THE UNIVERSITY OF ASTON IN BIRMINGHAM

(Department of Chemical Engineering)

Gaseous Heat Transfer in Cross Flow

by

A.M. KARIM

being a thesis submitted in support of an application for the degree of Doctor of Philosophy.

October 1982

The University of Aston in Birmingham

Gaseous Heat Transfer in Cross Flow

Adil M. KARIM

Oct. 1982

SUMMARY

An investigation was carried out into gas phase heat transfer in a single-pass cross flow heat exchanger supplied by NU-WAY ECLIPSE Ltd., to find reasons why over design occured when standard correlations were used.

The heat exchanger was of industrial scale with a burner heat duty of 10^6 Btu hr-1, (290Kw). Some of this heat was recovered by fresh air flowing through the bundle of 60 stainless steel tubes of 42 inch,(97cm) length. The combustion gases flowed transversly across the tube bundle.

An experimental programme was planned and implemented. It included developing mathematical models for both radiative and convective heat transfer.

It was found originally that air flow was uneven on both shell and tube sides. This situation was greatly improved by simple modifications.

The heat transfer coefficients on tube side were found to be higher than those obtained from standard correlations, while the heat transfer coefficients on the shell side were found to be similar to those obtained from standard correlations.

The thermal radiation, emitted from the refractory walls and radiating gases in the combustion chamber to the bundle of tubes was found to have no significant effect on the heat transfer coefficients of either shell or tube sides.

The main reasons for the over design were found to be that standard liquid-liquid correlations are not suitable for gas-gas heat transfer, the relative shortness of the tubes and end effects at entry and exit.

Heat transfer correlations, for both tube and shell sides, were developed, their application will enable over design to be avoided:-

Tube side correlation

$$Nu_T = 0.0028\ Re_T^{1.08} Pr^{0.33}$$

Shell side correlation

$$Nu_S = 0.89\ Re_S^{0.42} Pr^{0.33}$$

Key words

Heat transfer   Gaseous   Cross flow

ACKNOWLEDGEMENTS

The author wishes to express his thanks to Dr. J.K. Maund for his helpful, friendly and valuable supervision of this research project.

He would also like to thank all the staff of the Department of Chemical Engineering including those of the engineering and workshop departments for their help throughout the course of the work.

Finally he wishes to thank his wife, Carole, for typing the thesis.

List of Contents

List of Figures

List of Tables

NOMENCLATURE

Symbol	Significance	Dimensions
A	Effective heat transfer surface of sink	ft^2 m^2
A'b	Effective heat transfer of sink	ft^2 m^2
Ac	Tube area exposed to radiation	ft^2 m^2
Acp	Equivalant cold surface replacing a bank of tubes	ft^2 m^2
A_L	Inside tube longitudinal area	ft^2 m^2
A_{Lo}	Outside tube longitudinal area	ft^2 m^2
a_s	Shell side flow area	ft^2 m^2
A_t	Tube cross sectional area	ft^2 m^2
B	Baffle spacing	inch,cm
C_1, C_2, C_3, C_4	Constants for parameters in error calculation	-
C'	Clearence between tubes	inch,cm
CFL	Fresh air volumetric flow	$ft^3/hr, m^3/hr$
Cp_B	Specific heat capacity of hot gases	$Btu/Lb^oF, J/kg^oC$
cp_m	Fresh air specific heat capacity	$Btu/Lb^oF, J/kg^oC$
D	Inside tube diameter	inch,cm
D_o	Outside tube diameter	inch,cm
De	Shell equivelant diameter	inch,cm
Dev	Shell volumetric equivelant diameter	inch,cm
E	Emissive power	$Btu/hrft^2$
F	Factor to allow for both the geometry of the system and the non black emissivities of hot and cold bodies	-

Symbol	Significance	Dimensions
f	Friction factor.	-
F_I	Entrance configuration factor	-
F_A	Geometry factor	-
F_a	Tube arrangement factor for convection heat transfer	-
Fe	Emissivity factor	-
Fs	Safety factor in McAdams equations (1.21 and 1.22)	-
F_T	Correction factor for mean temperature difference	-
FT_p	Practical mean temperature difference correction factor.	-
g'	Air/fuel ratio	-
G	Mass velocity	$Lb/hrft^2, Kg/m^2hr$
G_t	Fresh air mass velocity	$Lb/hrft^2, Kg/m^2hr$
h	Heat transfer coefficient	$Btu/hrft^{2o}F, w/m^{2o}C$
HFL	Hot gas volumetric flow	$Ft^3/hr, m^3/hr$
h_m	Mean heat transfer coefficient	$Btu/hrft^{2o}F, w/m^{2o}C$
h_x	Asymptotic heat transfer coefficient	$Btu/hrft^{2o}F, w/m^{2o}C$
J_H	Factor for heat transfer	-
K	Fresh air thermal conductivity	$Btu/fthr^oF, w/m^oK$
K_f	Furnace wall thermal conductivity	$Btu/fthr^oF, w/m^oK$
K_w	Tube wall thermal conductibity	$Btu/fthr^oF, w/m^oK$
L	Size of individual eddies	-
L_m	Logarithmic mean temperature difference	$^oF, ^oC$
$\dot{m}$	Fluids mass flow	Lb/hr, Kg/hr
ma	Fresh air mass flow	Lb/hr, Kg/hr

Symbol	Significance	Dimensions
m_W	Molecular weight	mole/Kg
N	Number of major restrictions	-
n	Number of tube pases	-
Nu	Nusselt number	
P		
Pr	Prandtl number	
P_T	tube Pitch	inch,cm
Q_C	Heat imput from fuel	Btu/hr,Kw
Q_{con}	Heat transferred from hot gas to fresh air in a tube	Btu/hr,Kw
Q_F	Amount of heat taken out per hour by flue gases	Btu/hr,Kw
Q_{gt}	Amount of radiative heat transfer fromradiative gases to individual tube	Btu/hr,Kw
Q_L	Amount of heat loss per hour	Btu/hr,Kw
Qp	Overall amount of heat per hour recovered by fresh air	Btu/hr,Kw
Qw_t	Amount of radiation emitted by combustion chamber top wall	Btu/hr,Kw
Qw_b	Amount of radiation emitted by combustion chamber bottom wall	Btu/hr,Kw
Qw_L	Amount of radiation emitted by combustion chamber left wall	Btu/hr,Kw
Qw_R	Amount of radiation emitted by combustion chamber right wall	Btu/hr,Kw

Symbol	Significance	Dimensions
q_{Co_2}	Radiative heat flux from Co_2	Btu/hrft^2,w/m^2
q_{H_2o}	Radiative heat flux from H_2o	Btu/hrft^2,w/m^2
R	Temperature group	-
Re	Reynolds number	-
Re_x	Reynolds number at tube entrance	-
S	Temperature group	-
SL	Longitudinal Pitch	inch,cm
S_T	Transverse pitch	inch,cm
S_t	Stanton number	-
Ta_i	Fresh air temperature at tube inlet	^oF,^oC
Ta_o	Fresh air temperature at tube outlet	^oF,^oC
T_b	Fresh air bulk temperature	^oF,^oC
T_{Gi}	Inlet hot gas temperature	^oF,^oC
T_{Go}	Outlet hot gas temperature	^oF,^oC
Tw_i	Tube wall inlet temperature	^oF,^oC
Tw_o	Tube wall outlet temperature	^oF,^oC
T_1	Temperature of radiation source	^oR,^oK
T_2	Temperature of radiation sink	^oR,^oK
$\overline{U}$	Time average velocity in x direction	-
Ug	Velocity at the local main stream condition	-
$U\infty$	Free Stream Velocity	ft/s,(m/s)
V_{in}	Hot gas volumetric flow at combustion	ft^3/hr,(m^3/hr)
V_{os}	Hot gas volumetric flow	ft^3/hr,m^3/hr
VS	Hot gas velocity in the shell	ft/hr,m/hr
V_T	Velocity of fresh air in tubes	ft/hr,m/hr

Symbol	Significance	Dimensions
$\bar{V}$	Time average velocity in Y direction	ft/hr, m/hr
$\bar{w}$	Time average velocity in Z direction	ft/hr, m/hr
x_{ent}	Tube entrance length	inch, cm
x_L	Combustion furnace wall thickness	inch, cm
x_T	Tube wall thickness	inch, cm
yb	Width of boundary layer	inch, cm
Z	Intensity of turbulence	-
σ	Stefan Boltzman constant	0.173×10^{-8} ($Btu/hrft^2R4$), 5.67×10^{-8} (w/m^2K^4).
μ	Viscosity of fluids	Lb/fthr, (Kg/mhr)
μ_b	Viscosity of	Lb/fthr, (Kg/mhr)
μ_w	Viscosity of fluids at the tube wall temperature	Lb/fthr, (Kg/mhr)
	Density of fluids	Lb/ft^3, Kg/m^3
Ø	Viscosity ratio $(\mu/\mu w)^{0.14}$	-
x	Radiation effectiveness factor	-
Δ hi	Error involved in heat transfer coefficient tube side	$Btu/hr\ ft^{2\,o}F$, $w/m^{2\,o}C$
Δ ho	Error involved in heat transfer coefficient shell side	$Btu/hr\ ft^{2\,o}F$, $w/m^{2\,o}C$
Δ P	Pressure drop	inch H_2o, N/m^2
Δ TLM	Logarithmic mean temperature difference	^oF, ^oC
Δ RET	Error involved in Reynolds number tube side	-

Symbol	Significance	Dimensions
Δ Res	Error involved in Reynolds number shell side	-
Co_2	Emissivity of carbon dioxide	-
H_2o	Emissivity of water vapour	-
s	Emissivity of cold surfaces	-

Subscripts

i	tube inlet
o	tube outlet
t	tube side
s	shell side

INTRODUCTION

Heat recovery is one of the most important economical activities in any industrial plant, since costs and shortages of fossil fuels are increasing rapidly. Also heat is a form of energy that can be used for a large number of purposes, such as space heating, drying, boiling, chemical endothermic reactions, and many other uses.

The process designer involved in recovering heat to improve the economy of the process, has various applications and techniques, through which he can achieve an optimum and economic design, which would enhance the suitability of the equipment to that particular process. He has to consider the following points:-

a) The type of energy available to be recovered,
b) the specific requirements of the process to be considered,
c) the type of equipment used.

Heat recovery from a hot gas stream has often been ignored in industry, mainly because the heat transfer coefficients are usually low and it is often difficult to arrange the equipment for this secondary purpose.

This research work concerns in particular, gas to gas heat transfer in a heat exchanger, where waste organic fumes and solvents are incinerated. The process was simulated using an experimental rig manufactured by NU-WAY ECLIPSE LTD., which was donated by them to Aston University, Chemical Engineering Department, for research purposes. It consists of a combustion chamber with two gas burners and a heat exchanger of sixty stainless steel tubes, arranged in cross flow in a staggered arrangement. The tubes are arranged in such a way that the hot gaseous products from the incinerated organic fumes and solvents flow across the outside of the bank of tubes through the inside of which fresh air flows to recover heat from the hot gases, which may be used for various heating purposes.

The aim of this present research was to investigate the tendency to over design such units by understanding the behaviour of the air taking into account the different nature of its physical properties compared with liquids on which most heat transfer correlations are based. The performance of the heat exchanger, was also investigated in terms of thermal radiation, and aerodynamic effects.

As standard correlations for heat transfer assume a fully developed turbulent boundary layer with tube length to diameter ratio larger than 60 and based on liquid-liquid or gas-liquid systems (such as Sieder and Tate, Boelter-

Dittus, Kern...etc.) are applied generally and were applied in designing the present heat exchanger, and no regard was taken of end effects, and the nature and mechanism of gaseous heat exchange; the heat exchanger turned out to be overdesigned.

Heat transfer correlations for both shell and tube sides, based on experimental data from an operating air-air crossflow heat exchanger, would be very valuable from the economic point of view, as the correct design correlations would lead to lower costs in construction and materials because a smaller bank of tubes should be needed for the specified heat duty. Less operating expenses would be incurred as less energy would be needed, such as that for pumping air.

The expected design heat transfer correlations, for both shell and tube, would be expected to take the following form derived from dimensional analysis:-

$$Nu = \alpha Re^m Pr^n$$

where

Nu	=	Nusselt number	dimensionless.
Re	=	Reynolds number	dimensionless.
Pr	=	Prandtl number	dimensionless.

Another factor to cause overdesign might be radiation from most surfaces in the combustion chamber or from most gases from the combustion process to the tubes, so this was also investigated.

As this work concerns gaseous heat transfer in a single pass, crossflow heat exchanger taking into account the effect of thermal radiation on heat transfer coefficients, the pertinent literature to be consulted was in the years 1930 - 1965 and was rather scarce.

CHAPTER ONE

LITERATURE SURVEY

The objective of this chapter is to review previous work done by investigators into gaseous heat transfer in cross flow heat exchangers. This review also includes convective heat transfer and also radiative heat transfer, since in the present work, furnace process analysis is also considered.

Radiative heat transfer differs greatly from convective heat transfer, since the convective rate of heat transfer depends on the temperature difference between service and process while in the radiative process, the rate of heat transfer also depends on the temperature level. The two processes are additive and are very difficult to separate. At high temperature the radiative process is dominant, while at low temperatures, convective heat transfer makes the most important contribution to the process (9).

1.1 Convective Heat Transfer

Heat transfer by convection, which is produced by fluids in motion is of two kinds:

Free Convection when the fluid motion is not implemented by mechanical agitation, and Forced Convection when the fluid is mechanically agitated. It is forced convection which is the more efficient and of main interest to engineers.

The main objective of the mechanical agitation is to increase the heat transfer, in other words to enhance the heat transfer coefficient.

1.1.1 Heat Transfer Coefficient

At a given temperature difference the heat transfer coefficient and the surface area control the rate of heat transfer and are both governed by the layout and geometry of the equipment. An increase in surface area leads to an increase in the rate of heat transfer but may also increase the pressure drop across the exchanger. This loss in pressure in either flow medium must be compensated by the use of pumps or fans, therefore an optimisation technique for design would be of considerable interest to achieve the most economic heat transfer equipment.

Heat transfer of fluids flowing turbulently in closed circuits is one of the most important modes of industrial heat transfer. Therefore empirical correlations for turbulent-flow heat transfer were developed quite early and they have constantly been modified and improved as experimental techniques and results have become more refined.

The complicated nature of tubulent flow usually prevents an analytical approach.

In early studies, experimental work on turbulent heat transfer concentrated mainly on air and water, covering a Prandtl number range of 0.7 - 10. Later studies were made on higher viscosity oils having a Prandtl number range up to 1000.

1.1.2 Dimensional Analysis

It has been found experimentally that the heat transfer coefficient "h", depends on the following factors:

The fluid velocity "v", the fluid density "ρ" the fluid viscosity "μ", its thermal conductivity "k", the fluid specific heat capacity,"Cp", the pipe internal or external diameter, depending on whether it is an inside or outside heat transfer coefficient. It may also be necessary to include a conversion factor to allow for the case when all the energy terms are not expressed mechanically or thermally by the dimensions of the variables. If all the dimensions combine to give only thermal quantities (such as calories), K_H then must be unity. Using dimensional analysis and dimensionless groups and ignoring the bouyancy effects:

$$h = f(V^a \rho^b \mu^c K^d C_p^e D^f K_H^g) \quad \text{.....................(1.1)}$$

$$\frac{H}{L^2 \emptyset T} = (\frac{L}{\emptyset})^a (\frac{M}{L^3})^b (\frac{M}{L\emptyset})^c (\frac{H}{L\emptyset T})^d (\frac{H}{MT})^e (L)^f (\frac{ML^2}{H\emptyset^2})^g \ldots\ldots\ldots (1.2)$$

where

M = Mass		$\emptyset$ = time
H = Heat		t = temperature
L = Length		D = tube diameter

H	1 =	d+e-g	1	a	2
L	-2 =	a-3b-c-d+f+2g	2	b	2
$\emptyset$	-1 =	-a-c-d-2g	3	c	3
T	-1 =	-d-e	4	d	4
M	0 =	b+c-e+g	5	e	3

from 1 and 4 and solving in terms of a and e:

$d = 1-e$

$c = 1-a-d$

$\quad = 1-a-1+e$

$\quad = -a+e$

$b = e-c = a$

$f = -2-a+3b+c+d$

$\quad = -2-a+3a-a+3+1-e$

$\quad = a-1$

Rearranging

$$\frac{hD}{K} = \propto (\frac{pvD}{u})^a (\frac{cpu}{K})^e \quad \ldots\ldots\ldots\ldots\ldots\ldots\ldots (1.3)$$

or

$$Nu = \propto (Re)^a (Pr)^e \quad \ldots\ldots\ldots\ldots\ldots\ldots\ldots\ldots (1.4)$$

Empirical correlations for turbulent heat transfer in conduits and tubes using the same approach of dimensional analysis, would be in the same form as equation (1.4)

The most common form of equations relating these dimensionless groups for turbulent flow heat transfer is the one for Nusselt number and follows:

$$Nu = \alpha Re^{m} Pr^{n} \qquad \ldots\ldots\ldots\ldots\ldots\ldots\ldots\ldots (1.5)$$

The mean heat transfer coefficient for a circular tube of length L may be calculated from the following relation, (1):

$$h(\pi\ dL)(Tw - Tb)_{Lm} = \frac{d^2\pi}{4} GCp(Tb_2 - Tb_1) \ \ldots\ldots (1.6)$$

where Tb_1 and Tb_2 are, respectively the inlet and outlet bulk temperature of the fluid from equation (1.6), Nusselt number becomes:

$$Nu = \frac{d^2}{4L}\frac{GCp}{K}\frac{Tb_2 - Tb_1}{(Tw - Tb)_{L\ m}} \qquad \ldots\ldots\ldots\ldots\ldots\ldots (1.7)$$

where

Nu = Nusselt Number, dimensionless

h = heat transfer coefficient Btu/hr $ft^2 F^{\circ}$, $w/m^{2\circ}C$

d = tube diameter, inch, cm

Tb_2 = outlet bulk temperature, $^{\circ}F$, $^{\circ}C$

Tb_1 = inlet bulk temperature, $^{\circ}F$, $^{\circ}C$

k = fluid thermal conductivity, Btu/hrft$^{2\circ}F$, $w/m^{2\circ}C$

Cp = fluid specific heat capacity; Btu/Lb$^{\circ}F$, $J/k^{2\circ}C$

$(Tw-Tb)_{L\,m}$ = logarithmic mean temperature difference.

In the present work, it would be desired to see the effect of Re on Nu for different values of Re.

1.1.3 Effect of Temperature Difference on Heat Transfer Coefficient

If the properties of the fluid were constant, the use of equation (1.6) would be quite simple. However, the temperature of the fluid does not only vary across the section of the tube, but also along the length of the tube.

Since physical properties of fluids change with temperature, there is always the problem of choosing which temperature to use for evaluating the properties.

In early work, (9) where temperature differences were low and only air and water were studied, the bulk temperature of the fluid was suitable for evaluating all fluid properties, but when oil was used for example, in which the viscosity varies greatly with temperature, it was necessary to use an additional dimensionless group $(\mu_b/\mu_w)^{0.14}$, to allow for variations across the tube section to obtain a satifactory correlation of data. Another practice was also adopted to evaluate all fluid properties at what is called film temperature rather than using a viscosity - ratio correction. The usual film temperature for evaluating properties is taken as:

$$T_{0.5} = \frac{Tw + Tb}{2} \quad \ldots\ldots\ldots\ldots\ldots\ldots\ldots\ldots\ldots\ldots (1.8)$$

i.e. it is the arithmetic average of the wall and bulk temperature.

A large number of data for turbulent heat transfer were obtained by many investigators. Most of these data were correlated by other research workers.

Dittus and Boelter (2) proposed the equation

$$\frac{hD}{K} = 0.023 \left(\frac{DG}{\mu}\right)^{0.8} \left(\frac{Cpu}{k}\right)^{n} \ldots\ldots\ldots\ldots\ldots\ldots (1.9)$$

fluid properties were evaluated at arithmetic mean bulk temperature.

$n = 0.4$ for heating and 0.3 for cooling.

Equation(1.9)has limitations, such as Reynolds number should not be less than 10,000 which means it does not hold for turbulent flow over the range 2300 - 10,000. Also the $\frac{L}{D}$ ratio for tubes has to be more than 60, which means the equation is for a fully developed turbulent boundary layer. In the case of gases there is no need for n variation since Prandtl number is always less than unity.

It is not suitable for the present work, since air is used with a Reynolds number of less than 10,000 sometimes and $\frac{L}{D} = 40$.

Another disadvantage with equation (1.9) is that it has no viscosity-ratio correction when used for liquids with Prandtl number of up to 100 so it is not applicable to liquids with high Prandtl number

Colburn (3) presented the following correlation in which Stanton number was used instead of Nusselt number:-

$$\left(\frac{h}{GCp} \right) \left(\frac{Cp\mu}{K} \right) = 0.023 \left(\frac{DG}{\mu} \right)^{-0.2} \qquad \text{...........(1.10)}$$

The fluid properties are evaluated at film temperature except Cp in the Stanton group which was evaluated at the arithmetic average temperature.

Equation (1.10) also has limitations such as: Reynolds number should be higher than 10,000 and $\frac{L}{D}$ must be more than 60, therefore it can not be used for tubes with $\frac{L}{D} = 40$ where the turbulent boundary layer might not be fully developed early in the tube. The range of Prandtl number is wider than for equation (1.9), being 0.7 - 160. No account was taken of viscosity changes in longitudinal and radial directions, especially in oils where viscosity changes greatly for small temperature changes.

Sieder and Tate (4) developed an equation which is suitable for fluids with high Prandtl number

$$\frac{h}{Gcp} \left(\frac{cp\mu}{K}\right)\left(\frac{\mu w}{\mu b}\right)^{0.14} = 0.023 \left(\frac{DG}{\mu}\right)^{-0.2} \quad \ldots\ldots\ldots\ldots(1.11)$$

equation (1.11) has a viscosity ratio-correction which indicates it is suitable for viscosity changes. However, it is also not applicable when Reynolds number is less than 10,000 and $\frac{L}{D}$ less than 60.

Correlation (1.11) was tested by Drexel and McAdams (5), and they found when air was used a constant of 0.021 could be used, and the constant of 0.023 is suitable for correlating most available data.

Equation(1.11) should be suitable for the present research since air was used, but the $\frac{L}{D}$ ratio is different from the holding conditions, also the entrance effect is another factor, which is not considered here.

Equations (1.9), (1.10), (1.11) are applicable for moderate temperature differences.

At high temperature and high temperature difference, Humble et al (6) studied heat transfer to air flowing through a smooth circular tube by investigating various entrance configurations, the tube length, and tube wall temperatures. They developed the empirical relationship:

$$\frac{hD}{K} = 0.034\left(\frac{DG}{\mu}\right)^{0.8}\left(\frac{cp\mu}{K}\right)^{0.4}\left(\frac{L}{D}\right)^{-0.1} \quad \ldots\ldots\ldots\ldots(1.12)$$

All fluid properties were evaluated at the film temperature, since air was used.

Equation (1.12)is useful for the present work, since the medium used was air, also an account was taken of the entrance effect. It has a limiation in that Reynolds number should not be less than 10,000, $\frac{L}{D}$ ratio is to be as low as 30 up to 120 which makes the correlation more applicable to cases like the present work.

Another limitation is that the wall temperature must be in the range 600-3050 ^{o}R and (Tw/Tb) is in the range of 0.8 - 3.5. Equation (1.12)was substantiated by Weiland and Livinggood and Lowdermilk (7).

Kern (9) proposed the following equation:

$$\frac{h_i D}{k} = 0.027 \left(\frac{DG}{\mu}\right)^{0.8}\left(\frac{cu}{k}\right)^{0.33}\left(\frac{\mu}{\mu w}\right)^{0.14} \quad \ldots\ldots\ldots(1.13)$$

Equation (1.13)was an improvment on Sieder and Tate's equation (1.11) which was based on the data of Morris and Whitman (8), for a number of fluids principally petroleum fractions in horizontal and vertical tubes.

Equation (1.13)is suitable for turbulent flow, but it gave maximum mean deviations of approximately + 15 and -10 percent for Reynolds numbers above 10,000.

Although it was obtained for calculating heat transfer coefficients on the tube sides, it would also be used for pipes. Kern (9) reported that equation (1.13) is suitable for organic liquids, aqueous solutions, and gases. Differences in the natures of fluids, were not taken into account, since there is no need for a viscosity correction when gases are used, unlike liquids.

It was developed for a fully turbulent boundary layer, Kern suggested that a $\left(\frac{L}{D}\right)$ parameter could be incorporated in the equation to allow for the effect of length. He also developed a graphical representation for equation (1.13), using:

$$j_H = \frac{hD}{K}\left(C\mu/K\right)^{-\frac{1}{3}}\left(\frac{\mu}{\mu w}\right)^{-0.14} \qquad \ldots\ldots\ldots\ldots\ldots(1.14)$$

from which 'h' could be found from a calculation of Reynolds number.

The use of graphical charts increases the error since reading errors would be included.

Kern (9) also developed a correlation for Reynolds numbers varying from 2000 to 1,000,000 for calculating the Nusselt number on the shell side:

$$\frac{h_o D_e}{K} = 0.36\left(\frac{DeGs}{\mu}\right)^{0.55}\left(\frac{cp\mu}{k}\right)^{0.33}\left(\frac{\mu}{\mu w}\right)^{0.14} \quad ,.....(1.15)$$

in equation (1.15) the equivalant diameter was introduced to represent the shell overall diameter:

where

$$De = \frac{4 \times \text{free area}}{\text{wetted perimeter}} \quad \text{inch,(cm)} \; ....(1.16)$$

It agrees very well with the methods of Colburn (3),Short (10), and the test data of Breedenbach and O'Connell (11).

The large range of Reynold's numbers makes it very practical for a wide range of fluids, such as hydrocarbons, organic compounds, water and gases. However, it does not take into account the arrangement of tubes the pitch and clearance between tubes.

The viscosity ratio included,makes it more practical for fluids with high viscosity. It is also available in graphical form.

Carpenter et al (12) presented the following form of dimensionless correlation, for turbulent flow only. He claimed it is suitable for all fluids:

$$\frac{hD}{K} = 0.023\left(\frac{DG}{\mu}\right)^{0.8}\left(\frac{cp\mu}{k}\right)^{0.33}\left(\frac{\mu}{\mu w}\right)^{0.14} \quad ....(1.17)$$

equation (1.17)is identical to Kern's equation (1.13)

It is very practical in fluids with high viscosity, but it is also only applicable to a turbulent fully developed boundary layer.

Pierson (13) in his work on the influence of tube arrangement on convective heat transfer and flow resistance in cross flow of gases over tube banks,showed that the variation of heat transfer coefficients with lattice spacing increased as Reynolds numbers decreased, and these results were correlated by Grimson (14) from data of Huge (15) and Pierson (13) by the equation:

$$Uc = 0.284Fa \frac{K}{\mu^{0.61}} \frac{G^{0.61}}{D_t^{0.39}} \quad \ldots\ldots\ldots\ldots\ldots(1.18)$$

Uc = Convection conductance at solid boundary Btu/hr $ft^{2\,o}F$, $w/m^{2\,o}C$

D_t = tube diameter inch/cm

G = mass flow of gas lb/hr ft^2

Fa = arrangement factor for convection heat transfer such as in line or staggared.

equation(1.18) applies strictly to banks of a minimum of ten rows. Pierson (13) gave a correction factor for less rows for specific in-line and staggered arrangements. Grimson, (14) Huge and Pierson (15) covered a very wide area in predicting data on flow resistance and heat transfer for cross flow of gases over tube banks.

They presented a great deal of information taking into account the effect of size of the bundle of tubes, and the behaviour of fluids towards the tube diameter clearance and depth of rows in the bundle.

Colburn (3) recommended the following correlation for gases flowing normal to banks of staggered unbaffled tubes, for Reynolds number from 2,000 to 40,000.

$$\frac{h_o D_o}{K} = 0.33\ (C\mu/K)^{1/3}(D_oG/\mu)^{0.6} \quad \ldots\ldots\ldots\ldots\ldots (1.19)$$

The properties of gases were evaluated at T_f where

$$T_f = \tfrac{1}{2}(T_w + T_b) \quad \ldots\ldots\ldots\ldots\ldots\ldots\ldots\ldots\ldots (1.20)$$

equation (1.19) is only suitable for a bundle of at least ten rows deep with staggered tube arrangement.

McAdams (16) suggested two general equations for flow of fluids normal to banks of tubes that are not baffled in a Reynolds number range 10,000 to 20,000:

$$\left(\frac{h}{CG}\right)_i (C\mu/K)^{2/3} = \frac{a/Fs}{(DG/\mu)_i^{\,1-no}} \quad \ldots\ldots\ldots\ldots (1.21)$$

$$\left(\frac{h}{CG}\right)_o (C\mu/K)^{2/3} = \frac{a/Fs}{(DG/\mu)_o^{\,1-ni}} \quad \ldots\ldots\ldots\ldots (1.22)$$

where subscripts i refer to inside

o refer to outside

for gases and water (Fs) could be taken as 1.25 generally.
for the recommended Reynolds number range

$$a_i = 0.023 \text{ and } ni = 0.8$$

with Reynolds number range 2,000 to 40,000, $a_2 = 0.33$ for staggered tubes and n_o is 0.6.

Equations(1.21) and(1.22) are applicable for turbulent flow without change in phase, and they are suitable for fluids with Prandtl number in the range of 0.7 - 120. Equation(1.21) applies to a Reynolds number range of 10,000 - 120,000 and $\frac{L}{D}$ ratios greater than 60. Equation (1.22) is of some interest, since the tube arrangement is taken into account, but there is no viscosity ratio correction for use when liquid with high Prandtl number is used, also the entrance effect is obviously not taken into account.

1.1.4 Effect of Turbulence on Heat Transfer

There are two factors that can effect the average and local heat transfer coefficients to or from a tube in cross flow, namely:

1) Intensity of turbulence.
2) Scale of turbulence.

1.1.4.1 Intensity of Turbulence

This is a measure of the amplitude of random oscillation of the flow under consideration. If turbulence is taken into consideration, then the dimensionless heat transfer equations (local and average) become:

$$Nu = f(Re, Pr, Z) \quad \text{.......................} (1.23)$$

Mathematically the intensity of turbulence Z is:

$$Z = \frac{1}{3} \frac{(\bar{U}^2 + \bar{V}^2 + \bar{W}^2)}{U\infty} \quad \text{.......................} (1.24)$$

where

$\bar{U}$ = Time average velocity in x direction

$\bar{V}$ = Time average velocity in y direction

$\bar{W}$ = Time average velocity in z direction

The effect of turbulence on heat transfer cannot be determined theoretically, due to the difficulty in mathematically handling random fluctuations, so it has to be determined experimentally.

Comings et al(17) were among the first to obtain experimental results for the effect of intensity of turbulence. For a Reynolds number of 5,800, they varied the intensity of turbulence from 1.8% to 21.6% and found that over this range, the heat transfer increased by 10% with the majority of the increase of heat transfer being in the range of 1.8% to 8% turbulence.

Schlichting(18), showed that the inter-dependance between pressure gradient and turbulence intensity could be understood qualitatively using the theory of Lin(19) for non-steady boundary layer flows in which the average balance of forces in the laminar boundary layer involved an additional term J, of the form

$$J = \tfrac{1}{2}U_g \times \frac{du_g}{dx} f(\frac{y}{\delta}) \qquad \ldots\ldots\ldots\ldots\ldots\ldots(1.25)$$

where

J = unit force, an additional term arising from the average balance of forces in the laminar boundary layer.

δ = Boundary layer thickness.

Ug = velocity at the local main stream condition.

for the case of a harmonic oscillation $U\infty(x)$ Sin nt super-imposed on an average velocity $\bar{U}\infty(x)$.In this example the amplitude U has the same effect as the intensity of turbulence which is a measure of the r.m.s of the amplitude of random oscillation. The term J vanishes when the rate of change of amplitude $\frac{du}{dx} = 0$. According to this reasoning,strong deceleration and subsequent acceleration of a stream as occurs in the neighborhood of the stagnation point on a tube will cause the rate of change of the intensity of turbulence to become large, hence the effect of heat transfer will be greatest at this point. This has been confirmed experimentally by Seban (20), Kestin (21), Sagin and Subramanian (22), and Perkins and Leppert (23).

1.1.5 Scale of Turbulence

The scale of turbulence is a measure of the size of individual eddies and is defined by a charateristic length, L,

where

$$L = \quad R(y)dy$$

where

$$R(y) = \text{correlating coefficient.}$$

The effect of scale of turbulence upon heat transfer has been the subject of fewer investigations than intensity of turbulence. The most comprehensive experimental study has been carried out by Hegge Zinjen (24) who measured rates of heat transfer from wires and tubes for Reynolds numbers of between 60 - 25800 and ratios of scale of turbulence to tube diameter $\frac{L}{dc}$ between 0.31 - 240. Results showed that at constant Reynolds number and intensity of turbulence heat transfer increased with increasing scale ratio to a maximum when the ratio $\frac{L}{dc}$ was about 1.5 - 1.6 and then steadily decreased. Most of the increase in heat transfer occured in the range of scale of turbulence 0.5 - 7.

Hegge Zijnen explained this variation by assuming that the effective frequency of turbulence was proportional to $\frac{U_\infty}{L}$, and equalled the frequencies of eddies shed by the tube (Strouhal effect) over the range of $\frac{L}{dc}$ of 1.5 - 1.6 (the value of maximum effect on heat transfer).

Fallon (25) described the variables affecting the performance of tubes in a cross-flow arrangement:

i) as turbulence intensity at the entrance of the bank increases, the heat transfer in the first row is enhanced.

ii) There appears to be no general rule about the effect of row depth except that a tube bank has to be at least six rows deep to simulate conditions in an infinitely deep heat exchanger. The effect varies with tube arrangement and geometry.

iii) Even a thin layer of carbon deposits forming on the external surface of the tubes can change the heat transfer significantly. This problem could be over-come by controlling the fuel/air ratio so that less carbon deposits would be formed.

Although turbulence intensity would normally enhance the heat transfer there are other factors which could lead to a decrease in the heat transfer rate, such as swirling of fluids and zoning near the first rows. Thompson et al (26) and Snyder (27) did some work on this phenomenon and found that using a bundle of ten rows deep and air flows normal to the bank,average Nusselts number increases up to the third row, decreases slightly, and then remains essentially constant. Reynolds number was kept constant at 10,000 in Snyder's experiment.

Huge (15) studied the effect of tube size as a factor in heat transfer and pressure drop, for gases flowing transversly over the tube bank of a given arrangement. He reported that the values of both gas boundary conductance and friction factors for a given tube arrangement are consistent for all tube sizes. Bergelin et al (28) developed data and charts based on a study of effect of tube spacing and size on heat transfer and fluid friction during viscous flow across banks of tubes. Having used different tube arrangements and spacing, they concluded the following:

1. When the pitch is increased for a given arrangement and tube size:

   a) At constant velocity, the pressure drop is lower and the coefficient of heat transfer is lower.

   b) At constant pumping power, the heat transfer coefficient is slightly lower.

2. When the tube diameter is increased for a given arrangement and constant pitch ratio:

   a) At constant velocity the pressure drop is lower and the heat transfer coefficient is lower.

   b) At constant pumping power the coefficient of heat transfer is considerably lower.

3. The highest coefficients of heat transfer were obtained with the smaller tube sizes and tube pitches in staggered arrangements.

4. The use of volumetric equivalent diameter in the Reynolds number gives somewhat better correlation of heat transfer data than does the use of tube diameter.

This research is of interest in the present work since the bundle arrangement and tube size play a big role in the performance of the heat exchanger. Although the data was based on highly viscous fluids, unlike the air used in the present work.

Omhandre et al (29) disclosed certain perculiarities in fluid flow and heat transfer in their work on the effect of Reynolds number which was investigated further for a variety of tube sizes and arrangements.

They suggested that the viscosity ratio-correction $\mu/\mu w$ should possibly be some function of the rate of flow in order to bring friction factor for oil-cooling in line with isothermal data. It may be possible that part of the irregularity in the flow velocity regime may be due mainly to uneven distrubution of flow and only partly due to an improper exponent applied to the viscosity ratio.

In consideration of this possibility they considered it advisable to investigate the variation in flow distribution for tube banks of different properties before assigning a specific function of the viscosity ratio correction. The data is based on oil of which viscosity changes have considerable effect on friction factor and heat transfer coefficients, so errors in temperatures could lead to drastic errors in viscosity. In gases errors will not be as large as in viscous liquids, such as oil, also the flow profile will not be affected so much.

1.1.6 Flow in the Entrance Section of Tubes

When a fluid enters a tube, the boundary layer begins forming at the entrance.

A fully developed velocity profile exists when the edge of the boundary layer coincides with the axis of the tube. The fluid dynamic conditions at the entrance of the tube greatly influence the length required for a fully developed velocity profile to form.

The configuration of the entrance is an important factor in turbulent fully-developed flow in determining the dynamics of flow downstream. The ratio of length to diameter at which the flow becomes fully developed depends on the type of entry and the Reynolds number.

According to the theory of Latzko (30) for turbulent flow in a tube with bull mouth entry, laminar boundary layers build up on the wall in the inlet region of the tube and meet at the critical or starting length given by:

$$\frac{L}{D} = 0.693\ Re^{0.25} \qquad (1.26)$$

Stanton (31) showed that mean heat transfer coefficients in tubes were the same between values of (L/D) from 30 to 60.

Nusselt (32) studied the effect of entrance length and recommended introducing the factor $(\frac{L}{D})^{-0.054}$

$\frac{L}{D}$ ratio has to be more than 10 and less than 400.

Equation (1.28) has been used extensively for predicting heat-transfer coefficients in entrance regions.

Aladyev (33) presented charts for local and mean heat transfer coefficients for fluids with Pr = 0.7 flowing in the entrance region using $\frac{h_m}{h_\alpha}$ versus $\frac{x}{d}$ at constant Reynolds number. These could be of interest for the present research work. Reynolds numbers covered of the range 10^4-10^5 and extrapolated to 10^6.

Deissler (34) presented analytical results for predicting heat transfer coefficients in circular tubes, indicating the variation of the mean Nusselt number Nu_m with $\frac{L}{D}$ ratio at various Reynolds numbers. The curves apply for air since Prandtl number was 0.73.

He showed that the neat Nüsselt number bec omes essentially constant at values of $(\frac{L}{D})$ more than 30.

Boelter et al (35) studied the effect of entrance configuration on heat transfer coefficients in circular tubes. They investigated the heat transfer to air in the entrance section of a tube in which the wall temperature was essentially constant and recommended the following equation:

$$\frac{h_m}{h_\alpha} = 1+F_1 \frac{L}{D} \quad \text{..............................(1.27)}$$

where $\frac{L}{D}$ must be more than 5

F_1 is an entrance configuration factor.

1.1.7 Pressure Drop

As has been said earlier in this chapter, heat transfer coefficients and the surface area are closely linked and governed by the lay-out and form of the tubes. An increase in surface area and heat transfer coefficient leads additionally to loss of pressure in the flow medium which has to be compensated by the use of pumps. The energy required for this is derived from the simple equation:

$$E = V_m \Delta p \quad \ldots\ldots (1.28)$$

where

V_m is the flowrate, and

ΔP is the pressure loss in the flow medium.

Winding (36) presented his observations on the effect of the shape on heat transfer coefficients in staggered tube banks. He found that stream-lined tubes gave a lower pressure drop through the tube bank but this gave low coefficients of heat transfer in all rows except the first and second. Oval tubes gave lower rates of heat transfer than other shapes.

Huge and Pierson (15),(13) derived independently equations for calculating pressure drops and presented:

$$\Delta P = \frac{fNG^2}{10.84 \times 10^8 P} \quad \ldots\ldots (1.29)$$

where

N = number of major restrictions

The constant 10.84×10^8 includes the acceleration of gravity in ft per hr^2 and the pressure conversion from lbs per ft^2 to inches of water.

The physical properties in equation(1.29)are evaluated at the mean gas - boundary or film temperature. This is the generally accepted correlation for calculating resistance to flow across banks.

Sieder and Tate (4) gave a correlation for pressure drop in tubes:

$$\Delta P = \frac{f G_t^2 L n}{5.22 \times 10^{10} D_t \times S \times \emptyset_t} \quad \ldots\ldots\ldots\ldots\ldots\ldots\ldots (1.30)$$

They correlated friction factors for fluids being heated or cooled in tubes.
where L is the tube length and n is the number of tube passes, and S is the specific gravity of fluid.

Equation(1.33) has a deviation which was accepted by the Tubular Exchanger Manufactures Association.

Kern (9) developed in the same manner the following equation for calculating the shell side pressure drop:

$$\Delta P_s = \frac{fG^2{}_s\, D_s(N+1)}{5.22\times10^{10} DeS\phi_s} \quad \ldots\ldots\ldots\ldots\ldots\ldots\ldots\ldots (1.31)$$

Equation(1.31) has been widely used for industrial design, and has been found reasonably reliable since a viscosity ratio correction is inserted. It does not take into account tube arrangements and spacing.

Gunter and Shaw (37) suggested that pressure drop could be highly influenced by the spacing of the succeeding rows of tubes, their layout and closeness, and recommended the following correlation:

$$\frac{f}{2} = \frac{-Pg\ Dv}{G^2 L}\left(\frac{\mu}{\mu w}\right)^{0.14} \times \frac{Dv}{ST}^{-0.4} \times \frac{SL}{ST}^{-0.6} \quad \ldots . (1.32)$$

where: D_v = volumetric equivalent diameter

$$= \frac{4 \times \text{net free volume}}{\text{wetted perimeter}} \ldots\ldots\ldots\ldots (1.33$$

ST = centre to centre distance between the logitudinal rows(transverse pitch)

SL = center to centre distance between the tubes in adjacent transverse rows (longitudinal pitch)

Equation(1.32) is very useful since spacing and layout of tubes are taken into account. Clearly SL and ST would be factors affecting the friction factor for flow of fluid through a shell of tubes. This makes it possible to optimise tube arrangement within the shell.

1.2 Heat Transfer by Radiation

There is a large amount of information on heat transfer available, but appropriate literature for cross flow heat transfer in gas-gas system is rather scarce. Therefore it would be beneficial to review closely related research work, so that a background for the present work would be readily provided to investigate the effect of radiation on heat transfer coefficients in tubes - in the present work. There are radiant interchanges between surfaces, and also between gases as a source of radiation and solid surfaces in an enclosure. This situation leads to consideration of the view the surfaces have of each other and their emitting and absorbing charactristics.

The gases radiative behaviour has to be considered also.

1.2.1 Radiation from non-luminous gases and flames

Gases encountered in heat transfer equipment, carbon monoxide, hydro-carbons, water vapour, carbon dioxide, sulfur dioxide, ammonia, hydrogen chloride, and the alcohols are among those with emmission bands of sufficient magnitude to merit consideration.

Gases with symmetrical molecules, hydrogen, oxygen, nitrogen etc..., have been found not to show absorption bands in those wavelength regions of importance in radiant heat transmission at temperatures met in industrial practice.

Heat radiation by flames can arise either from the hot gases of the flame or from suspended hot particles of soot, ash, or injected solids.

When the radiation is from the hot gases, then only those gases which radiate strongly at the temperature range of interest need be considered. Ordinarly, these will include the asymmetric molecules, such as water vapour, carbon monoxide, cabon dioxide and sulfur dioxide.

The radiation emanating from a unit volume of a radiating gas will be partially absorbed and re-radiated by the gas lying between the unit volume and a heat sink and the effects of all unit volumes, lying along the path will be cumulative, so that the gas emissivity as judged by the sink(radiation compared with that recieved from a black body at gas temperature) is dependent upon the path length.

Patrick and Patel (38) tried to develop a heat transfer coefficient in towns gas heated equipment.

They operated at temperatures of not more than $700^{o}F$ and used towns gas of 500 BTU/ft^3. They relied on experimental work by other groups of researchers working on the same project and established an equation of the following form.

$$U = 0.001\ N^{0.8} (Q/A)^{0.9} \qquad \text{.....................(1.34)}$$

where N is called air number defined as ratio of quantity of air supplied to that required stochio metrically for combustion.

No real account was taken of the heat transferred by radiation, also no parameters were established for the process and equipment.

Debaufre (39) presented an empirical correlation for heat transfer in a combustion chamber as:

$$Q = A_c E \left(\frac{T_G}{1000}\right)^4 - \left(\frac{T_s}{1000}\right)^4 \qquad \text{..............(1.35)}$$

where

Q = heat transfer rate. Btu/hr

A_c = tube area exposed to radiation ft^2.

T_G = Absolute temperature of products of combustion leaving furnace chamber R^o

T_s = Absolute temperature of cooling medium inside tubes or cooled surfaces.

E = effectiveness factor

This correlation would be of value if E were easily evaluated. He suggested that E should have a maximum value of 1723.(Stefan-Boltzman constant BTU/(hr)(ft^2)$\overset{o}{R}{}^4$) ($5.67 \times 10^{-8} w/K^4 m^2$). No account was taken for the configuration of the furnace and tubes, also the radiative interaction between tubes in the bundle.

Hottel (40) produced a breakthrough in radiative heat transfer, since he considered that radiation between tubes and gases in intertube spaces is often a factor of great importance in tube-bank performance. He presented the following equation:

$$Q = F_A F_e A \sigma (T_1^4 - T_2^4) \qquad (1.36)$$

where

Q = heat flow by radiation alone to A BTU/hr

A = effective heat transfer surface of sink, ft^2

T_1 = temperature of radiation source ^oR

T_2 = temperature of sink ^oR

F = factor to allow for both the geometry of the system and the non-black emissivities of the hot and cold bodies, dimensionless

σ = Stephan-Boltzman constant, $0.I73xI0^{-8}$ BTU/hr ft^2 R^4 ($5.67x10^{-8} w/K^4 m^2$)

Application of this equation to practical engineering problems requires a number of assumptions and simplifications, which might create inaccuracy in determining the heat transferred by radiation. Some supporting information is needed also such as the view factor, emissivity, absorptivity, and details of any cavities on surfaces.

Mulliken (41) presented an equation to evaluate the effective heat transfer surface for various boiler tubes as:

$$(\alpha\, AC_p)_s = AC_p\, F_c F_e F_s \quad \ldots\ldots\ldots\ldots\ldots\ldots\ldots (1.37)$$

Acp = an equivelant cold plane surface replacing a bank of tubes.

α = effectiveness factor

F_c = conductivity factor, dimensionless

F_e = emissivity factor, dimensionless

F_s = slag factor, dimensionless

In equation (1.35) the tube emissivity is introduced in the evaluation of the effective surface while in equation (40), the tube surface emissivity was considered in the exchange factor "F".

The emissivity of a particular gas mass is a function of the product of the partial pressure of the radiating constituent times mean beam length (L).

Hottel (40) presented a gas radiation equation for the two radiative combustion gases Co_2 and H_2o and it is accepted universally:

$$Q_G = 0.173\, F_G \left[(e_c + e_w)_{T_G} \left(\frac{T_G}{100}\right)^4 - (e_c + e_w)_{T_b} \left(\frac{T_G}{100}\right)^4 A_b \right] \ldots (1.38)$$

$(e_c+e_w)_{T_G}$ = emissivity of gas at T_g

e_c = emissivity of gas Co_2 at P_{co_2}, L and T_G

e_w = emissivity of H_2o at PH_2O, L and T_G

$(e_c+e_w)_{Tb}$ = emissivity of gas at Tb

A'b = effective heat transfer surface of black body ft^2, (m^2)

There is also additional radiant heat transfer from the refractory side walls which adds to the average flux.

Since it was very difficult to evaluate the effect of the refractory surface contribution quantitatively, as Kern states in his text book (9). Hottel (40) established an equation which has been accepted worldwide, it is applicable for determining the overall exchange factor:

$$Fe = \frac{1}{\frac{1}{e_f} + \frac{1}{e_s} - 1} \quad \text{..................(1.39)}$$

where

e_s = the emissivity of the cold surface

e_f = the emissivity of the furnace cavity

Kern(9) suggested that the overall exchange factor may be obtained from the furnace and cold surface emmisivities, but he strongly warned that only in simplified calculations should these be used in an equation of the Stefan-Boltzman type for calculating the radiant heat transfer, simplifying the calculation to the following equation:

$$Q = 0.173F\left((\frac{T_G}{100})^4-(\frac{T_s}{100})^4\right) \propto ACp \quad \text{............(1.40)}$$

Q = radiant heat flow BTU/hr.

F = overall exchange factor to allow for the geometry , and emissivity dimensionless.

α = effectiveness factor

Acp = Area of cold plane replacing a bank of tubes ft^2

Other investigators in the field of furnace technology carried on the work of Hottel and presented several correlations.

Orok-Hudson (42) gave a correlation for a quick check on the performance of furnaces under differing operating conditions. It can be used to estimate the effects of changes in firing rate or air-fuel ratio for boilers fired with oil or coal. It is of limited value for design work:

$$Q = \frac{Q_F}{1 + G' /(CR/27)} \qquad \text{.......................(1.41)}$$

where CR is the pounds of fuel/hr ft^2 of projected radiant heating surface.

G' = ratio of air/fuel

Q_F = heat liberated by fuel, BTU/hr

Wilson et al (43) presented an empirical correlation of the form

$$Q/Q_F = \frac{1}{1+(G'/4200)/ Q_F/\alpha \, Acp} \qquad \text{................(1.42)}$$

Equation (1.45) is only useful for box type furnaces fired with oil or refinery gas when fluxes lie between 5000 and 30,000 BTU/hr per ft^2 of circumferential tube surface.

Also air to fuel ratio must be between 5-80% and the tube surface must be 400^oF lower than the radiant section exit gas temperature. Mean beam length should be at least 15ft.

Wohlen Berg et al (44) developed a complex method for evaluating the heat absorption in boiler furnaces. It is of no use for oil or gas fired furnaces. It appears from reviewing the radiative heat transfer correlations presented by other workers that they are all highly influenced by Hottel's work, and the simplifications and assumptions are still the designer's responsibility, since each design casediffers greatly from the other.

Lihou (45) presented a review of furnace design methods, and the suitability of these methods for various industrial furnaces is discussed. He concluded that the method to choose depends on the temperature and velocity distribution of the furnace gas and on the precision with which heat flux distribution to the sink needs to be predicted.

Methods Discussed were

1) The long furnace model with combustion at

one end, plug flow, with transverse mixing and no axial radiation,

2) the stirred furnace model with complete or incomplete mixing of combustion products,

3) the zoned furnace model having isothermal gas and surface zones and where heat transfer is by bulk flow, radiation, convection and conduction between zones,

4) the flux method which considers radiative flux through gases as beams of photons which are absorbed and scattered according to the laws of astrophysics,

5) the Monte Carlo method which calculates radiative exchange between zones by tracing "parcels" of radiation moving along random paths.

1.3 Mean Temperature Difference

The rate of heat flow between two fluids in a heat exchanger has customarily been expressed as being equal to the product of the area of the exchanger, the temperature difference between the fluids averaged with respect to the length or area of the exchanger, and a coefficient of heat transfer, where the coefficient of heat transfer can be assumed constant throughout the apparatus. It has been proved in the early stages of the heat exchanger design, that the logarithmic mean of the temperature differances between the hot and cold fluids at the ends of the heat exchanger is the most reasonable average to use. For fluids, experimental data later showed that the heat transfer coefficient varies with temperature and thus with length of the exchanger, so the logarithmic mean of the temperature difference is not the correct average value.

Colburn et al (46) reported that to make a correct design for such a case, it is necessary to apply a graphical solution using values of temperature difference and coefficient of heat transfer occuring at small temperature intervals along the apparatus. This point is of interest to the present work.

Bowman et al (47) derived equations, from which a correction factor (FT), to correct the mean temperature difference in cross flow arrangements, could be determined. Charts were also provided for each case concerning the process conditions such as degree of fluid mixing. The following equations were adopted:

$$K = \frac{T_1 - T_2}{T_1 - t_1}$$

$$S = \frac{t_2 - t_1}{T_1 - t_1}$$

$$(r) = \frac{\Delta t}{T_1 - t_1}$$

$$R = \frac{K}{S} = \frac{T_1 - T_2}{t_2 - t_1}$$

(r) may be expressed as an implicit function:-

$$(r) = \frac{S}{\ln 1/1 - \frac{S}{K} \ln(\frac{1}{1-K})} \quad \ldots\ldots\ldots\ldots\ldots\ldots (1.43)$$

equation(1.43)was adopted for the present process conditions (fluids mixed in the shell, unmixed in the tubes).

$$\text{and} \qquad FT = \frac{(r)}{(r)\ \text{counter flow}} \qquad \text{.........(1.44)}$$

where

$$(r)\ \text{counter flow} = \frac{LM\Delta T}{T_1 - t_1}$$

$$= \frac{(T_1-t_2) - (T_2-t_1)}{(T_1-t_1)\ \ln \dfrac{T_1-t_2}{T_2-t_1}} \qquad \text{......(1.45)}$$

equation(1.45)was derived by both Bowman (47) and Kern (9)

Kern (9) made an algebraic error when expressing $(r)_{\text{counter flow}}$ in terms of the temperature groups K and S thus:-

$$(r)_{\text{counter flow}} = \frac{(K-S)/S}{\ln(\frac{1-S}{1-K})} \qquad \text{...........(1.46)}$$

when this incorrect equation(1.46)was used to find (FT) it always gave a very low result. Substituting for K and S in terms of T_1, T_2, t_1 and t_2 in equation (1.46) would lead to the following:-

$$(r)_{\text{counter flow}} = \frac{(T_1-t_2)-(T_2-t_1)}{(t_2-t_1)\ \ln \dfrac{T_1-t_2}{T_2-t_1}}$$

which results in values of FT very different from the charts reproduced in Kern (9)

For example taking the following data to compare both situations with the charts, in Kern (9) and Bowman et al (47)

$$T_1 = 256^{\circ}C \qquad T_2 = 87^{\circ}C$$

$$t_1 = 27^{\circ}C \qquad t_2 = 80^{\circ}C$$

$$K = \frac{256-87}{256-27} \qquad S = \frac{80-27}{256-27}$$

Using equation (1.43)

$$(r) = \frac{0.23}{\ln 1/(1 - \frac{0.23}{0.3} \times \ln \frac{1}{1 - 0.3}} = 0.72$$

and using equation (1.46)

$$(r)_{\text{counter flow}} = \frac{(0.3 - 0.23)/0.23}{\ln \frac{1 - 0.23}{1 - 0.3}} = 3.2$$

$$\therefore \quad FT = \frac{(r)}{(r)_{\text{counter flow}}} = \frac{0.7}{3.2} = 0.21$$

Using the charts, FT = 0.98

The correct correlation of $(r)_{\text{counter flow}}$ should be shown:-

$(r)_{\text{counter flow}} = \dfrac{LM\Delta T}{T_1 - t_1}$ which comes from

$$(r)_{\text{counter flow}} = \frac{K-S}{\text{lm}\,\frac{1-S}{1-K}} \quad \text{.............(1.47)}$$

when using equation (1.47)

$$(r)_{\text{counter flow}} = \frac{0.3 - 0.23}{\text{lm}\,\frac{1 - 0.23}{1 - 0.3}}$$

$$= 0.73$$

and $$FT = \frac{r}{(r)_{\text{counter flow}}}$$

$\therefore$ $$FT = \frac{0.72}{0.73}$$

$$= 0.98$$

where

FT = correction factor of mean temperature difference for cross flow arrangement

which compares well with the chart value.

Stevens et al (48) presented mean temperature difference for one, two, three passes with counter current and cocurrent flow.

Their theory was based on effectiveness E, thermal capacity ratio z, and number of transfer units NTU.

where

$$E_A = \frac{\Delta t_A}{t_1 - T_1}, \quad E_B = \frac{\Delta T_B}{t_1 - T_1}$$

$$Z_A = \frac{(Mcp)A}{(Mcp)B} \quad \ldots\ldots\ldots\ldots\ldots\ldots\ldots\ldots (1.48)$$

$$Z_B = (mcp)_B/(mcp)_A \quad \ldots\ldots\ldots\ldots\ldots\ldots\ldots\ldots (1.49)$$

$$NTU_A = UA/(mcp)_A \quad \ldots\ldots\ldots\ldots\ldots\ldots\ldots\ldots (1.50)$$

$$NTU_B = UA/(mcp)_B \quad \ldots\ldots\ldots\ldots\ldots\ldots\ldots\ldots (1.51)$$

charts were also presented for various cases of crossflow concerning mixing situations.

Although this work has been based on Bowman and Nagel (47), it is more comprehensive and the correlations handle more complicated cases, such as multi-pass crossflow.

Ratzel et al (49) proposed a method of determining the mean temperature difference for air-cooled crossflow heat exchangers, when the outlet temperature of the fluid is not known.

An explicit and approximate equation, together with empirical coefficients, were presented for the fast calculation of the mean temperature difference of eight cross flow arrangements. It is calculated from the effectiveness of the process stream and the number of transfer units on the air side.

The following equation was found to be suitable for any computerised work:

$$r = r_1 + \sum_{i=I}^{m} \sum_{K=I}^{n} bi,K.\ P_i \left(\frac{S}{S+1}\right)^K \ldots (1.52)$$

where

r = dimensionless mean temperature difference.

r_1 = dimensionless mean temperature difference for one row

m and n = maximum value of i and K, respectively

bi,K = coefficients for the number of rows and passes

P_i = effectiveness of stream

S = number of transfer units on air side

The correction factor F_T is calculated from the following:

$$F_T = 1 - \sum_{i=1}^{m} \sum_{K=1}^{n} a_i\ K\ (1-r_{i.m})^K \sin(2.i.\text{arc tan } \frac{p}{q}) \ldots (1.53)$$

1.4 Operational Effects

Where it is desired to obtain an individual heat transfer coefficient between a fluid and a surface by direct measurement, the problem of determining the true temperature of the solid surface arises.

When the temperature difference between wall and fluid is small, an error of a given number of degrees in measuring the tube wall will introduce a large percentage error in the temperature difference, as the temperature difference increase the effect will be less serious.

Rohenow and Hunsaker (50) reported that when a hot gas is flowing in a duct, then the walls of the duct are at a lower temperature than that of the gas. They presented charts for correcting the measured temperatures by the following situations:

1) exposed thermocouples
2) enclosed thermocouples
3) protected thermocouples.

They also made an allowance for the case where radiation could have an effect. This was mainly for a very high temperature technique, where radiation has a large effect.

McAdams (16) reported methods of installing thermocouples in walls.

1. A groove is cut in that part of the outer surface later to be located in a substantially isothermal zone, the bare junction is placed in direct contact with the metal wall of the tube, the electrically insulated leads are installed in the grove so that at least one inch of each lead is in the groove, and the groove is filled with

suitable material. If surface conditions are important as in boiling or condensing, it is advisable to plate the assembly with a suitable coating of metal.

2. The function is threaded through a chordal hole, each lead is submerged in a circumferential groove for at least one inch, and the groove is filled with suitable material.

This method does not disturb the surface of the metal near the junction. A modification of this method involves placing the junction in the hole drilled at an angle to the axis of the tube.

Concerning methods 1 and 2. These are not practical on a thin walled tube like the one in use for the present research.

CHAPTER TWO

Experimental equipment and modifications

2.1 Experimental equipment before modification

The experimental rig was a Nu-Way Eclipse, air to air cross-flow, gas-fired heat exchanger, with staggered tube arrangement. The over-all dimensions were 13ft x 8ft x 6ft, (4m,2.4m,1.8m). Heat was supplied by two Eclipse 126TA burners fired by natural gas, with an overall design heat duty of 10^6 Btu/hr,(290 Kw). See figure (2.1)

Primary and secondary air was fed to the burners by a Breeza fan, equipped with a 12 inch, (30cm)suction duct. The flow diagram of the rig is shown in figure (2.2)

The primary air flow was controlled by a butterfly flow control valve on each burner. The secondary air flow was controlled by a damper fitted in the fan discharge duct.

The furnace chamber was 14 inch (36cm), high and 34 inch, (86cm) wide over the 42 inch, (107cm) long tube-bundle of the heat exchanger.

The heat exchanger consisted of a tube bundle of sixty nominal one inch, (2.54cm) diameter, schedule 5A/S/321 stainless steel tubes on a 1.5 inch, (3.8cm) triangular pitch as shown in fig (2.3a)and (2.3b).

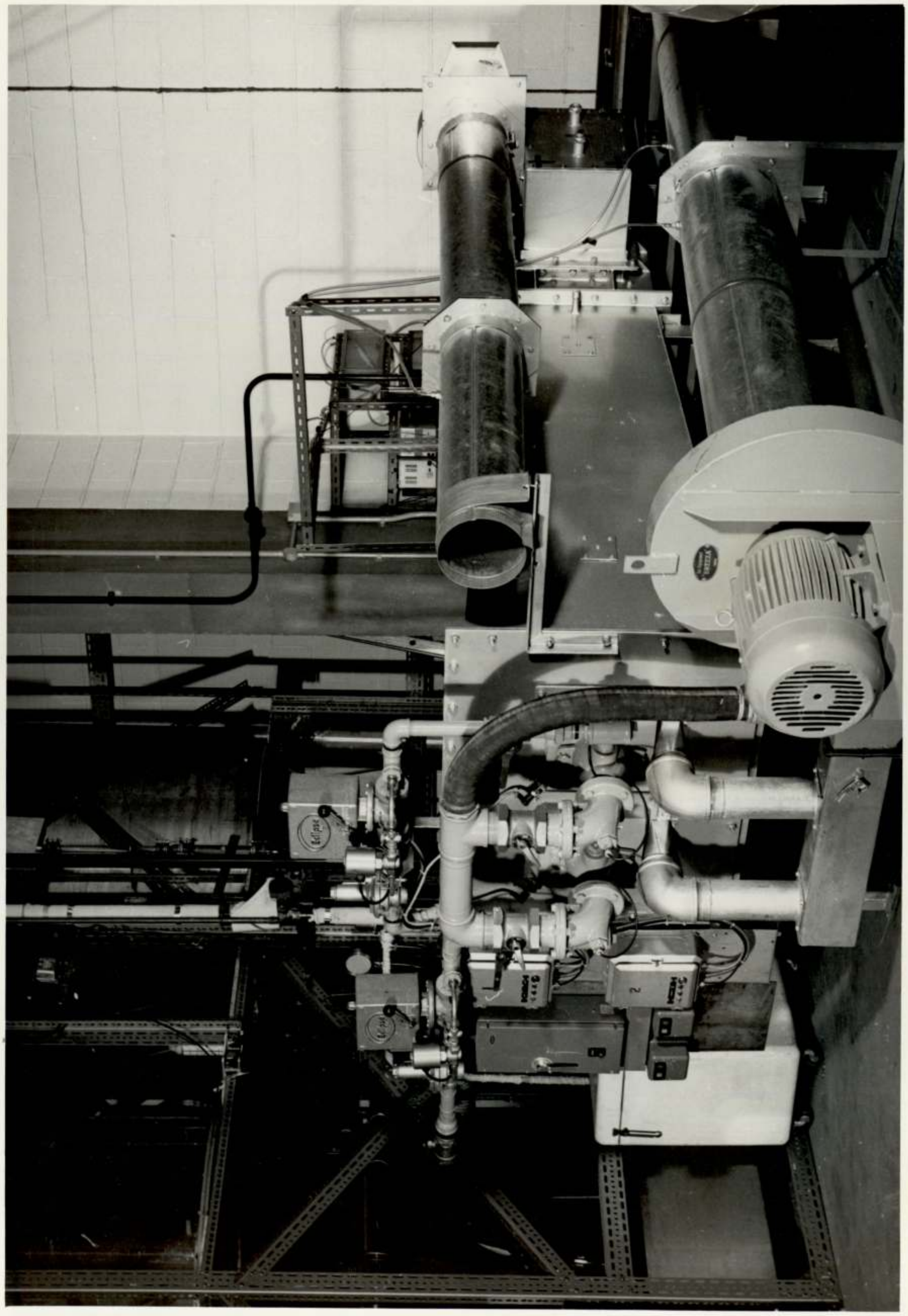

Figure (2.1) The Experimental Rig

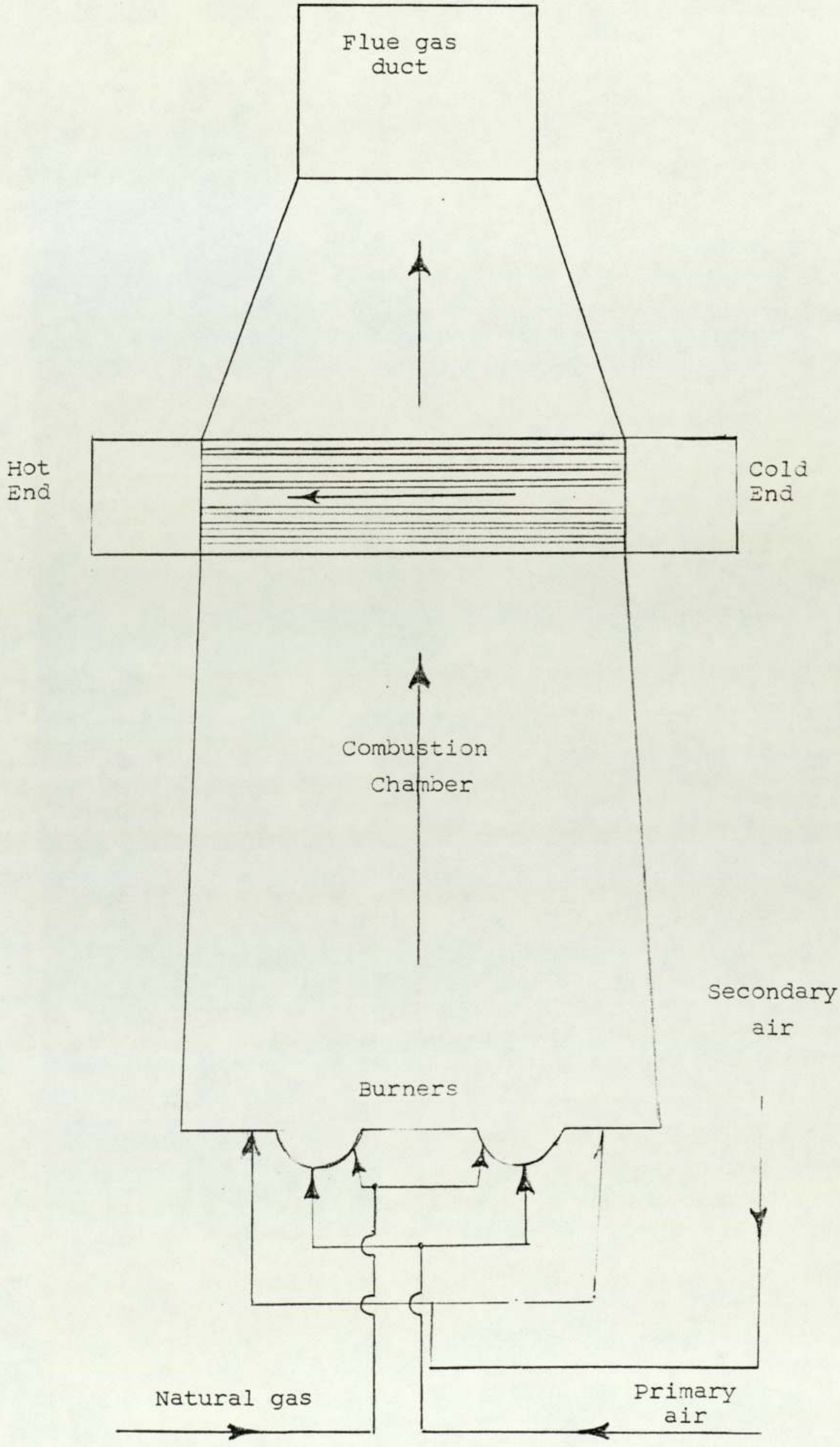

Fig (2.2) Experimental rig flow diagram

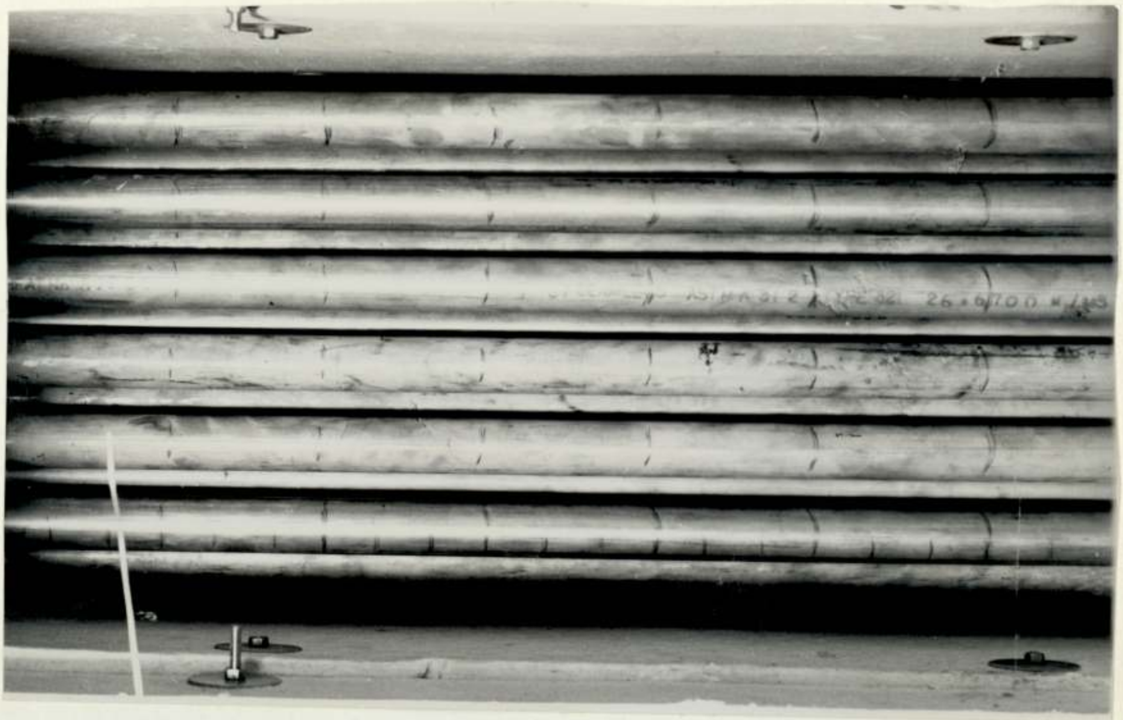

Fig. (2.3a) Front View of the Bundle

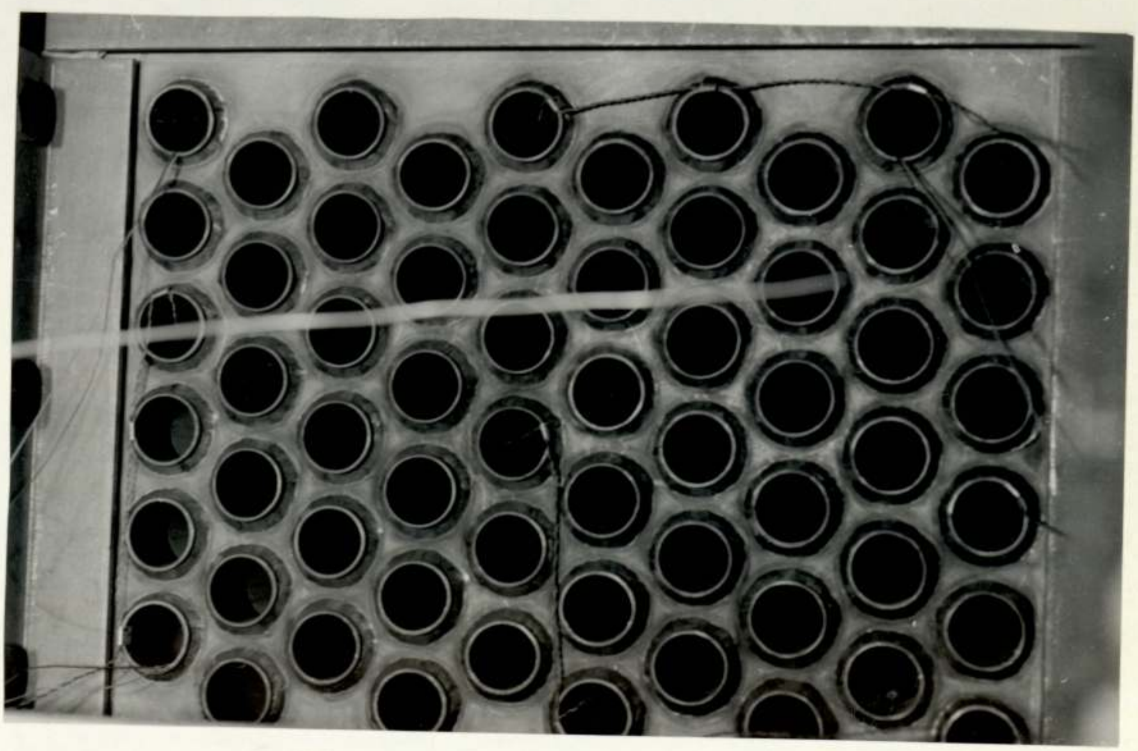

Fig. (2.3b) End View of the Bundle

The tubes were designed to be heated by the products of combustion diluted by secondary air.

A small fan equipped with a 9 inch, (22.9cm) suction duct supplied fresh air to the tubes of the heat exchanger chest of 500 ft^3/min, ($14.2m^3/min$), at a temperature of 500^oF, ($260\ ^oC$) with the inlet air at ambient temperature.

A damper on the fan suction duct was fitted to enable the fresh air flowrate to be controlled.

The cooled products of combustion leaving the shell side of the heat exchanger passed through a short tapered duct before leaving through the exit stack. A dilution air fan was installed at the base of the stack to cool the flue gases. Design conditions at the exhaust outlet were, a flow rate of 1000 ft^3/min, ($28.4m^3/min$) at a temperature of 630^oF, (332.2^oC).

Since heat transfer depends mainly on flow rate and temperature difference, flowrate measurement instruments such as orifice plates, and manometers, were fitted to the rig where appropriate. Many thermo couples were installed for gas and surface temperature measurements.

HOT END

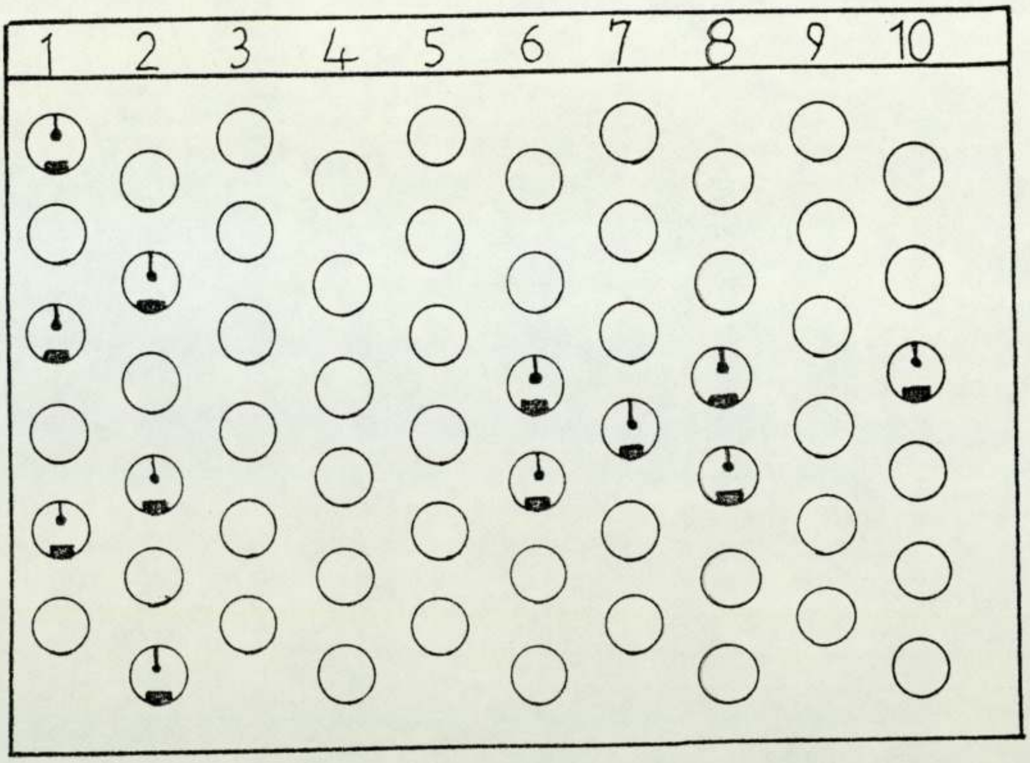

KEY

■ wall thermocouples

⬇ air thermocouples

COLD END

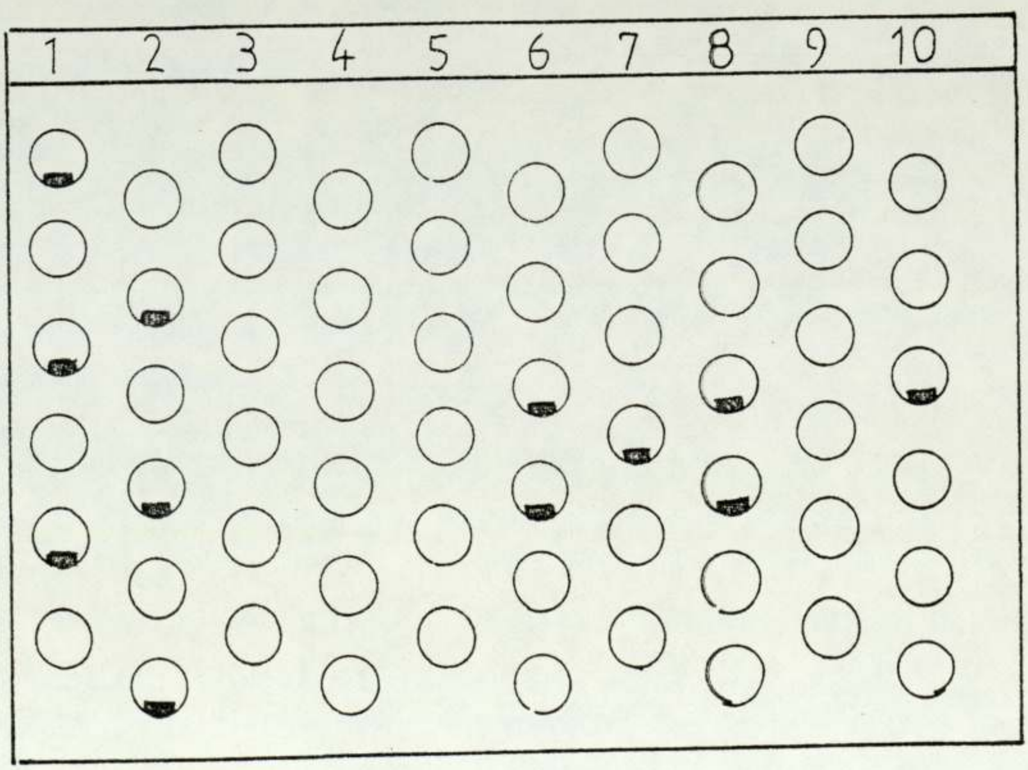

FIG. (2.4) Thermocouple positions in tubes in the bundle

2.2 Modified experimental equipment

It was decided that the first and second rows of tubes, in the front of the bundle, facing the burners, would constitute a "wall" that receives the radiation emitted by the combustion gases and the refractory walls, since the tubes are in a staggered arrangement.

To find the effect of radiation on the heat transfer coefficient, twelve tubes were chosen for sampling the performance of the heat exchanger as shown below:-

i) Three tubes on the first row

1:1 1:3 1:5

ii) Three tubes on the second row

2:2 2:4 2:6

iii) Six tubes in the middle and back rows

6:3 6:4 7:4 8:3 8:4 10:3

See figure (2.4)

The chosen twelve tubes were fitted with high temperature thermo couples(Ni-Cr/Ni-Al, with fibre glass sleeving) for measuring the following temperatures:-

i) inlet tube wall

ii) inlet air

iii) outlet tube wall

iv) outlet air

To measure the refractory wall temperatures so that the amount of radiation emitted could be calculated, and since the walls are heated by the combustion gases two probe thermo couples, (Ni-Cr/Ni-Al, type K/M1530L,range 1000^{o}C) were fitted in different positions on each wall, so that an average temperature could be taken.

The probe thermo-couples were fitted to the centre of the following walls:

i) left side refractory wall
ii) right side refractory wall
iii) top refractory wall
iv) bottom refractory wall

Although the combustion gases inside the chamber were assumed to be well mixed, it was decided to design and make a probe 0.25 inch,(6mm) diameter, with a thermo-couple fitted inside it, so that temperature scanning could be carried out at several spots inside the combustion chamber, and an average temperature could be taken that would represent the bulk of gases inside the combustion chamber. The probe was 4ft, (1.2m) long so that spots at the bottom and corners of the combustion chamber could be reached.

It was also desirable to measure the temperature of air surrounding the tubes individually, so that heat transfer rates between hot air on the shell side and the tube, could be calculated as temperatures vary across the bundle. A probe of 1/8 inch, (3mm), diameter and 3ft, (0.9m) long was made and a thermo couple, (Ni-Cr, K/M1530L.), (51), was fitted inside it to measure temperatures at several spots around the tubes and between the rows of tubes. This temperature scanning, would also enable the temperature profile in the shell to be understood.

It was desirable to investigate the temperature profile inside specific tubes in the bundle under various process conditions such as, various secondary air and fresh air flow rates, alternative burners in operation, and different natural gas flowrates, so that the effect of these conditions on the temperature profile inside specific tubes would be understood. A probe to measure the tube wall and the flowing air temperature was designed, with dimensions, 5.5ft, (1.56m) long and 0.25 inch(6mm), diameter, with springs on each side of the measuring end to ensure reasonable contact with the tube inside wall, see figure (2.5). Several points along the inside walls of the tubes, were measured, also temperature scanning at four radial positions along the tubes could be carried out using this technique.

Three long pitot tubes were neededfor flow scanning inside the combustion chamber. The main aim of using these pitot tubes was to check the uniformity of flow pattern inside the combustion chamber. They were designed according to B.S 1042 ,and calibrated against a standard pitot tube

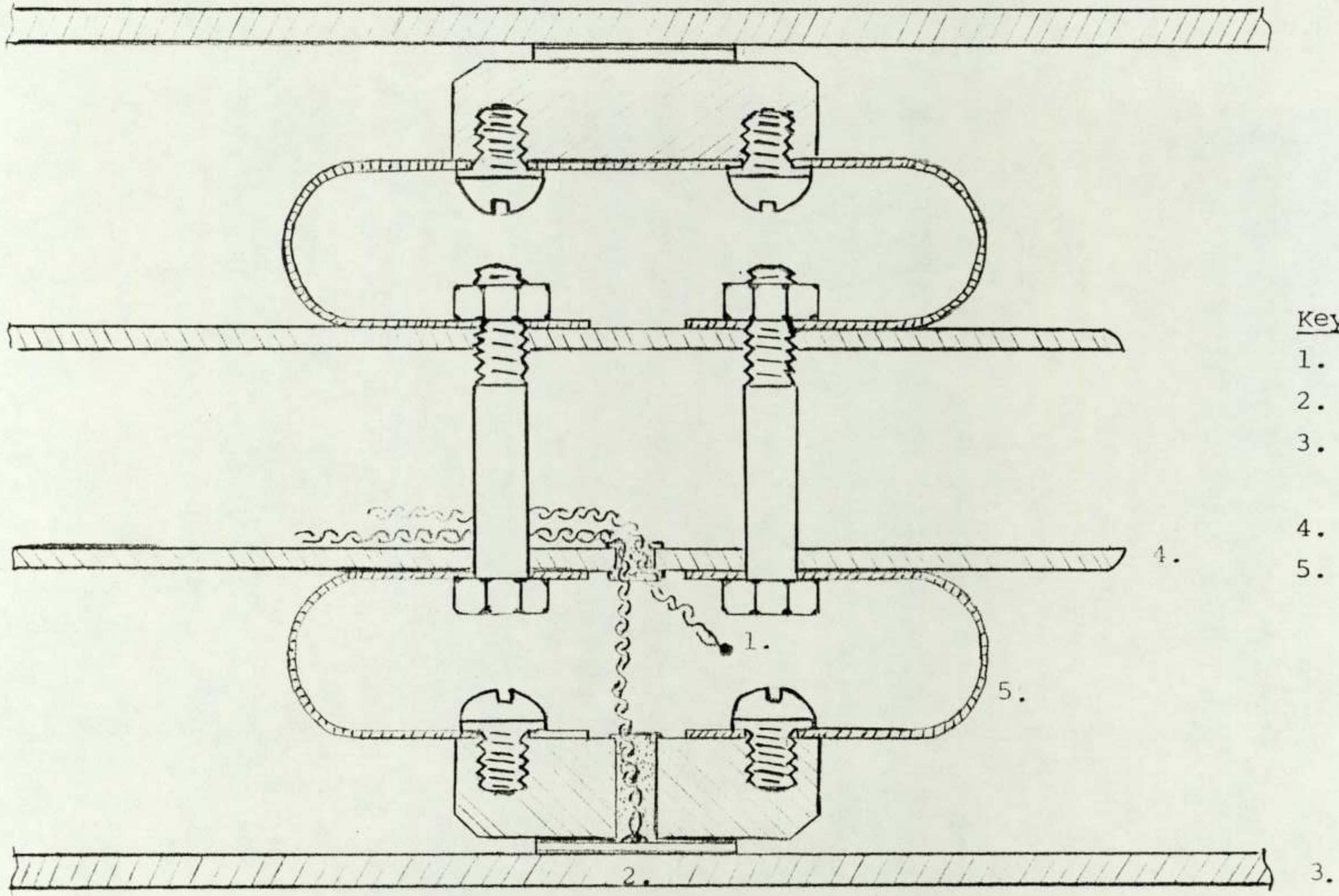

Key

1. Air thermocouples
2. Wall thermocouples
3. Heat Exchanger
   tube wall
4. Probe wall
5. Phosphor Bronze
   Spring

Fig. (2.5) Wall air temperature probe for inside Heat Exchanger tubes.

(52),. They were 0.25 inch,(6mm) diameter and 3ft,(0.9m) long.

During test operations, it was observed that the primary air for both burners and the secondary air for cooling the hot gases in the combustion chamber were both supplied by the same air fan, making it very difficult to control and measure each burner flow. The primary air flow was separated and an air fan with a 3 inch,(7.6cm) internal diameter suction pipe was fitted to supply primary air for the burners. An orifice plate was designed according to B.S 1042, calibrated against a standard pitot tube and was fitted to measure the primary air flow to both burners.

After the above arrangements were made, it was found that measurement and control of each individual flow of secondary and primary air was easy.

The primary air on each burner was controlled using a "butterfly" flow control valve, fitted on each individual burner air supply duct. The orifice on the main primary air duct, was used to measure the total amount of air flowing to both burners. The amount of stoichiometric air needed was fixed for all of the experiments, as the upper limit was taken, therefore, there were no primary air flowrate variations.

During test operation, it was observed that burner number 2, was not igniting easily. After some search for the reason, it was found that it was starved of primary air due to the feed duct arrangements. The flow rate of air was measured on each inlet duct, just infront of the burners and it was found that the air was not evenly distributed as burner number"1",received most of the air while burner number "2"was receiving almost nothing. The arrangement of the inlet ducts, as shown in figure (2.6a) was such that the air passed straight to burner number 1, without sufficient air being diverted into the first inlet duct.

The inlet ducts were re-designed, so that the air flow was distributed evenly between the two inlet ducts see figure (2.6b). This was checked by pressure scanning across the inlet ducts, and the volumetric air flow rates were calculated and compared with each other. A standard pitot tube was used for this purpose, (52).

Pressure taps were fitted to both inlet ducts and connected to manometers permanently, so that an equal amount of air flow to each burner was ensured.

Since these modifications were made, burner number "2"has operated normally.

To enable the combustion chamber to be pressure scanned during operation, access had to be made for the

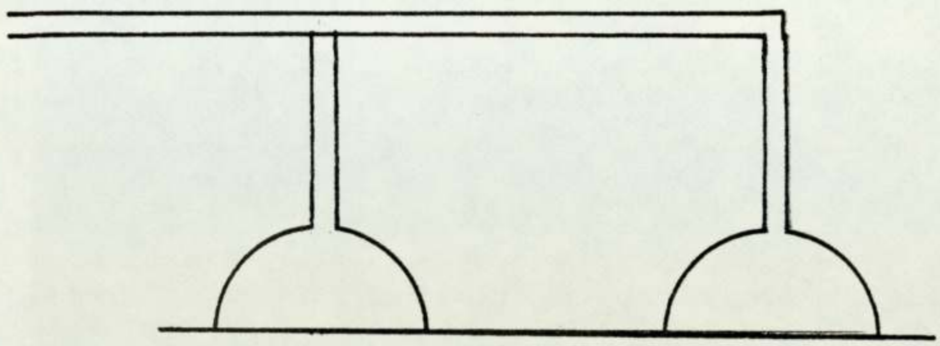

Fig. (2.6a) Old primary air inlet duct arrangement.

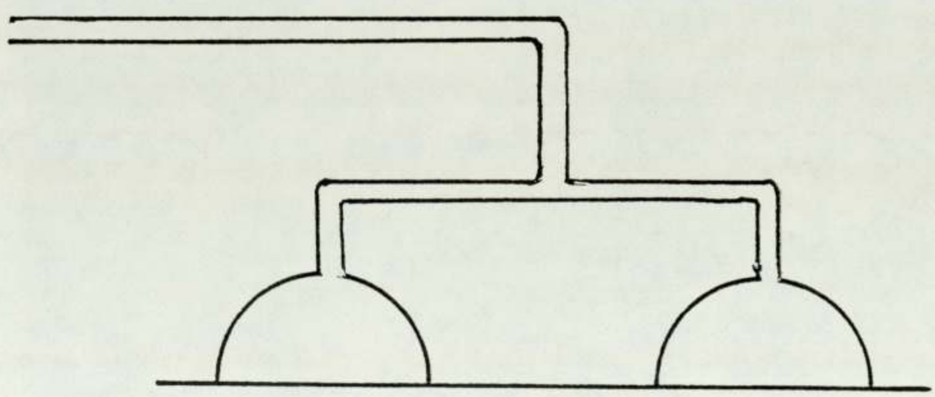

Fig(2.6b) Modified primary air inlet duct arrangement pitot tubes, so several holes were drilled on the top and sides of the chamber.

During the scanning, it was found that the right hand secondary inlet duct was recieving much less air than the left hand one, so the flow of air into the inlet duct was measured using a standard pitot tube and mal-distribution was confirmed. Also during hot operation the entrance side (cold end), appeared to be hotter than the exit end (hot end), also the right hand side wall was much hotter than the left hand side wall, as there was not enough secondary air to cool the right hand side wall. Spot pressure scanning inside the chamber showed the irregularity of the air flow pattern inside the combustion chamber see table (2.1).

Several attempts were made to improve the flow profile inside the combustion chamber. As the secondary air ducts were arranged in such a way, that the air passed straight to the second and far inlet and little air was recieved by the first inlet of the chamber, as shown in figure (2.7a).

The ducts were modified, as shown in figure (2.7b) in such a way that the secondary air was evenly flowing into both ducts which lead to the combustion chamber.

Although pressures on the inlet ducts of the

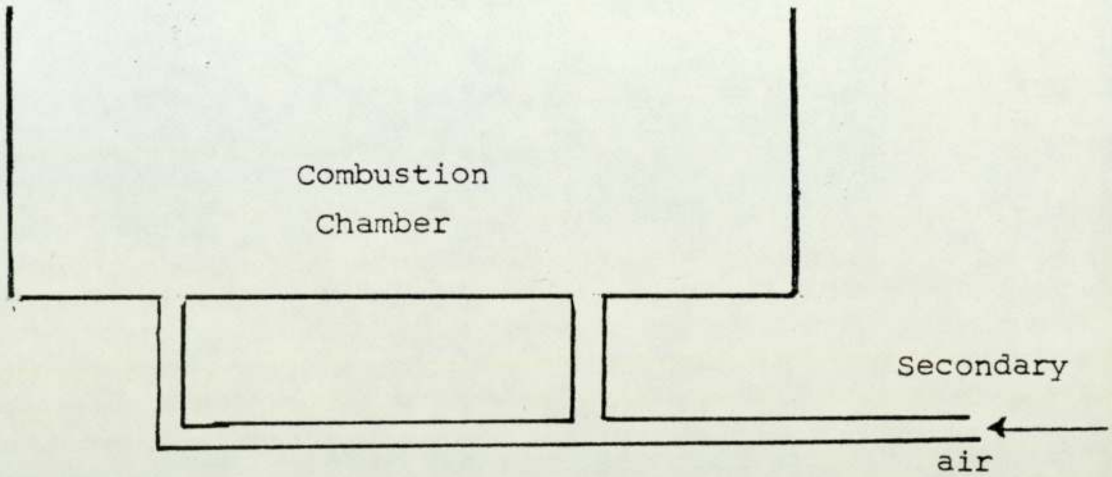

Fig.(2.7a) Old secondary air inlet ducts arrangement

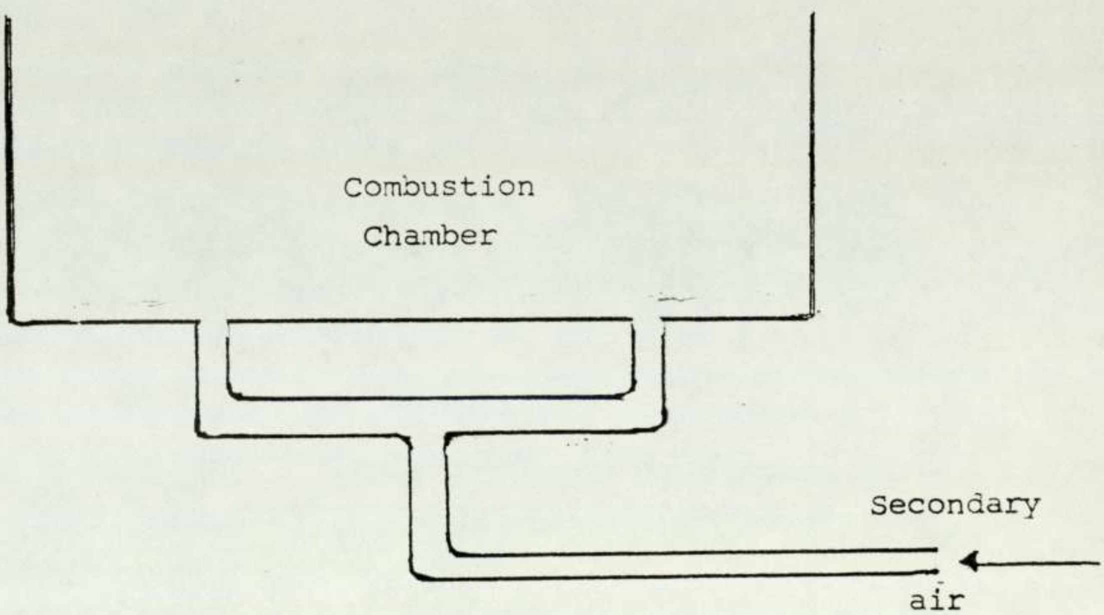

Fig. (2.7b) Modified secondary air inlet ducts arrangement.

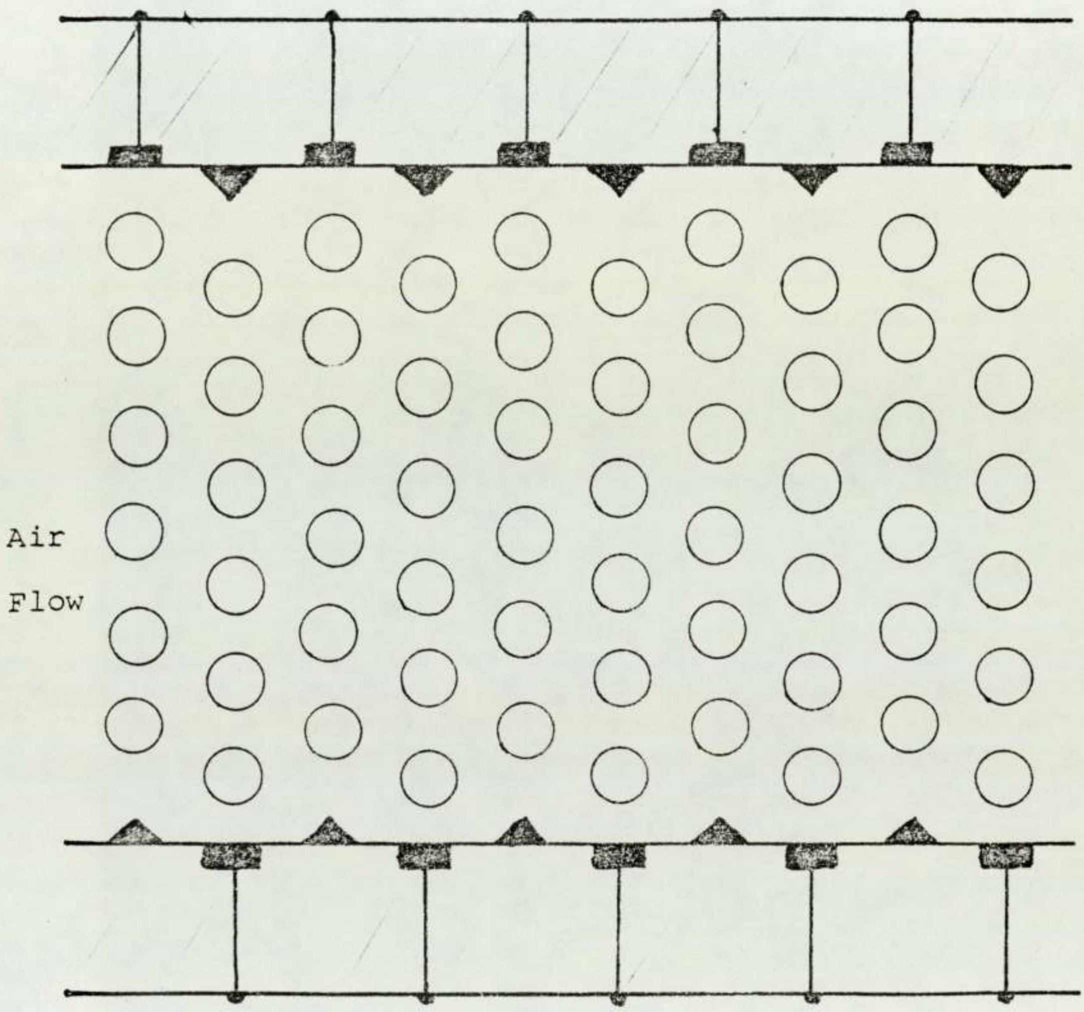

Key

▲ half tube dummy

Fig.(2.8) End view of tube bank with dummy
half tube effect.

secondary air were measured and found to be the same, some high pressure spots, were observed during pressure scanning across the combustion chamber. See table (2.2)

Perforated plates were fitted between the ducts and the inlet holes of the combustion chamber, to improve the flow profile inside the chamber in both dimensions, vertical and horizontal. Although this method was useful in improving the pressure profile, which evens the flow inside the chamber, it is not economically advisable. Since it cut the air flow considerably.

Since the number of thermo-couples used for this work was higher than the available multi-way thermometer selector could handle, a similar one was installed on the rig, and connected to the electronic thermometer. Each selector's capacity was twenty thermo-couples. All wires were connected to the thermo-couples and to the selector, and labeled, showing the position of the thermo-couples on the tubes, and the connection points on the selector. see table (2.3).

During the experimental programme, it was decided to use a non-radiating fluid pumped across the bundle, so that no radiative heat transfer was taking place. A steam heat exchanger was therefore fitted to the rig to provide hot air to the combustion chamber with the two burners switched off. This experimental work was left to be carried out near the end of the experimental programme, since fitting the proposed heat exchanger in the secondary air duct would reduce the flow.

Earlier experiments had shown that some by-passing of the tubes was taking place around the heat exchanger sides so it was decided to enhance the fluid mixing inside the shell and make the exchanger more representative of a large unit, that baffles had to be fitted to each side of the bundle top and bottom. Half cylindrical shapes would have been ideal, but they were difficult to obtain, so triangular baffles were used instead, as shown in figure (2.8).

One way of investigating the degree of turbulence would be to compare practical pressure drops across individual tubes with those predicted from a standard correlation based on Reynolds number. A pressure probe designed to be similar to the static tapping of a pitot tube (to avoid velocity head effect) was made to measure static air pressure along the length of the tubes.

Table (2.1) Hot Pressure Profile inside the chamber before rearrangement.

			Positions from both side walls					
Secondary air volumetric flowrate	Pitot direction		4"	8"	16"	16"	8"	4"
32,850 ft^3/hr	Burners	Pitot tube readings (inchs water)	0.01	0.01	0.09	0.02	0.02	-0.02
	Downwards		-0.01	-0.01	-0.02	0.09	-0.01	-0.01
	Bundle		0.0	0.0	0.0	0.04	0.0	0.0
	Upwards		0.0	0.0	-0.03	0.04	0.01	-0.01
72,260 ft^3/hr	Burner		0.01	0.02	0.09	0.02	-0.01	-0.02
	Downwards		-0.01	-0.01	-0.02	-0.01	-0.01	0.01
	Bundle		0.0	0.02	0.06	0.01	-0.02	-0.05
	Upwards		0.0	-0.01	0.01	-0.02	0.02	-0.01

Table(2.2) Hot Pressure Profile inside the chamber
After rearrangement

			Position from both side walls					
Secondary air volumetric flowrate	Pitot direction		4"	8"	16"	16"	8"	4"
32,850 ft^3/hr	Burners	Pitot tube readings (inchs water)	0.02	0.02	0.06	0.05	0.04	0.03
	Downwards		-0.01	-0.01	-0.02	-0.02	-0.01	-0.01
	Bundle		0.0	0.0	0.0	0.04	0.01	0.01
	Upwards		0.0	0.0	0.02	0.04	0.01	0.01
72,260 ft^3/hr	Burner		0.03	0.03	0.07	0.07	0.04	0.04
	Downwards		-0.01	-0.01	-0.01	-0.02	-0.02	-0.01
	Bundle		0.0	0.0	0.01	0.01	0.01	0.01
	Upwards		0.0	0.0	0.03	0.02	0.01	0.01

Table 2.3 Thermocouple positions on tubes and Electronic thermometer

TUBE	POSITION	ELECTRONIC THERMOMETER	
		HOT	COLD
1	1:1W	2B	18B
	1:1A	3B	17C
2	1:3W	5B	19B
	1:3A	4B	17C
3	1:5W	7B	15C
	1:5A	6B	17C
4	2:2W	8B	2A
	2:2A	9B	17C
5	2:4W	14A	3A
	2:4A	19A	17C
6	2:6W	16A	13C
	2:6A	15A	17C
7	6:3W	11A	15B
	6:3A	18A	17C
8	6:4W	9C	16B
	6:4A	6C	17C
9	7:4W	4C	12C
	7:4A	3C	17C
10	8:3W	7C	11C
	8:3A	5C	17C
11	8:4W	12A	13B
	8:4A	10C	17C
12	10:3W	8C	17B
	10:3A	13A	17C

20B	Bottom Wall	2C	Top Wall
19C	Left Front	17A	Back Left
1C	Right Front	20C	Right Back
9A	Probe 1	14B	Probe 2

Key

W = wall A = air

CHAPTER THREE

3. Experimental Procedure

The first step was to plan a primary experimental programme and modify the experimental rig and prepare it according to the designated experimental programme requirements. This involved redesigning the secondary and primary air ducts, so that the air flow was uniform in the shell, also some work had been done on the thermal and flow measuring instrumentation .

The measurement instruments were a very important factor in this research, so a great amount of attention was paid to this particular area principally to minimise errors in the thermal and air flow measurements

3.1 Instrumentation and Precision

Thermal instrumentation

All thermocouples, such as ones on the tube walls of both inlet and outlet, as well as air thermocouples were all checked before and after every operation, making sure they are in position, if they were not they would still give a reading but, of course, they would give wrong readings, therefore, it was necessary to keep them in good order.

Thermo-couples on the combustion chamber walls were always checked to make sure they were situated just near the inner side of the wall of the combustion chamber. Before any operation all thermo-couples had to read near to the ambient air temperature in the pilot plant, as this indicates that they are in good order, then it was made sure they were all in position. Some thermo-couples were damaged during the operation. They were replaced by new ones and the experiment involved was repeated.

The first set of thermo-couples used for this work proved difficult to ensure contact with the tube wall when in use so all of them were taken out and replaced by the present set of thermo couples, and all results obtained using the first set of thermo couples were ignored, as it was thought the errors involved, could be high.

As thermal radiation was suspected to exist in the combustion chamber, the thermo couples used to temperature scan inside it to obtain an average gas temperature,were shielded by inserting them inside a steel tube to avoid errors due to radiation. A similar procedure was used for temperature scanning in the bundle and between the tube rows. Three temperature readings for each tube row were taken, so that a reasonable average of the gas temperature around the tube would be obtained. The thermo couples fitted in the probe were always checked and especially the one for the combustion temperature scanning was checked and replaced very often for the reason that the temperature of the hot gas was very high.

When reading temperatures from the electronic thermometer, there was some approximation made, as divisions on the electronic thermometer were of 1 degree C , so $\pm$ 0.5 C^{o} error may be expected to take place, especially when small fluctuations were taking place.

As air physical properties, such as density, viscosity, thermal conductivity and specific heat capacity were functions of temperature, an averaged temperature would be desirable for calculating the air and flue gas physical properties, for all the regions such as the combustion chamber, over the bundle, and across the tubes length.

A few runs were made first to assess the reliability of the instruments, and also the time needed for the experimental rig to reach steady state was determined. Temperature variations were recorded ,in several positions, against time and it was found to be two hours approximatly from the start up.

The time needed for the experimental rig to reach steady state after adjusting the fresh air flow rate through the tube bundle, using the same approach as above, was found to be around 40 minutes.

3.2 Air flow measurements

Since the air flow profile in the original combustion chamber design was not uniform, experimental work could not proceed until this problem was solved. A standard pitot tube was used to investigate the flow possible in several positions in the combustion chamber. Four directions of scanning were adopted, namely, forwards burner, bundle, upward adn downward. Using this technique, the redesigning the inlet flow ducts, it was found possible to maintain a reasonably uniform flow profile in the combustion chamber and in the shell.

Three pitot tubes were permenantly fitted in the combustion chamber to check the flow under different operating conditions, such as gas temperature and flow-rate variations.

To analyse the general performance of the heat exchanger, knowledge of individual tube air flow would be needed for calculation of Reynolds number and heat transfer coefficient. Therefore, a standard pitot tube was used to measure the air flow in each individual tube in the bundle, for the following overall fresh air volumetric flowrates:-

49,900 ft^3/hr 44,700 ft^3/hr 38,700 ft^3/hr 31,600 ft^3/hr
22,350 ft^3/hr

so that a range of Reynolds number would be obtained (see tables 3.1 to 3.5)

It was decided to make three sets of measurements for each overall air flow rate and take an average. The reason for doing this averaging was because of the possibility of "Yaw", which may take place while positioning the pitot tube in the centre of the tube exit.

Another check made on the measurements taken, was to compare the overall volumetric flowrate measured by an orifice plate with the total tube volumetric flowrate. This proved to be acceptable match.

This velocity of the fresh air through the tube was calculated by the following equation. (52).

$$V = 4000 \sqrt{\frac{30}{B} \times \frac{T}{528} \times hp} \quad \ldots\ldots\ldots\ldots (3.1)$$

where

v	=	air velocity	ft/min
B	=	barometric pressure	inch Hg
T	=	temperature of fluids	R^{o}
hp	=	pressure drop	inch, water gauge

Positioning the pitot tube in the centre of the tube and against the stream of fluids, would only read the maximum velocity. To obtain the average velocity a factor of 0·8 must be used (53) as shown below:-

$$V(\text{average}) = V(\text{measured}) \times 0.8 \quad \ldots\ldots\ldots\ldots (3.2)$$

Measuring the secondary air flow rate using a standard orifice plate would involve less errors than measuring the individual tubes as the latter was done by the aid of a portable pitot tube where "Yaw" might take place.

After redesigning the inlet flow ducts and improving the flow profile in the combustion chamber, the secondary air flow was reduced and the highest flowrate possible was 76,200 ft^3/hr,(2,157 m^3/hr). Therefore an upper limit was imposed for the secondary air flow, the lower limit would obviously be the lowest flow under which the rig would not over-heat, which was found to be 28,300 ft^3/hr,(801 m^3/hr).

The primary air was also measured by an orifice plate designed and calibrated to B.S 1042. The primary air was kept constant for all the experimental work at 20% excess air above stoichiometric to avoid Co formation.

3.3 Experimental Programme

Since the investigation of radiation effects on heat transfer coefficients was one of the objectives in this work six of the twelve tubes chosen for the experimental work were in the first and second rows.
The twelve tubes chosen were as follows:

1:1	1:3	1:5	2:2	2:4	2:6
6:3	6:4	7:4	8:3	8:4	10:3

The first six tubes on the first and second rows were used for two purposes, firstly, to calculate the amount of radiation falling on them, since they form a wall acting as a radiation sink, secondly, they were used together with the other six as sample tubes for calculating Reynolds numbers and Nusselt numbers, so that a correlation could be based on them to represent the bundle of sixty tubes.

It was noticed after a few runs that the graphs of Reynolds against Nusselt number based on the first six tubes do not correlate very well, due to reasons which will be discussed in detail later. It was, therefore, decided to concentrate on the second set of six tubes in the centre and back of the bundle for developing a convective heat transfer correlation.

It was decided that the first set of experiments which would be carried out by varying the secondary air flow rate with fresh air flowing inside the tubes, and keeping the primary air and the natural gas flow rates constant at 20% excess air and 450 ft^3/hr respectively. see table (3.6). The main objective of doing this set of experiments was to compare the amount of radiation from both refractory walls and radiative gases(Co_2 and H_2o) recieved by the sink which is the front of the bundle for each secondary air flow rate. This would show the effect of the secondary air flow rate on the radiation process. Also a heat transfer correlation of the following form

$$Nu = \alpha Re^{m} Pr^{n} \qquad (3.3)$$

would be obtained, for both tube and shell sides.

One of the objectives of this work was to increase the range of Reynolds numbers, so that the heat transfer correlation would represent a wide range of flow rates. Therefore some of the tubes in the bundle were blocked, using plugs randonly around the sample tubes in the centre and edges of the bundle, so that the fresh air flow rate in the rest of the tubes would be increased. Results obtained, showed that Nu_T - Re_T points of each individual sample tube were very scattered and cannot be correlated. The reason was thought to be, that the plugged tubes became much hotter than the other tubes, with fresh air flowing through them, so this random selection created a non uniform heat profile in the bundle.

Another approach was adopted which was to block tubes well away from the sample tubes especially the front rows, the top and bottom of the bundle, as shown in figure (3.1). This situation should not disturb the heat profile across the bundle. The fresh air flow rates of six sample tubes were measured with the aid of a standard pitot tube and proved to have higher fresh air flowrates than before.

Blocking tubes would create resistance against the air blower, and subsequently lower the overall flow to the bundle.

The same experimental work as in the first set of experiments was repeated for this condition as shown in table(3.7).

Since all experimental work so far was carried out with both burners in operation, it was desirable to have one burner in operation at a time since this procedure s often used in industry, and to compare the effect of this condition with the other previous results, also to see the difference in the general form of the heat transfer coefficients, the constant α, and the ower of Reynolds number, m. This work was carried out for the highest and lowest secondary air flow rates, see table(3.8).

Since air is not a radiative gas, it would be advantageous if hot air were to be pumped across the bundle and then the heat transfer coefficients calculated could be compared with the ones when the burners were in operation i.e. with combustion taking place. After a steam heat exchanger was fitted to the rig, and it was tested, this experimental work was carried out.

The reason for varying the secondary air flow was to understand the effect of this flow rate on the amount of radiation received by the bundle, and the hot air flow rate variation would not have a similar effect as air is not radiative gas. Therefore the highest possible hot air flow rate of 69,300 ft^3/hr,(1,962m^3/hr) was chosen and kept constant for all fresh air flow variations.

The hot air flow rate mentioned above was the highes possible, since the steam heat exchanger fitted in the secondary air stream, reduced the air flow rate. Considering the limitations on the steam temperature available in the department and the steam heat exchanger, a low air flow rate should ensure a reasonbly high temperature of air flowing across the bundle of tubes.

The following measurements were adopted in each run:

i) The refractory wall temperatures.

ii) Tube wall and air temperatures at inlet and outlet.

iii) Temperatures of hot gases between rows and infront and behind the tube bundle.

iv) Temperatures at various positions inside the combustion chamber.

v) Inlet and outlet temperatures of the total air flowing through the bundle.

vi) Secondary and primary air flow rates.

vii) Natural gas flow rate.

viii) Pressures at various positions inside the combustion chamber.

To measure the temperature profile along the tube length, and to evaluate the heat transfer coefficient variations along the tube length under different process conditions, four position wall temperature scans were made for several tubes in the bundle, with the aid of a probe that can measure wall and air temperatures, as explained in Chapter two. Eleven positions were measured along the tubes. This technique was adopted for the following conditions:

i) Both burners in operation.

ii) Hot air flowing across the heat exchanger transversley, burners off.

iii) One burner in operation at a time.

iv) Constant secondary air and fresh air, but varying natural gas flow.

v) Different fresh air flow rates.

Measuring the fresh air temperature along the sample tube was carried out easily, but measuring the wall temperatures at four positions for each interval presented a few practical problems. Firstly, contact between the tube wall and the thermo-couple junction, was not always ensured, especally ~~at~~ the far end of the tubes. This problem was over come by comparing the air temperature, at that interval with that wall temperature obtained, when the latter should be reasonably higher. Secondly, friction between the inside wall of the tube and the probe springs when moving along and rotating around the tube wall caused the thermocouple junction to be eroded. To avoid this problem grease was used to decrease the friction. Development of probes were carried out to obtain the most suitable one for this type of work. Regular maintenance of the probe was necessary during this work.

Finally, pressure scanning through a specific tube was carried out to compare the practical pressure drop with the calculated pressure drop using standard correlations. A static pressure probe was used in this work. The main objective of doing this work was to compare the practical pressure drop with the theoretical one, calculated by using standard correlations.

The data obtained from this work should enable the investigation of the tendency to over-design gas/gas heat exchangers and also to establish an overall heat transfer correlation, for both shell and tube sides.

Table. 3.1 Fresh air flow distribution 49900 ft^3/hr
from front to back rows

1	2	3	4	5	6	7	8	9	10
1164		1005		948		928		1035	
	1011		992		1005		1005		1081
1053		992		928		928		1023	
	1017		992		1005		941		1081
1005		941		980		867		992	
	992		1005		992		992		1035
999		941		948		1005		999	
	967		922		961		1005		901
1070		915		961		915		986	
	961		948		922		922		1076
928		1064		1087		1110		888	
	961		992		928		928		1041

Table. 3.2 Fresh air flow distribution 44700 ft^3/hr from front to back rows

1	2	3	4	5	6	7	8	9	10
1076		999		928		915		1011	
	1017		980		874		961		992
1041		992		999		915		941	
	1005		928		888		874		859
1017		948		992		915		867	
	1017		992		901		915		867
954		922		974		915		852	
	961		999		901		928		859
1005		928		901		859		901	
	888		980		941		915		888
1017		948		961		941		986	
	935		980		915		928		928

Table. 3.3 Fresh air flow distribution 38700 ft^3/hr from front to back rows

1	2	3	4	5	6	7	8	9	10
915		800		785		785		800	
	874		785		785		815		800
859		859		785		823		777	
	823		800		800		852		728
800		800		823		808		785	
	830		785		808		769		800
808		785		823		830		753	
	815		800		777		769		761
852		785		785		736		785	
	852		823		800		719		777
874		815		845		702		761	
	800		792		785		785		792

Table. 3.4 Fresh air flow distribution 31600 ft^3/hr
from front to back rows

1	2	3	4	5	6	7	8	9	10
666		666		618		684		628	
	693		656		656		666		666
647		684		656		656		587	
	637		618		637		608		608
647		666		656		656		656	
	628		656		597		597		693
647		656		656		647		628	
	608		675		618		608		628
684		628		618		608		618	
	666		608		656		628		666
702		628		693		684		736	
	656		656		666		608		702

Table. 3.5 Fresh air flow distribution 22350 ft^3/hr

from front to back rows

1	2	3	4	5	6	7	8	9	10
508		496		496		457		484	
	532		471		484		415		496
520		532		520		457		457	
	520		471		457		508		444
532		508		508		508		430	
	496		520		457		430		444
496		496		496		484		484	
	484		496		430		415		444
508		471		496		496		471	
	508		520		496		430		496
520		496		508		520		508	
	484		496		496		444		496

Table 3.6 Variation of secondary air flow with fresh air flow

Secondary air flow ft^3/hr	Fresh air flow ft^3/hr				
76200	49900	44691	38704	31602	22346
69368	49900	44691	38704	31602	22346
61720	49900	44691	38704	31602	22346
52980	49900	44691	38704	31602	22346
42479	49900	44691	38704	31602	22346
28319	49900	44691	38704	31602	22346

Table 3.7 Variation of secondary air flow with fresh air flow with blocked tubes

Secondary air flow ft^3/hr	Fresh air flow ft^3/hr				
76200	40594	36308	31444	25674	18534
69368	40594	36308	31444	25674	18534
52980	40594	36308	31444	25674	18534
42479	40594	36308	31444	25674	18534

Table 3.8 Variation of secondary air flow with fresh air flow for one burner in operation

Secondary air flow ft^3/hr	Fresh air flow ft^3/hr				
76200	49900	44691	38704	31602	22346
28319	49900	44691	38704	31602	22346

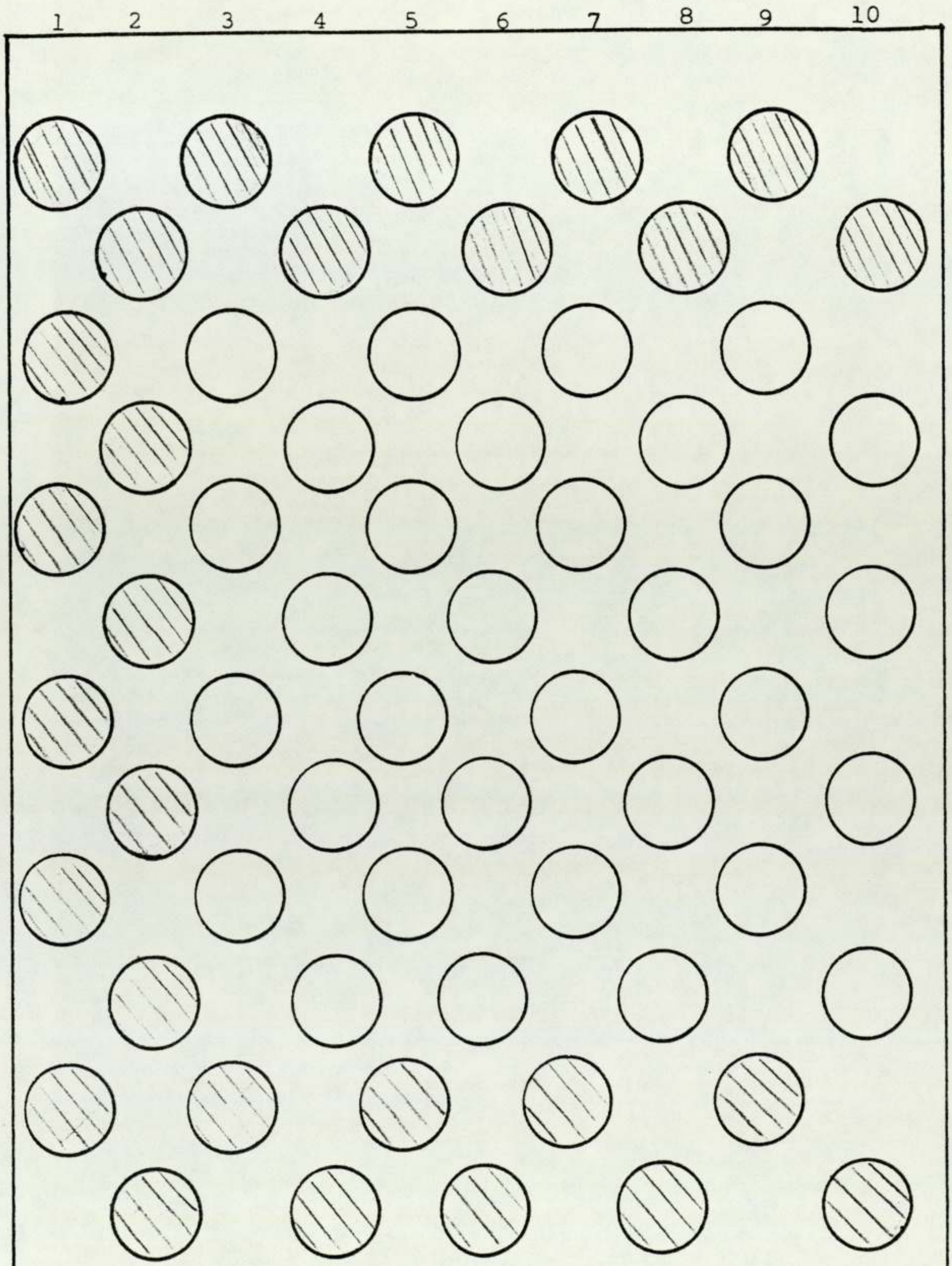

Fig. 3.1 End view of the bank with plugged tubes
from front to back rows

CHAPTER FOUR

Experimental results and calculations

4.1 Experimental results

After the experimental programme was successfully completed and the experimental data were obtained, several computer programmes were developed to process and analyse the data. The following results were extracted:-

i) The radiation effect on heat transfer coefficients was found to be very small and has no significance. The average ratio of the amount of radiation from the refractory walls and the radiating gases, to the energy input from the natural gas, was found to be only 0.9% .

ii) The insignificant effect of radiation was also confirmed by using hot air flowing across the bundle while the burners were not in operation.

4.1.1 Developed Heat Transfer Correlations

The following correlation was developed for the hot air conditions on the tube side:-

$$NU(\text{hot air}) = 0.009\ Re^{0.98}\ Pr^{0.33} \quad \ldots\ldots\ldots\ldots(4.1)$$

The experimental points, shown in figure (4.1) were clearly in line with each other and a uniform straight line trend with a high degree of correlation was obtained.

Comparing equation (4.1), with the following correlation, developed for the same fluid flow conditions as before but with both burners in operation:-

$$Nu(burners) = 0.01\ Re^{0.95} Pr^{0.33} \quad \text{..........(4.2)}$$

it will be noticed, that the power of Reynolds number in equation (4.1) is slightly higher, but when applying both equations (4.1), and (4.2) to a typical Reynolds number from this work, such as 18,000 Nusselt numbers would be reasonably close for both correlations as shown below:-

equation (4.1), $Nu(\text{hot air}) = 120$

equation (4.2), $Nu(\text{burners}) = 102$

Both graphs look very similar when compared see graphs in figures (4.1) and (4.3).

Since the secondary air flowrate was varied with fresh air, six overall tubeside correlations were developed for the following secondary air flow rates:-

76.200 ft^3/hr 69,300 ft^3/hr 61,700 ft^3/hr
52,940 ft^3/hr 42,446 ft^3/hr 28,299 ft^3/hr

which were as follows according to the secondary air flow rates in order:-

i) $NU = 0.008\ Re^{1.2}Pr^{0.33}$ ....(4.3)

ii) $NU = 0.01\ Re^{0.95}Pr^{0.33}$ ....(4.4)

iii) $NU = 0.009\ Re^{0.98}Pr^{0.33}$ ....(4.5)

iv) $NU = 0.003\ Re^{1.1}Pr^{0.33}$ ....(4.6)

v) $NU = 0.001\ Re^{1.2}Pr^{0.33}$ ....(4.7)

vi) $NU = 0.004\ Re^{1.05}Pr^{0.33}$ ....(4.8)

The experimental results were plotted in figures (4.2) to (4.7). Small differences were noticed on the slopes i.e., the power of Reynolds numbers, and also in the constants (intercepts). Slopes were fluctuating around unity for all of these correlations, which may be due to the secondary air flow rate variations, since the latter was the only variable. The change in the intercepts has no significance since they were all in the third decimal points.A high degree of correlation (0.8 - 0.9) was obtained, which means a linear trend existed.

To provide a wider range of Reynolds number on the tube side, some of the tubes were blocked and four correlations were developed, based on the following secondary air flow rates:-
76195 ft^3/hr 69315 ft^3/hr 52940 ft^3/hr 42446 ft^3/hr
which are:-

$NU = 0.0019\ Re^{1.18}Pr^{0.33}$ ....(4.9)

$NU = 0.029\ Re^{1.09}Pr^{0.33}$ ....(4.10)

$NU = 0.04\ Re^{1.065}Pr^{0.33}$ ....(4.11)

$NU = 0.019\ Re^{1.18}Pr^{0.33}$ ....(4.12)

KEY

SYMBOL		TUBE POSITION IN THE BUNDLE
■	=	6:3
●	=	6:4
◆	=	7:4
□	=	8:3
○	=	8:4
×	=	10:3

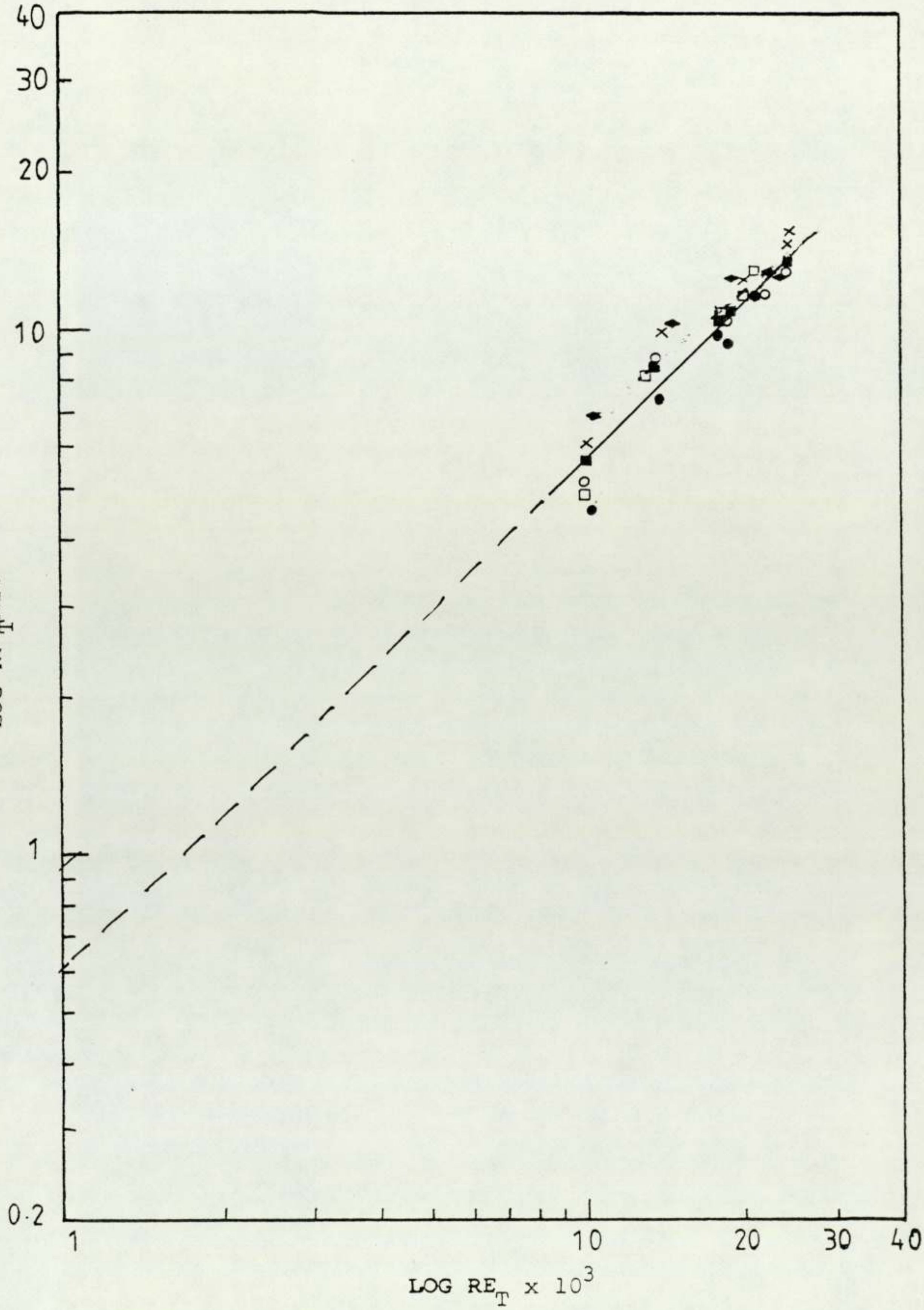

FIG: 4.2 Variation of Nusselt Number with Reynolds Number with both burner on and secondary air flow ($76200ft^3/hr$)

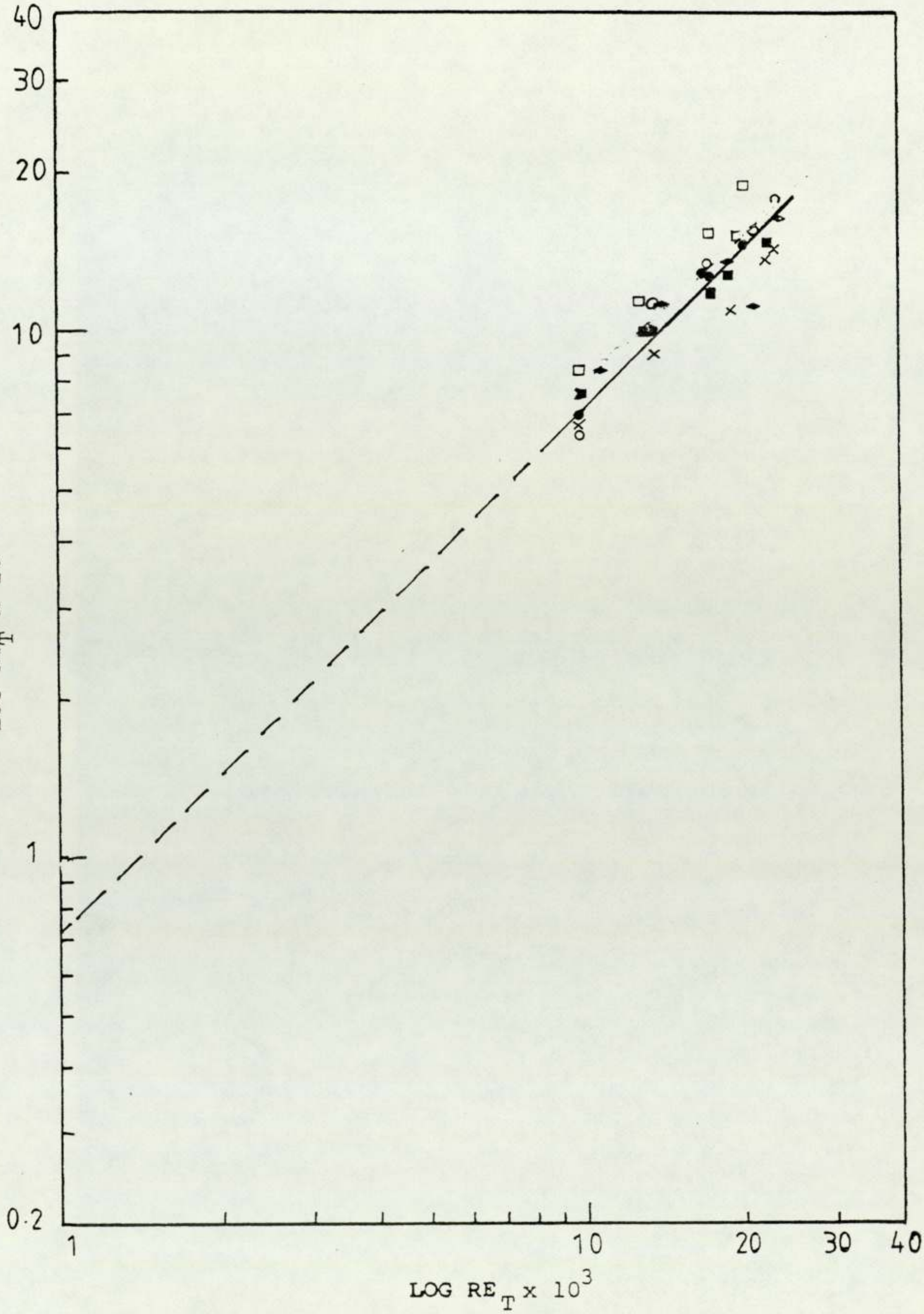

FIG: 4.1 Variation of Nusselt Number with Reynolds Number with hot air flowing over the bundle and secondary air flow (69368ft^3/hr)

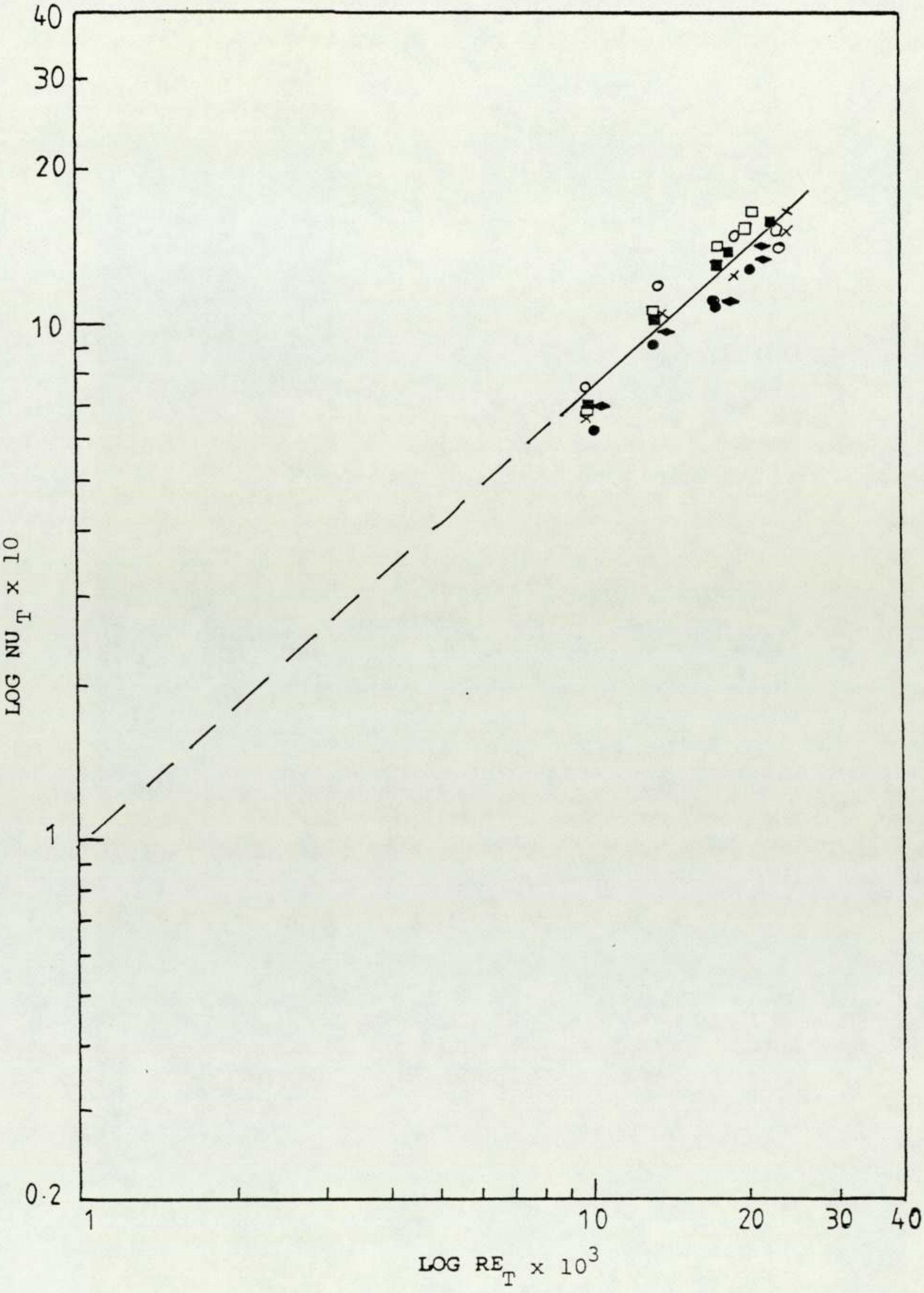

FIG:4.3 Variation of Nusselt Number with Reynolds Number with both burners on and secondary air flow ($69368\ ft^3/hr$)

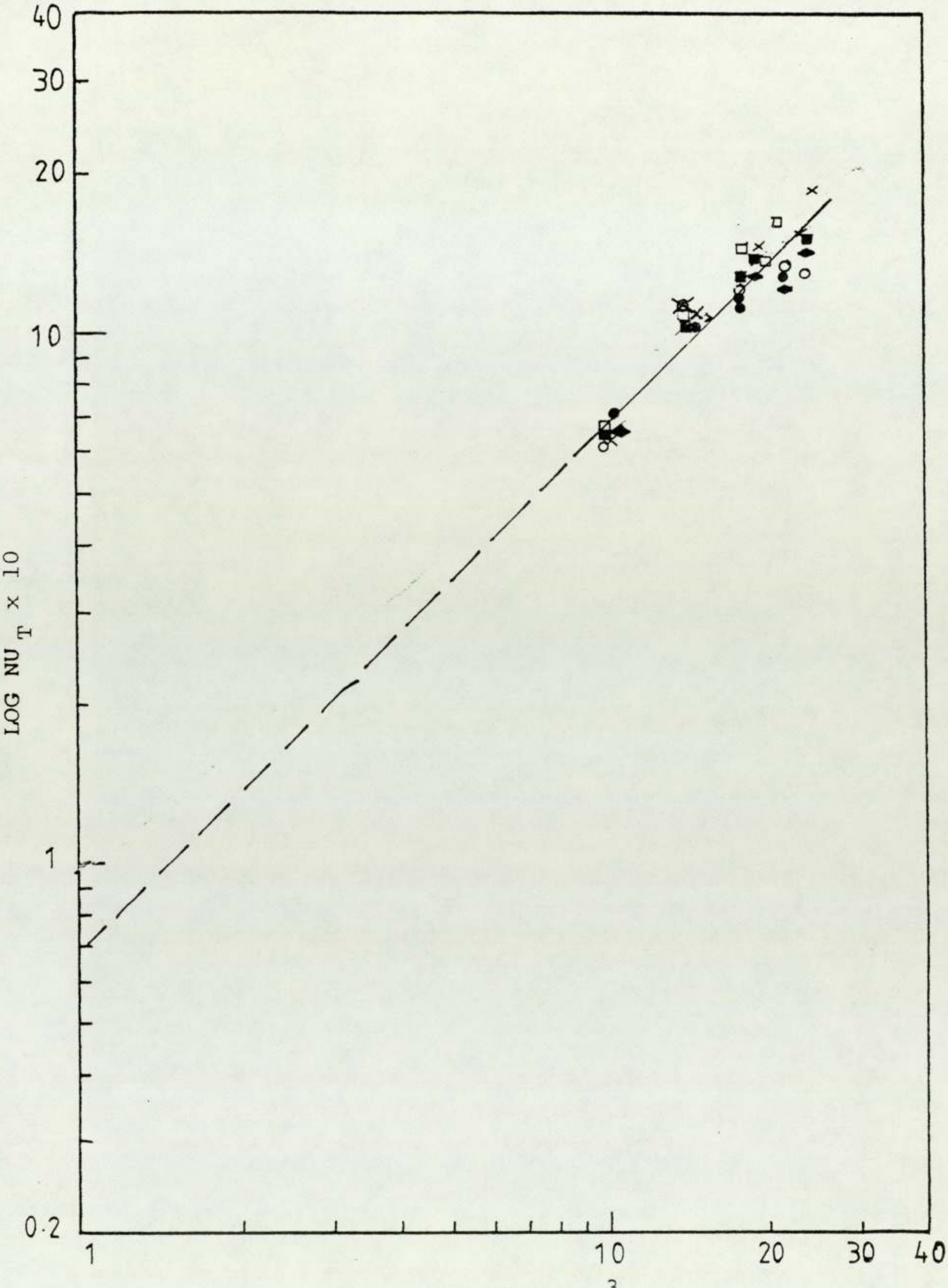

FIG:4.4 Variation of Nusselt Number with Reynolds Number with burners on and secondary air flow ($61720\ ft^3/hr$)

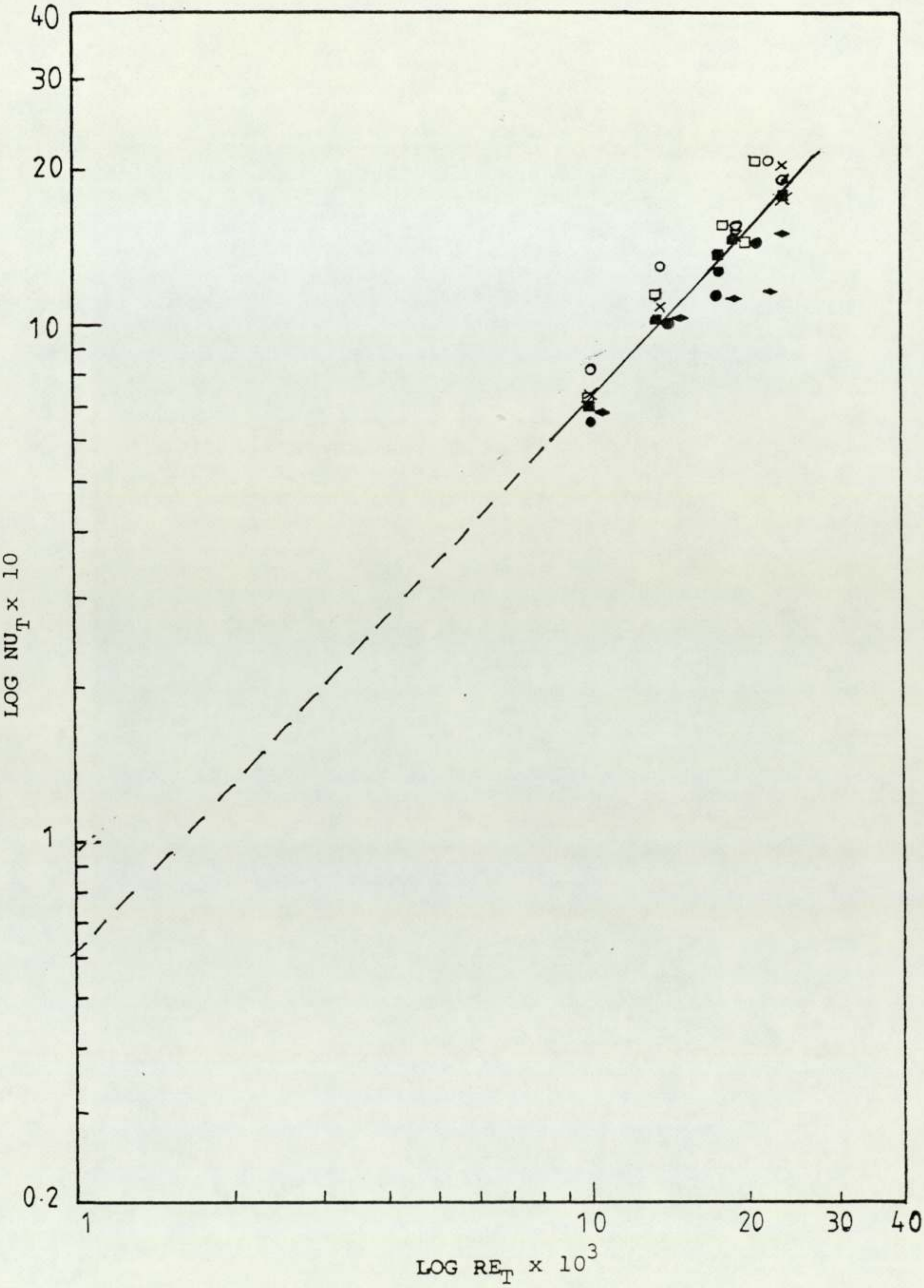

FIG:4.5 Variation of Nusselt Number with Reynolds Number with both burners on and secondary air flow ($52980\ ft^3/hr$)

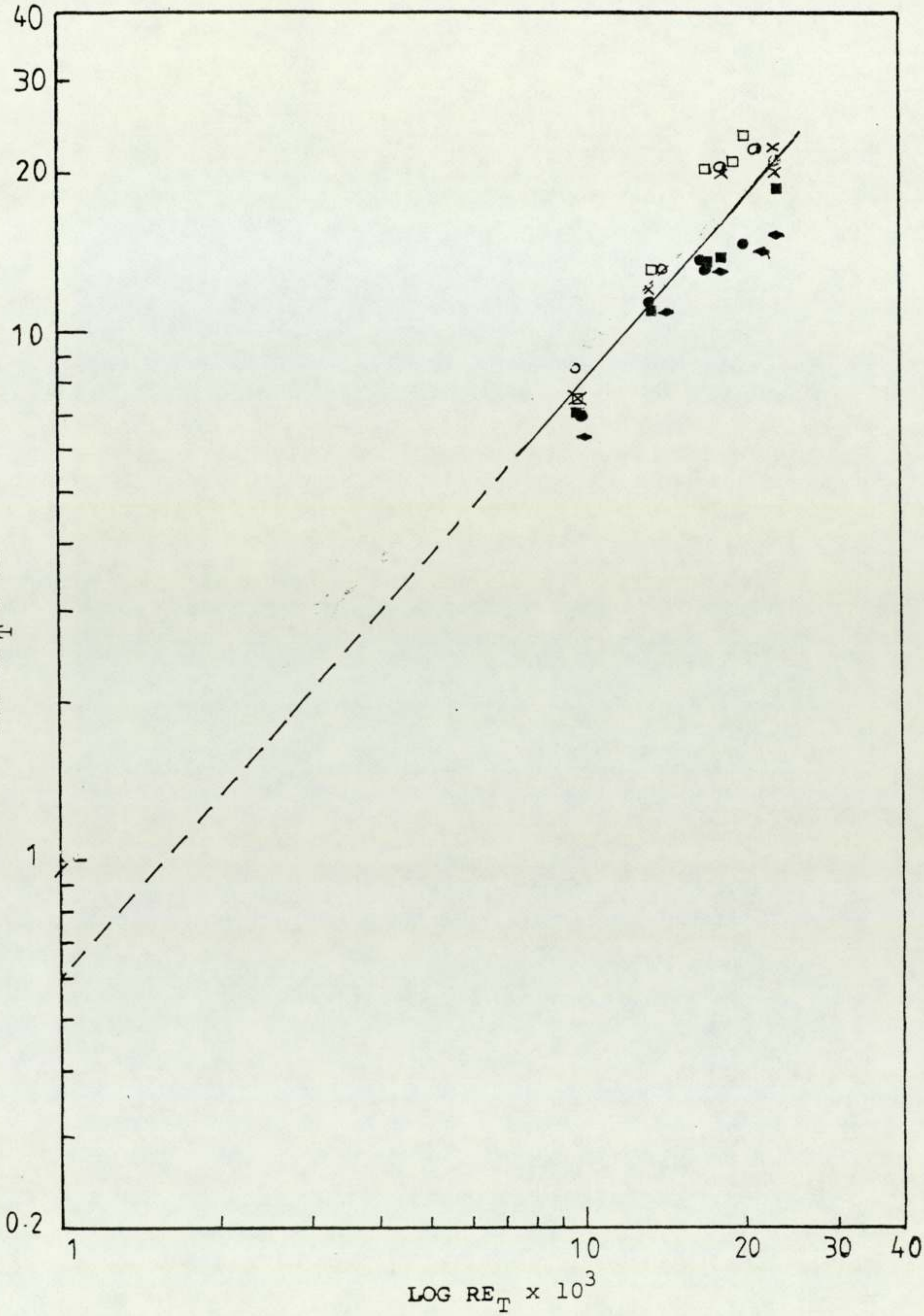

FIG:4.6 Variation of Nusselt Number with Reynolds Number with both burners on and secondary air flow ($42479\ ft^3/hr$)

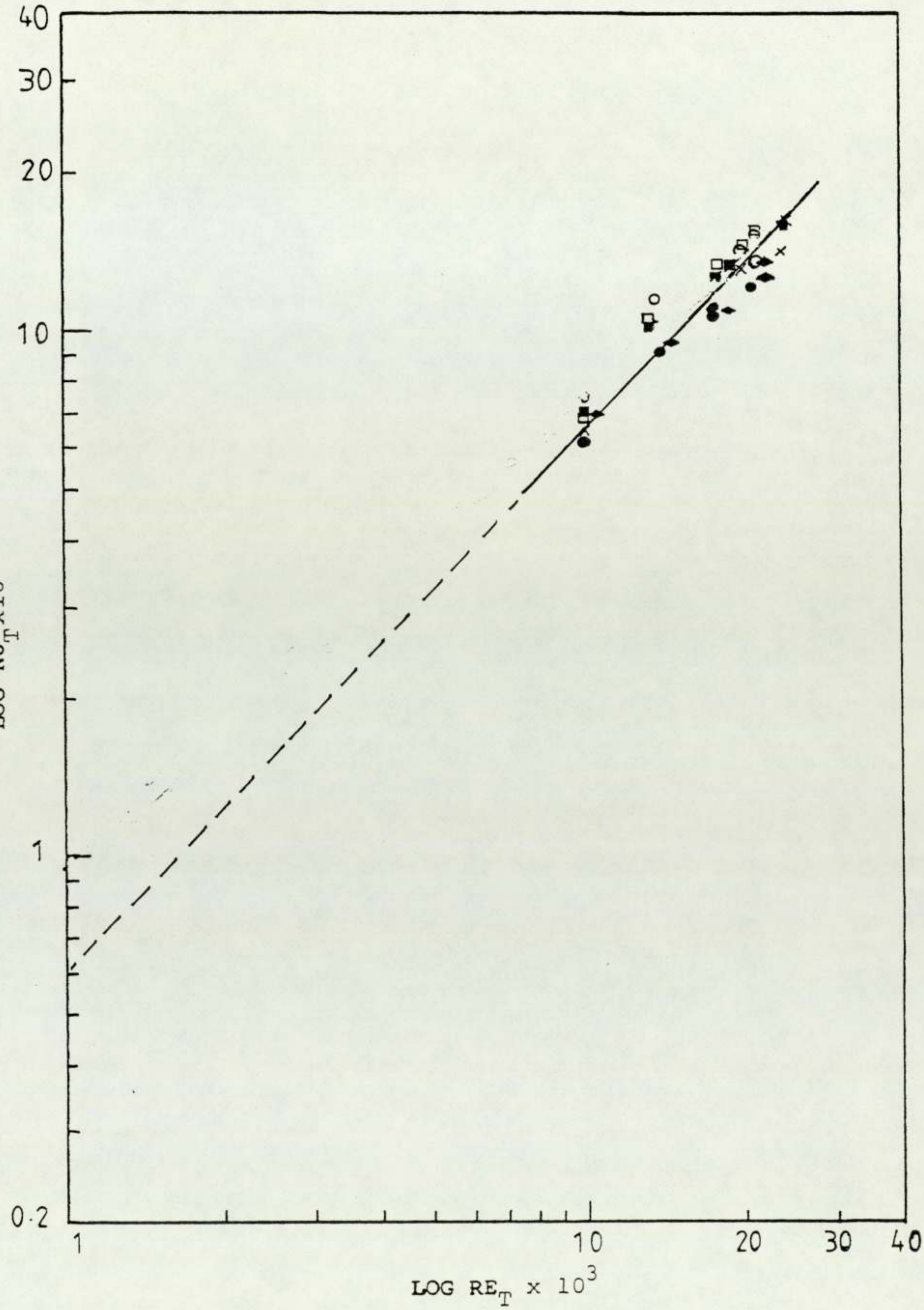

FIG: 4.7 Variation of Nusselt Number with Reynolds Number with both burners on and secondary air flow ($28319 ft^3/hr$)

The above equations were very simillar to the previous equations(4.4) to (4.8), and they cover a wider range of Reynolds number. No deviation was noticed on the graphs, obtained, in figures (4.8) to (4.10). The slopes were also fluctuating around unity. A high degree of correlation was obtained.

An overall tube side correlation was established for data obtained for a single burner in operation. These are:-

i) burner number one in operation at the highest possible secondary air flowrate 76200 ft^3/hr ($2058m^3/hr$)

$$Nu = 0.006 \, Re^{1.01} Pr^{0.33} \quad \ldots\ldots\ldots\ldots (4.13)$$

ii) burner one in operation at the lowest possible secondary air flow rate 28300 ft^3/hr ($764m^3/hr$)

$$Nu = 0.007 \, Re^{1.02} Pr^{0.33} \quad \ldots\ldots\ldots\ldots (4.14)$$

iii) burner number two in operation at the highest possible secondary air flow rate 76200 ft^3/hr ($2057m^3/hr$)

$$Nu = 0.006 \, Re^{1.01} Pr^{0.33} \quad \ldots\ldots\ldots\ldots (4.15)$$

iv) burner number two at the lowest possible secondary air flow rate 28300 ft^3/hr, ($764m^3/hr$)

$$Nu = 0.006 \, Re^{1.034} Pr^{0.33} \quad \ldots\ldots\ldots\ldots (4.16)$$

looking at graphs in figures (4.11) and (4.12), it will be observed that when burner two was in operation i.e., the one near the cold end, the individual tube lines are clear and there is no intermixing between individual points. More scatter was observed on graphs (4.13) and (4.14) which were plotted for burner number one in operation.

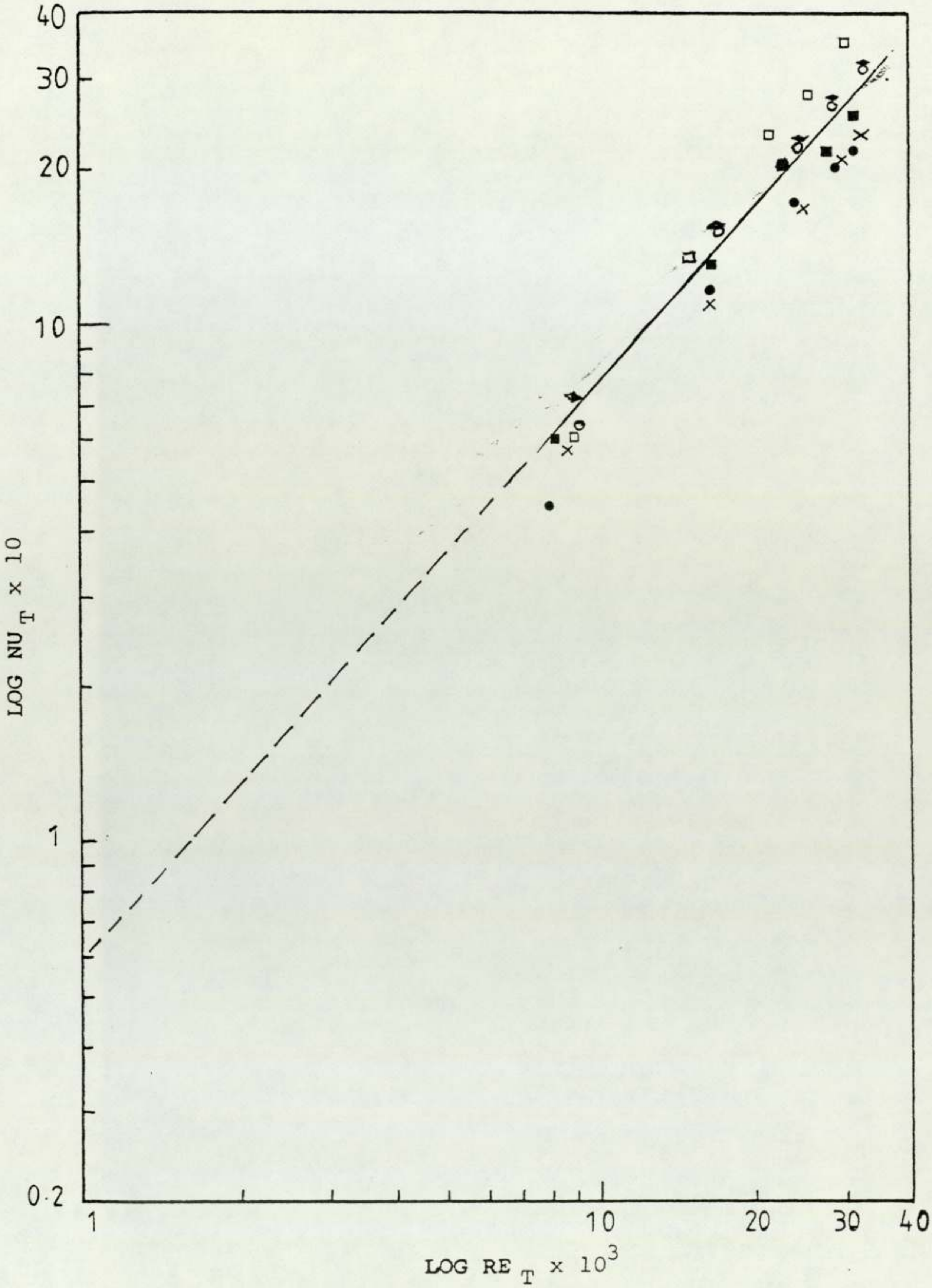

FIG: 4.8 Variation of Nusselt Number with Reynolds Number

blocked tubes and both burners on with secondary air flow (76200 ft^3/hr)

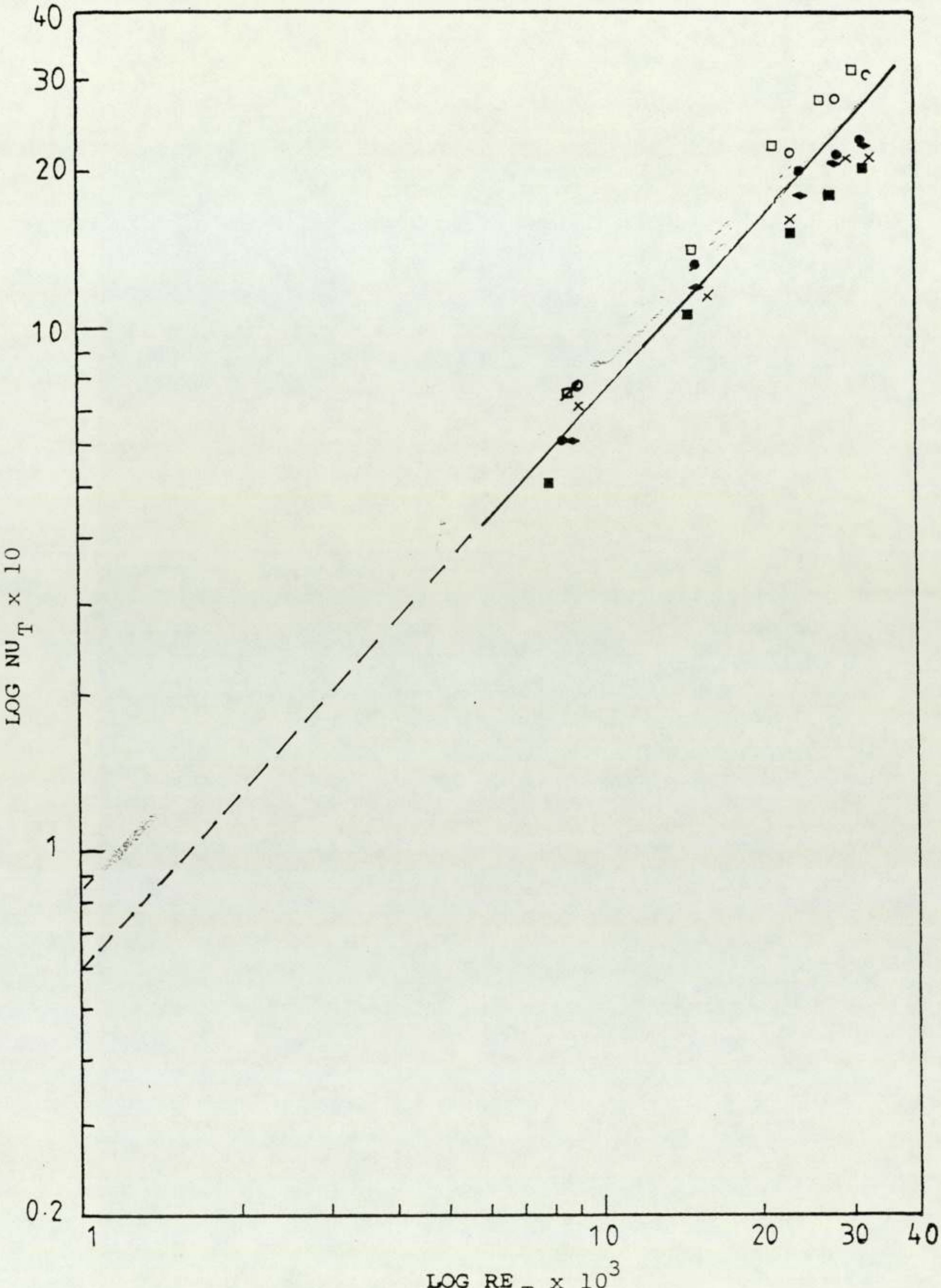

FIG: 4.9 Variation of Nusselt Number with Reynolds Number blocked tubes and both burners on with secondary air flow (69368 ft^3/hr)

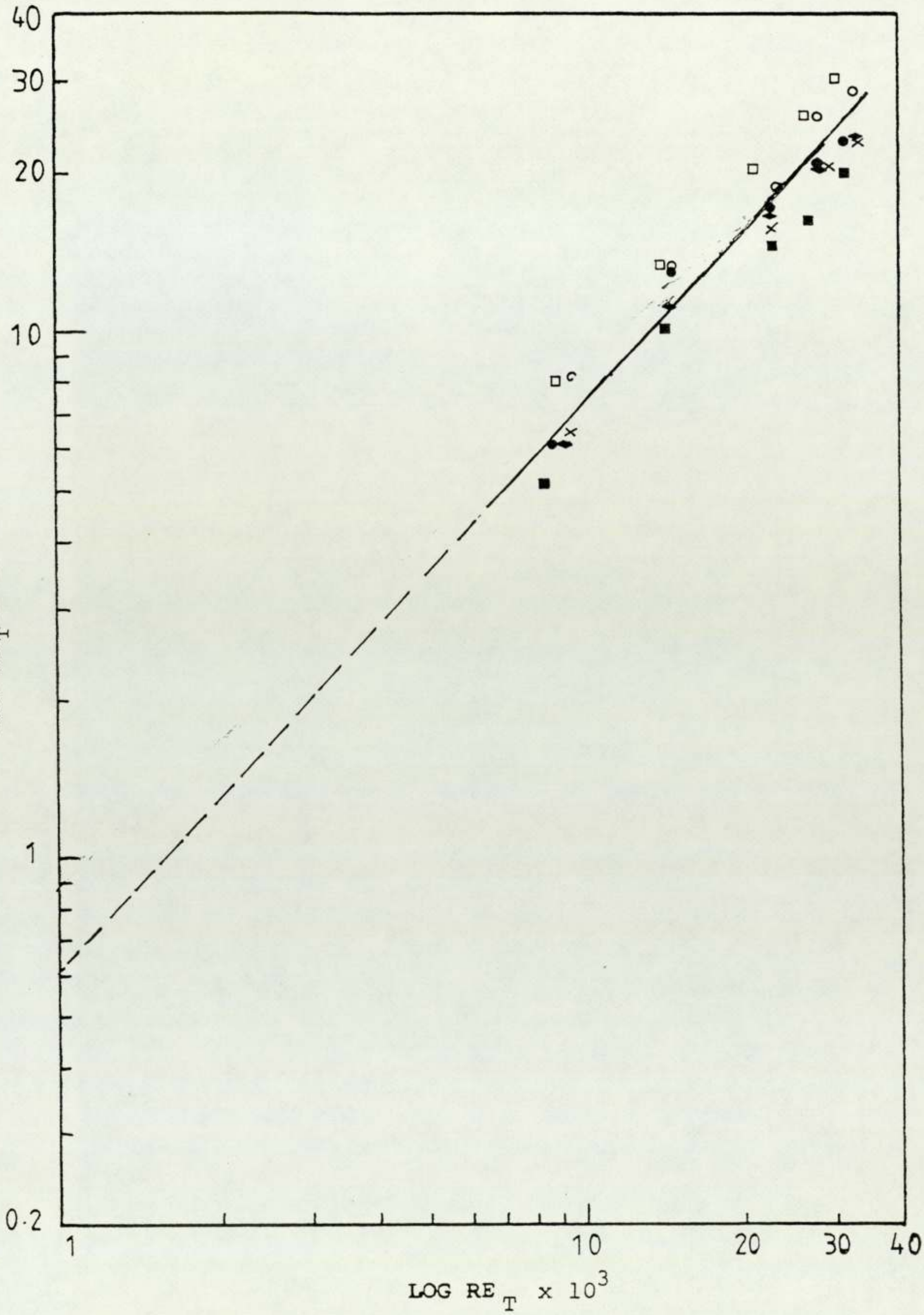

FIG: 4.10 Variation of Nusselt Number with Reynolds Number blocked tubes and both burners on with secondary air flow (52980 ft^3/hr)

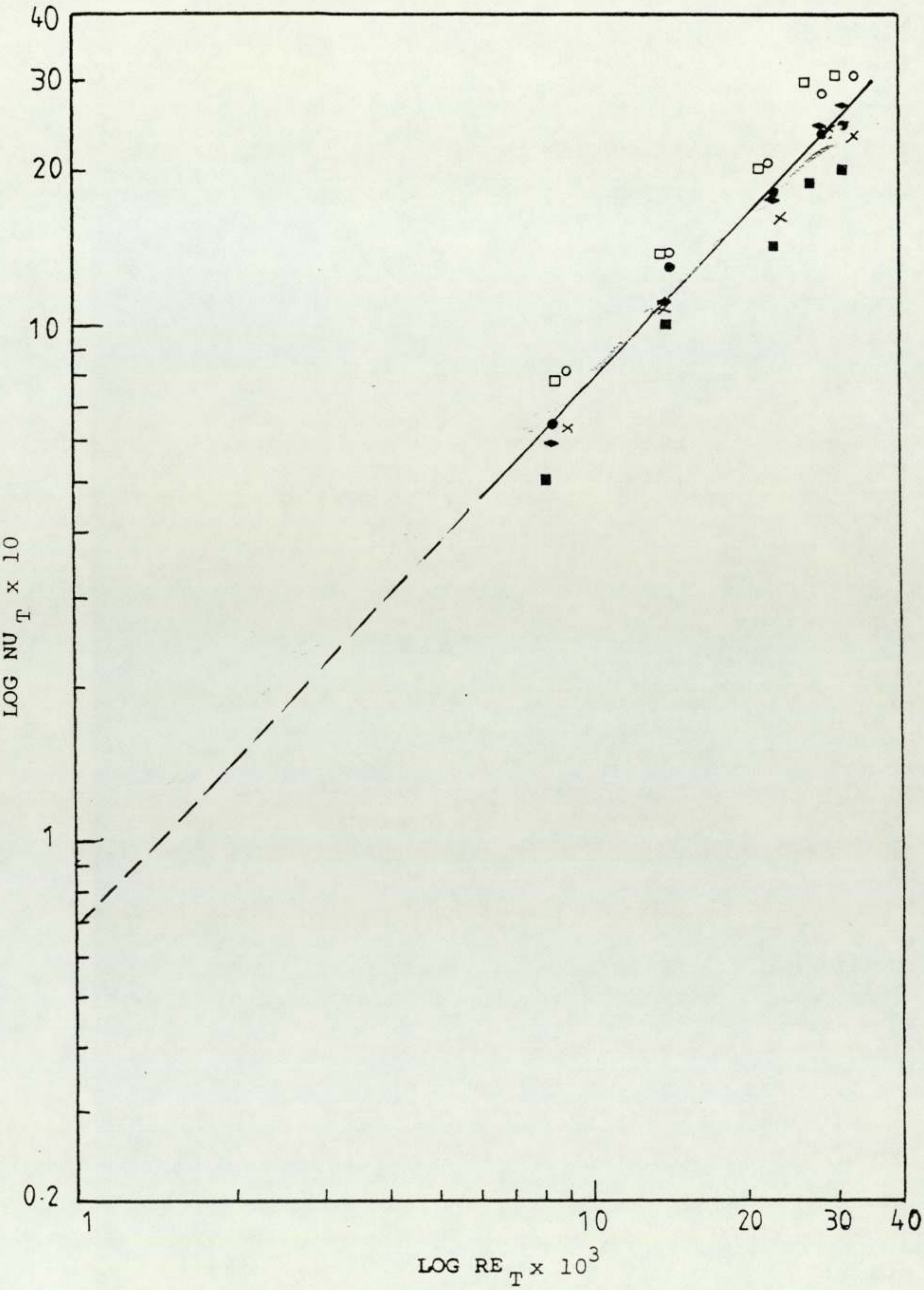

FIG: 4.11 Variation of Nusselt Number with Reynolds Number blocked tubes and both burners on with secondary air flow (42479 ft^3/hr)

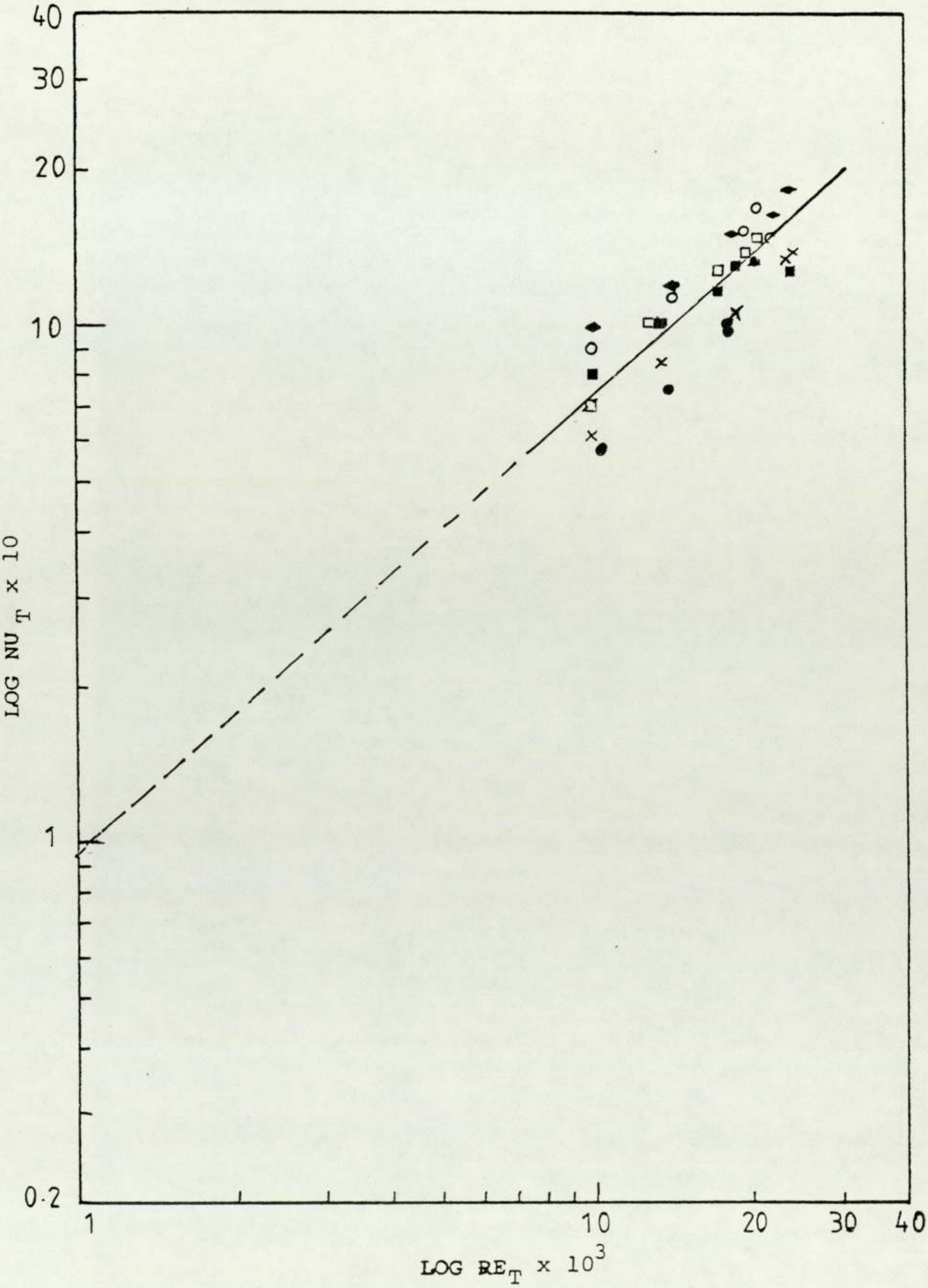

FIG: 4.12 Variation of Nusselt Number with Reynolds Number burner number two on with secondary air flow ($76200\ ft^3/hr$)

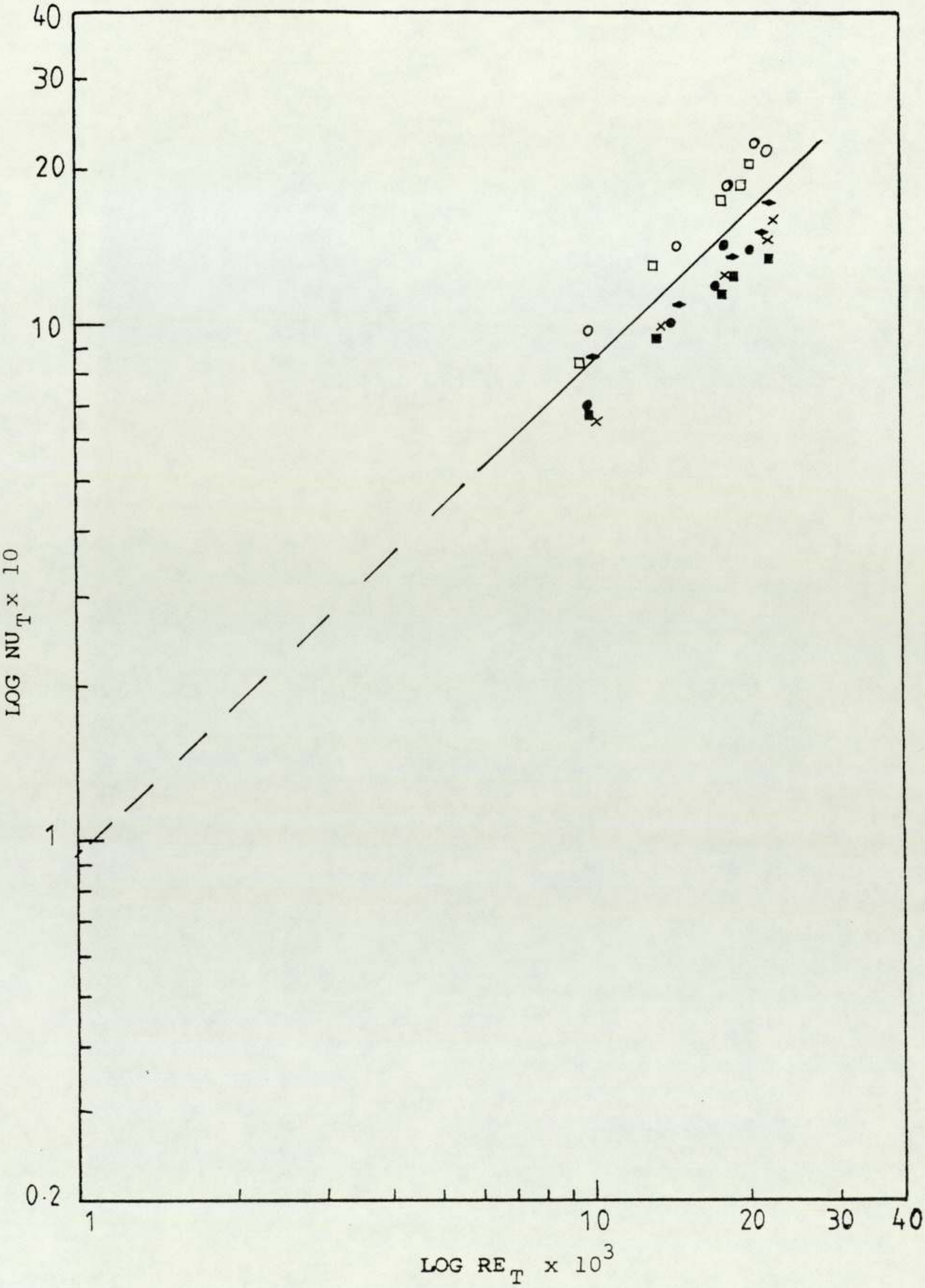

FIG:4.13 Variation of Nusselt Number with Reynolds Number burner number two on with secondary air flow (28319 ft^3/hr

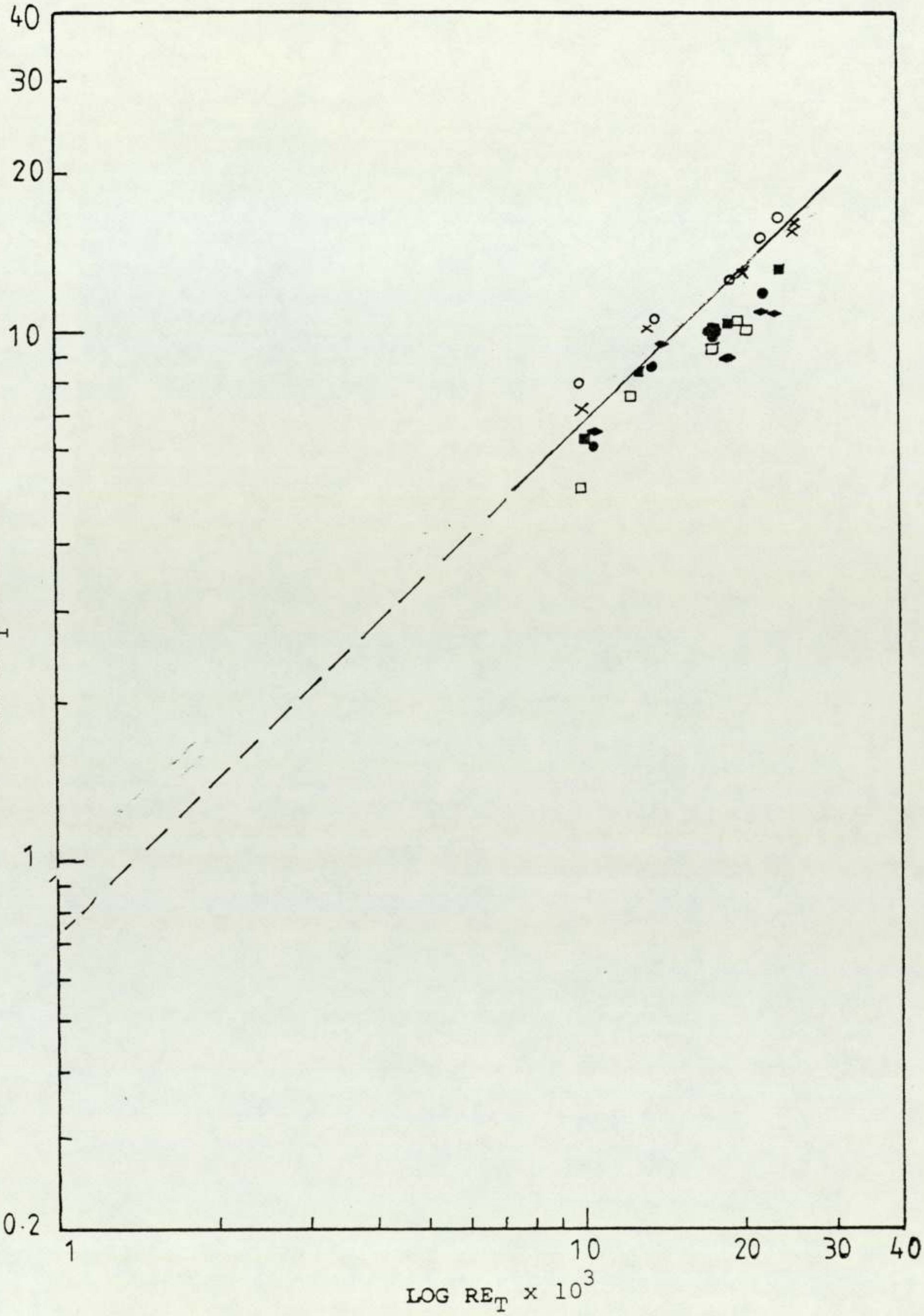

FIG: 4.14 Variation of Nusselt Number with Reynolds Number
burner number one on with secondary air flow
(76200 ft^3/hr)

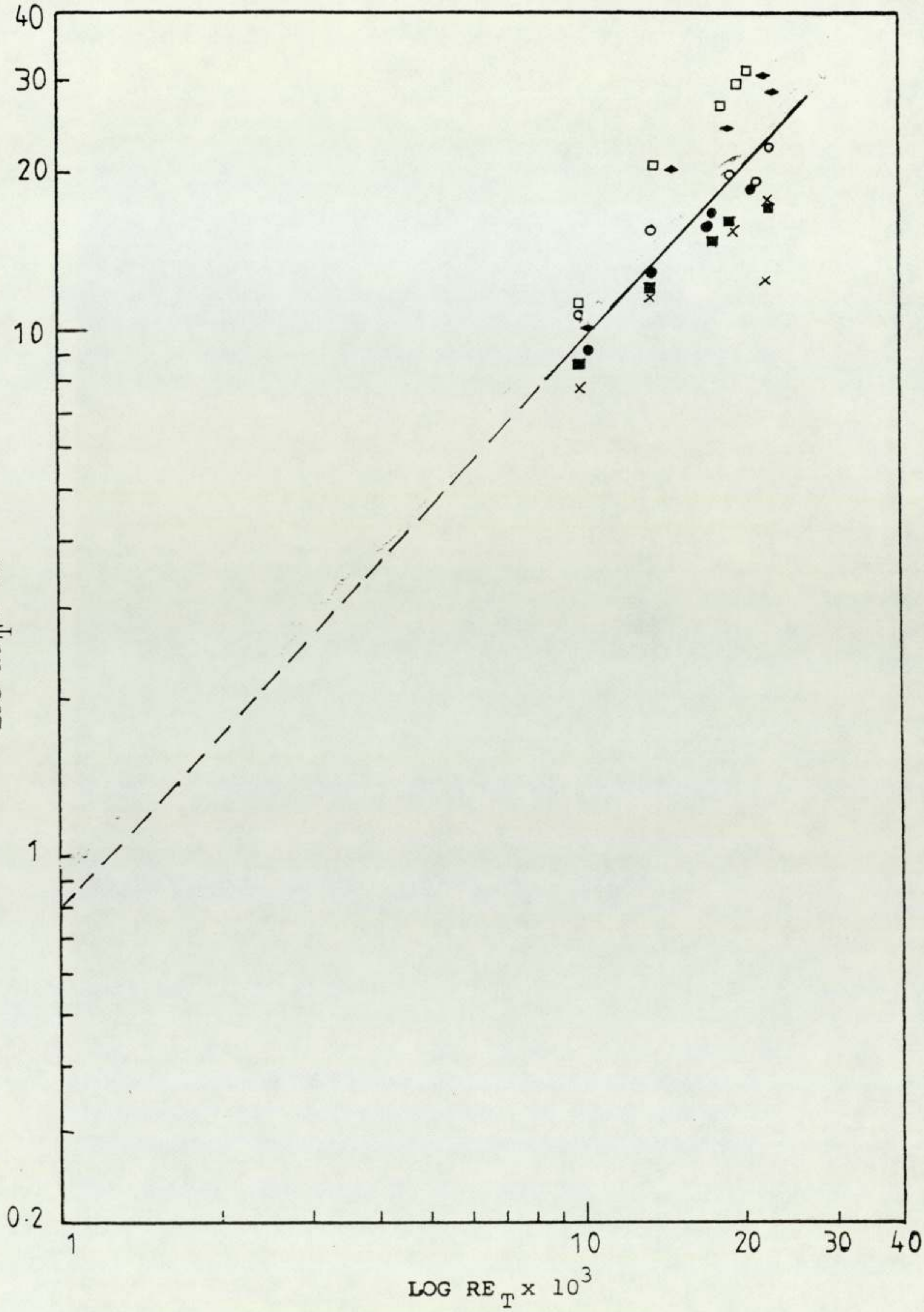

FIG: 4.15 Variation of Nusselt Number with Reynolds Number burner number one on with secondary air flow ($28319 \ ft^3/hr$)

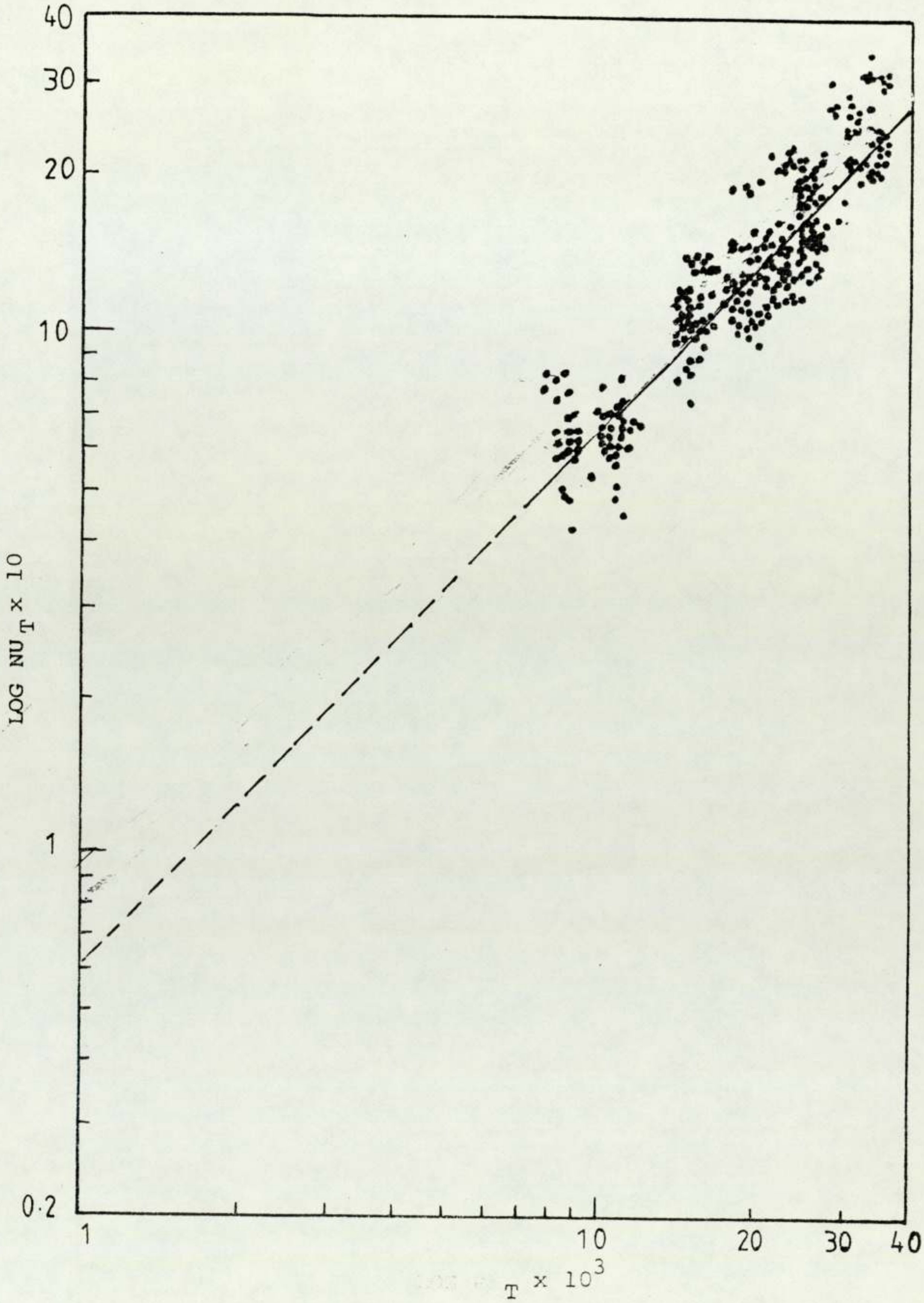

FIG:4.16 Variation of Nusselt Number with Reynolds Number on tube side for overall experimental data

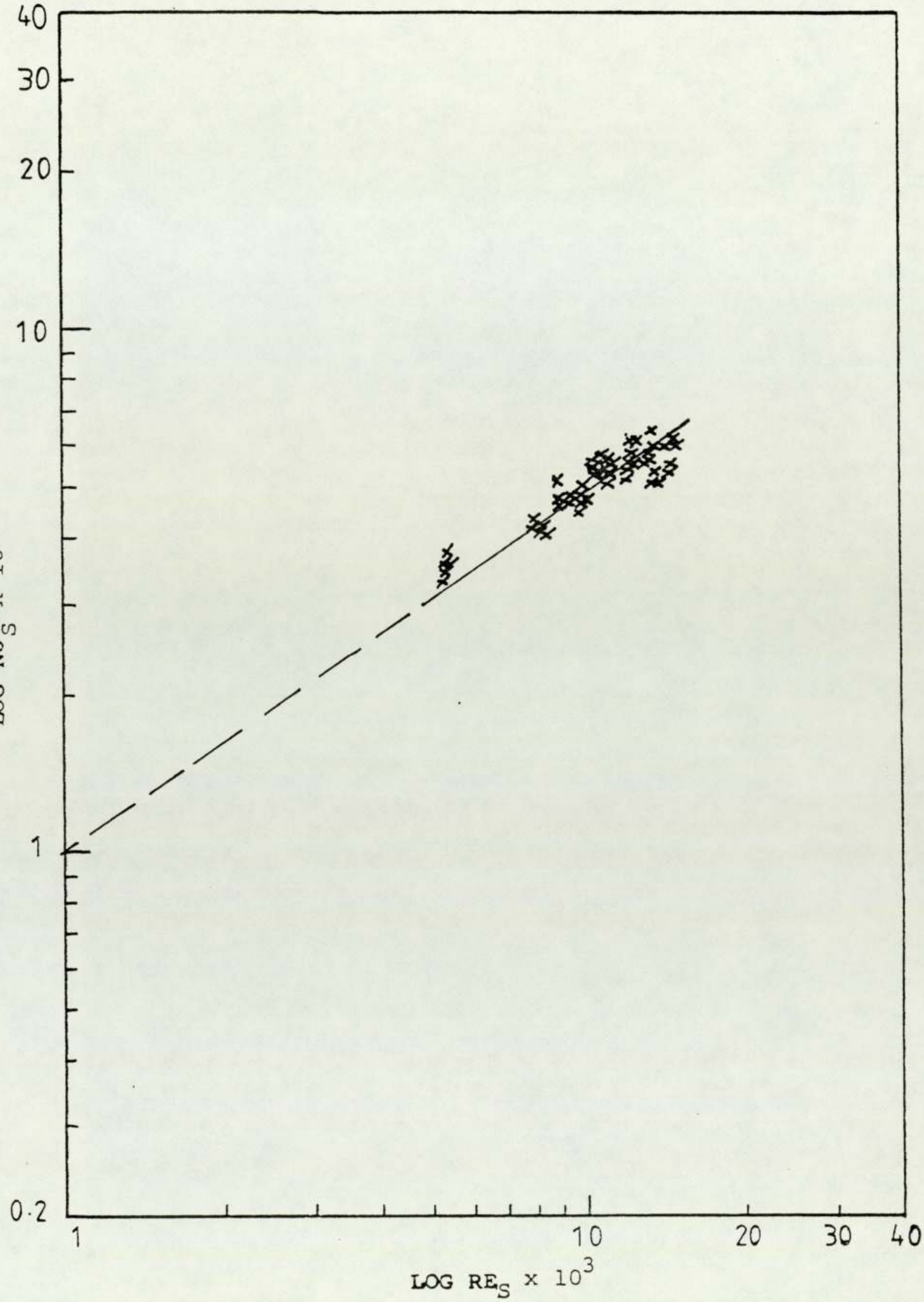

FIG: 4.17 Variation of Nusselt Number with Reynolds Number on shell side for overall experimental data

No real difference was noticed in the slopes i.e., powers of Reynolds numbers. The degree of correlation was slightly lower than in the earlier work.

To provide a good representation of the experimental data in correlations for both tube and shell sides under a range of operating conditions, experimental data were fed into the computer for an overall correlation of both tube and shell sides, see plotted graphs in figures (4.15) and (4.16).

Tube Side Correlations

$$NU_T = 0.0028\ Re^{1.08} Pr^{0.33} \quad \ldots\ldots\ldots\ldots\ldots\ldots (4.17)$$

Shell Side Correlation

$$NU_S = 0.89\ Re^{0.42} Pr^{0.33} \quad \ldots\ldots\ldots\ldots\ldots\ldots (4.18)$$

The shell side correlation of (NU_S-Re_S) was based on the calculated Nusselt number and Reynolds number based on the shell side when different secondary air flow rates were used. A computer package with least square method analysis was used for both shell and tube correlations. See appendices (A.2.2)

4.1.2 Temperature Scans

Four radial position temperature scanning through specific tubes, was carried out for the following process variables:-

i) hot air flow across the bundle

ii) one burner in operation at a time

iii) various natural gas flow rates

iv) various secondary and fresh air flowrates.

It was noticed from the graphs in figures (4.17 to 4.54), that experimental points were scattered for the first and second row tubes, and that stagnation points along the tube length on the front face, showed irregularity in the wall temperatures for all the data.

Temperature scans for hot air flowing across the bundle with burners switched off showed that for tube (1:1) in figure (4.18) points were scattered and a disturbance was noticed on the top face of the tube, Tube (1:5) in figure (4.19) showed a similar profile. Tubes (2:6),(2:3),(4:3) in figures (4.20)(4.21) and (4.22) show a more uniform wall temperature profile although the stagnation points showed a slightly higher temperature than other faces.

Temperature scans for two different fresh air flow rates 49900ft^3/hr,(1412m^3/hr)and 31602ft^3/hr,(894m^3/hr),see Figures (4,23)-(4.28) indicate that tubes (1:1),(1:5), (2:3), and (2:6) had very irregular wall temperature profile, while tubes at the back and centre of the bundle such as tubes (6:3) and(8:1) had reasonably uniform wall

TEMPERATURE SCANNING

KEY

SYMBOL		TUBE WALL FACE
□	=	Burners
×	=	Top
○	=	Back
◇	=	Bottom
●	=	Air in the centre of tube

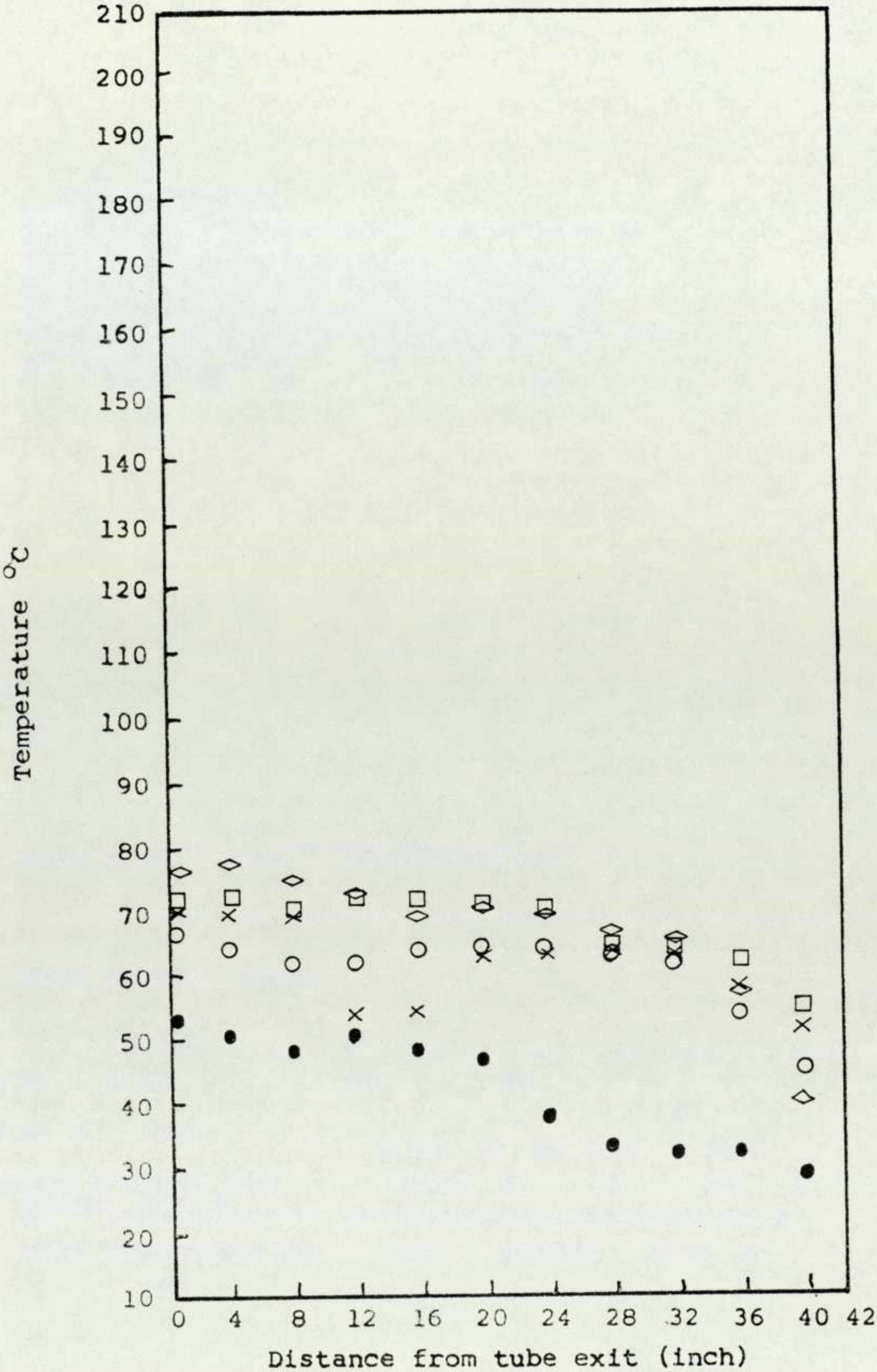

FIG.4.18 Variation of wall temperature along tube (1:1) with burners switched off and hot secondary air flow (76200 ft^3/hr)

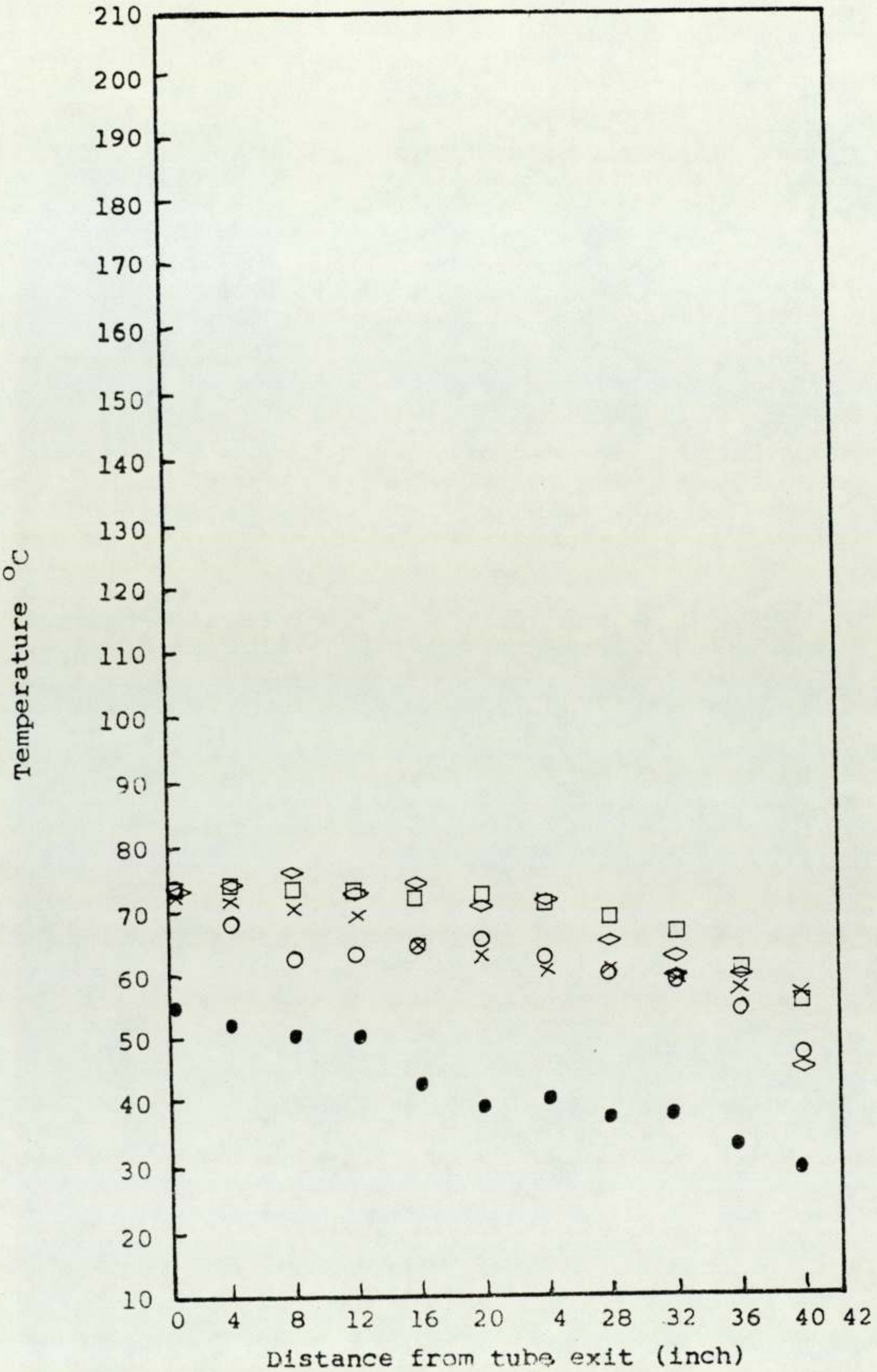

FIG.4.19 Variation of wall temperature along tube (1:5) with burners switched off and hot secondary air flow (76200 ft^3/hr)

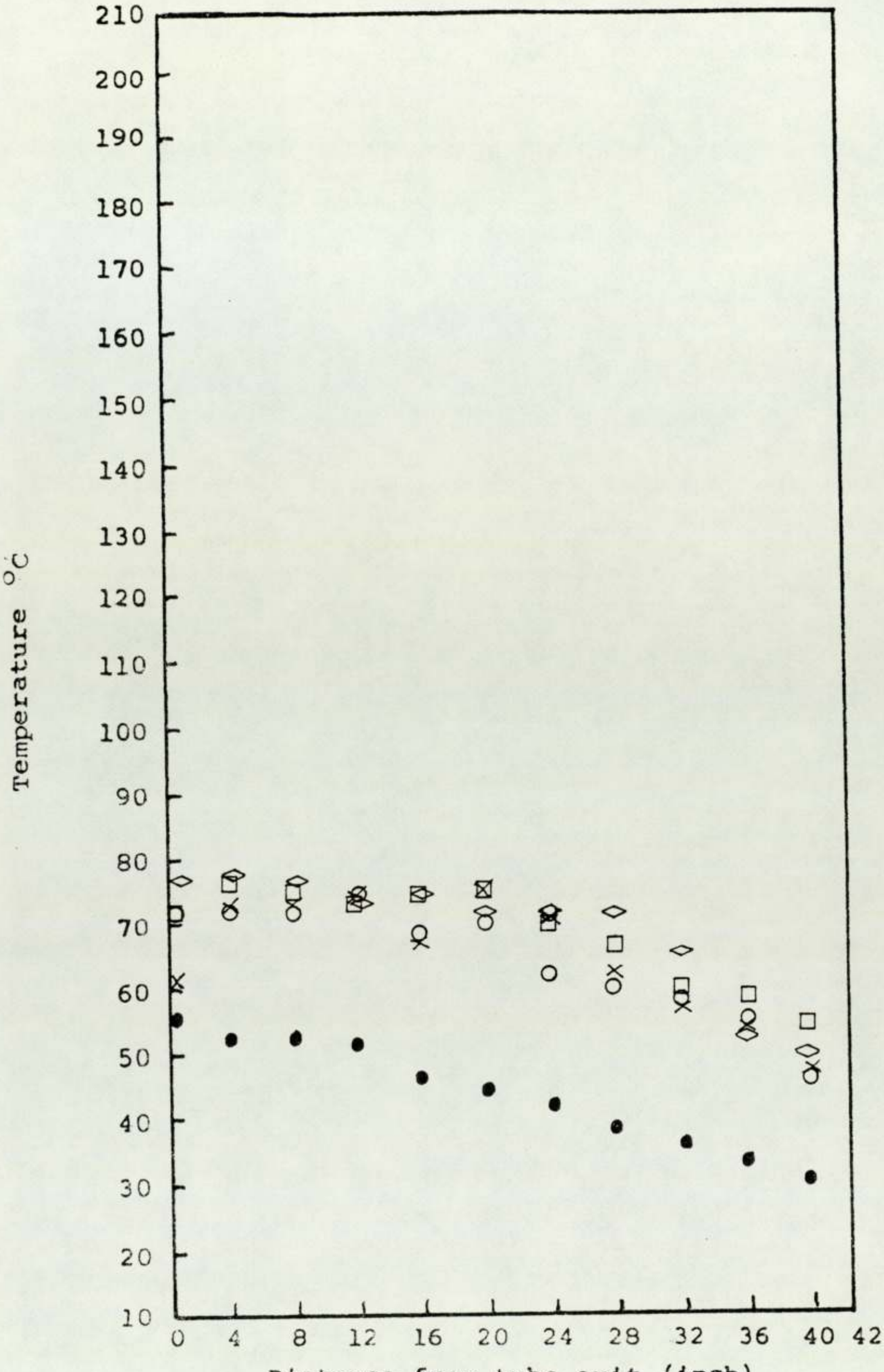

FIG.4.20 Variation of wall temperature along tube (2:6) with burners switched off and hot secondary air flow (76200 ft^3/hr)

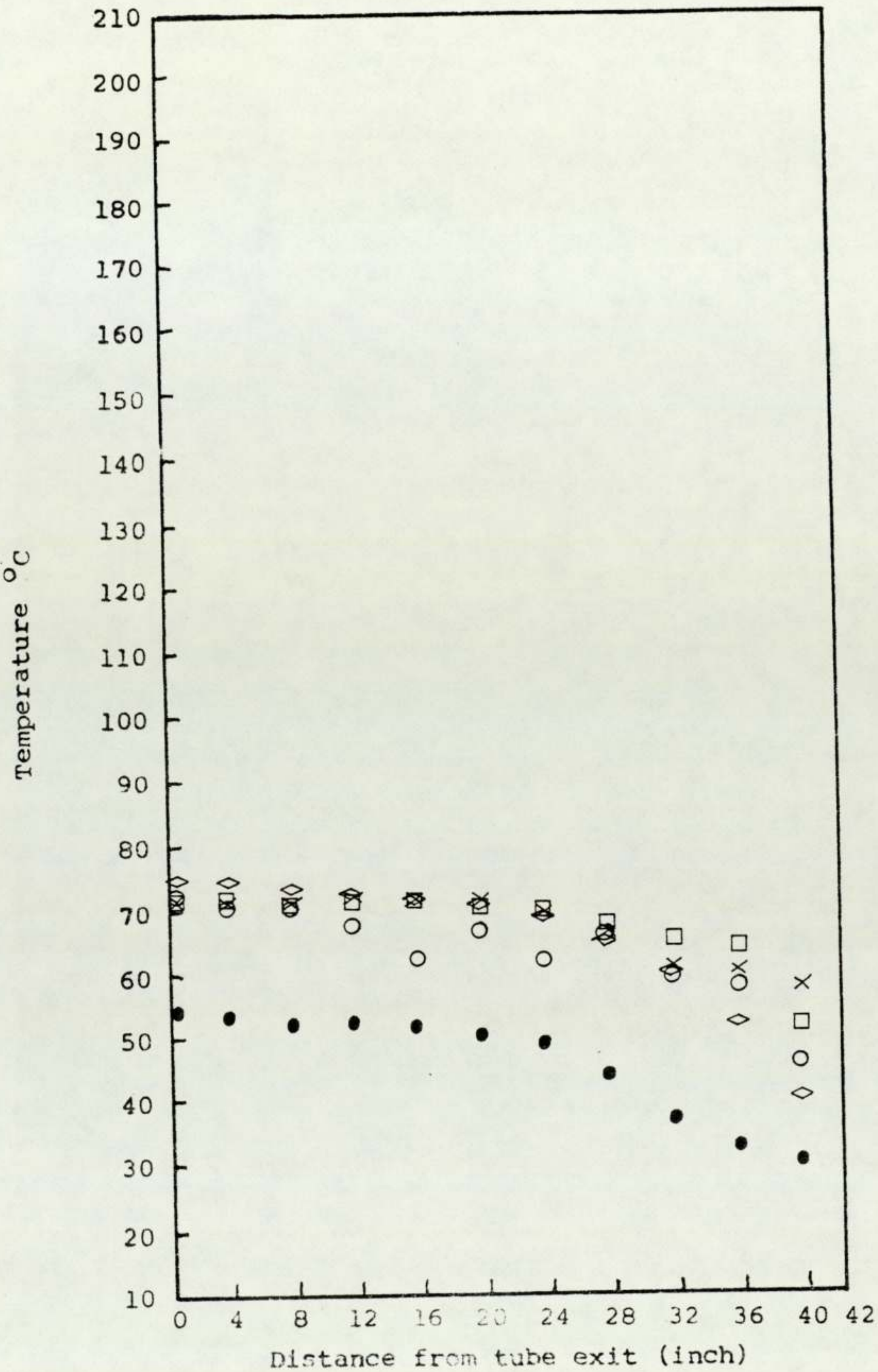

FIG.4.21Variation of wall temperature along tube (2:3) with burners switched off and hot secondary air flow (76200 ft^3/hr)

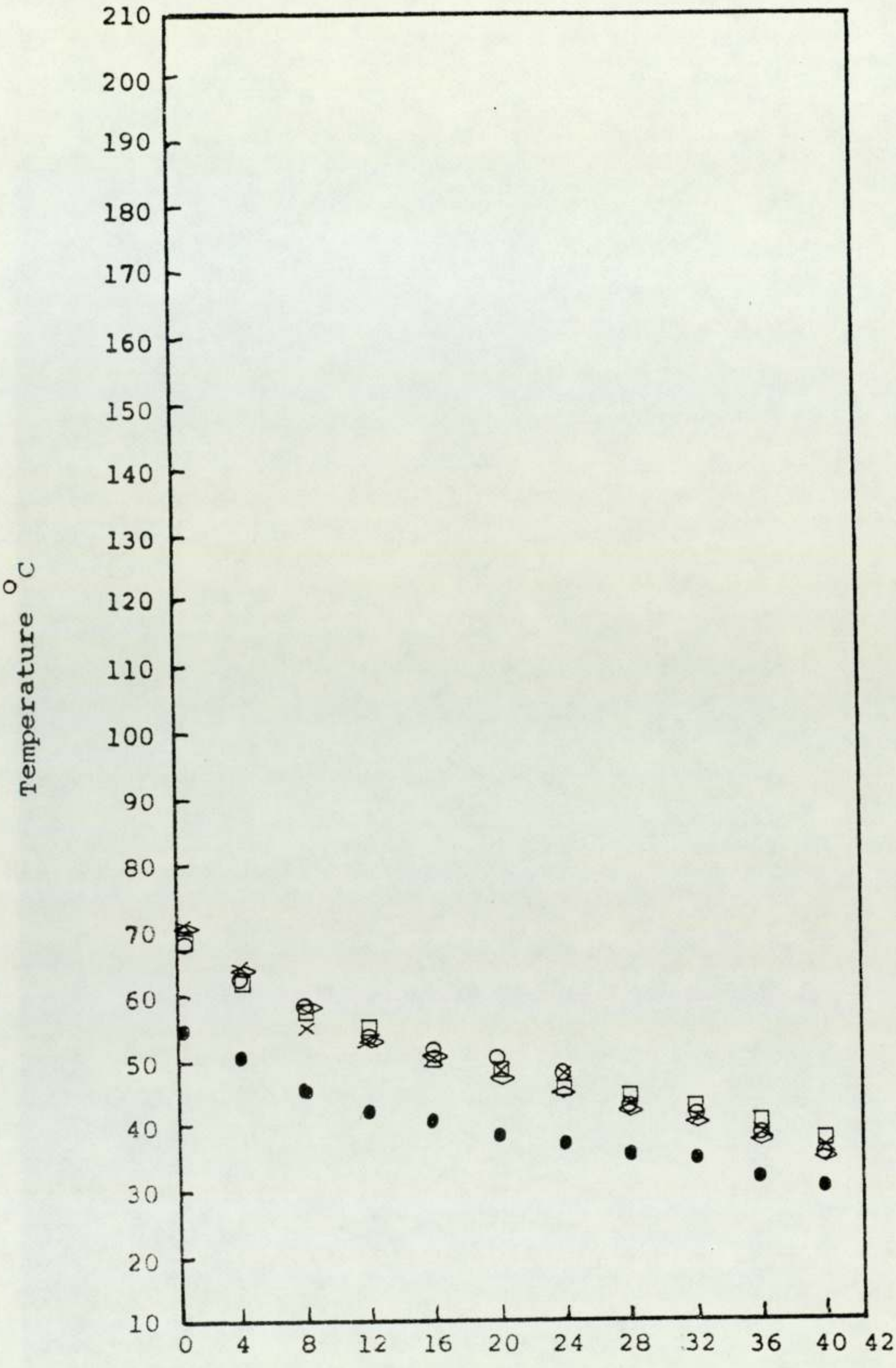

FIG.4.22 Variation of wall temperature along tube (4:3)
with burners switched off and hot secondary
air flow 76200 ft^3/hr)

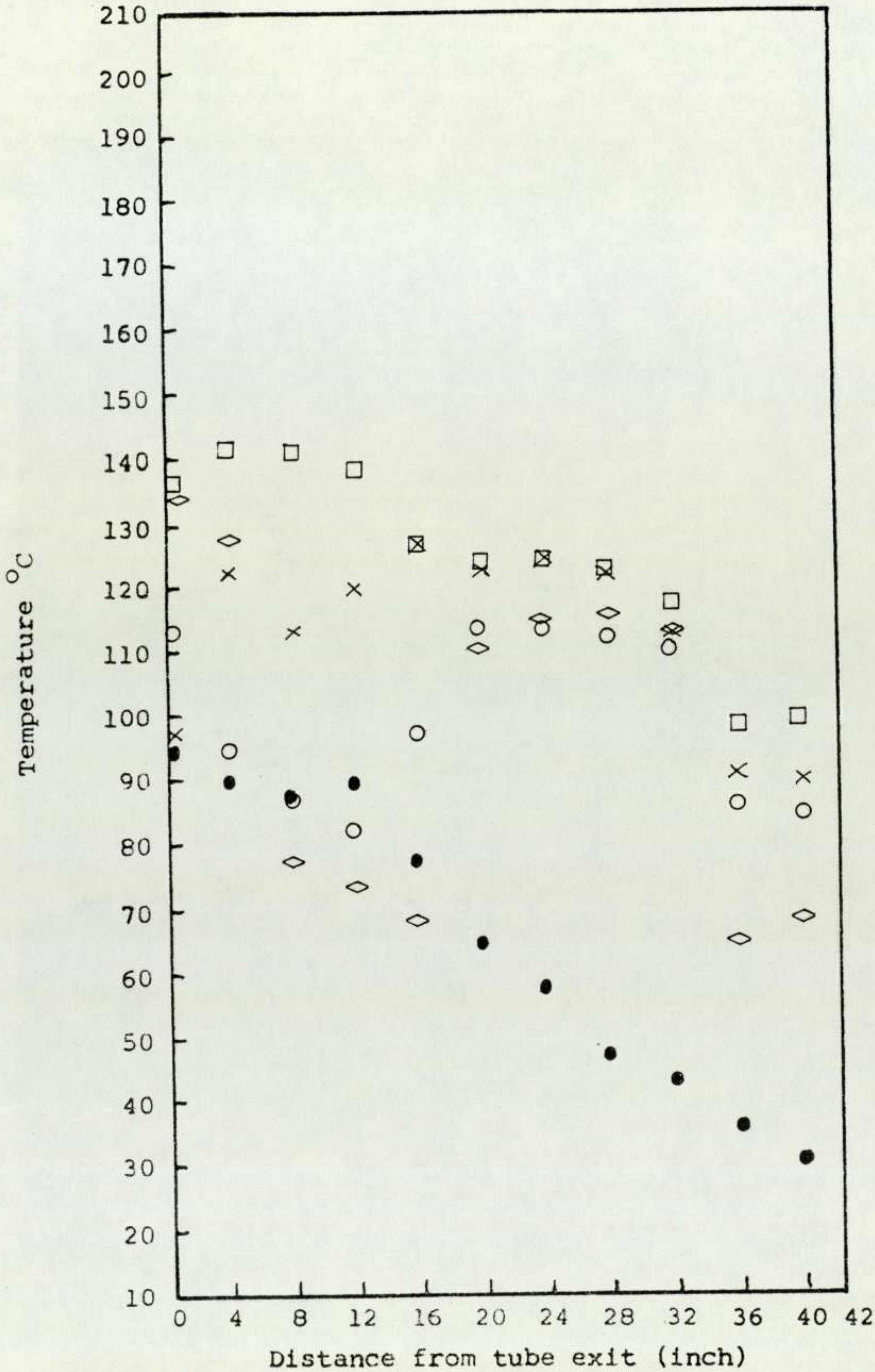

FIG.4.23 Variation of wall temperature along tube (1:1)

fresh air flow 49900 ft^3/hr and Secondary air flow 76200 ft^3/hr

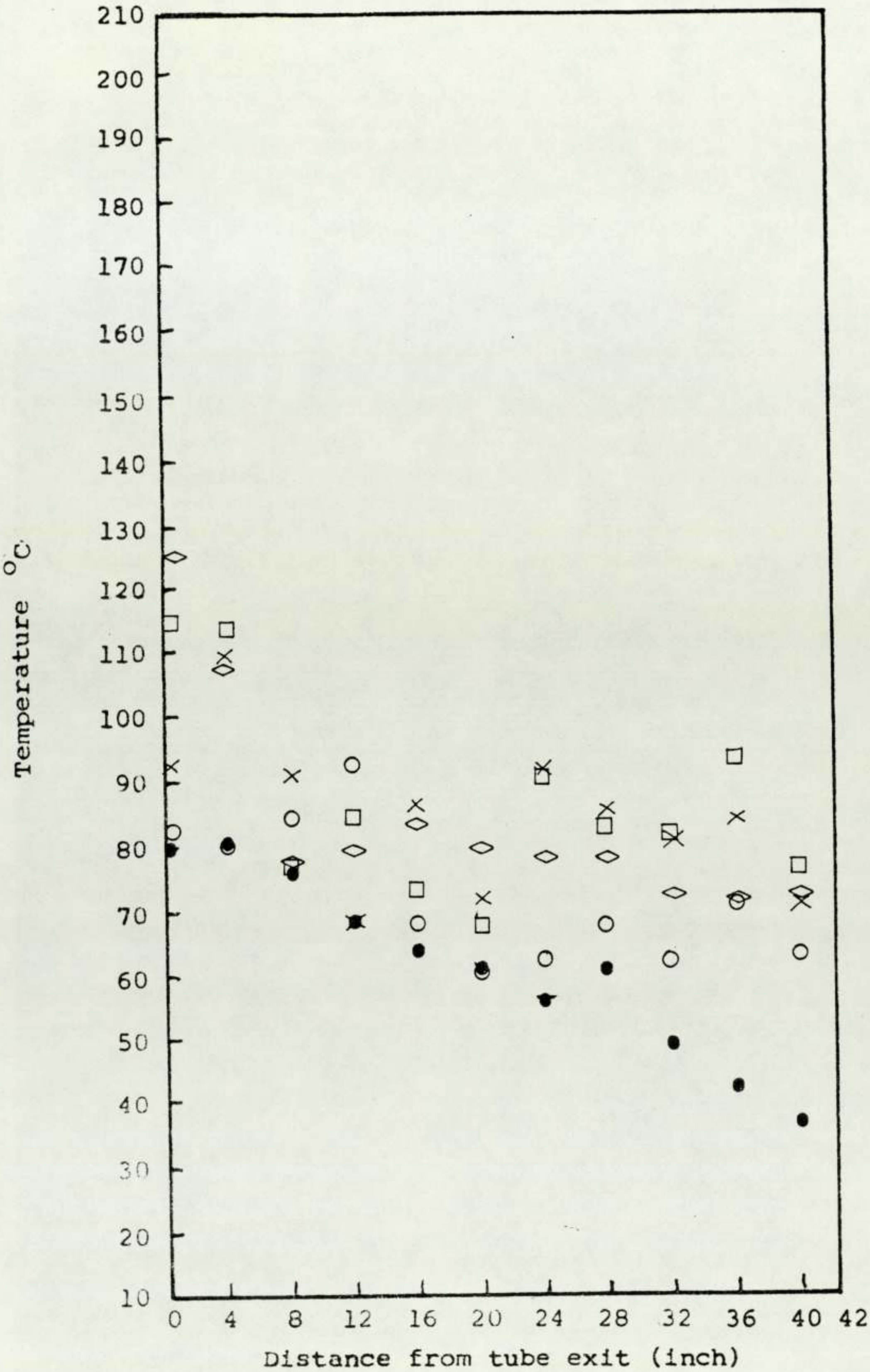

FIG.4.24 Variation of wall temperature along tube (1:5)
fresh air flow 49900 ft^3/hr and secondary
air flow 76200 ft^3/hr.

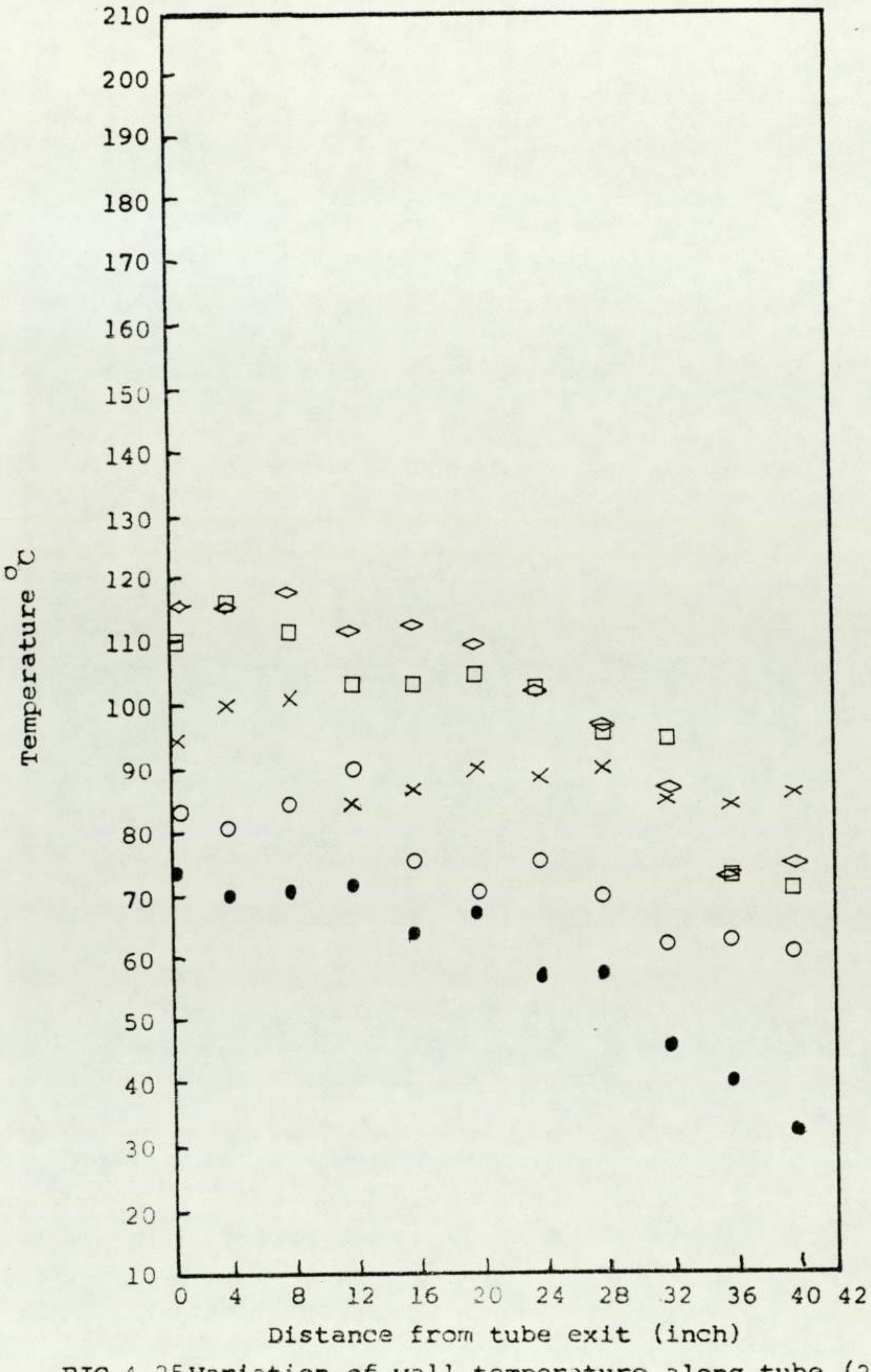

FIG.4.25 Variation of wall temperature along tube (2:3) fresh air flow 49900 ft^3/hr and secondary air flow 76200 ft^3/hr

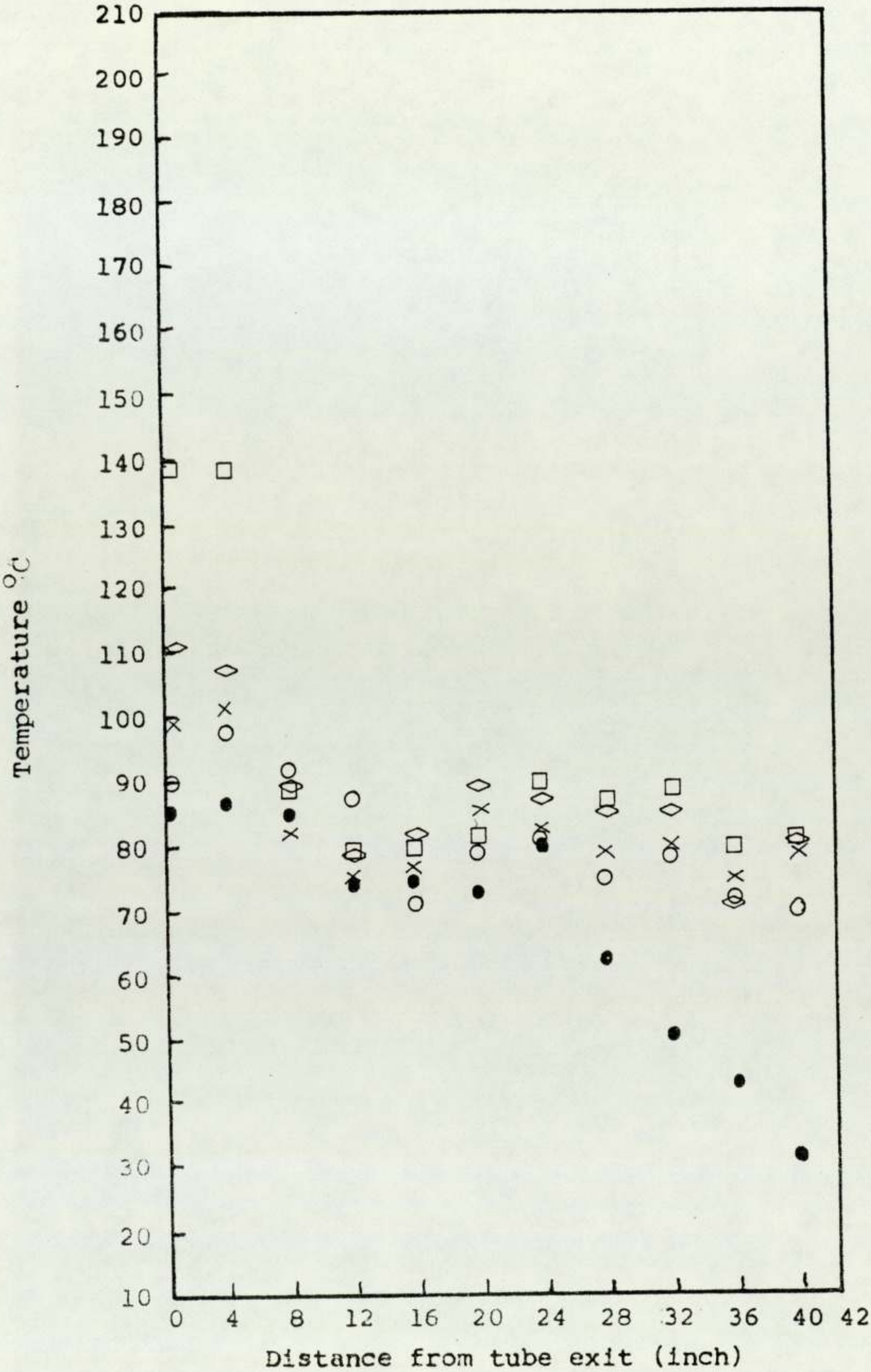

FIG.4.26 Variation of wall temperature along tube (2:6)
fresh air flow 49900 ft^3/hr and secondary
air flow 76200 ft^3/hr

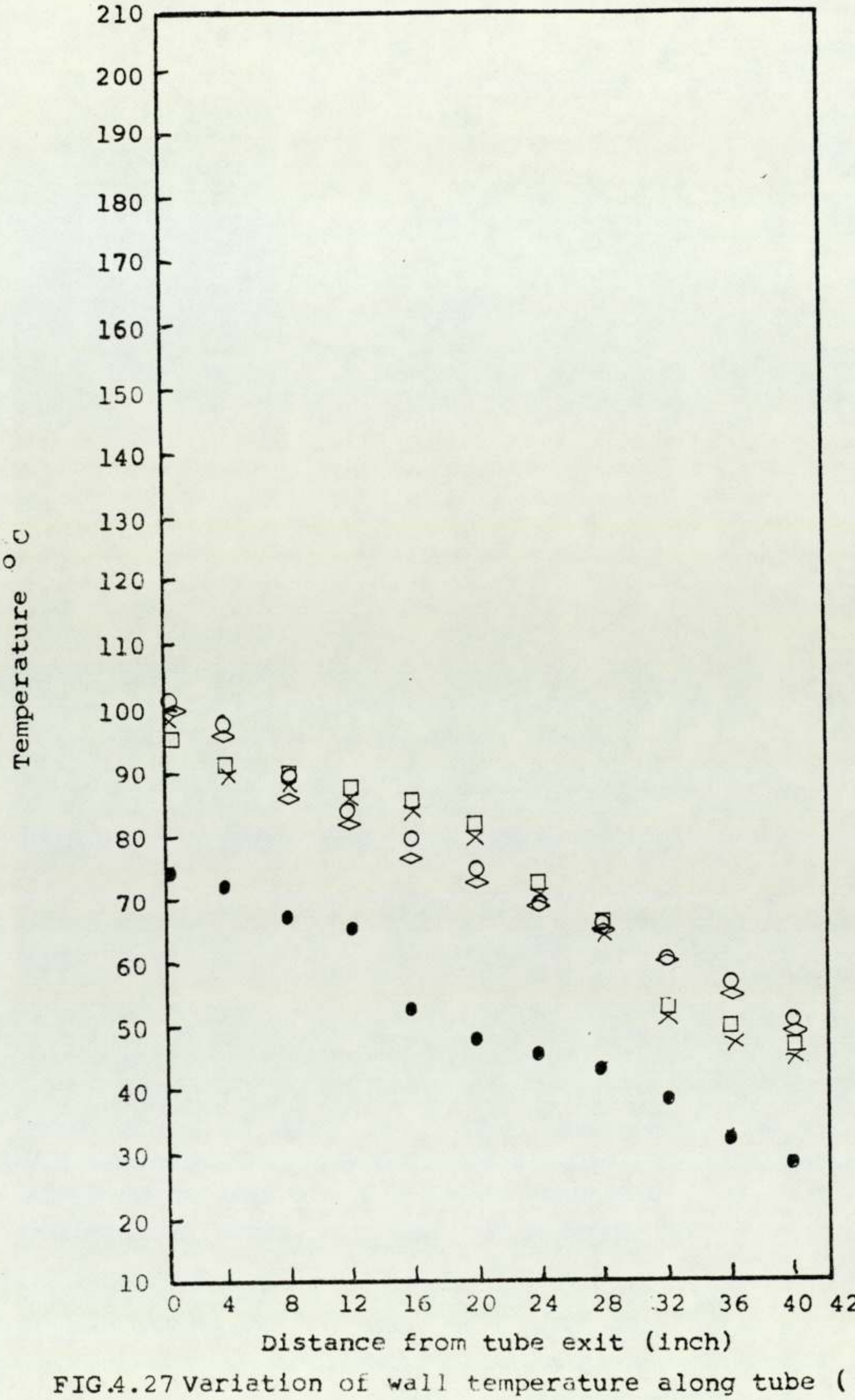

FIG.4.27 Variation of wall temperature along tube (6:3)
fresh air flow 49900 ft^3/hr and secondary
air flow 76200 ft^3/hr

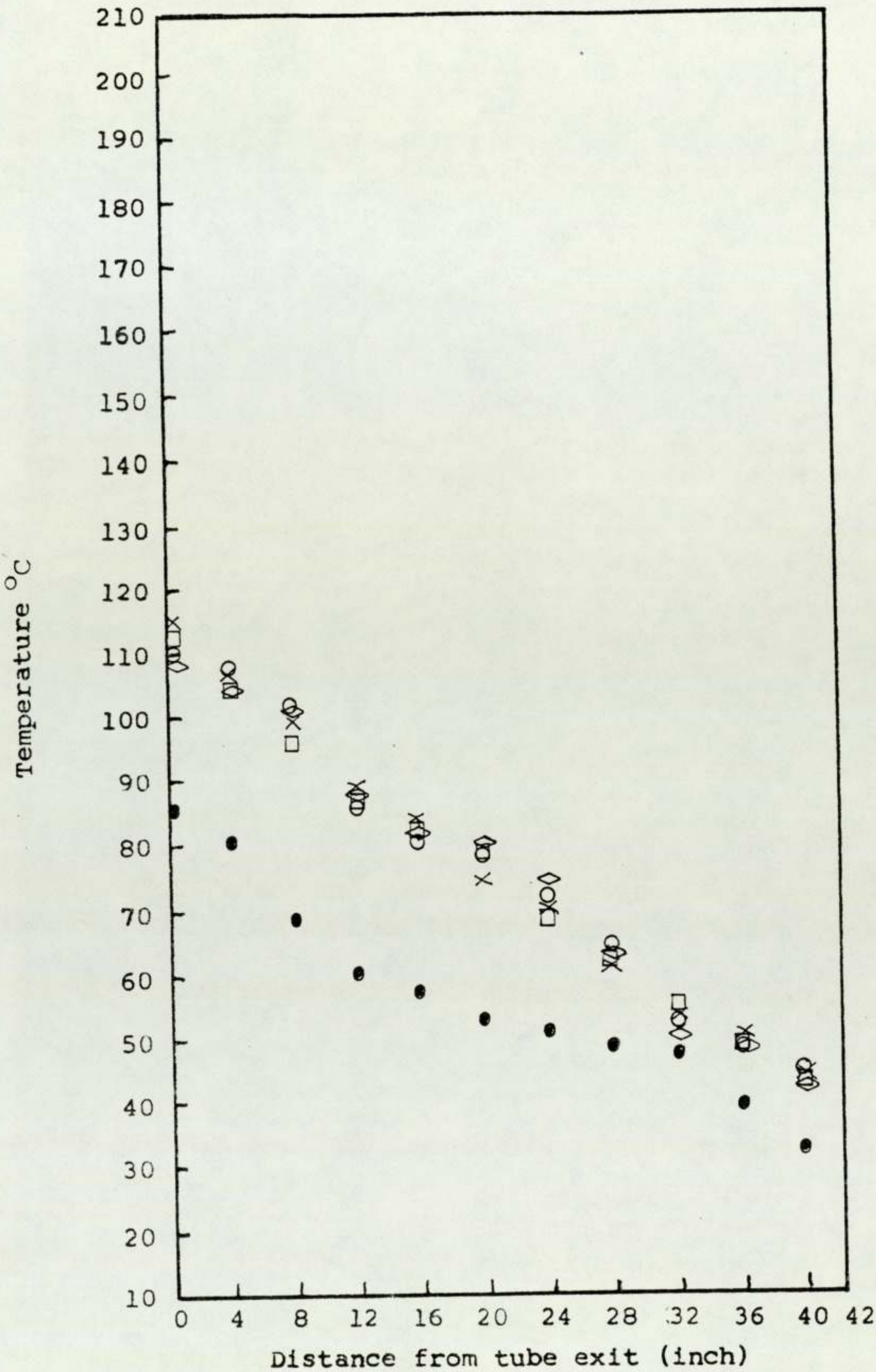

FIG.428 Variation of wall temperature along tube (8:1)
fresh air flow 49900 ft^3/hr and secondary
air flow 76200 ft^3/hr

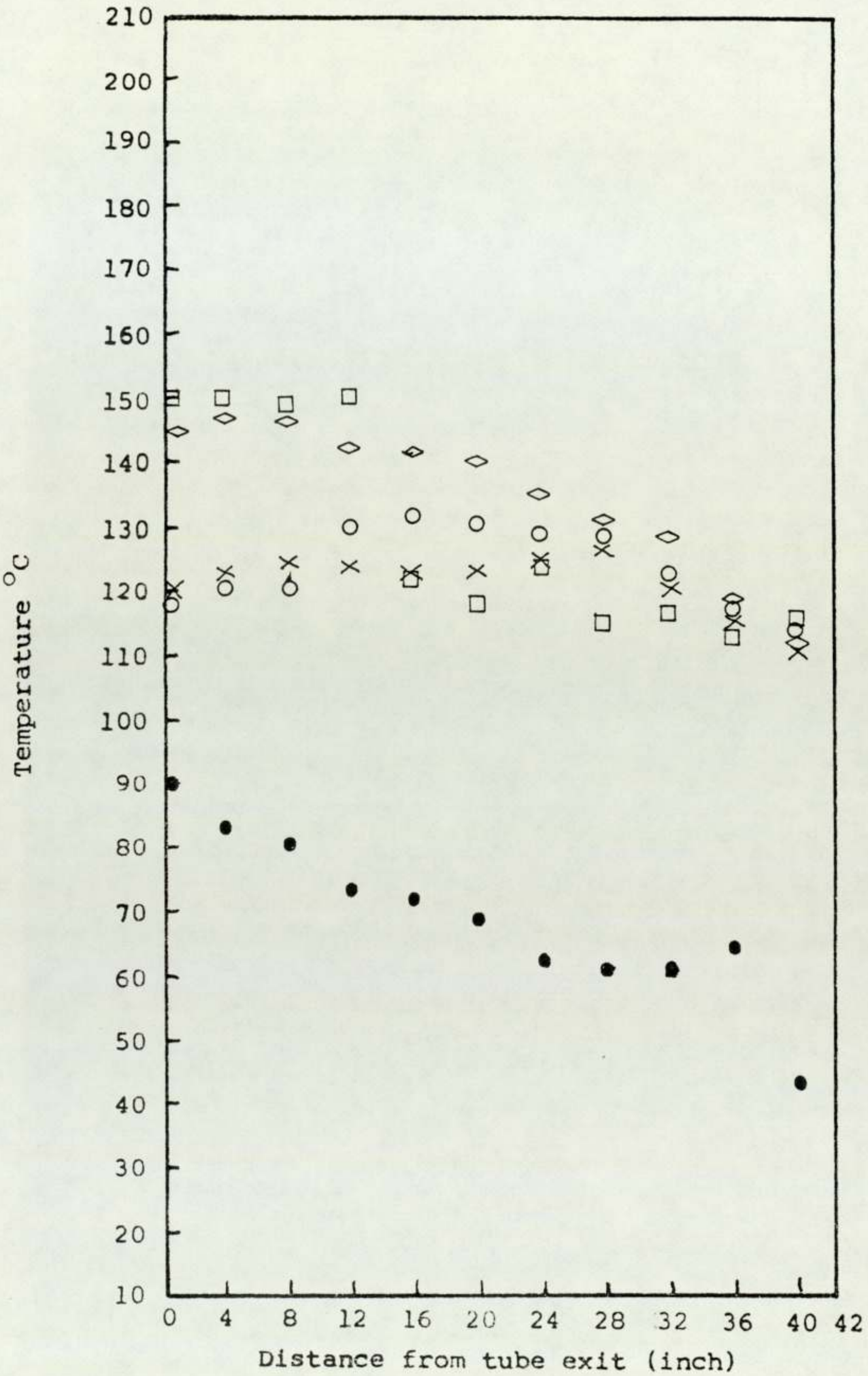

FIG.4.29Variation of wall temperature along tube (1:1)
fresh air flow 31602 ft^3/hr and secondary air flow 76200 ft^3/hr.

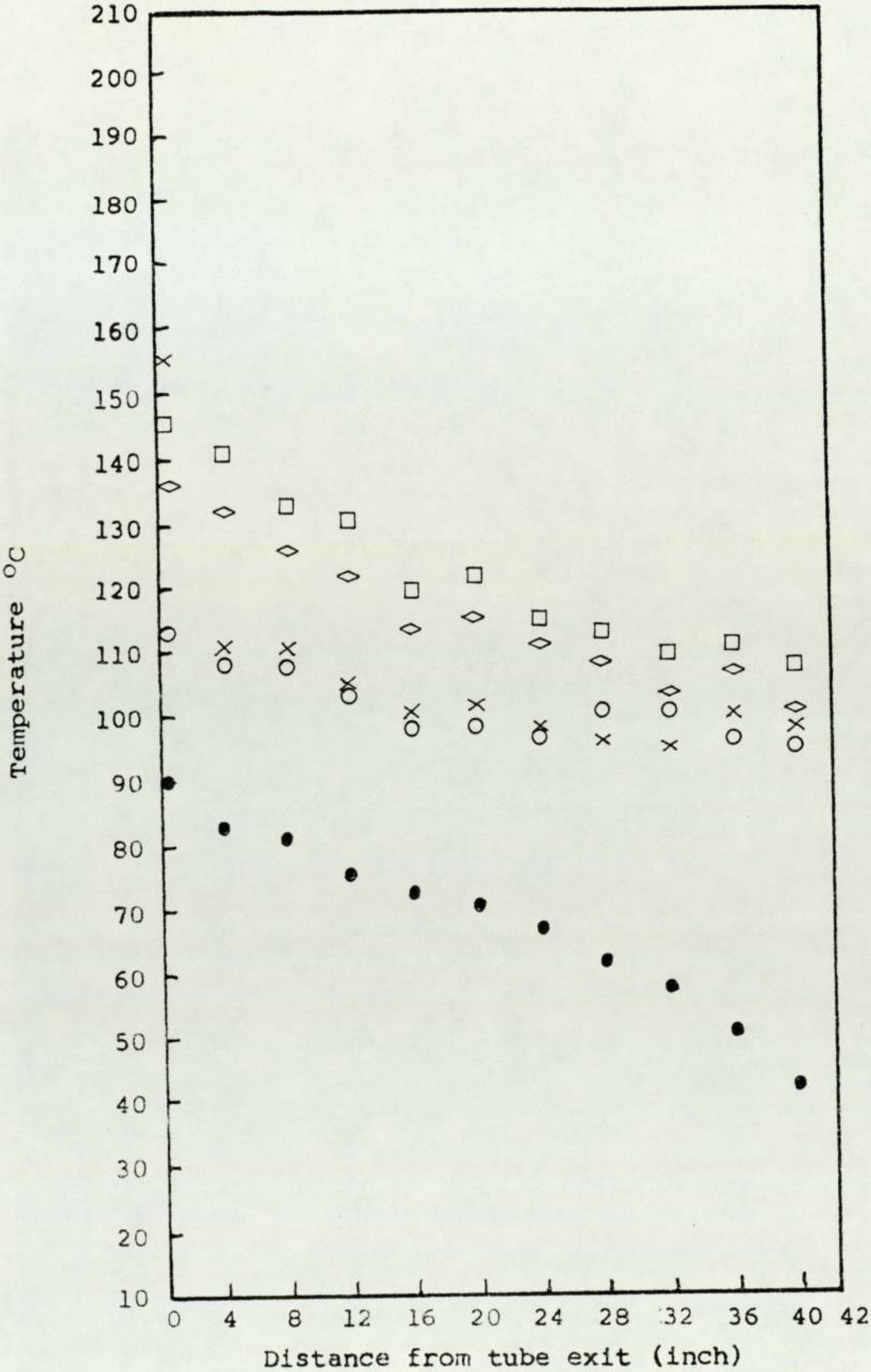

FIG.4.30 Variation of wall temperature along tube (1:5)

fresh air flow 31602 ft^3Hr and secondary

air flow 76200 ft^3/hr.

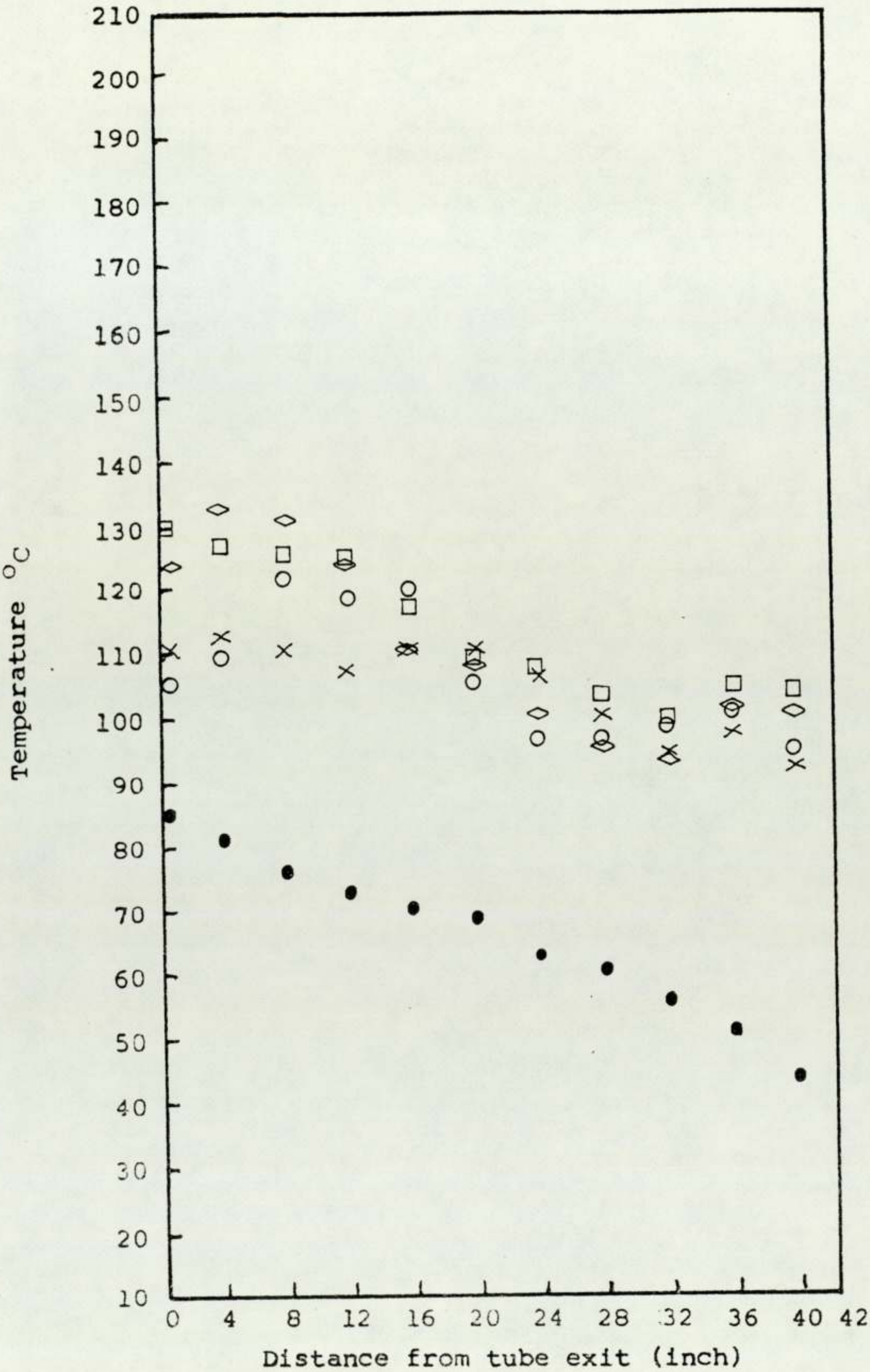

FIG.4.31 Variation of wall temperature along tube (2:3)

fresh air flow 31602 ft^3/hr and secondary

air flow 76200 ft^3/hr.

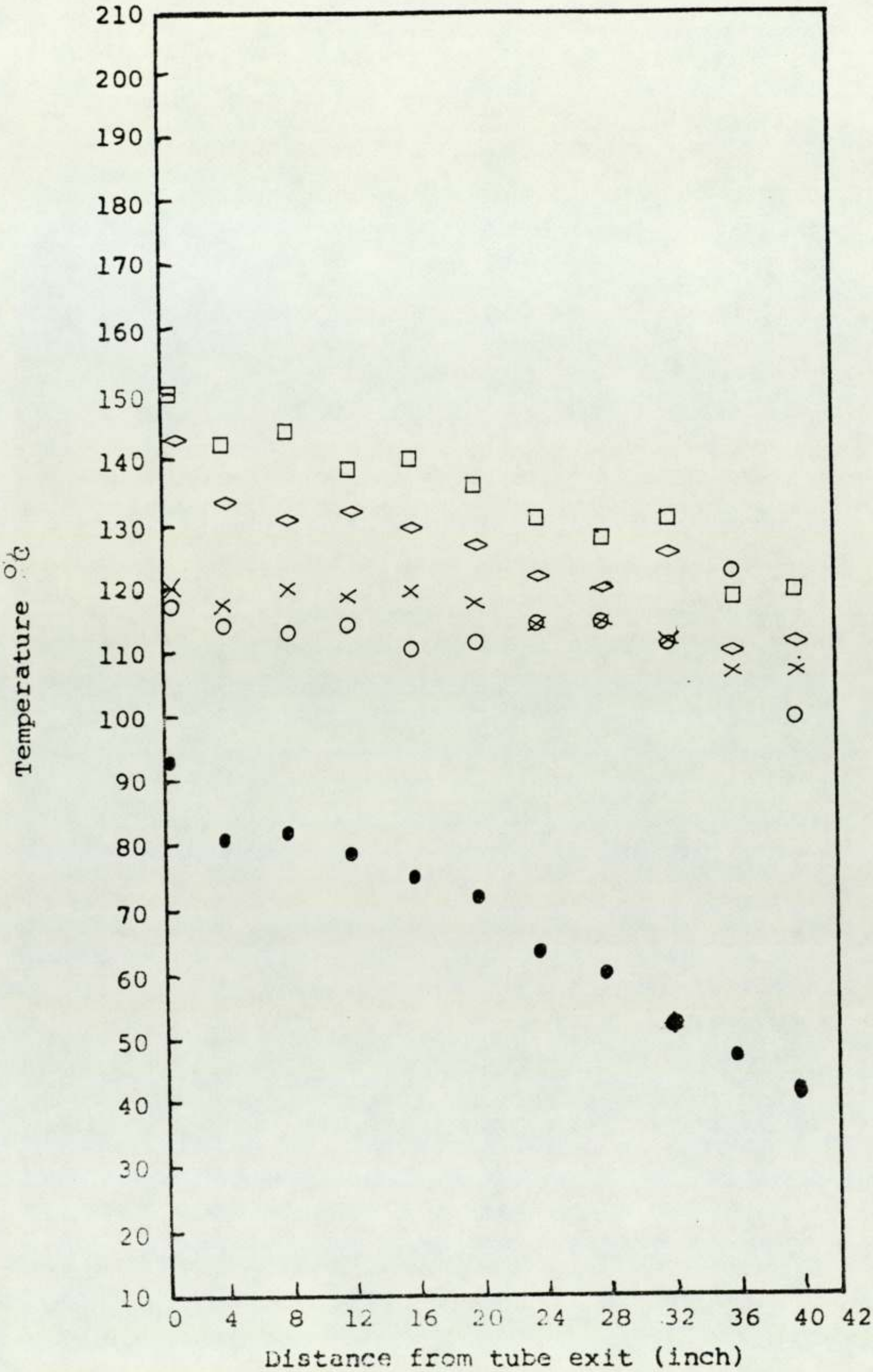

FIG.4.32 Variation of wall temperature along tube (2:6)
fresh air flow 31602 ft^3/hr and secondary
air flow 76200 ft^3/hr.

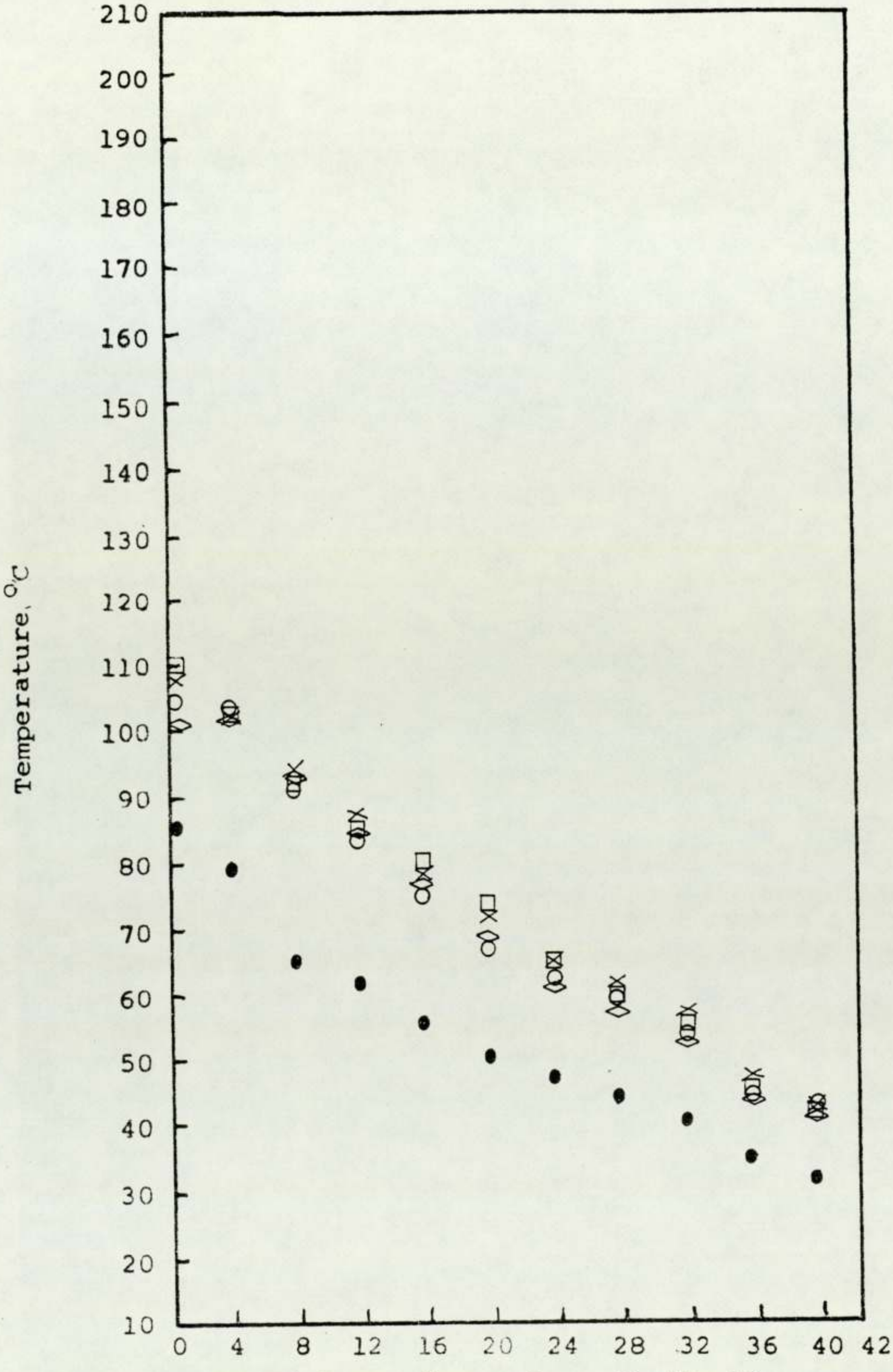

FIG.4.33 Variation of wall temperature along tube (6:3) fresh air flow 31602 ft^3/hr and secondary air flow 76200 ft^3/hr.

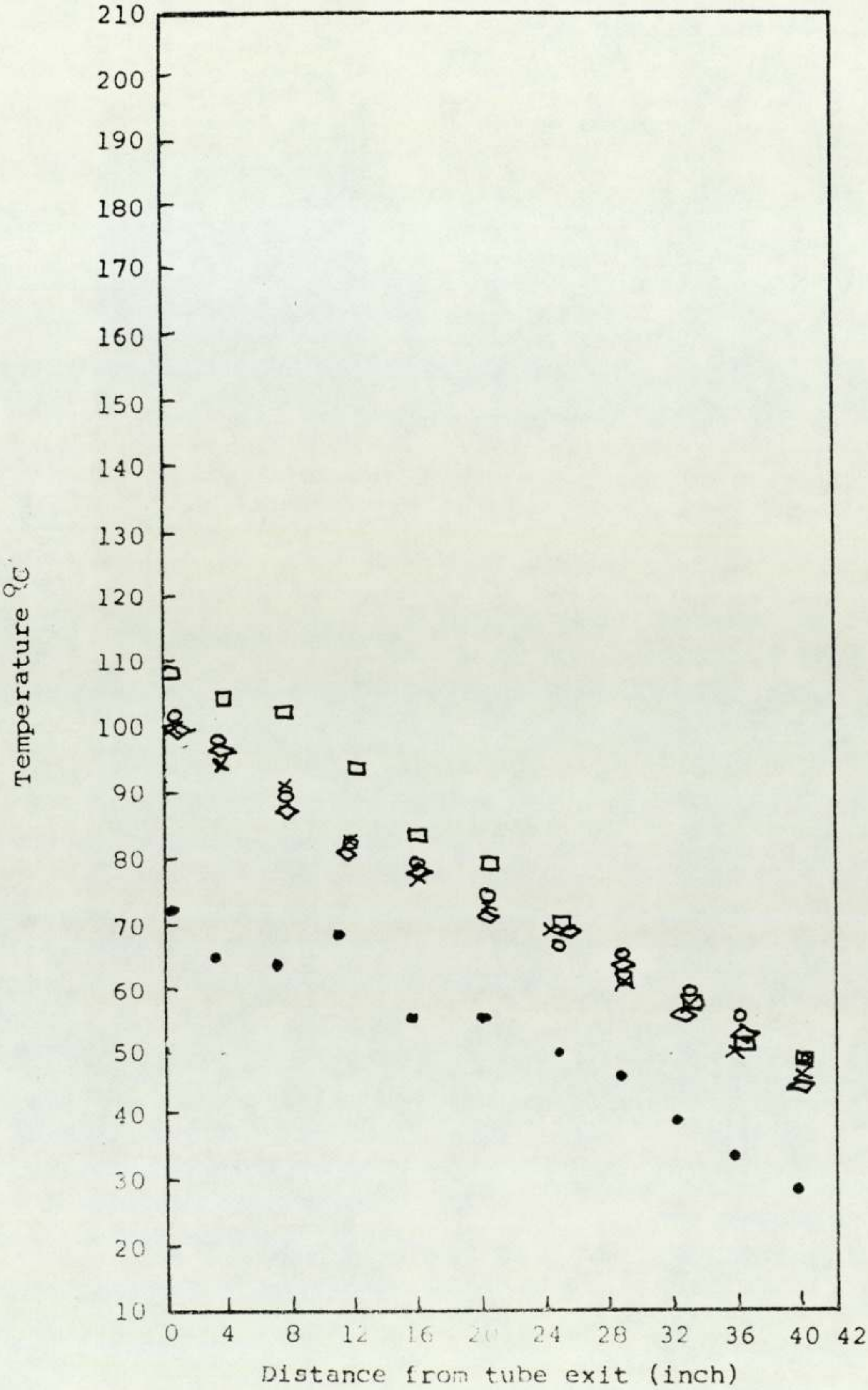

FIG.4.34 Variation of wall temperature along tube (8:1) fresh air flow 31602 ft^3/hr and secondary air flow 76200 ft^3/hr.

temperature profile. Radial wall temperatures did not show significant differences and were very near to each other, including the stagnation point face. See figures (4.29) to (4.34).

Changing fresh air flow did not cause any noticeable difference in wall temperature profile.

In order to judge whether the effect on the wall temperature profile on the frontal tubes in the bundle, was due to radiation effects or flow irregularity, (i.e., entrance effect at the bundle front) the secondary air flow rate was kept constant at 76200ft^3/hr, (2157m^3/hr) and two natural gas flow rates (300 ft^3/hr, (8.5m^3/hr) and 600 ft^3/hr,) (17 m^3/hr) were used. It follows from figures (4.35 to 4.42) that when the natural gas flow was increased from 300ft^3/hr, (8.5m^3/hr) to 600ft^3/hr, (17 m^3/hr) more scattering was observed on the frontal tubes (1:1), (2:6), (1:5) and (2:3). This means, that since at a natural gas flow of 300ft^3/hr, (8.5m^3/h) scattering was also noticed and it increased greatly at 600 ft^3/hr, (17 m^3/hr) the radiation effect must exist, though on a small scale. The flow disturbance also has an appreciable effect.

It was noticed from figures (43 to 46) for tubes (1:3), (1:6), (4:4), and (8:3) for burner number two in operation, that the wall temperatures were not decreasing along the tube length from exit to inlet ends for the

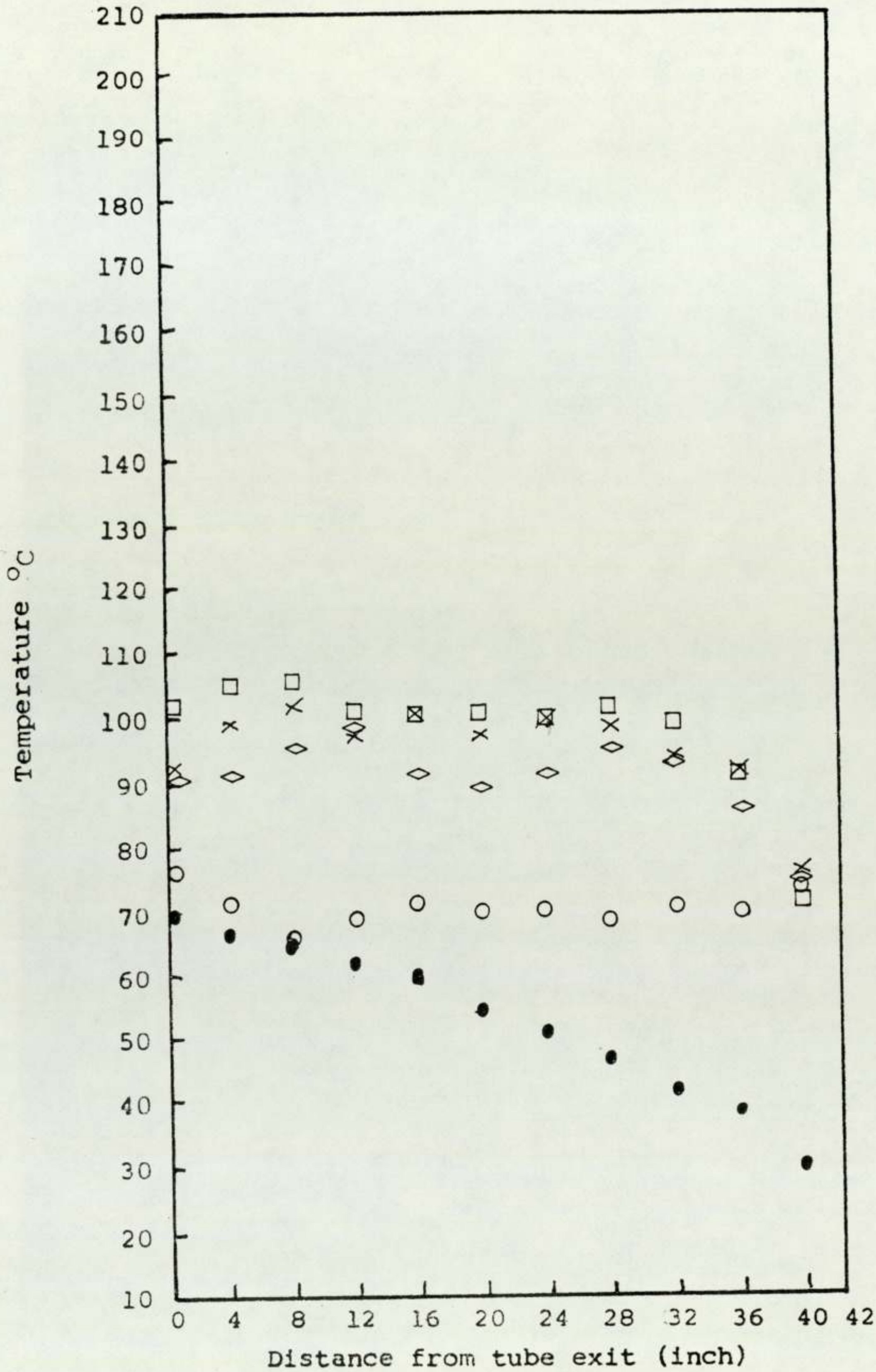

FIG.4.35 Variation of wall temperature along tube (1:1)

Natural gas flow 300ft^3/hr and secondary air flow 76200 ft^3/hr.

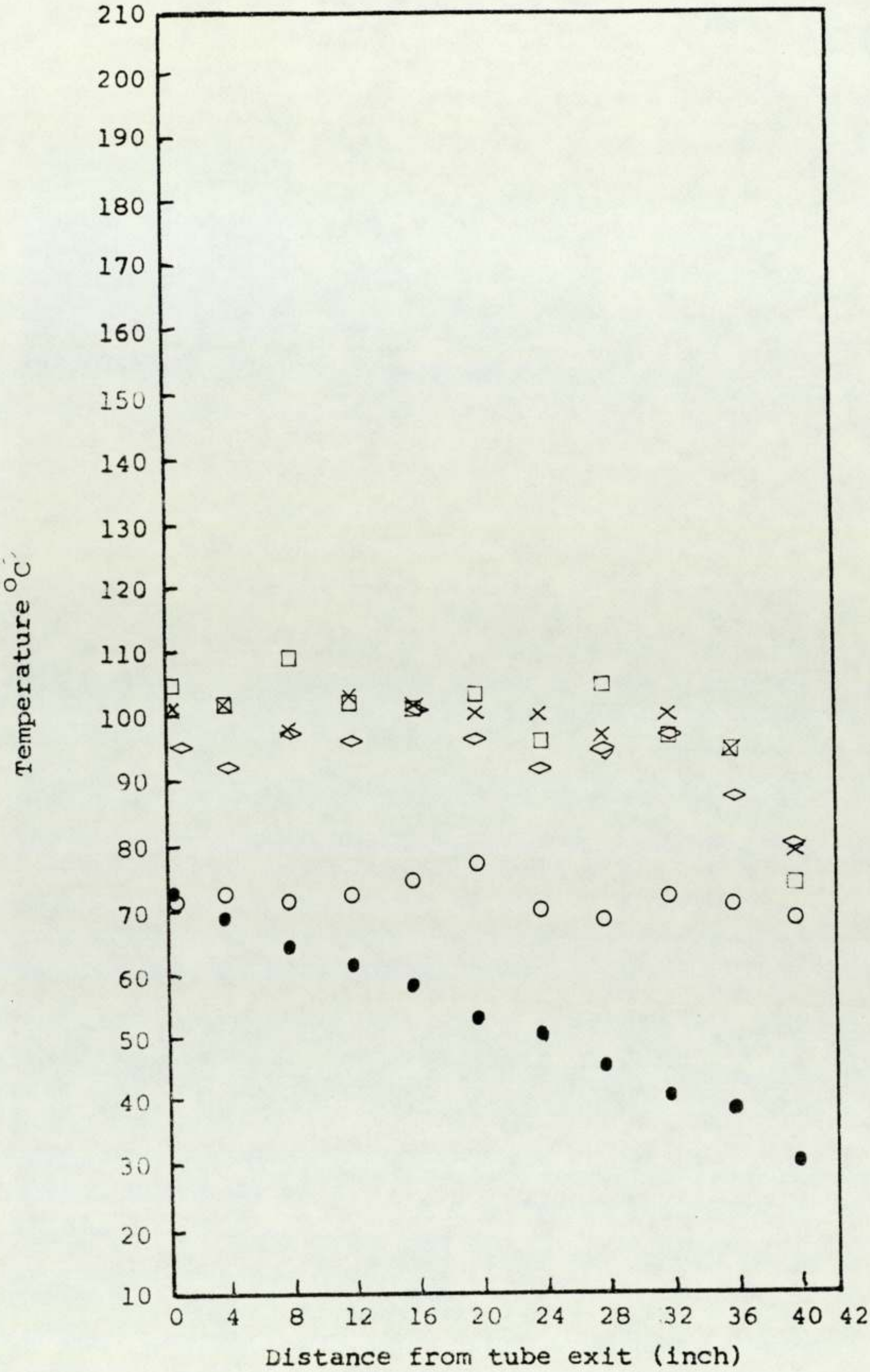

FIG.4.36 Variation of wall temperature along tube (1:5)

Natural gas flow 300 ft^3/hr and secondary air flow 76200 ft^3/hr.

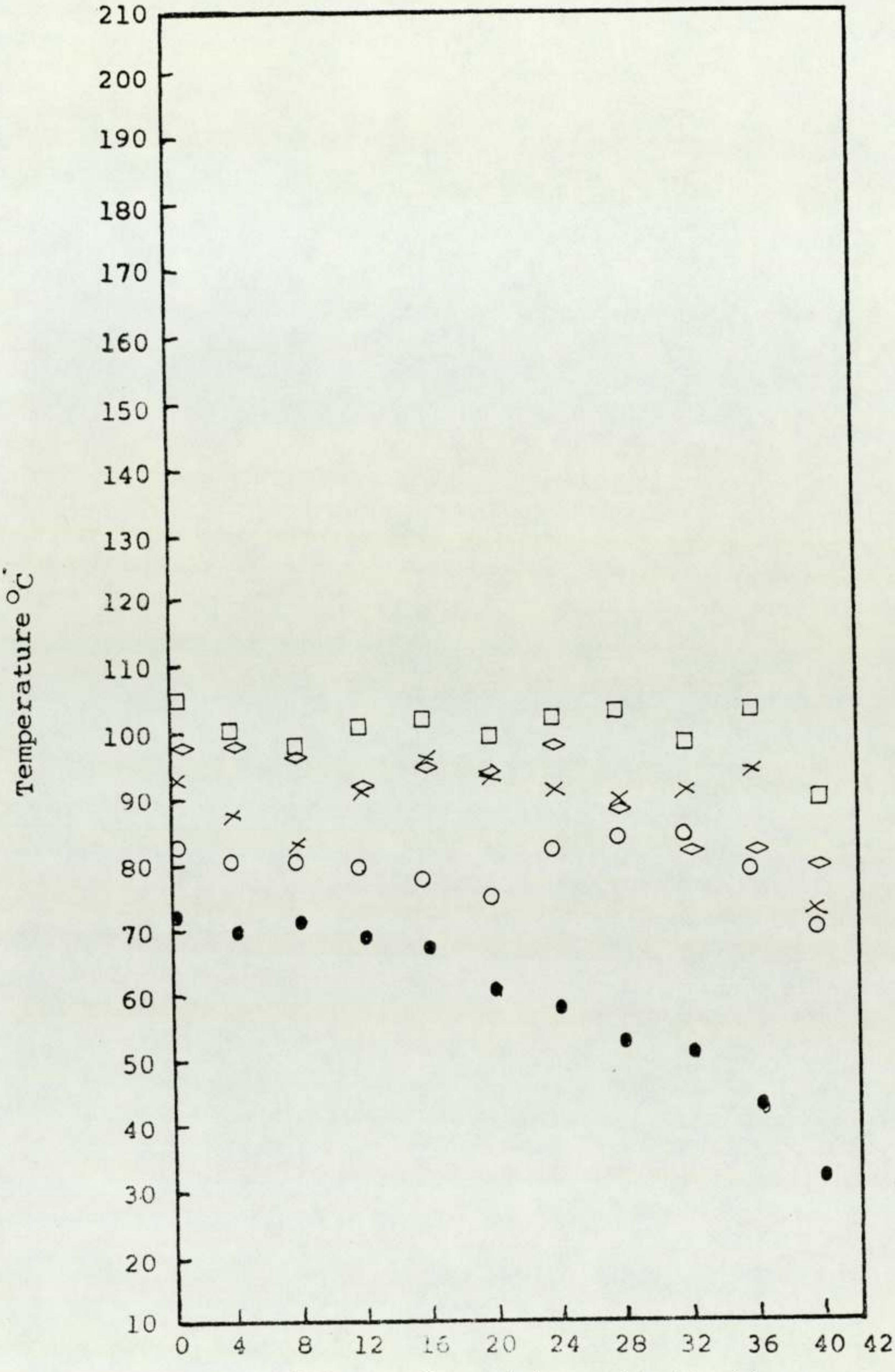

FIG.4.37 Variation of wall temperature along tube (2.3)

Natural gas flow 300 ft^3/hr and secondary air flow 76200 ft^3/hr.

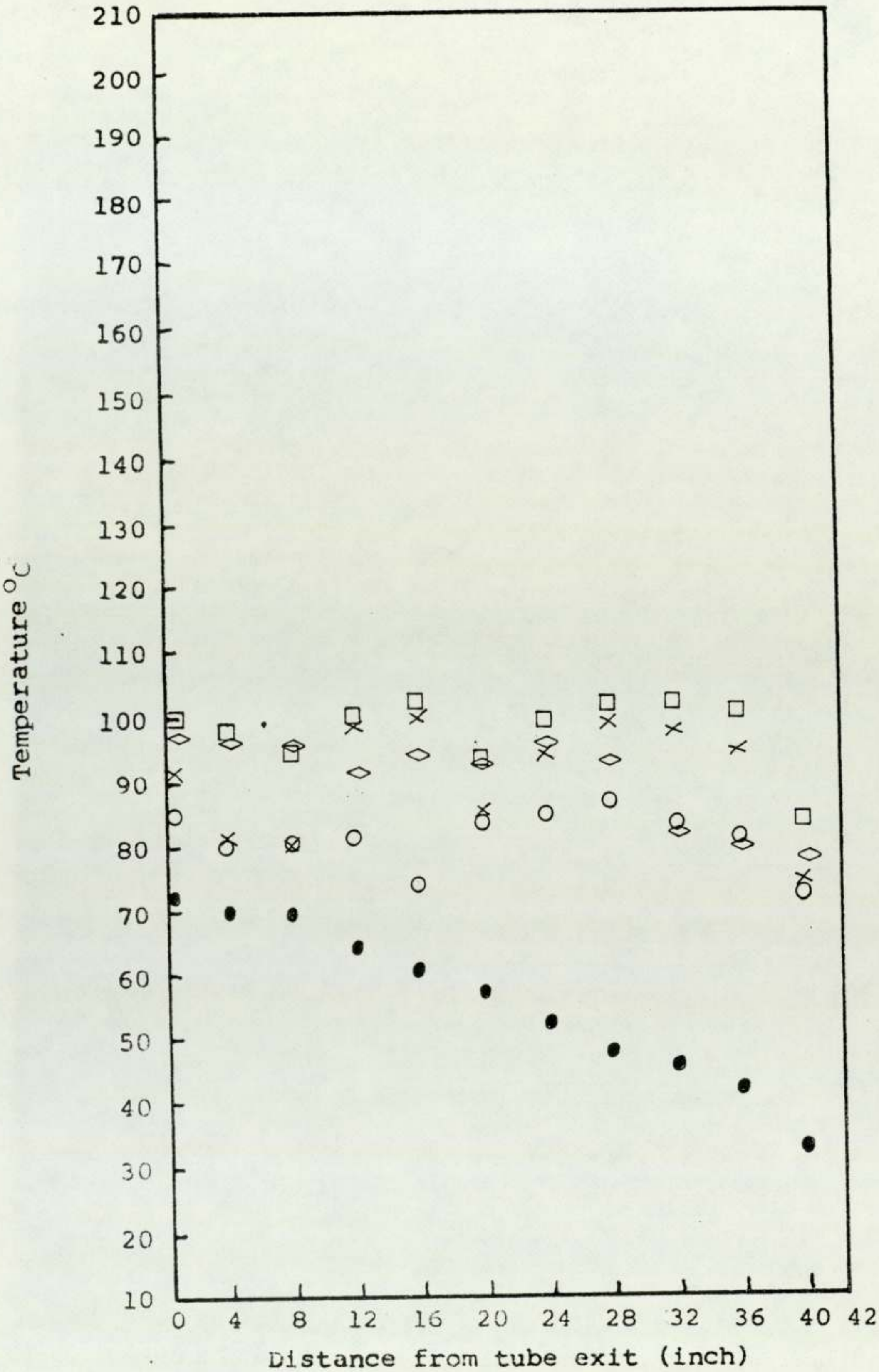

FIG.4.38 Variation of wall temperature along tube (2:6)

Natural gas flow 300 ft^3/hr and secondary air flow 76200 ft^3/hr.

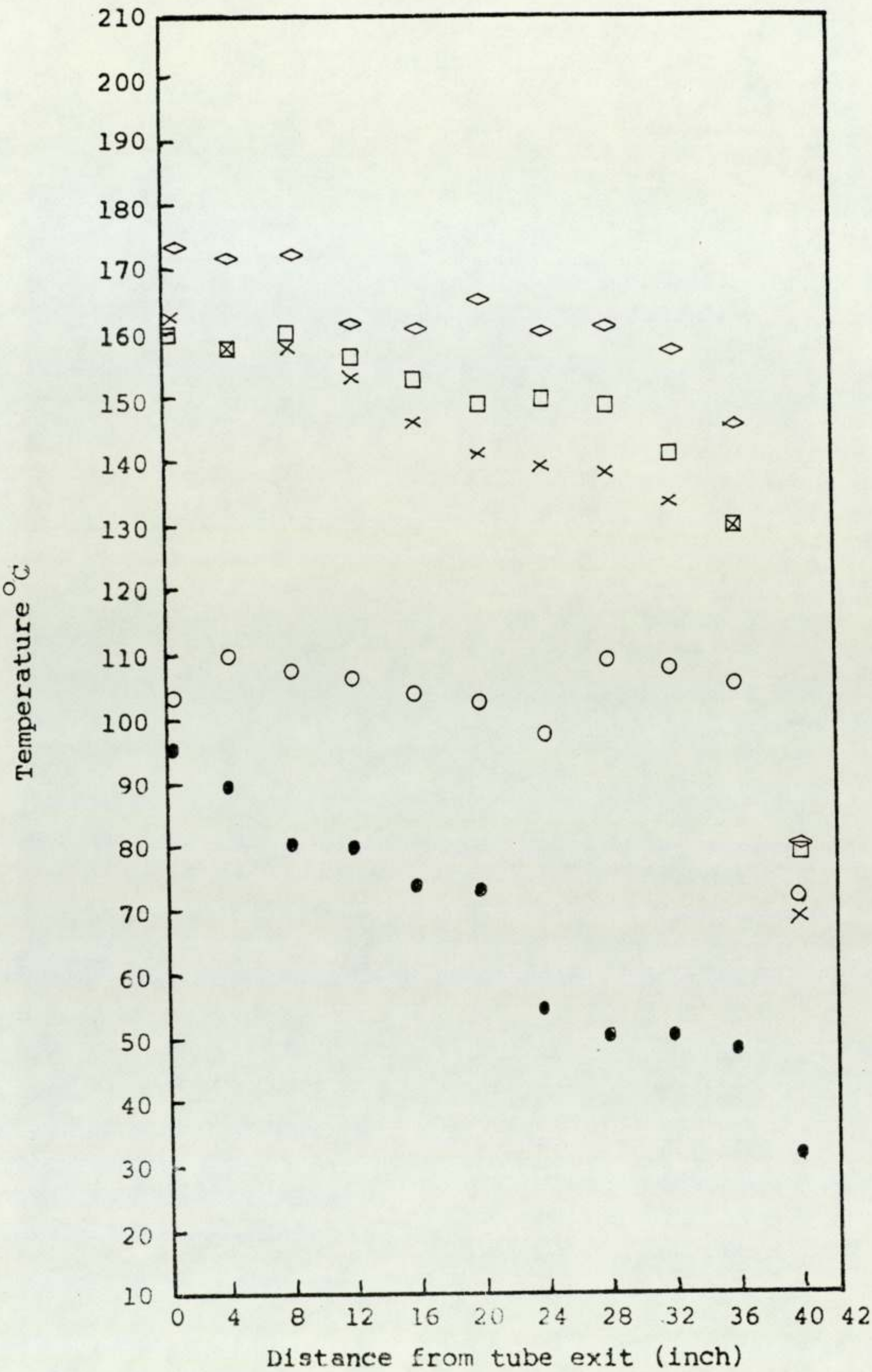

FIG.4.39 Variation of wall temperature along tube (1:1)

Natural gas flow 600 ft^3/hr and secondary air flow 76200 ft^3/hr.

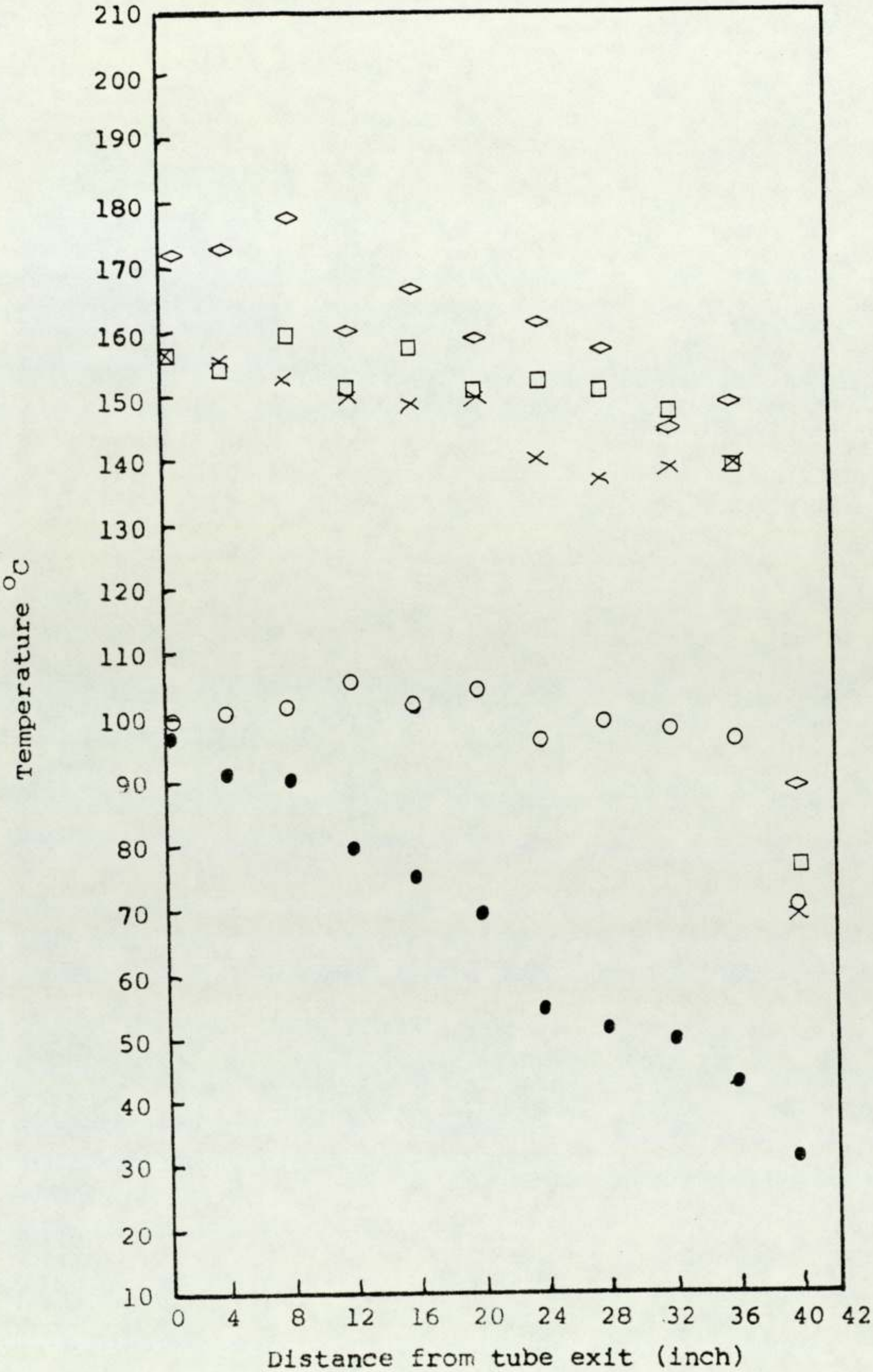

FIG.4.40 Variation of wall temperature along tube (1.5)
Natural gas flow 600 ft^3/hr and secondary air flow 76200 ft^3/hr.

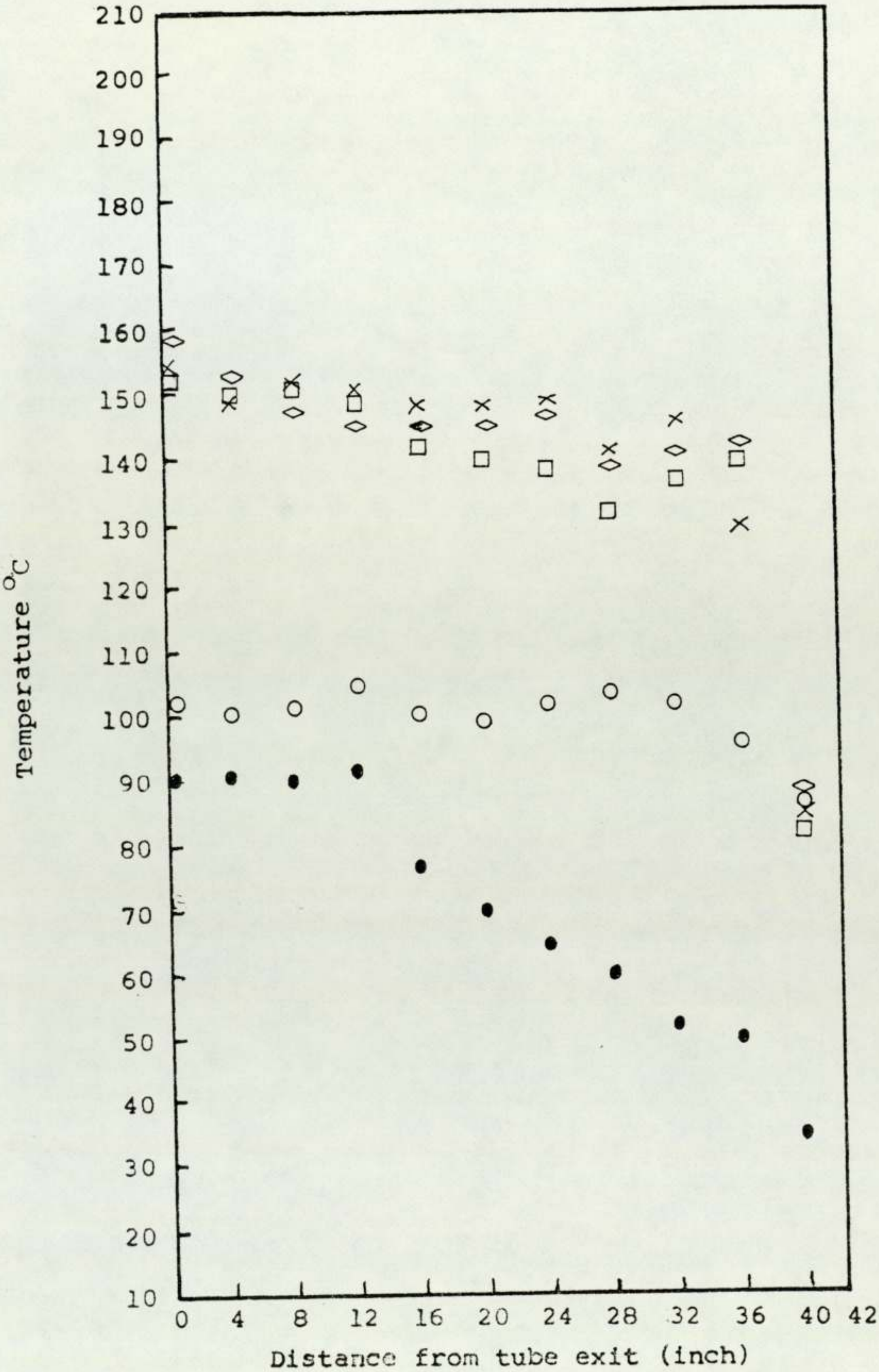

FIG.4.41 Variation of wall temperature along tube (2:3) Natural gas flow 600 ft^3/hr and secondary air flow 76200 ft^3/hr.

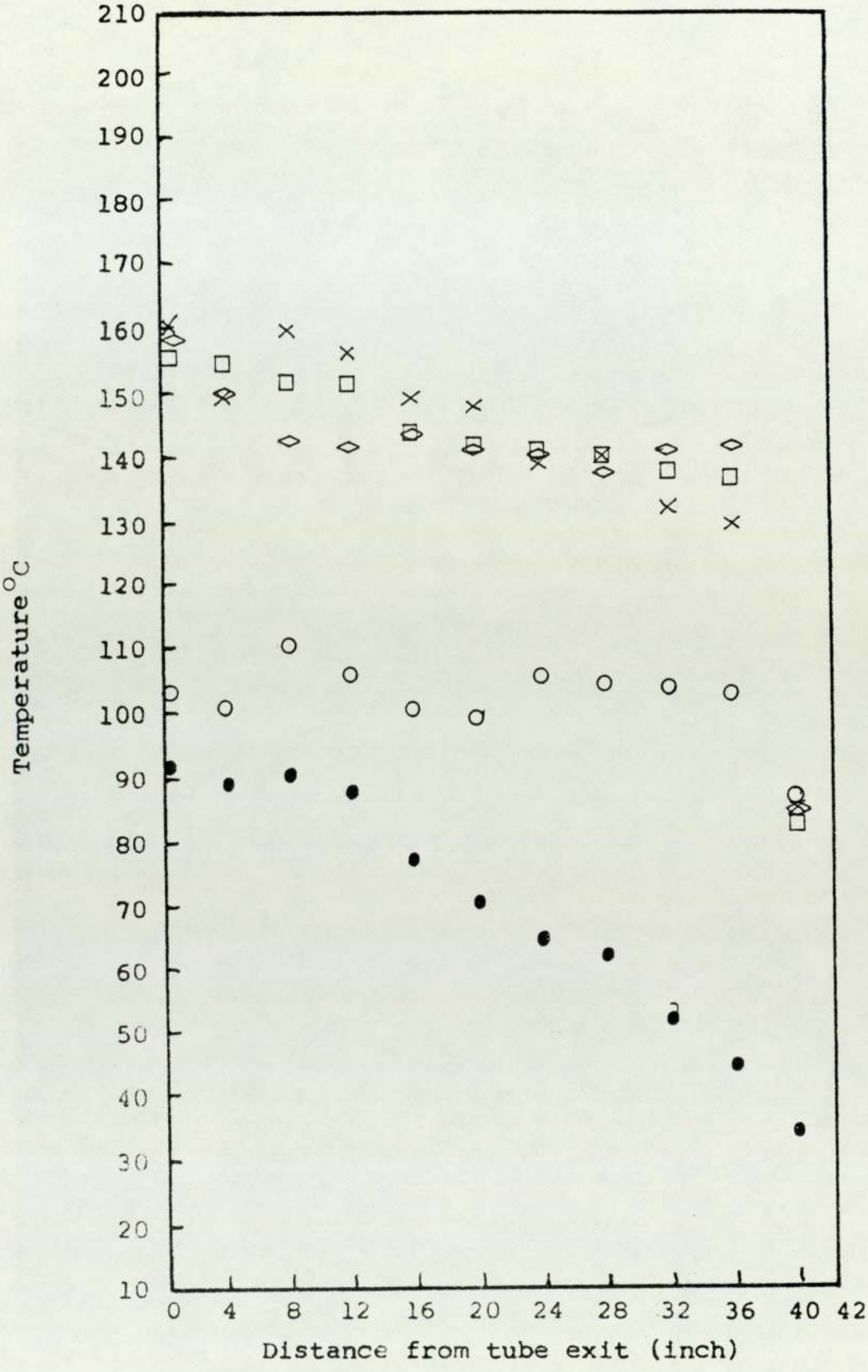

FIG.4.42 Variation of wall temperature along tube (2.6)

Natural gas flow 600 ft^3/hr and secondary air flow 76200 ft^3/hr.

stagnation points only while burner one is in operation also the wall temperature decrease along the tube length, see figures (47 to 50). This means a much higher degree of mixing is needed in the chamber if one burner only is used.

From the incremental heat transfer coefficients, calculated for 100mm intervals along tubes in the bundle, it was noticed that tubes in the frontal rows of the bundle (1:1),(1:5),and (2:3), showed irregularity of inside wall heat transfer coefficients, along the tube length, in figures (4.51)(4.52)and(4.53) much more uniform patterns were observed on tubes (3:1), (7:6) and (10:3) in figures (4.54)(4.55)and(4.56).

An overall conclusion can be drawn that the frontal tubes suffer from disturbance by both radiation and flow entrance effects, and the central and back region of the bundle is much more reliable for correlation.

Results for incremental heat transfer coefficients were obtained by the aid of a computer programme, which includes statistical analysis. See appendix (A.2.3)

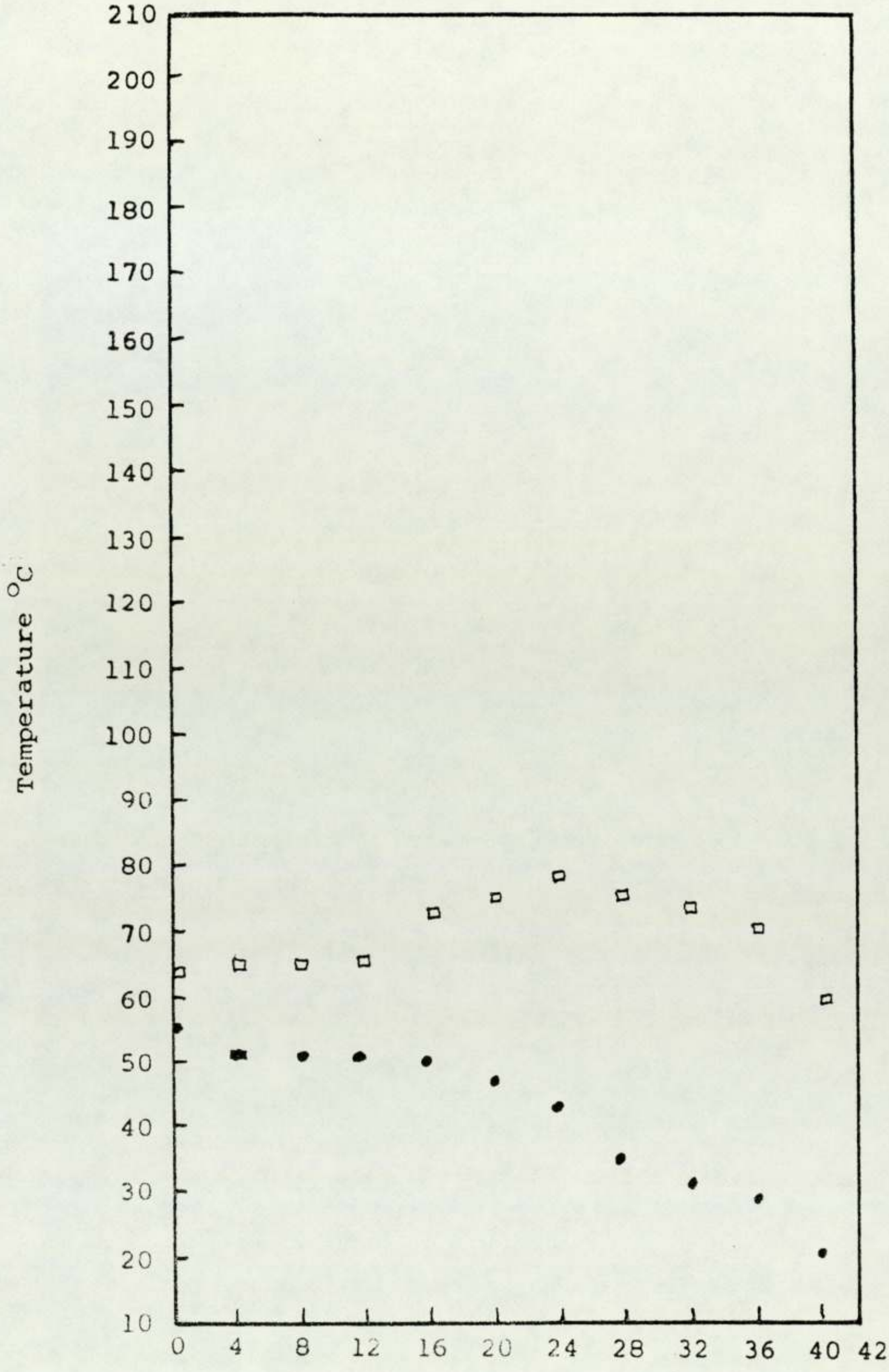

FIG.4.43 Variation of wall temperature along tube (1.3)

with burner number two on.

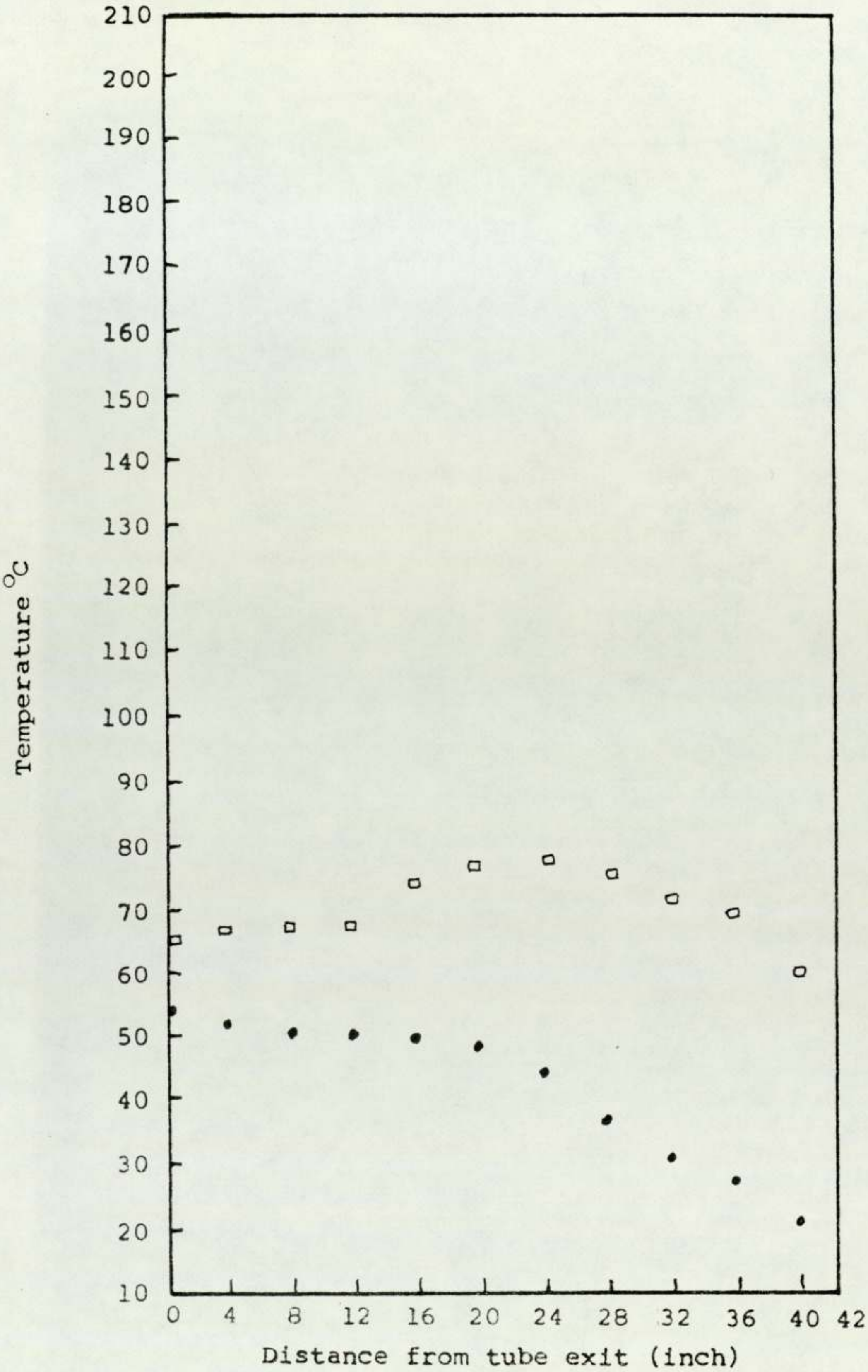

FIG.4.44Variation of wall temperature along tube (1:6)

with burner number two on.

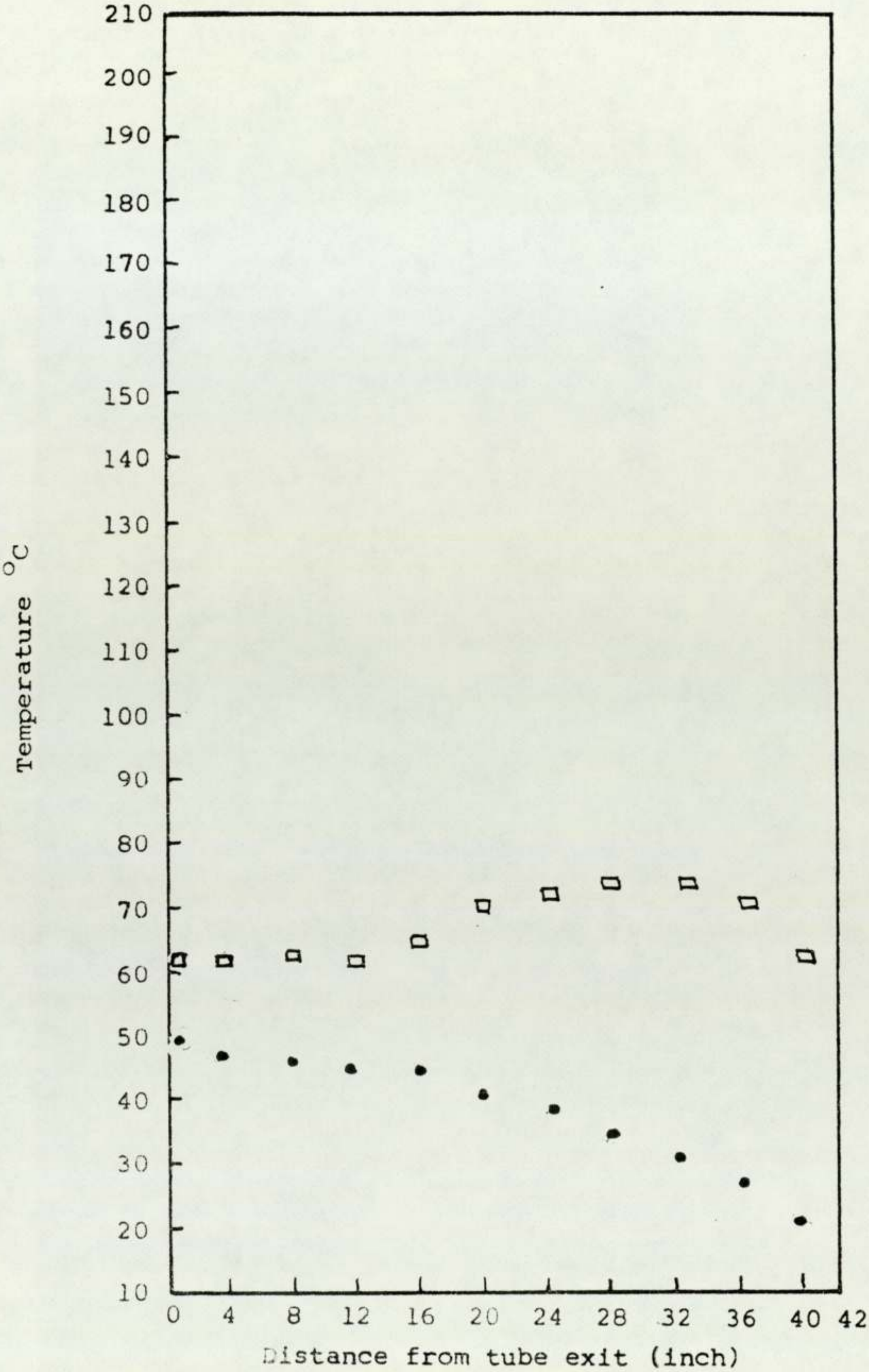

FIG.4.45 Variation of wall temperature along tube (4:4) with burner number two on.

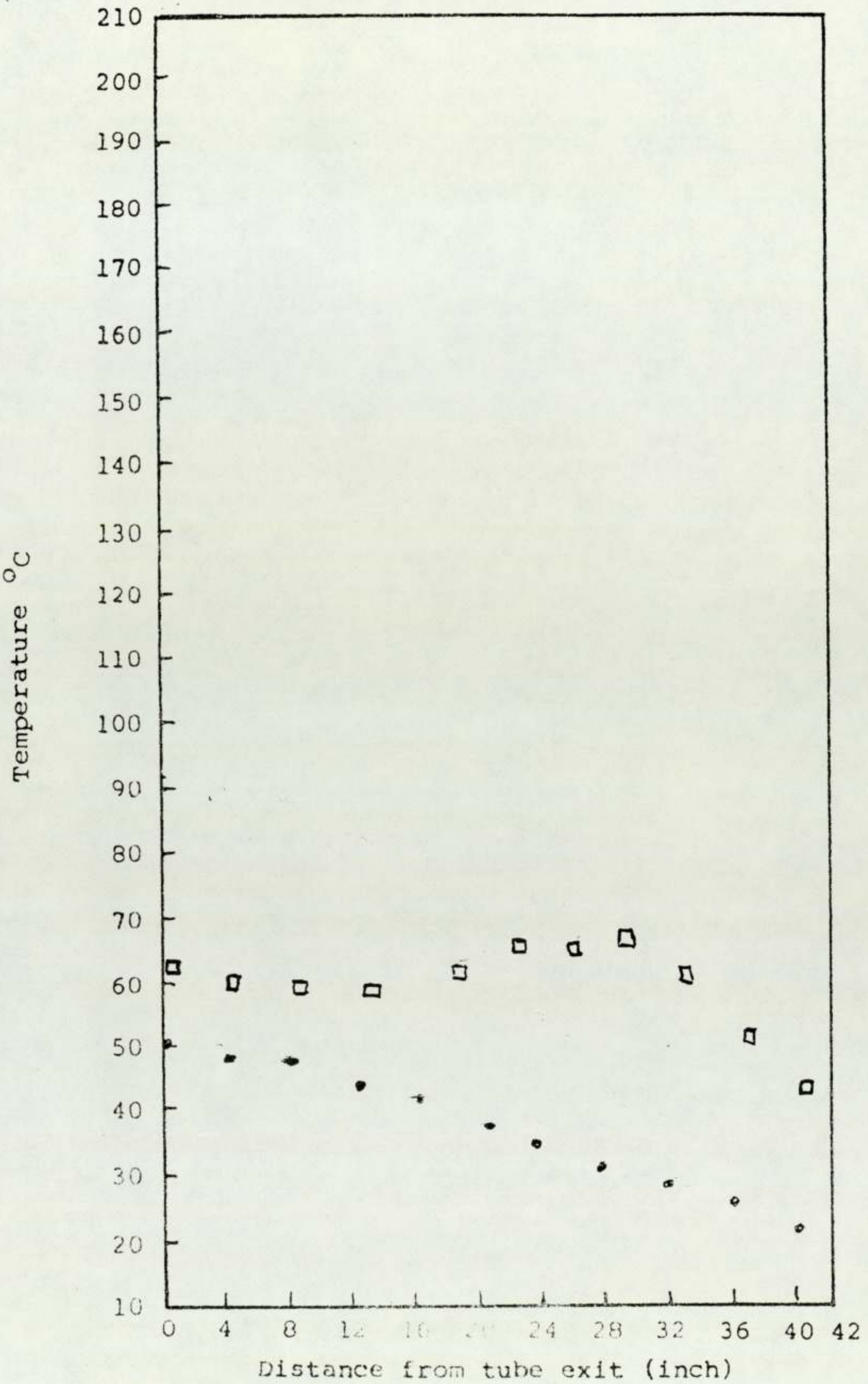

FIG.4.46Variation of wall temperature along tube (8:3)

with burner number two on.

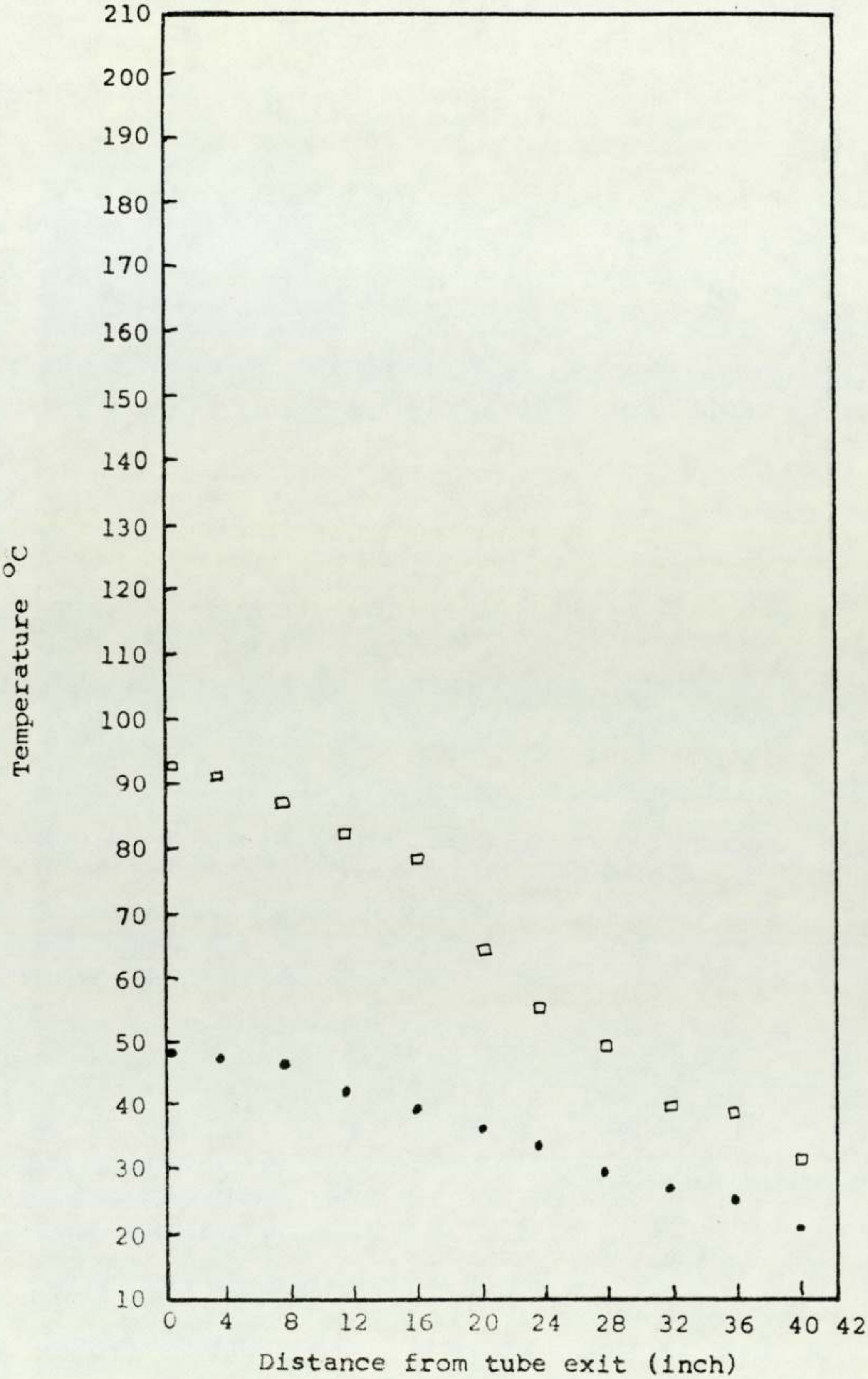

FIG.4.47Variation of wall temperature along tube (1:3)

with burner number one on.

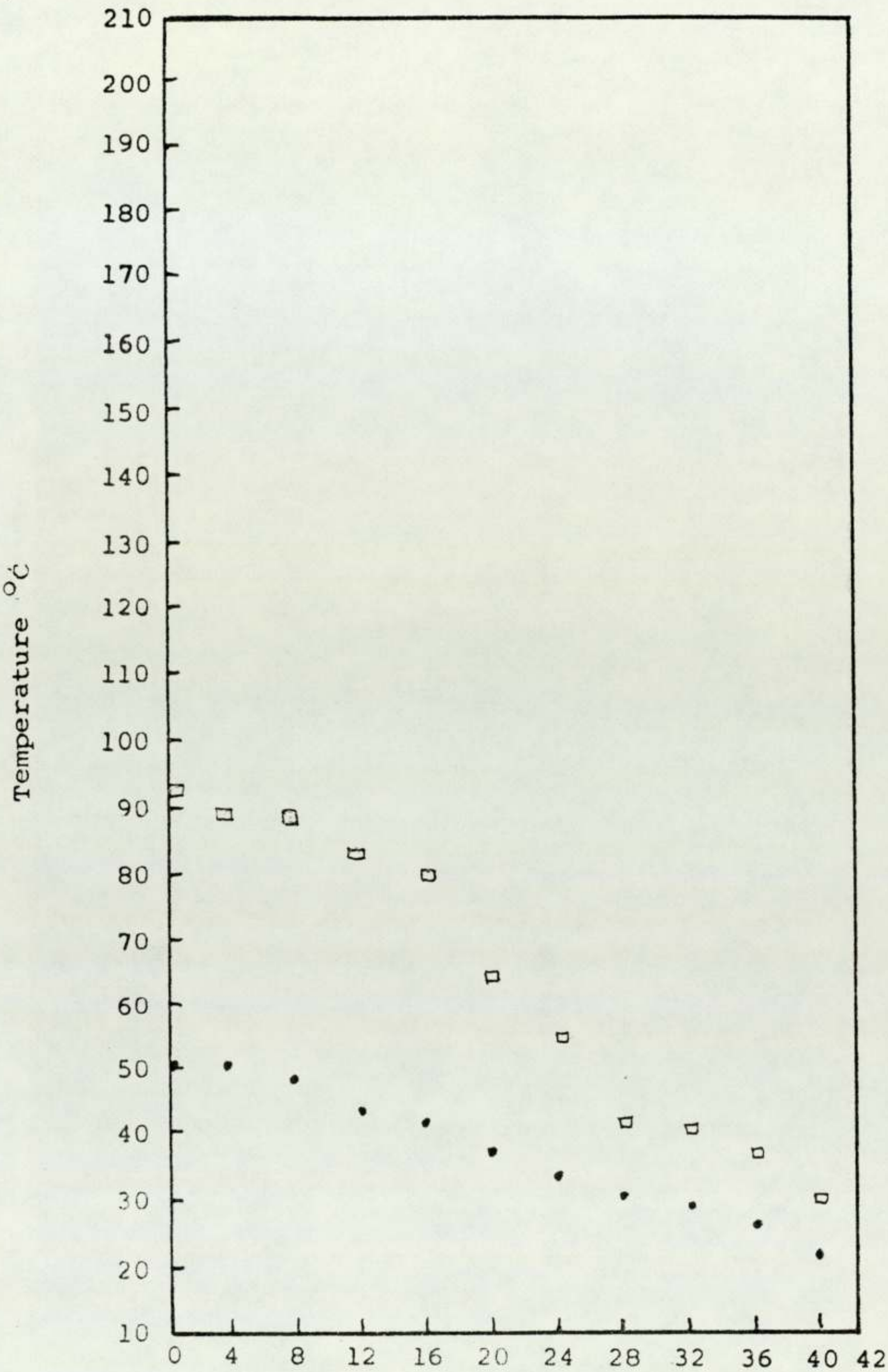

FIG.4.48 Variation of wall temperature along tube (1.6)
with burner number one on.

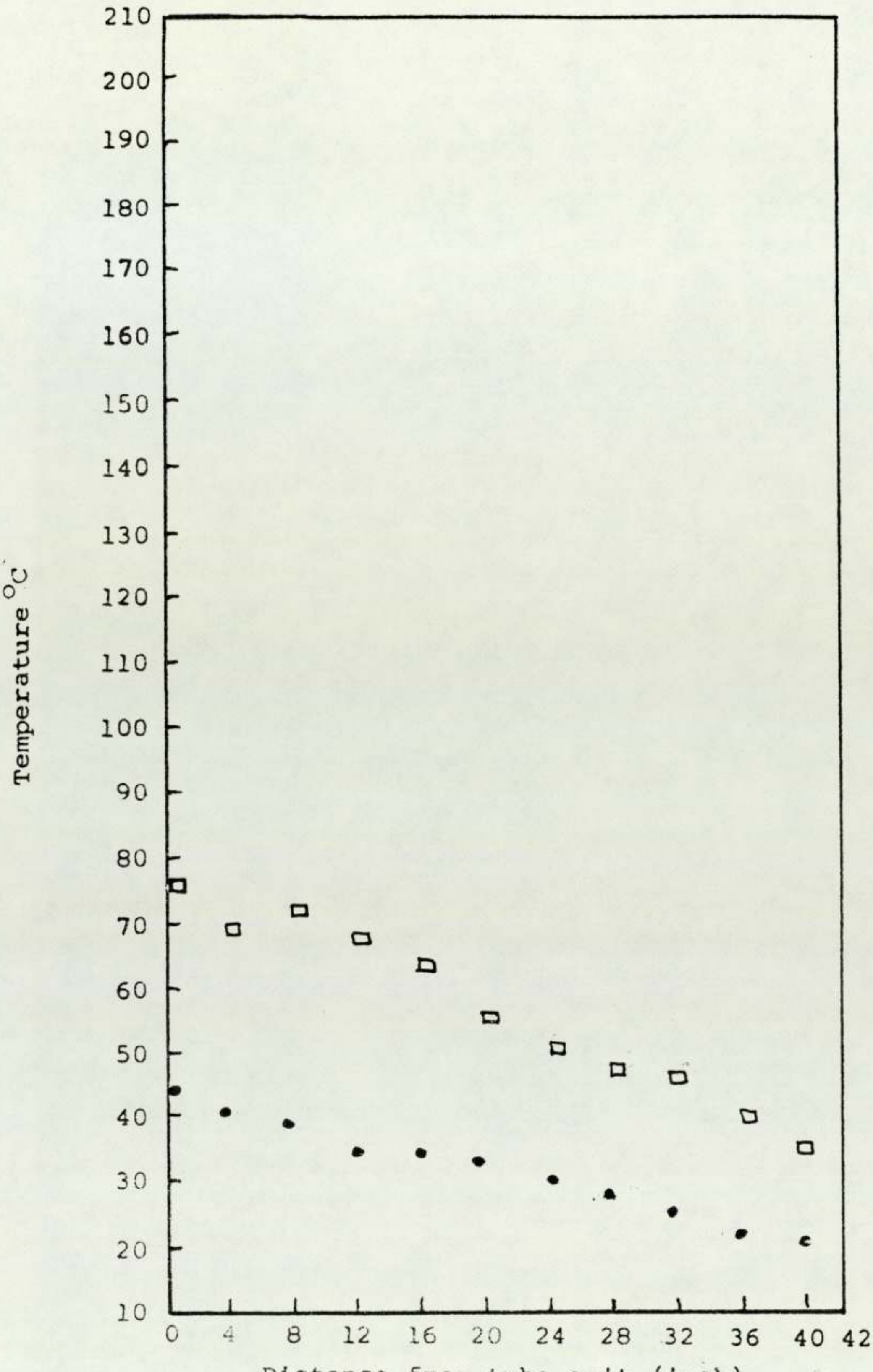

FIG.4.49 Variation of wall temperature along tube (4:4) with burner number one on.

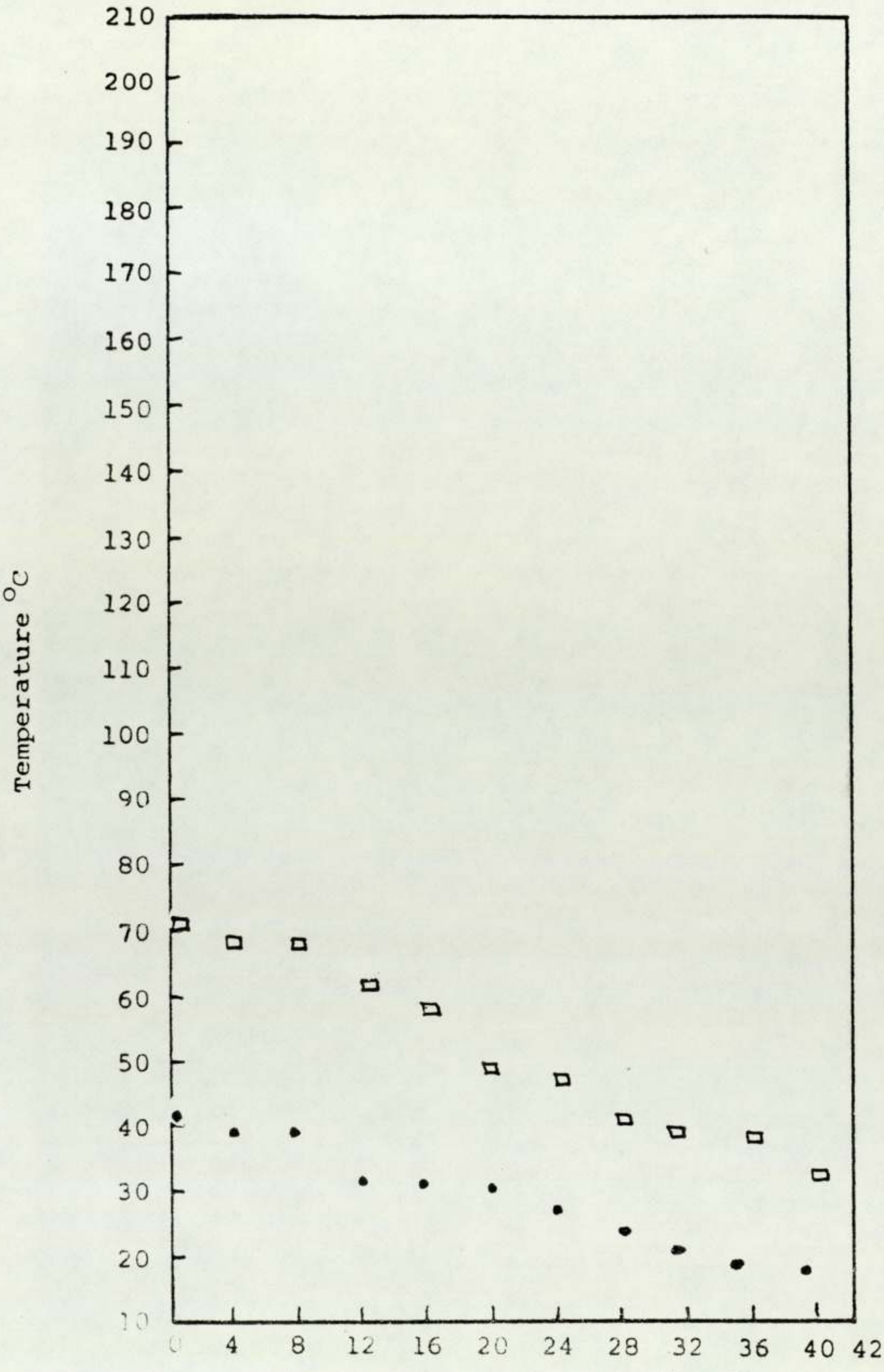

FIG.4.50 Variation of wall temperature along tube (8:3) with burner number one on.

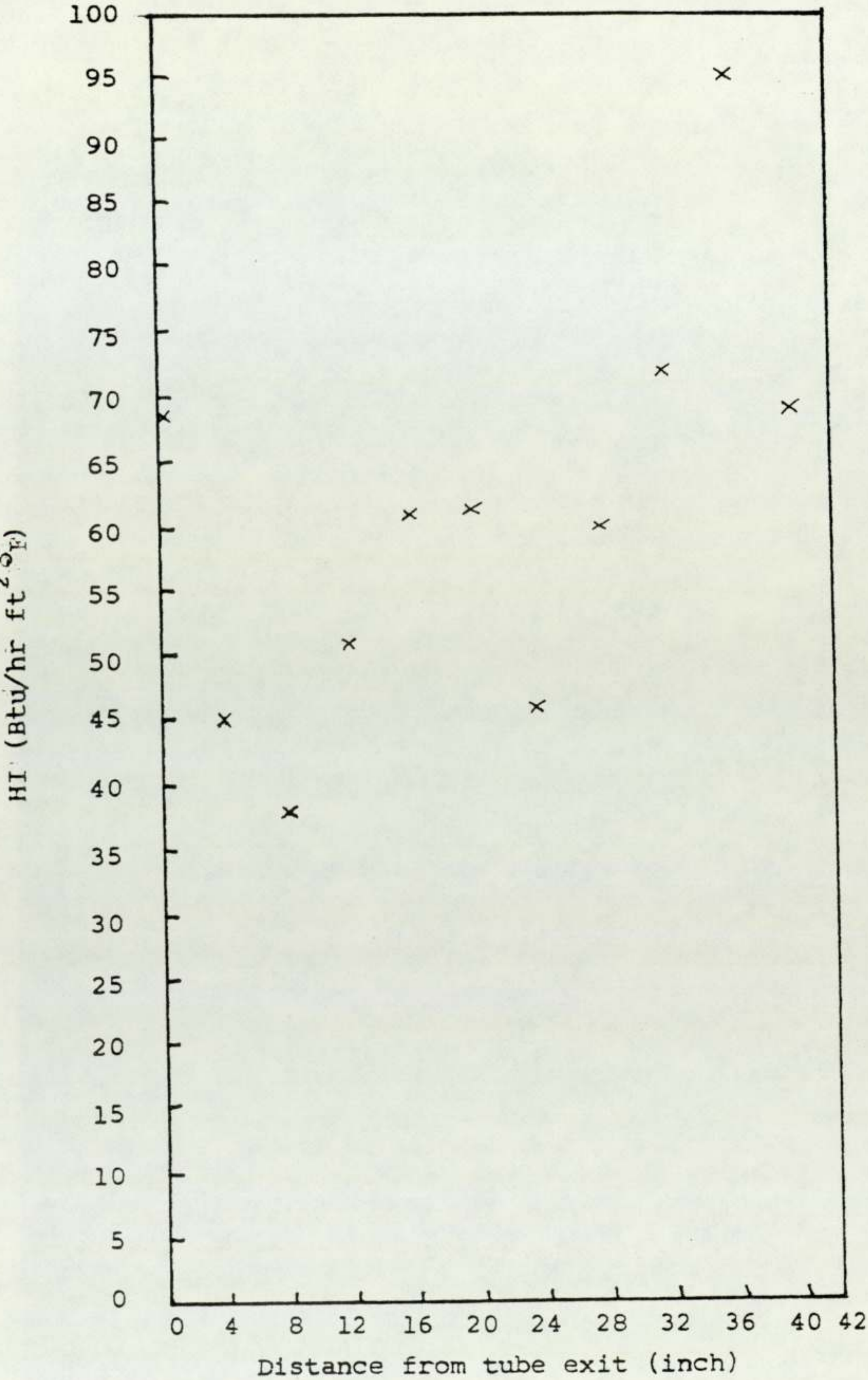

FIG. 4.51 Variation of heat transfer coefficients (tube side) along tube (1:1).

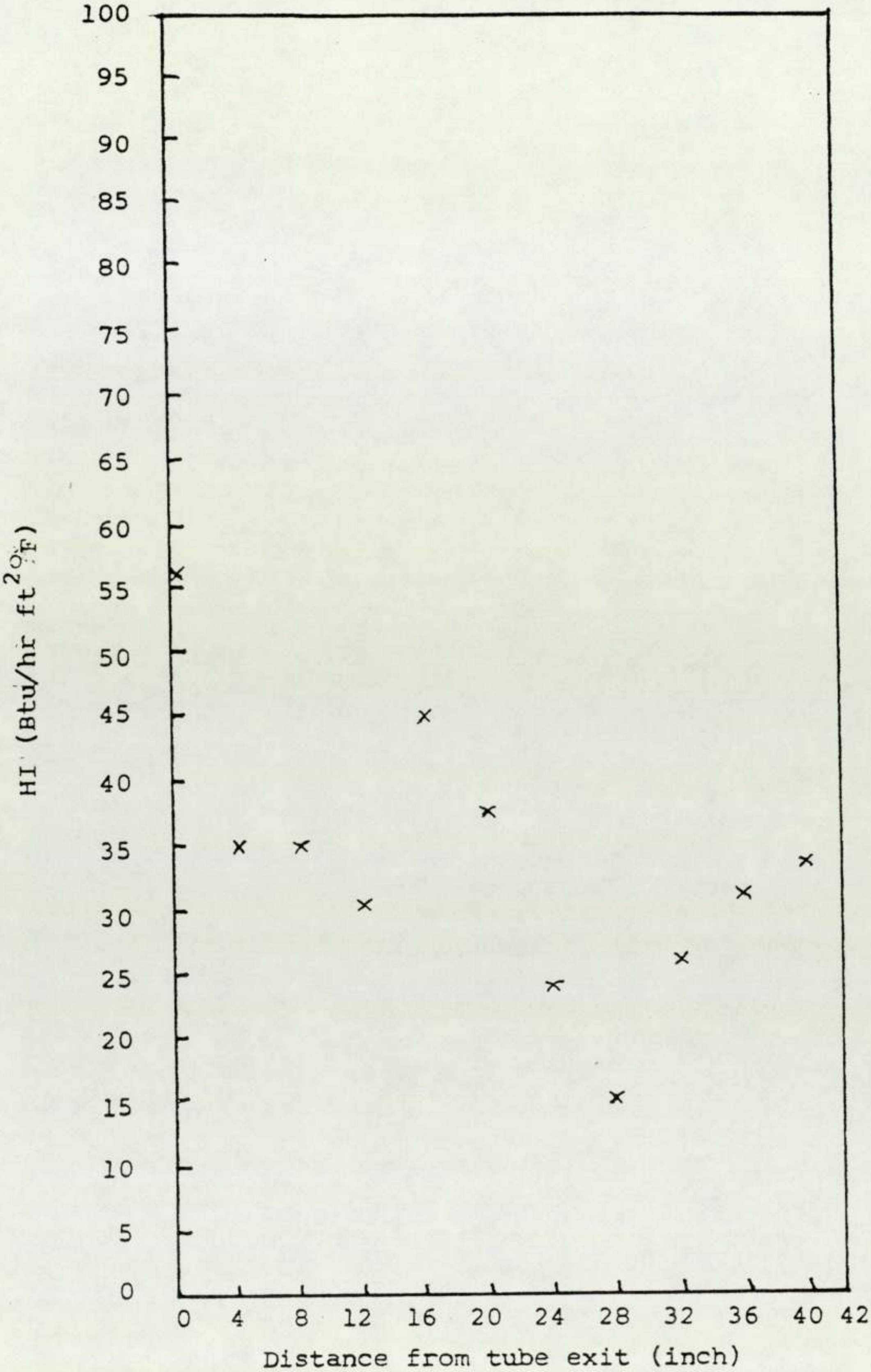

FIG. 4.52 Variation of heat transfer coefficients (tube side) along tube (1:5).

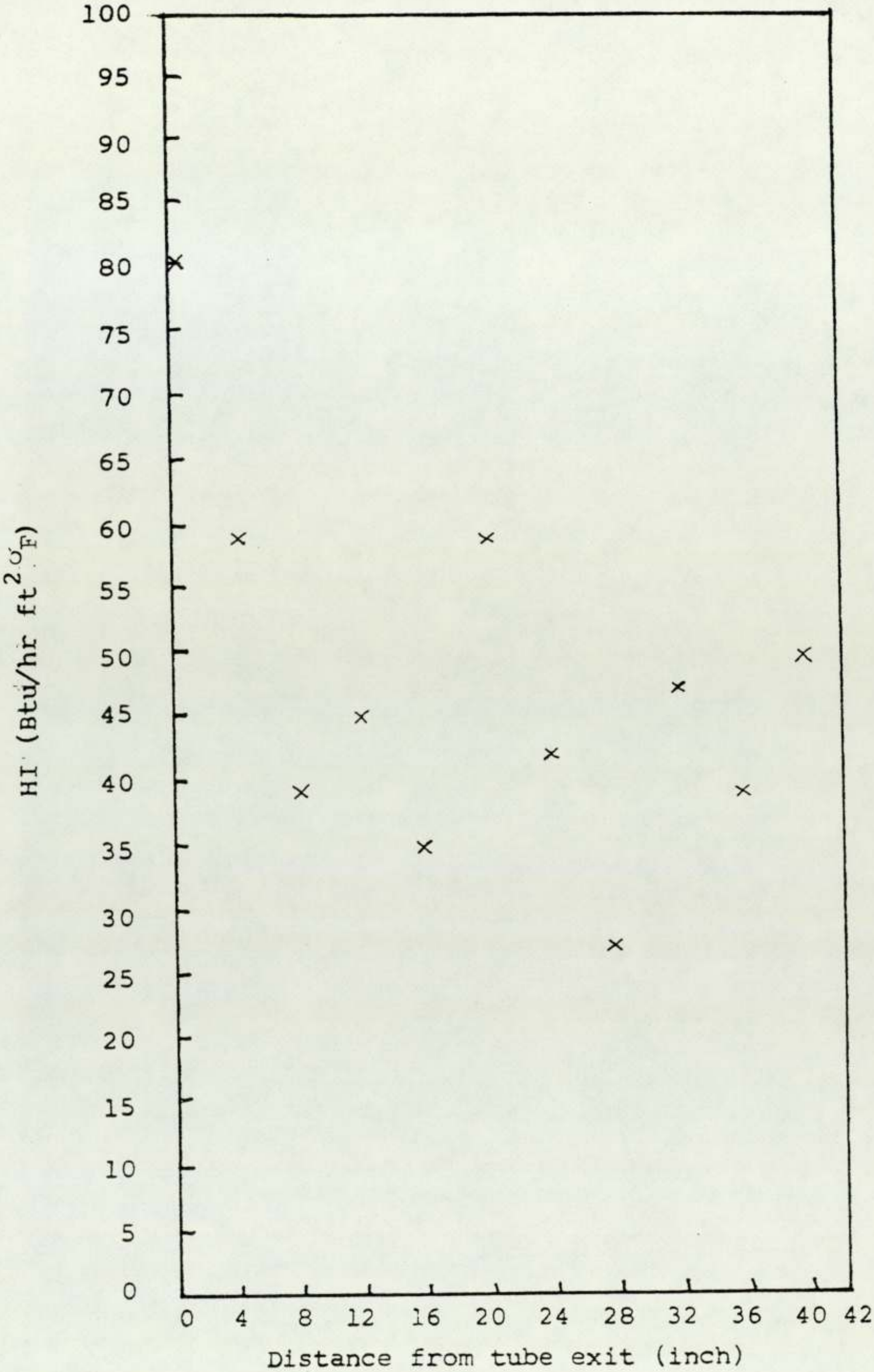

FIG.4.53 Variation of heat transfer coefficients(tube side) along tube (2:3).

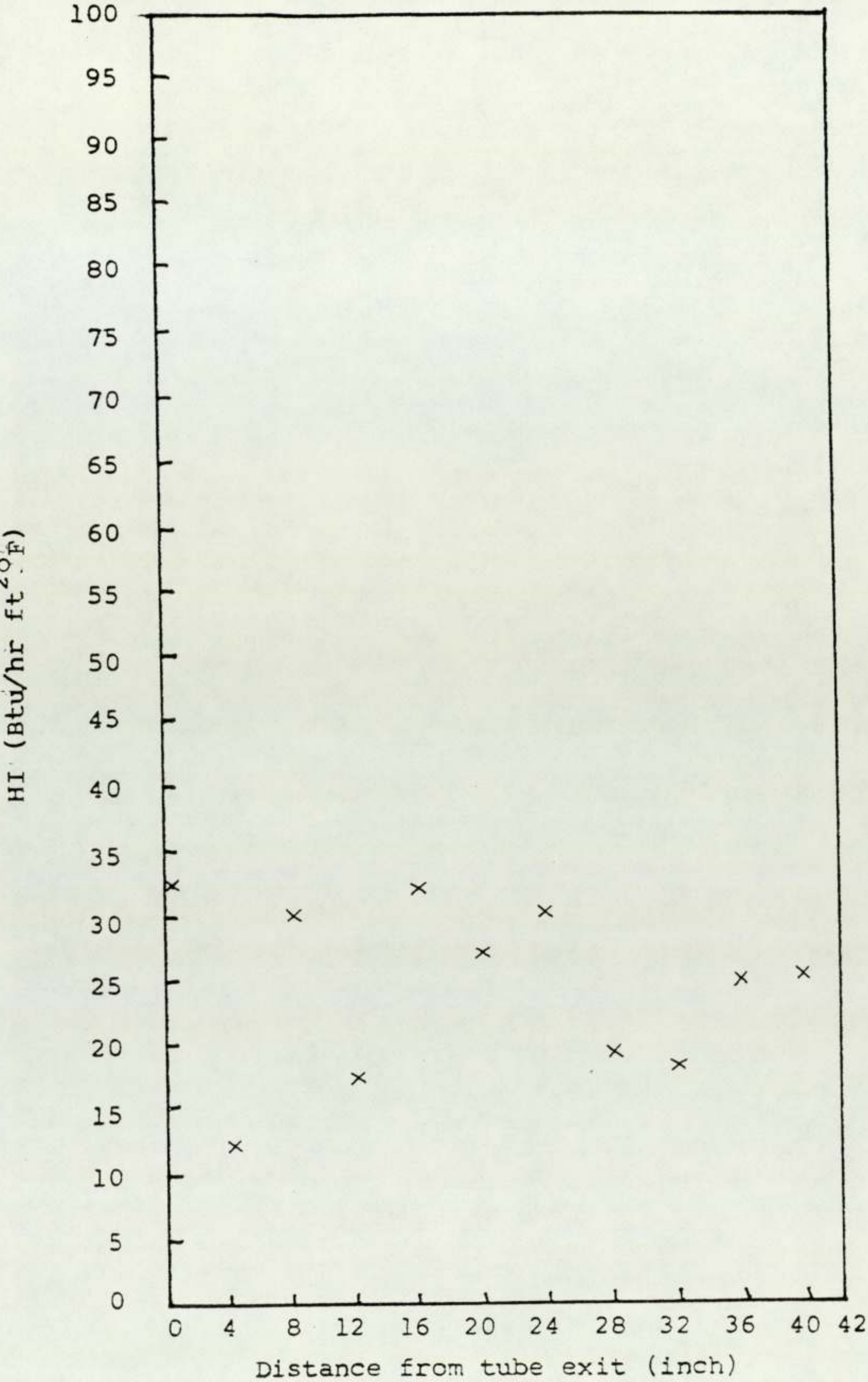

FIG.4.54 Variation of heat transfer coefficients(tube side) along tube (3:1).

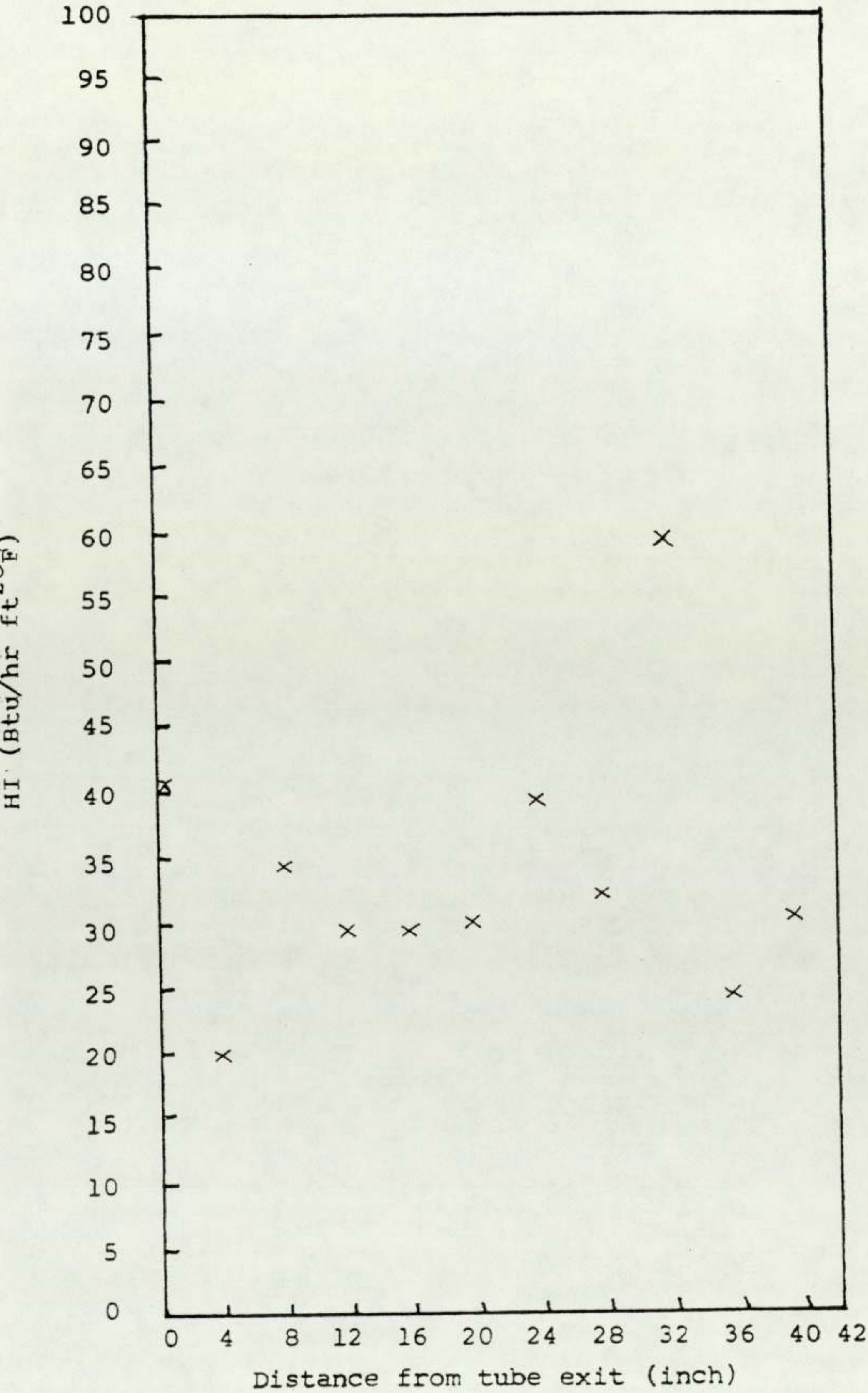

FIG. 4.55 Variation of heat transfer coefficients (tube side) along tube (7:6).

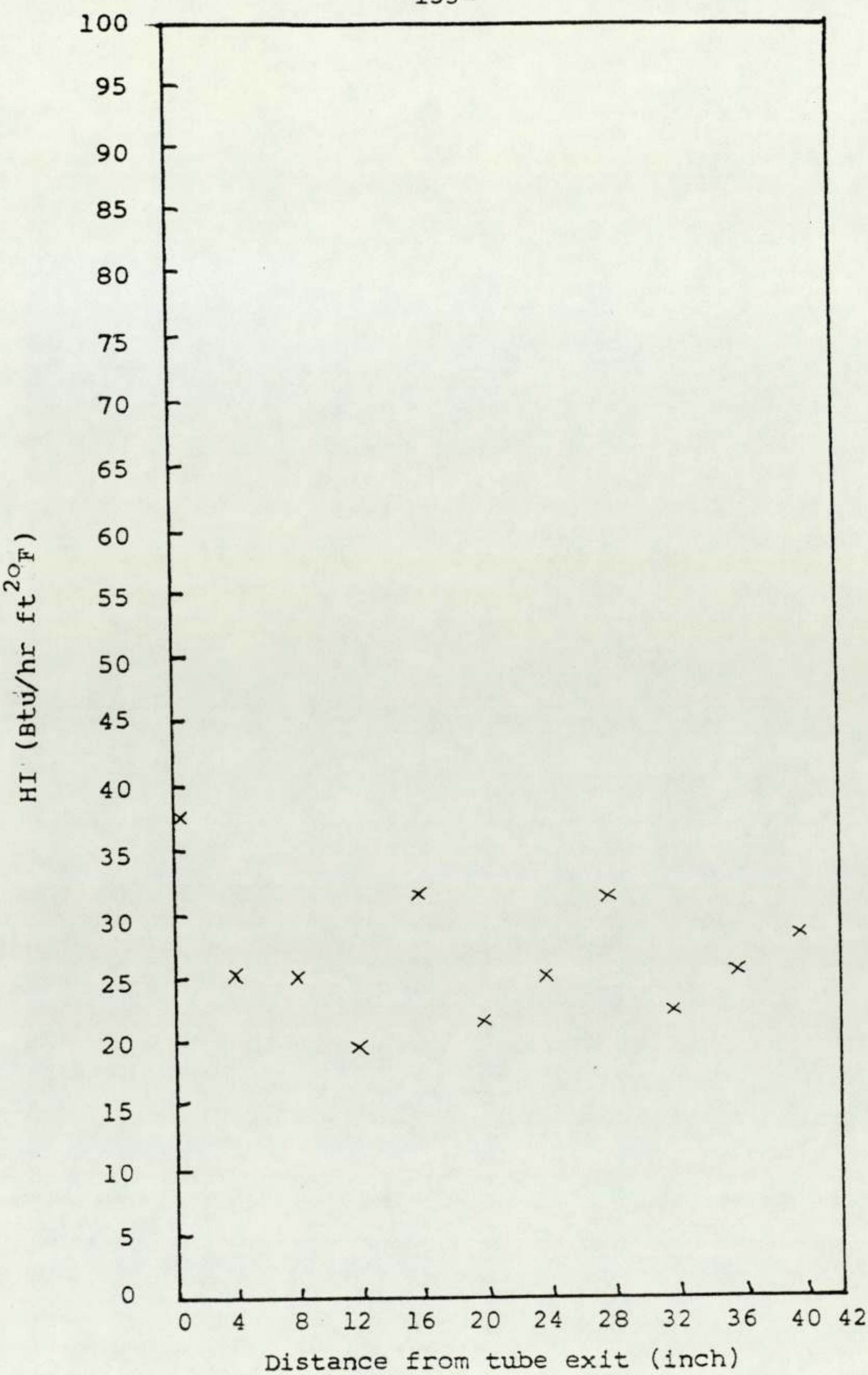

FIG. 4.56 Variation of heat transfer coefficients(tube side) along tube (10:3).

4.1.3 Overall Mean Temperature Difference

In order to compare various methods of finding the overall mean temperature difference, three ways of calculation were adopted.

i) Linear mean temperature difference

$$\Delta T_L = \left(\frac{T_{G_o} + T_{G_i}}{2}\right) - \left(\frac{T_{a_i} + T_{a_o}}{2}\right) \quad \text{.............. (4.19)}$$

ii) logarithmic mean temperature difference

$$\Delta T_{L_M} = \frac{\left(T_{G_i} - T_{a_o}\right) - \left(T_{G_o} - T_{a_i}\right)}{\ln \dfrac{T_{G_i} - T_{a_o}}{T_{G_o} - T_{a_i}}} \quad \text{................. (4.20)}$$

iii) Practical mean temperature difference

ΔTp was calculated from the calculated U(overall heat transfer coefficient) and Q(heat transfer rate Btu/hr).

where

$$Q = UA_{L_o} \Delta T_p \quad \text{......................... (4.21)}$$

also

$$\frac{1}{U} = \frac{1}{h_o} + \frac{1}{h_i} + \frac{xT}{K_w} + 0.001 \quad \text{................. (4.22)}$$

$$\therefore \Delta T_p = \frac{Q}{A_{L_o} \times \left(\dfrac{1}{1/h_o + 1/h_i + xT/Kw + 0.001}\right)} \quad \text{... (4.23)}$$

(i and ii)

Comparing the methods with the practical methos (iii) showed that the linear mean temperature difference deviated from the practical one, in several data calculations, but logarithmic mean temperature difference was very near to the practical one, which means, when a crossflow correction factor is used it would be the most suitable for this work.

In order to calculate a correction factor (FT) for the logarithmic mean temperature difference in cross-flow on the shell side, two methods were adopted:-

Method of Bowman and Nagle (44), in which the effectiveness of process parameters, such as mixing degree on both shell and tube are taken into account which is as follows:-

$$F_T = \frac{r(\text{cross flow})}{r_o(\text{counter current flow})} \quad \text{..........(4.24)}$$

where

r(cross flow)

$$= \frac{q}{\log_e \dfrac{1}{1-\dfrac{q}{p}\log_e \dfrac{1}{1-p}}} \quad \text{...........(4.25)}$$

r_o(counter current flow)

$$= \frac{p-q}{\log \dfrac{1-q}{1-p}} \quad \text{...........(4.26)}$$

$$p = \frac{T_1 - T_2}{T_1 - t_1} \quad \text{..........................(4.27)}$$

$$q = \frac{t_2 - t_1}{T_1 - t_1} \quad \text{.........................(4.28)}$$

T_1 = inlet temperature, shell side F^o

T_2 = outlet temperature, shell side F^o

t_1 = inlet temperature, tube side F^o

t_2 = outlet temperature, tube side F^o

ii) The practical correction factor

$$FT_p = \frac{\text{Practical mean temperature difference}}{r_o\text{(counter current flow)}} \quad \text{.....(4.29)}$$

The two measured were used to calculate the correction factor for all the data available, and it was found that the correction factor was around unity using both methods.

The first method of Bowman and Nagle is of advantage, as the degree of mixing was considered as a factor affecting the correction factor and it could be readily integrated into a computer programme. A computer programme was developed for the above three methods. See appendix (A.2.4)

It was found that an average of incremental logarithmic mean temperature differances based on intervals along a sample tube was very close to the logarithmic mean temperature difference based on both tube ends.

4.1.4 Pressure drop scans

The practical pressure drop, measured across a sample tube in the bundle, using a long pitot probe, was found to be o.68 inch of water, ($159 N/m^2$) while the calculated pressure drop through Reynolds number and friction factor, using the following correlation (9),

$$\Delta P_t = \frac{f\, G^2_t\, L_n}{5.22 \times 10^{10} \times D_t \times S \times \phi_t} \quad \ldots\ldots\ldots(4.30)$$

where

G_t = Mass flow $\frac{Lb/hr}{ft^2}$

L_n = path length ft

S = fluid specific gravity, dimensionless

ϕ_t = $(\mu/\mu w)^{0.14}$

was found to be 0.47 inch of water, (116.56N/m^2). This shows that since the practical pressure drop was higher, there is a possibility of eddies fluctuating in every direction within the tube. Figure (4.57) shows a plot of pressure drop against the distance inside the tube, from the exit.

4.1.5 Statistical Results

In order to be certain that the variations of secondary air flow, and fresh air flow, especially in the case of blocked tubes, should not cause incompatibility among the sets of data obtained from the experimental programme, since it was known, that changing variables could cause errors when all sets of data are pooled together for one correlation to be obtained, as in this present work, a computer programme was written (see appendix (A.2.5)) and variance calculations

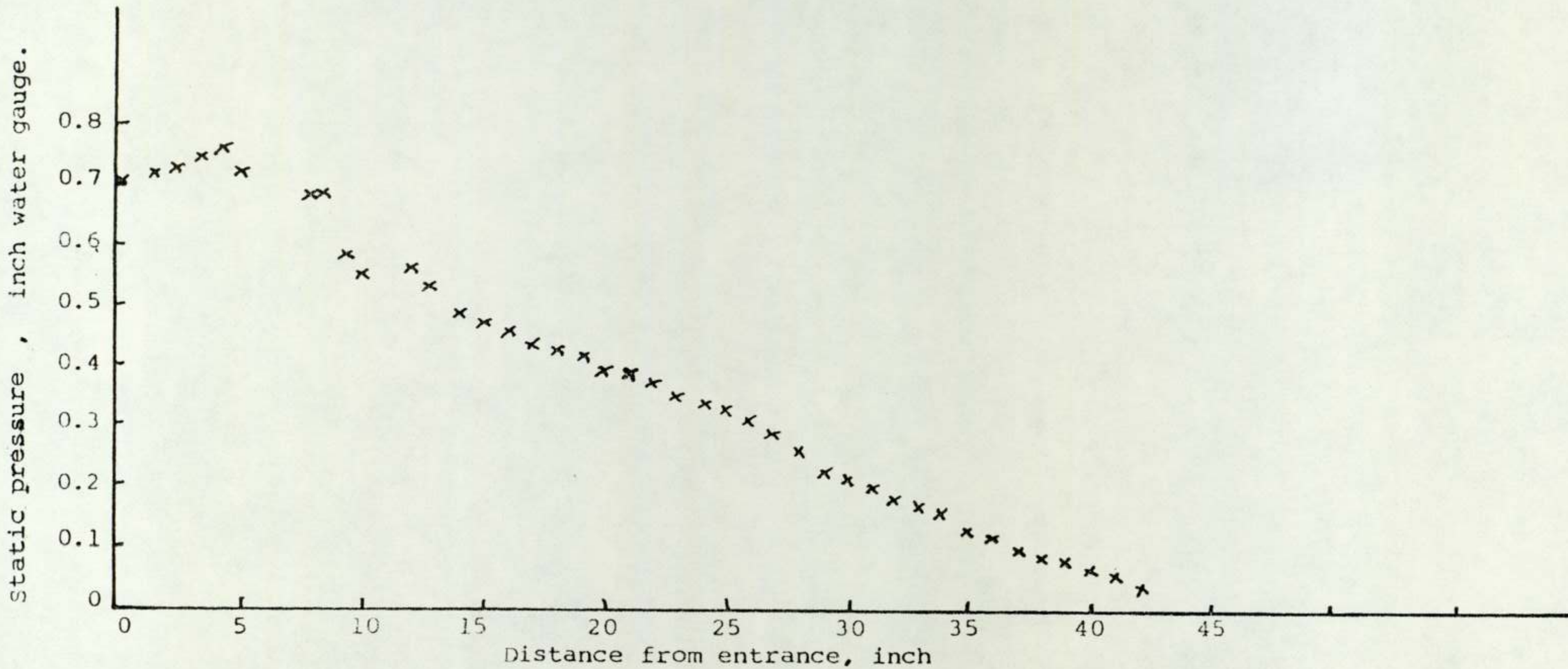

FIG (4.57) Variation of static pressure with distance from tube entrance.

with "F test" were executed for the followingsets of data:-

i) first run of secondary air flow 76200 ft^3/hr, and the sixth run of secondary air flow 28319ft^3/hr

ii) first run of blocked tubes of secondary air flow 76200ft^3/hr and the fourth run of blocked tubes of secondary air flow 42479 ft^3/hr

iii) first run of secondary air flow 76200 ft^3/hr and the fourth run of blocked tubes of secondary air flow 42479 ft^3/hr

Results obtained from this calculation showed that the sets of data obtained from the experimental programme are compatible, since errors are not significant. Therefore, the data could be pooled together for on correlation. Texts used for this purpose were (54), (55), (56).

4.2 Experimental Calculations

To analyse the results it was decided that a mathematical model needed to be developed to represent the radiative and convective modes of heat transfer.

The experimental rig consisting of a heat exchanger, and a combustion chamber, was arranged in such a way that with a number of assumptions, its complexity could be simplified, therefore the following assumptions were introduced.

i) As the tubes in the bundle were in a staggered arrangement, it would be reasonable to assume that the first and second rows, form a wall that picks up most of the radiation emitted by the radiating gases and the refractory walls in the combustion chamber.

ii) The secondary air, which was a non-radiating gas, was considered to be the dominant component of the hot gases in the chamber. This would allow the physical properties of the hot gases in the chamber and the shell to be assumed to be the same as air properties.

iii) The tube wall was thin (0.065 inch),(1.65mm), so it was assumed that there was no temperature gradient through the tube walls.

iv) Hot gases on the shell side were assumed to be well mixed especially after the shell was "baffled".

v) Tube surfaces were checked and proved to be very clean, which leads to a very low fouling factor.

vi) Since the flame was from a gas fuel, and dark blue in colour it was assumed that the amount of radiation emitted from the flame was zero.

Using these assumptions, the following mathematical model was established:-

Considering the heat transfer process as shown in figure (4.58)

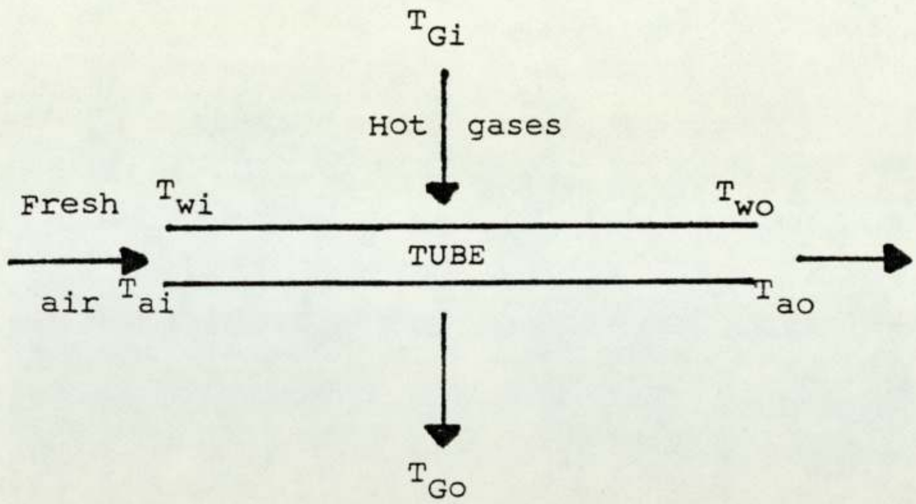

Fig.4.58 Hot gas flows across sample tube in the bundle.

Heat transferred from tube wall to fresh air flowing through the tube, (Q)

$$Q = Ma\ cp_m(Ta_o - Ta_i) \quad \ldots\ldots\ldots\ldots\ldots\ldots\ldots (4.31)$$

where

Ma = fresh air mass flow rate (Lb/hr), (Kg/hr)

cp_m = Mean air specific heat capacity (Btu/Lb ^oF), (KJ/Kg ^oC)

Ta_i = Air inlet temperature to tube ^oF, ^oC

Ta_o = Air outlet temperature from tube ^oF, ^oC

also

$$Q = hi\ A_t \triangle t_m \quad \ldots\ldots\ldots\ldots\ldots\ldots\ldots\ldots (4.32)$$

where

hi = heat transfer coefficient based on the inside wall (Btu/hr ft^{2o}F), (W/m^{2o}C)

A_t = logitudinal area of the tube based on the inside wall. (ft^2, m^2)

Δt_m = logarithmic mean temperature difference F^{o}.

$$= \frac{(Tw_o - Ta_o) - (Tw_i - Ta_i)}{\ln \frac{Tw_o - Ta_o}{Tw_i - Ta_i}} \quad \ldots\ldots\ldots\ldots\ldots (4.33)$$

$$\therefore \quad hi = \frac{Ma\ cp_m (Ta_o - Ta_i)}{A_t \Delta t_m} \quad \ldots\ldots\ldots\ldots\ldots\ldots (4.34)$$

Also

$$Q = h_o A_o \left[T_G - \frac{(Tw_o + Tw_i)}{2} \right] + Qw_t + Qg_t \quad \ldots. (4.35)$$

where

Qw_t = amount of radiative heat transfer from refractory walls to individual tube.

Qg_t = amount of radiative heat transfer from radiative gases to individual tube.

T_G = temperature of hot gases that surround specific tube.

The overall heat transfer coefficient (U), is given by:-

$$\frac{1}{U} = \frac{1}{hi} + \frac{1}{ho} + \frac{xT}{Kw} + \text{fouling factor} \ldots. (4.36)$$

where

xT = Tube wall thickness (inch)(mm)

Kw = Tube wall thermal conductivity Btu/ft hr^{o}F, (w/m ^{o}K)

Qw (heat transferred from refractory walls to the sink), may be calculate d as follows:-

The general equation of heat transfer by radiation (9)

$$Q_w = F_A \times F_e \times A_o \times \sigma \times (Tw^4 - Ts^4) \ldots\ldots\ldots\ldots (4.37)$$

where

F_A is the geometrical factor, which allows for the configurations of the radiating and receiving surfaces. Charts from which the factor may be extracted, are available in Reference (9).

F_e is the emissivity factor which depends on the two surface emissivities, source and reciever. Charts are available in Reference (9).

Tw and Ts are the average temperature of the surfaces involved in the prcess.

σ = Stephan Boltzman constant, $(5.67 \times 10^{-8} w/m^2K^4)$

The amount of radiation recieved by the sink from the radiating gases in the combustion chamber, which are Co_2 and H_2o, depends on the gas beam length, partial pressure, and temperature. The emissivities of the gases depend upon the temperature as well as the partial pressure.

The following equations, (9), were used to calculate the heat flux transferred from the radiating gases, Co_2 and H_2o.

$$q_{Co_2} = 0.173\ E_{Co_2}\left(\frac{T_G}{100}\right)^4, \text{at } P_{Co_2}.L \text{ and } T_G \quad ..(4.38)$$

$$q_{H_2o} = 0.173\ E_{H_2o}\left(\frac{T_G}{100}\right)^4, \text{at } P_{H_2o}.L \text{ and } T_G. \quad (4.39)$$

where

q_{Co_2} and q_{H_2o} are the rates of radiative heat flux.

4.2.1 Sample Calculations

The following calculation, was based on the first experimental work, with the secondary air flowrate 76200 ft^3/hr,(2156m^3/hr), and fresh air flow rate 44271 ft^3/hr,(1253m^3/hr).

4.2.1.1 Radiative Heat transfer Calculations

i) Refractory wall radiation

Average wall temperature over the first and second rows of the bundle

$$= \frac{\text{(inlet and outlet wall temperatures of 12 tubes)}}{12}$$

$$T_{ave} = (54+109.5+86+119+44.5+100.5+41+120+59.9+104+69.5+96)/12$$

$$= 83.7\ C^o$$

To convert to absolute temperature (Rankine)

$$83.7 \times \frac{9}{5} + 32 + 460 = 643\ R^{o}$$

Using the charts

$F_A = 0.15$ for side walls

$= 0.36$ for top and bottom walls

$$F_e = \varepsilon_{source} \times \varepsilon_{sink}$$

$$= 0.52 \times 0.8$$

$$= 0.42$$

Using equation (4.36)

$$Qw_L = 0.15 \times 0.42 \times 0.173 \times 12.9 \times \left[\left(\frac{933.9}{100}\right)^4 - \left(\frac{643}{100}\right)^4 \right]$$

$$= 829 \text{ Btu/hr}$$

$$Qw_R = 0.15 \times 0.42 \times 0.173 \times 12.9 \times \left[\left(\frac{928.5}{100}\right)^4 - \left(\frac{643}{100}\right)^4 \right]$$

$$= 805 \text{ Btu/hr}$$

$$Qw_T = 0.36 \times 0.42 \times 0.173 \times 14.16 \times \left[\left(\frac{877.2}{100}\right)^4 - \left(\frac{643}{100}\right)^4 \right]$$

$$1559 \text{ Btu/hr}$$

$$Qw_B = 0.36 \times 0.42 \times 0.174 \times 14.16 \times \left[\left(\frac{760.2}{100}\right)^4 - \left(\frac{643}{100}\right)^4 \right]$$

$$= 602 \text{ Btu/hr}$$

where

Qw_L = radiative heat transferred from the left hand side wall.

Qw_R = radiative heat transferred from the right hand side wall.

Qw_T = radiative heat transferred from the top wall

Qw_B = radiative heat transferred from the bottom wall

Qw_{Total}

= 829 + 805 + 1559 + 602

= 3795 Btu/hr, (400 J/hr)

ii) Gaseous radiation calculations

Natural gas flow rate, was kept constant at $450 ft^3/hr$, $(12.6 m^3/hr)$.

Considering the chemical equation of the combustion process.

$$CH_4 + 2O_2 \longrightarrow CO_2 + 2H_2O$$

molecular weight

16 64 36 44

CH_4 mass flowrate = 450 x 0.0445 = 20.025 Lb/hr

$\therefore$

O_2 needed = 80.1 Lb/hr (36.5Kg/hr)

CO_2 produced = 45.1 Lb/hr (20.5Kg/hr)

H_2O produced = 55.1 Lb/hr (25Kg/hr)

amount of stochiometric air needed

$$= \frac{100}{21} \times 80.1$$

$$= 381.4 \text{ Lb/hr } (173.4\text{Kg/hr})$$

Using 20% excess air to prevent carbon monoxide formation, the actual air flow

$$= 381.4 \times 1.2$$

$$= 457.7 \text{ Lb/hr}, (208\text{Kg/hr})$$

density of air at 20C^{o}

$$= 0.075 \text{ Lb/ft}^3, (1.2 \text{ Kg/m}^3)$$

Volumetric flow rate of primary air

$$= \frac{457.68}{0.075}$$

$$= 6102 \text{ ft}^3\text{/hr}, (172.7 \text{ m}^3\text{/hr})$$

Primary air constituents:-

$$N_2 = 457.8 \times \frac{79}{100} = 361.7 \text{ Lb/hr}, (164.4\text{Kg/hr})$$

$$O_2 = 457.8 \times \frac{21}{100} = 96.14 \text{ Lb/hr}, (43.7\text{Kg/hr})$$

Secondary air volumetric flowrate

$$= 527.3(5.8)^{0.5}x60$$

$$= 76195 \text{ ft}^3\text{/hr}$$

Mass flow rate of secondary air

$$= 76195 \times 0.075$$

$$= 5715 \text{ Lb/hr}$$

Secondary air constituents:-

$N_2 \quad = \quad 5715 \times \frac{79}{100} \quad = \quad 4515$ Lb/hr, (2047.5Kg/hr)

$O_2 \quad = \quad 5715 \times \frac{21}{100} \quad = \quad 1200.2$ Lb/hr, (544.4Kg/hr)

Partial pressure of Co_2

$$= \frac{\frac{MCo_2}{MwCo_2}}{\frac{MCo_2}{MwCo_2} + \frac{Mo_2}{Mwo_2} + \frac{MN_2}{MwN_2} + \frac{MH_2o}{MwH_2o}} \text{ atm} \quad \text{..........(4.40)}$$

$$= \frac{\frac{45.1}{44}}{\frac{45.1}{44} + \frac{16.02+1200.2}{32} + \frac{361.7+4515}{28} + \frac{55.1}{18}} \text{ atm}$$

$= \ 0.0047$ atm

Partial pressure of H_2o

$$= \frac{\frac{55.1}{18}}{\frac{45.1}{44} + \frac{16.02+1200.2}{32} + \frac{361.7+4515}{28} + \frac{55.1}{}} \text{ atm}$$

$= \ 0.014$ atm

The average temperature of the gases in the combustion chamber

$= \ 203 \times \frac{9}{5} + 32$

$= \ 397.4F^o$

The beam length of the gas depends on the combustion chamber volume(9)

$$\text{Beam length} = \frac{2}{3}\sqrt[3]{\text{gas volume}} \quad \ldots\ldots\ldots\ldots\ldots\ldots\ldots (4.41)$$

$$= \frac{2}{3}\sqrt[3]{\frac{60\text{x}34\text{x}\left(\frac{14+12}{2}\right)}{12\text{x}12\text{x}12}}$$

$$= 1.66\text{ft}, (0.5\text{m})$$

Since height of combustion chamber was 60 inch (1.52m), allowing for insulation which was 4 inch, (10cm) thick on each side

∴ Combustion chamber net length 60 inch, (1.5m)

The width of the combustion chamber

= 34 inch, (0.86m)

The average height

= (14+12)/2

= 13 inches (0.33m)

Using charts in literature (9) to find Co_2 and H_2o emissivities respectively, at average gas temperature, and partial pressures

$$\varepsilon_{Co_2} = 0.015$$

$$\varepsilon_{H_2o} = 0.03$$

Using equations (4.38), (4.39)

The gas radiative heat flux:-

$$q_{Co_2} = 0.173\text{x}0.015\text{x}\left(\frac{397.4+460}{100}\right)^4$$

$$= 14 \text{ Btu/hr ft}^2$$

$$q_{H_2O} = 0.173 \times 0.03 \times \left(\frac{397.4+460}{100}\right)^4$$

$$= 28 \text{ Btu/hr ft}^2$$

The area of the receiver (front of the bundle)

$$= \frac{9}{12} \times \frac{34}{12}$$

$$= 2.1 \text{ ft}^2$$

rate of heat transferred to the sink from the gas

$$= (14+28) \times 2.1$$

$$= 88.2 \text{ Btu/hr}$$

Total amount of radiative heat transfer from gas and wall

$$= 3795 + 88.2$$

$$= 3883 \text{ Btu/hr.}$$

4.2.1.2 Convective heat transfer calculations

Hot air flow rate through the shell

= Secondary air flow + Natural gas flow + primary air flow

$$= 76195 + 450 + 6102.4$$

$$= 82747.4 \text{ ft}^3\text{/hr}, (2342 \text{ m}^3\text{/hr})$$

The shell equivalant diameter, De

$$De = \frac{4 \times \text{ area}}{\text{wet perimeter}} \quad \ldots\ldots\ldots\ldots\ldots\ldots (4.42)$$

$$= \frac{4 \times 10 \times 30}{22+2 \times 30}$$

$$= 13.6 \text{ inch } (34.5 \text{ cm })$$

Shell flow area as

$$= \frac{De \times C' \times B}{P_T \times 144} \quad \text{..........................(4.43)}$$

where

C'	=	clearence between tubes	inch
B	=	baffle spacing	inch
P_T	=	Tube pitch	inch

$$as = \frac{13.6 \times 0.95 \times 30}{144 \times 1.5}$$

$$= 0.85 \ ft^2$$

Volumetric flow change due to temperature change

inlet fluid temperature

$$= 205 \times \frac{9}{5} + 32 + 460$$

$$= 536.1 \ R^{o}$$

Shell fluid temperature

$$= 162.4 \times \frac{9}{5} + 32 + 460$$

$$= 784 \quad R^{o}$$

$$\frac{V_{in}}{T_{in}} = \frac{Vos}{Ts} \quad \text{..................................(4.44)}$$

where

V_{in} = hot gases volumetric flow at inlet temperature ft^3/hr, m^3/hr

T_{in} = inlet temperature flow ^{o}R

Vos = hot gases volumetric flow at the shell temperature ft^3/hr, m^3/hr

Ts = gas temperature in the shell ^{o}R

$$Vos = \frac{784}{536} \times 82747.4$$

$= 121034 \ ft^3/hr$

velocity of hot gases through the shell

$$Vs = \frac{121034}{0.85}$$

$$Vs = 142393 \ ft/hr$$

physical properties of hot fluids on the shell side

$$Density = (144x14.7)/(53.36x1.8x(162.4+273))$$

$$= 0.051 \quad Lb/ft^3$$

Thermal conductivity

$$= 0.0139 \ x(398/(162.4 + 273 + 125)x(\frac{162.4+273}{273})^{1.5}$$

$$= 0.051 \quad Btu/ft \ hr \ ^oF$$

equivalent diameter with tubes in the shell

$$= \frac{4(0.5_{P_T} \times 0.86 \times - \frac{1}{2} \pi d^2_o/4}{\frac{1}{2} \pi d_o}$$

$$= \frac{4(\frac{1}{2}x1.5x0.86x1.5 - \frac{1}{2} \pi x(1.05)^2/4)}{\frac{1}{2} \pi \times 1.05}$$

$$= 0.110 \ ft$$

$$Res = \frac{Dens \ x \ Vs \quad x \ De}{viscs} \quad \ldots\ldots\ldots\ldots\ldots\ldots (4.45)$$

$$Res = \frac{0.05 \times 142393 \times 0.110}{0.051}$$

$$= 15378$$

Prandtl number on shell side

$$= \frac{0.049 \times 0.231}{0.0198}$$

$$= 0.6$$

Heat loss from the out-side of the combustion chamber Q_L

$$Q_L = \frac{A_c}{x_L} \times K_F \times (T_{wc} - T_{ar}) \quad \text{.................(4.46)}$$

where

A_c = total mean area of the combustion chamber $ft^2, (m^2)$

x_L = combustion chamber wall thickness ft, (m)

K_F = thermal conductivity of the combustion chamber walls

T_{wc} = average of temperature of the inside walls of the combustion chamber

T_{ar} = temperature of the air in the room ^{o}C

$$Q_L = \frac{42}{0.375} \times 2.2 \times (218.25 \times \frac{9}{5} + 2) - (24.75 \times \frac{9}{5} + 32)$$

$$= 86780 \text{ Btu/hr}, (25.4 \text{ Kw})$$

Heat taken out by flue gases (QF)

$$Cp_b = 6.713 + 0.4697 \times (\frac{144 + 273}{1000}) \times \frac{1}{29}$$

where

Cp_b = the specific heat capacity of hot gases at the bundle

$$Q_F = HFL \times Dens_{in} \times Cp_b \times (T_b - T_{in}) \text{.......(4.47)}$$

where

HFL = hot gases volumetric flow at inlet temperature

$Dens_{in}$ =hot gases density at inlet temperature Lb/ft^3, (Kg/m^3)

T_B = Temperature of hot gases at the bundle $F^o, (C^o)$

T_{in} = temperature of hot flow at inlet temperature $F^o, (C^o)$

$$Q_F = 0.075 \times 82747 \times 0.238((144 \times \frac{9}{5} + 32 - (24.5 \times \frac{9}{5} + 32))$$

$$= 292573 \text{ Btu/hr}, (85.7 \text{ Kw})$$

Heat recovered by fresh air (Q_P)

Specific heat capacity of fresh air

$$cpp = (6.713+(0.4697 \times ((\frac{69.5 + 24.75}{2})+273)/1000) \times \frac{1}{29}$$

$$= 0.237 \text{ Btu/Lb } F^o$$

$$Qp = CFL \times Densp \times cpp\ (Ta_o - Ta_i) \quad \text{..........(4.48)}$$

where

CFL = fresh air volumetric flowrate through the bundle of tubes

Densp = density of fresh air at the inlet temperature

$$Qp = 44271 \times 0.074 \times 0.237 \times ((69.5 \times \frac{9}{5} + 32) - (24.75 \times \frac{9}{5} + 32))$$

$$= 62541 \text{ Btu/hr} (18.3 \text{ Kw})$$

Heat exchanger efficiency

$$= \frac{Qp}{Q_c - Q_L} \quad \text{........................ (4.49)}$$

where

Q_c = rate of heat of combustion from natural gas Btu/hr

$$= \frac{62541}{402750 - 86780}$$

$$= 20\%$$

The heat exchanger efficiency was regarded as the ratio of the amount of heat recovered by the heat exchanger, to the amount of heat of combustion, taking into account the heat losses from the combustion chamber walls.

The gross calorific value of the natural gas

$= 1035\ Btu/ft^3$

The net calorific value of the natural gas

$= 895\ Btu/ft^3$

$\therefore$ The heat of combustion

$= 895 \times 450$

$= 402750\ Btu/hr$

Considering the whole efficiency of the rig, as the ratio of the heat recovered by the fresh air, to the heat of combustion from the natural gas ($\frac{Q_P}{Q_c}$), where the heat losses were not considered. This ratio would show how efficient the insulation system and the heat exchanger are.

$$\text{The rig efficiency} = \frac{62541}{402750}$$

$$= 15.5\%$$

4.2.1.3 Heat Transfer on the Tube Side

fresh air average physical properties

$Dens_{in}$ = (144x14.7)/(53.36 x 1.8x(24.5+273))

= 0.074 Lb/ft^3

$Dens_{out}$ = (144x14.7)/(53.36 x 1.8x(66.5+273))

= 0.065 Lb/ft^3

CP_{in} = $(6.173+(0.4967x(24.5+273)/1000)x \frac{1}{29}$

= 0.218 Btu/Lb F^o

CP_{out} = $(6.173+(0.496x(66.5+273)/1000)x \frac{1}{29}$

= 0.219 Btu/Lb F^o

$AKon_{in}$ = $0.0139x(398/(24.5+273+125)x((24.5+273)/273)^{1.5}$

= 0.015

$AKon_{out}$ = $0.0139x(398/(66.5+273+125)x((24.5+273)/274)^{1.5}$

= 0.012

$Visc_{in}$ = $0.044x(393/(24.5+273+120)x((24.5+273)/273)^{1.5}$

= 0.047 Lb/ft hr

$Visc_{out}$ = $0.044x(393/(66.5+273+120)x((66.5+273)/273)^{1.5}$

= 0.045 Lb/ft hr

Logarithmic mean temperature difference

$$LM\,\Delta T = \frac{(Tw_o - Ta_o) - (Tw_i - Ta_i)}{\ln \dfrac{Tw_o - Ta_o}{Tw_i - Ta_i}} \quad \ldots\ldots\ldots (4.50)$$

where

Tw_o = Tube wall temperature at exit $^oF, ^oC$

Tw_i = Tube wall temperature at inlet $^oF, ^oC$

Ta_o = Air temperature at exit $^oF, ^oC$

Ta_i = Air temperature at inlet $^oF, ^oC$

$$= \frac{(212.9-151.7)-(112.1-76.1)}{\ln \dfrac{212.9 - 151.7}{112.1 - 76.1}}$$

$$= 47.6\ C^o\ (117.7\ F^o)$$

Heat transfer to fresh air through the sample tube

$$Q_{Con} = V_T \times A_T \times Dens_{in} \times Cp_{ave}(Ta_o - Ta_i) \ldots (4.51)$$

where

Q_{con} = convective heat transfer to fresh air

and V_T = velocity of fresh air through tube

$$\therefore\ Q_{con} = 189954 \times 0.0049 \times \left(\frac{0.065+0.074}{2}\right) \times \left(\frac{0.218+0.219}{2}\right) \times \left(\left(66.5 \times \frac{9}{5}+32\right)-\left(24.5 \times \frac{9}{5}+32\right)\right)$$

$$= 1068\ \text{Btu/hr}$$

Heat transfer coefficient on tube side

$$h_i = \frac{Q_{con}}{AL\ LM\Delta T} \ldots\ldots\ldots\ldots\ldots\ldots\ldots\ldots\ldots (4.52)$$

$$= \frac{1068}{0.87 \times 47.6}$$

$$= 25.7\ \text{Btu/hr ft}^2,\ F^o (144\ w/m^{2o}C)$$

Heat transfer coefficient on shell side

$$h_o = \frac{Q_{con}}{AL_o \times (Tbundle - ((Tw_i \times \frac{9}{5} + 32) + (Tw_o \times \frac{9}{5} + 32)) \times 0.5} \quad \ldots\ldots\ldots\ldots\ldots (4.53)$$

$$h_o = \frac{1068}{0.96 \times ((131.5 \times \frac{9}{5} + 32) - ((\frac{44.5+97}{2}) \times \frac{9}{5} + 32))}$$

$$= 10 \text{ Btu/ hr ft}^{2\,o}\text{F}, (56 \text{ w/m}^{2\,o}\text{C})$$

Overall heat transfer coefficient "U"

$$\frac{1}{U} = \frac{1}{ho} + \frac{1}{hi} + \frac{x_T}{w_K} + 0.001 \quad \ldots\ldots\ldots\ldots\ldots\ldots\ldots\ldots\ldots (4.54)$$

$$= \frac{1}{10} + \frac{1}{25.7} + \frac{0.065}{12 \times 26} + 0.001$$

$$\therefore U = 7.14 \text{ Btu/hr ft}^2\text{F}^o \quad (40 \text{w/m}^{2\,o}\text{C})$$

Although the tubes of the bundle, were found to be reasonably clean, a small fouling factor was introduced for any future possibility of carbon deposition.

Nusselt number on tube side

$$Nu_i = \frac{h_i \times D_i}{K_{air}} \quad \ldots\ldots\ldots\ldots\ldots\ldots\ldots\ldots\ldots\ldots\ldots (4.55)$$

$$= \frac{25.7 \times 0.079}{\frac{0.015 + 0.013}{2}}$$

$$= 145$$

Nusselt number on shell side

Air Density (57)

$$Dens_A = (14.7/144)/(53.6 \times 1.8 \times (T+273)) \quad \ldots\ldots (4.56)$$

Air Viscosity (58)

$$VISC_A = 0.044 \times \left(\frac{393}{T+273+120}\right)\left(\frac{T+273}{273}\right)^{1.5} \quad \ldots\ldots (4.57)$$

Air Specific Heat Capacity (59)

$$CP_A = \left(6.713+\left(0.4697 \times \left(\frac{T+273}{1000}\right)\right) \times \frac{1}{29}\right) \quad \ldots\ldots (4.58)$$

Air Thermal Conductivity (60)

$$K_{air} = 0.01391 \times \left(\frac{398}{T+273} + 125\right) \times \left(\frac{T+273}{273}\right)^{1.5} \quad \ldots (4.59)$$

where

T = air temperature C^{o}

4.3 Error Calculations

In every process, when readings are taken from measuring instruments, errors may be involved. The effect of errors varies, depending on how sensitive is the calculation of results to that particular variable with which errors are involved, also depending on how great the error value is to the actual measured variable. In this present work, heat transfer calculation mainly depends on fluid velocity and temp-

$$Nu_o = \frac{h_o x D_o}{K_{hot\ air}} \quad \text{..........................(4.60)}$$

$$= \frac{10 \times 0.088}{0.0199}$$

$$= 44.2$$

A computer program was used to do the same calculation, as above, for the twelve sample tubes, and for the various fresh air and secondary air flow rates, including radiation calculation. See appendix (A.2.6)

A computer package, already available in the computer library, was also used to analyse the experimental data obtained, which presents the following facilities:-

i) best fit of Nusselt number Vs Reynolds number based on the theory of "Least Squares", by calculating the slope and intercept of the line.

ii) correlation coefficient, which indicates the degree of representation of the experimental points, by the fitted line.

iii) standard errors of the slope and intercept.

The following air physical properties equations were incorporated in the computer program after they had been checked against physical properties charts in Perry (61), and were found to be reasonably accurate:-

erature, and also on tube wall temperature. Errors involved in these measurements, would certainly have an effect on the results.

4.3.1 Heat Transfer Coefficients on Tube Side

The heat transferred from hot gases to fresh air flowing in a specific tube, (QCON) given in equation (4.61).

$$QCON = Dens_1 \times V_T \times A_T \times \left(\frac{Cp_1+Cp_2}{2}\right)(Ta_o - Ta_i) \ldots (4.61)$$

$$h_i = \frac{QCON}{AL_1}\left(\frac{Tw_i+Tw_o}{2}\right)-\left(\frac{Ta_i+Ta_o}{2}\right) \ldots\ldots\ldots\ldots\ldots (4.62)$$

The variables in equation ( ) are:-

Tw_i, Tw_o, Ta_i, Ta_o, V_T

The parameters are:-

A_T, $Dens_1$, Cp_1, Cp_2, A_L

$$h_i = f(Tw_i, Tw_o, Ta_i, Ta_o, V_T)$$

$$C_1 = \frac{Dens_1}{A_L} \times \left(\frac{Cp_1+Cp_2}{2}\right)$$

$$\Delta h^2 = \left(\frac{\partial h_i}{\partial Tw_i}\right)(\Delta Tw_i)^2 + \left(\frac{\partial h_i}{\partial Tw_o}\right)^2(\Delta Tw_o)^2 +$$

$$\left(\frac{\partial h_i}{\partial Ta_i}\right)^2(\Delta Ta_i)^2 + \left(\frac{\partial h_i}{\partial Ta_i}\right)^2(\Delta Ta_i)^2 +$$

$$\left(\frac{\partial h_i}{\partial Ta_o}\right)^2(\Delta Ta_o)^2 + \left(\frac{\partial h_i}{\partial V_T}\right)(\Delta V_T)^2 \ldots\ldots\ldots (4.63)$$

$$h_i = C_1 \times \frac{V_T(Ta_o - Ta_i)}{(Tw_i+Tw_o)-(Ta_i+Ta_o)}$$

Now

$$\frac{\delta h_i}{\delta Ta_i} = \frac{C_1 V_T(Tw_i+Tw_o-2Ta_i)}{(Tw_i+Tw_o-Ta_i-Ta_o)^2}$$

$$\frac{\delta h_i}{\delta Ta_i} = \frac{C_1 V_T(2Ta_o-Tw_i-Tw_o)}{(Tw_i+Tw_o-Ta_i-Ta_o)^2}$$

$$\frac{\delta h_i}{\delta Tw_i} = \frac{C_1 V_T(Ta_o-Ta_i)}{(Tw_i+Tw_o-Ta_i-Ta_o)^2} = \frac{\delta h_i}{\delta Tw_o}$$

$$\frac{\delta h_i}{\delta V_T} = \frac{C_1(Ta_o-Ta_i)}{(Tw_i+Tw_o-Ta_i-Ta_o)}$$

$$\left[\Delta h_i\right]^2 = \left[\frac{C_1 V_T(Ta_o-Ta_i)}{(Tw_i+Tw_o-Ta_i-Ta_o)^2}\right]^2 \times \left[\Delta Tw_i\right]^2 +$$

$$\left[\frac{C_1 V_T(Ta_o-Ta_i)}{(Tw_i+Tw_o-Ta_i-Ta_o)^2}\right]^2 \times \left[\Delta Tw_o\right]^2 +$$

$$\left[\frac{C_1 V_T(2Ta_o-Tw_i-Tw_o)}{(Tw_i+Tw_o-Ta_i-Ta_o)^2}\right]^2 \times \left[\Delta Ta_i\right]^2 +$$

$$\left[\frac{C_1 V_T(Tw_i+Tw_2-2Ta_i)}{(Tw_i+Tw_o-Ta_i-Ta_o)^2}\right]^2 \times \left[\Delta Ta_o\right]^2$$

$$= \left[\frac{Tw_oTa_i+Ta_oTw_o-Ta_o^{\,2}-Ta_i-Ta_iTw_o+Ta_i^{\,2}}{(Tw_i+Tw_o-Ta_i-Ta_o)^2}\right]^2 \times$$

$$\left[\Delta V_T\right]^2 \quad \ldots\ldots\ldots\ldots\ldots\ldots\ldots\ldots\ldots\ldots (4.64)$$

In order to find the ratio of Δh_i to h_i, R.H.S must be divided by h_i and the square root taken.

$$\frac{\Delta h_i}{h_i} = \sqrt{\frac{R.H.S}{h_i}}$$

4.3.2 Heat Transfer Coefficients on Shell Side

The heat transferred from hot gas to the tube wall QCON is given in equation (4.65)

$$QCON = h_o \times AL_o x(T_G-(\frac{Tw_o + Tw_i}{2})) \qquad \text{.......(4.65)}$$

$$\therefore \quad h_o = \frac{QCON}{AL_o(T_G-(\frac{Tw_o+Tw_i}{2})} \qquad \text{...........(4.66)}$$

and from equation (4.67).

$$QCON = Dens_1 \times V_T \times A_T x(\frac{Cp_1+Cp_2}{2})(Ta_o-Ta_i)$$

$$\text{...........(4.67)}$$

$$\therefore \quad h_o = \frac{Dens_1 x V_T x A_T x(\frac{Cp_1+Cp_2}{2})(Ta_o-Ta_i)}{AL_o(T_G-(\frac{Tw_o+Tw_i}{2}))}$$

$$\text{...........(4.68)}$$

The variables are:

Ta_o, Ta_i, Tw_o, Tw_i, T_G, V_T

The parameters are:

$Dens_1$, A_T, Cp_1, Cp_2

The physical properties were regarded to be parameters, for the reason that they are temperature dependant, and an error in temperature reading such as $\pm$ 0.5 ^{o}C, should not effect their values significantly.

Now

$$h_o = \frac{C_2 \times V_T(Ta_o \Delta Ta_i)}{T_G \,\Delta\, (\frac{Tw_o+Tw_i}{2})} \quad \ldots\ldots\ldots\ldots\ldots\ldots\ldots (4.69)$$

where

$$C_2 = \frac{Dens_1}{AL_o} \times A_T \times \frac{(Cp_1+Cp_2)}{2}$$

$$(\Delta h_o)^2 = (\frac{\delta h_o}{\delta Tw_o})^2 (\Delta Ta_o)^2 + (\frac{\delta h_o}{\delta Ta_i})^2 (\Delta Ta_i)^2 +$$

$$(\frac{\delta h_o}{\delta T_G})^2 (\Delta T_G)^2 + (\frac{\delta h_o}{\delta Tw_i})^2 (\Delta Tw_i)^2 \quad \ldots\ldots (4.70)$$

$$(\frac{\delta h_o}{\delta Ta_o}) = (\frac{CV_T}{T_G-(\frac{Tw_o+Tw_i)}{2}})^2$$

$$\frac{\delta h_o}{\delta Ta_i} = (\frac{CV_T}{(T_G-(\frac{Tw_o+Tw_i}{2}))})^2$$

$$\frac{\delta h_o}{\delta T_G} = \frac{-C_2V_T(Ta_o-Ta_i)}{(T_G-(\frac{Tw_o+Tw_i}{2}))^2}$$

$$\frac{\delta h_o}{\delta Tw_o} = \frac{\frac{1}{2}\times C_2V_T(Ta_o-Ta_i)}{(T_G-(\frac{Tw_o+Tw_i}{2}))^2}$$

$$\frac{\delta h_o}{\delta Tw_i} = \frac{\frac{1}{2}\times CV_T(Ta_o-Ta_i)}{(T_G-(\frac{Tw_o+Tw_i}{2}))^2}$$

$$\frac{\delta h_o}{\delta V_T} = = \frac{C_2(Ta_o-Ta_i)^2}{(T_G-(\frac{Tw_o+Tw_i}{2}))}$$

$$(\Delta h_o)^2 = \left(\frac{C_2V_T}{(T_G-(\frac{Tw_o+Tw_i}{2})^2}\right)^2(\Delta Ta_o)^2 +$$

$$\left(\frac{C_2V_T}{T_G-(\frac{Tw_o+Tw_i}{2})^2}\right)^2(\Delta Ta_i)^2 \ +$$

$$\left(\frac{-C_2V_T(Ta_o-Ta_i)}{(T_G-(\frac{Tw_o+Tw_i}{2}))^2}\right)^2(\Delta T_G)^2 + \left(\frac{\frac{1}{2}xCV(Ta_o-Ta_i)}{(T_G-(\frac{Tw_o+Tw_i}{2}))^2}\right)^2 \quad x$$

$$(\Delta Tw_o)^2 + \left(\frac{\frac{1}{2}xC_2V_T(Ta_o-Ta_i)}{(T_G-(\frac{Tw_o+Tw_i}{2})^2}\right)^2 x(\Delta Tw_i)^2 \quad +$$

$$\left(\frac{C(Ta_o-Ta_i)}{(T_G-\frac{Tw_o+Tw_i}{2})}\right)^2 \ x \ (\Delta V_T)^2$$

$$\frac{\Delta h_o}{h_o} = \sqrt{\frac{R.H.S}{h_o}} \ \ldots\ldots\ldots\ldots\ldots\ldots\ldots\ldots\ldots\ldots (4.71\ )$$

The errors in temperature readings we regarded to be in the range of $\pm$ 0.5 ^{o}C, since divisions on the electronic thermometer were in 1^{o}C intervals.

Errors of fresh air velocity through tubes are as explained below:-

The following equation was used for calculating the air velocity:-

$$V = 4000 \sqrt{\frac{30}{B} \times \frac{TR}{528} \times hp} \times 60 \quad \ldots. (4.72)$$

where

V = air velocity through tubes

B = Barometric pressure in. Hg

TR = absolute ambient air temperature R^{O}

hp = pressure drop measured by pitot tube inch of water gauge.

To smooth the readings which may have been effected by positioning the pitot tube at a wrong angle inside the tubes(Yaw), or taking slightly inaccurate readings from the manometer, three readings were taken, and the used value was the average of these three readings.

In this error calculation, three pressure drop values were taken as typical of the values obtained for the sample tubes:-

1.0" water   0.6"water   0.2"water

which cover the range of the measurements of pressure drops in tubes.

As the manometer range of division was in 0.01 therefore errors involved in readings, were regarded in the order of $\pm$ 0.005 inch of water.

$$V_T = 4000 \times \frac{30}{29.46} \times \frac{529.8}{528} \times 0.06 \times 60 \qquad \ldots.(4.73)$$

$$= \pm 17139$$

i) for 1.0" pressure

$$\frac{\Delta V_T}{V_T} = \frac{17139}{242388} = 0.09$$

ii) for 0.6"

$$\frac{\Delta V_T}{V_T} = \frac{17139}{187753} = 0.12$$

iii) for 0.2"

$$\frac{\Delta V_T}{V_T} = \frac{17139}{108399.2} = 0.2$$

$\therefore$ average ratio errors incurred in calculating fresh air velocity to the measured velocity $\left(\frac{\Delta V_T}{V_T}\right)$

$$= \frac{0.09 + 0.12 + 0.2}{3}$$

$$= 0.14$$

$$\therefore \quad \Delta V_T = 0.13 V_T$$

4.3.3 Errors in Reynolds Number on Tube Side

$$Re_T = \frac{\rho V_T D}{\mu} = \frac{(Dens_i + Dens_o) \times V_T \times D}{(Visc_i + Visc_o)} \quad \ldots.(4.74)$$

$$\Delta Re_T = \left(\frac{\partial Re_T}{\partial V_T}\right)^2 \times (\Delta V_T)^2$$

As (V_T) is the only variable with involved errors

$$(\Delta Re_T)^2 = \left(\frac{(Dens_i + Dens_o) \times D}{Visc_i + Visc_o}\right)^2 \times (0.13 V_T)^2 \quad \ldots.(4.75)$$

$$(\Delta Re_T)^2 = C_3^2 \times (0.13 V_T)^2 \quad \ldots\ldots\ldots\ldots\ldots\ldots\ldots(4.76)$$

Where $C_3 = \left(\frac{(Dens_i + Dens_o)}{Visc_i + Visc_o}\right)$

$$\frac{\Delta Re_T}{Re_T} = \frac{C_3^2 \times (0.13)^2}{Re_T} \quad \ldots\ldots\ldots\ldots\ldots\ldots\ldots(4.77)$$

4.3.4 Errors in Reynolds number on shell side

$$Re_S = \frac{Dens_S \times V_S \times Dev}{Visc_S} \quad \ldots\ldots\ldots\ldots\ldots\ldots(4.78)$$

$$(\Delta Re_S)^2 = \left(\frac{\partial Re_S}{\partial V_S}\right)^2 \times (\Delta V_S)^2 \ldots\ldots\ldots\ldots\ldots\ldots\ldots(4.79)$$

Since the hot gas velocity in the tubes was measured with a portable pitot tube more errors are likely than in measuring fresh air velocity, where orifice plates were used to measure the flow rate. So since the secondary air flow rate, primary air flow rate and natural gas flow rate was measured using reliable meters, the errors involved were assumed to be $\pm$ 0.07 V_S

$$(\Delta Re_S)^2 = C_4^2 \times (0.07V_S)^2 \quad \ldots\ldots\ldots\ldots\ldots\ldots\ldots (4.80)$$

where

$$C_4 = \frac{Dens_S \times Dev}{Visc_S}$$

$$\therefore \frac{\Delta Re_S}{Re_S} = \frac{C_4^2 \times (0.07V_S)^2}{Re_S} \quad \ldots\ldots\ldots\ldots\ldots\ldots\ldots (4.81)$$

The error calculations were carried out by the aid of a computer program, See Appendix (A.2.7)

The results obtained from this work are as follows:-

i) Error in calculating heat transfer coefficients on tube side was found to be $\pm$ 7%

ii) Errors in calculating heat transfer coefficients on shell side was found to be $\pm$ 4.2%

iii) Errors in calculating Reynolds numbers on tube side was found to be $\pm$ 13%

iv) Errors in calculating Reynolds umbers on shell side was assumed to $\pm$ 7%

4.3.5 Discussion of involved errors

Looking at the errors shown above, one concludes that due to the limitations of experimental equipment and instrumentations, as the rig is purely industrial, therefore,such degree of errors would be regarded as normal, especially on the tube side.

It was observed that, when heat transfer correlations of the form

$$Nu = x \, Re^{m} \, Pr^{n} \quad \ldots\ldots\ldots\ldots\ldots\ldots\ldots\ldots\ldots\ldots (4.82)$$

were developed for the following process conditions:-

i) Various secondary air flow rates
ii) Blocked tubes in the bundle, for wider range of Reynolds Number
iii) One burner in operation at a time
iv) hot air flowing across the bundle with both burners off

The power of Reynolds number "m" was ranging around unity giving an overall average of 1.08, which is a good representation of the whole experimental data.

CHAPTER FIVE

5. Discussion of Results

The practical heat transfer coefficients on the inside wall were found to be much higher than the calculated ones found by applying standard correlations such as Kern, Sieder-Tate, McAdams, and others. The reasons as will be discussed later, were due to the end effects, small ratio of tube length to diameter and gaseous nature of the fluids .

The results were correlated by plotting practical Nusselt numbers against their corresponding Reynolds numbers, for the individual twelve sample tubes which are the following:

1:1	1:3	1:5	2:2	2:4	2:6
6:3	6:4	7:4	8:3	8:4	10:3

It was observed that the first six tubes, which were in the frontal rows, namely, first and second, gave results, which when plotted, showed scattered points, so that the correlation factor was poor.

When each set of six tubes, the frontal, and the central of the bundle, were plotted separately, the obtained results, by the aid of a computer package, showed that the second six tubes, which were situated at the centre and rear of the bundle, showed much better correlation coefficients and standard deviations. It was decided, therefore to correlate on the second six tubes in the bundle, so that the heat transfer coefficients on the inside wall would be more reliable.

The same process was used for the heat transfer coefficients on the shell side, and the results supported the approach, as there was a large flow discrepency on the frontal part of the bundle as will later be discussed in this chapter.

An attempt was made to improve the correlation factor, in other words to make the individual plotted Nu-Re, for the inside wall, fall nearer each other by applying a correction factor. See figure (5.1)

It was thought, since the fresh air flow rates vary from one tube to another, due to uneven distribution of air flow through the bundle, and individual entrance effects are a function of Reynolds numbers, which were varying in the tubes, therefore, an entrance effect analysis would probably help to bring the individual tube lines together.

The following correlations were used (62)

$$St_{f,c} = 0.0204\ Re^{-0.195} Pr^{-0.585} \quad \text{..........(5.1)}$$

$$St_f = St_{f_{lc}} \times \left(\frac{Tw}{Tb}\right)^{-0.4} \quad \text{..............(5.2)}$$

$$St_e = St_f \times \int_{x=0}^{x=150} dx \quad \text{..............(5.3)}$$

$$St_{mean} = \frac{15D}{L} \times St_e + \left(\frac{L - 15D}{L}\right) St_f \text{......(5.4)}$$

where

$St_{f,c}$ = Stanton number appropriate to constant fluid properties and fully developed conditions.

St_f = Stanton number appropriate to fully developed conditions.

St_e = Stanton number, experimental value

T_b = air temperature evaluated of the bulk fluid F^o, (C^o)

Tw = wall temperature F^o, (C^o)

G = mass velocity lb/ft^2h, (kg/m^2s).

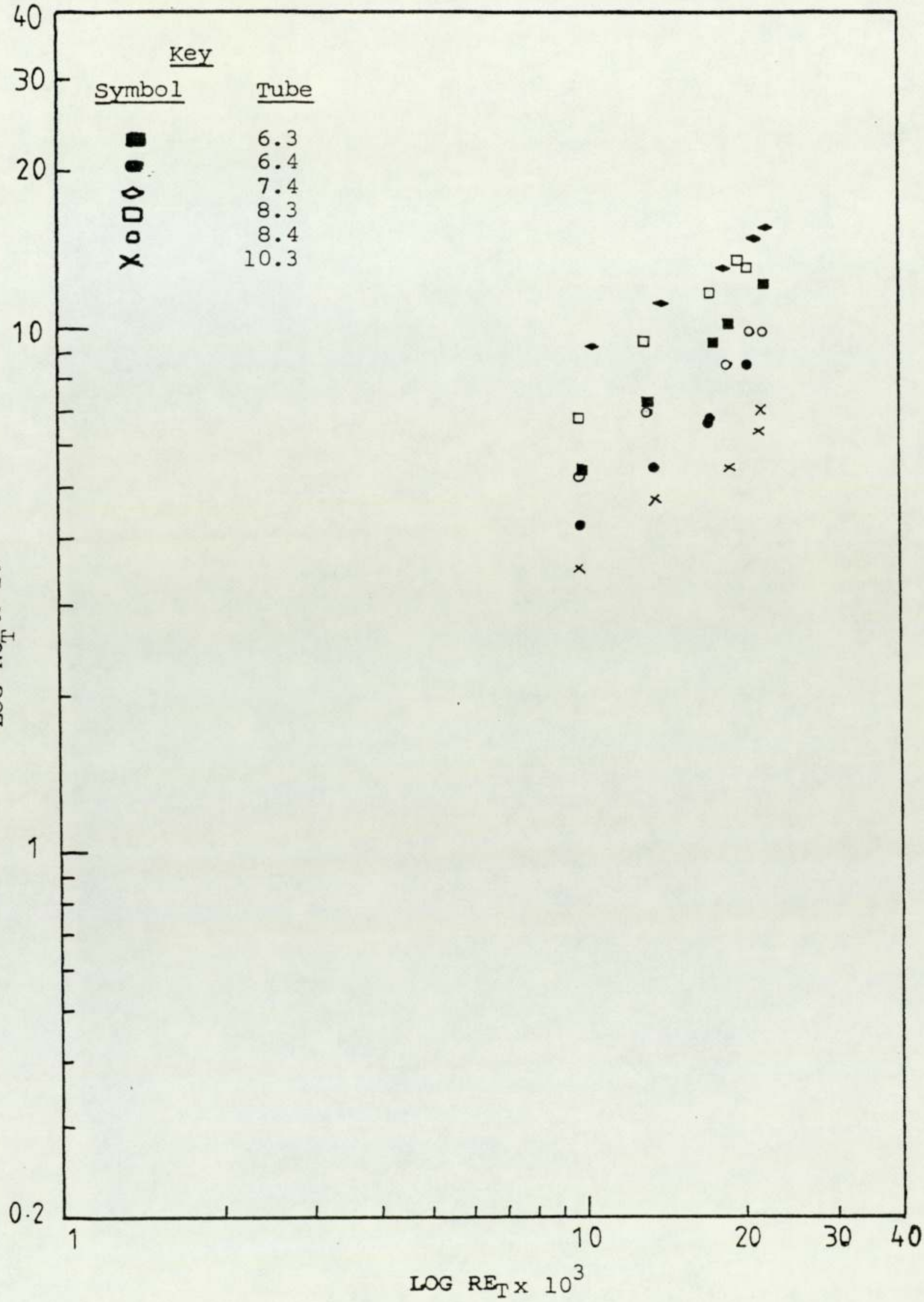

FIG:5.1 Variation of Nusselt Number with Reynolds Number of secondary air flow (69368 ft^3/hr) without correction factor

A computer program was used to calculate the mean Stanton number, $(\frac{h}{cpG})$, for each individual tube, making allowance for each entrance effect based on the corresponding Reynolds number. This work did not improve the correlation factor for the tubes, as the correlation factor was lower, and the standard deviation was higher for the heat transfer correlations Nu-Re on the six sample tubes which are as follows:-

6:3 6:4 7:4 8:3 8:4 10:3

The uncorrected correlation, based on the above six tubes, gave a lower standard deviation and higher correlation factor.

Since the position of the line seemed to depend on tube outlet air temperature a correction factor was proposed to improve the correlation even further. This turned out to be

$$\left(\frac{Ta_{mix}}{Ta_o}\right)^4$$

where

Ta_{mix} = air temperature in the outlet chest ^oC

Ta_o = air temperature at a particular tube outlet ^oC

The power "4" was found,by an iterative method to give the lowest standard deviation and highest correlation factor.

The reason for the variation in the individual tube heat transfer coefficients in the frontal region, was thought to be the turbulence and swirling of hot gases around the frontal tubes, In addition, some zoning, and variation in flow rates in the combustion chamber, would lead to an uneven temperature profile around the frontal tubes (first and second rows). Probe scanning along tubes (wall temperature, four radial positions), confirmed this irregularity in the frontal tubes.

5.1. Effect of Secondary Air Flow Rate on Radiation

The total amount of radiation emitted from the radiative gases Co_2 and H_2o, and the refractory walls to the bundle of tubes, was found to increase with a decrease of the volumetric flow rate of the secondary air, see figure (5.2).

The reason for this was that the increasing secondary air to the combustion chamber would lower the temperature of the hot gases and the refractory walls, which leads to lower amounts of radiation from both radiative gases and the refractory walls, as the temperature difference between them and the tube bundle would be lower. Also an important factor is the partial pressure of Co_2 and H_2o which would decrease for an increase in secondary air flow, causing low radiation from the gas bulk.

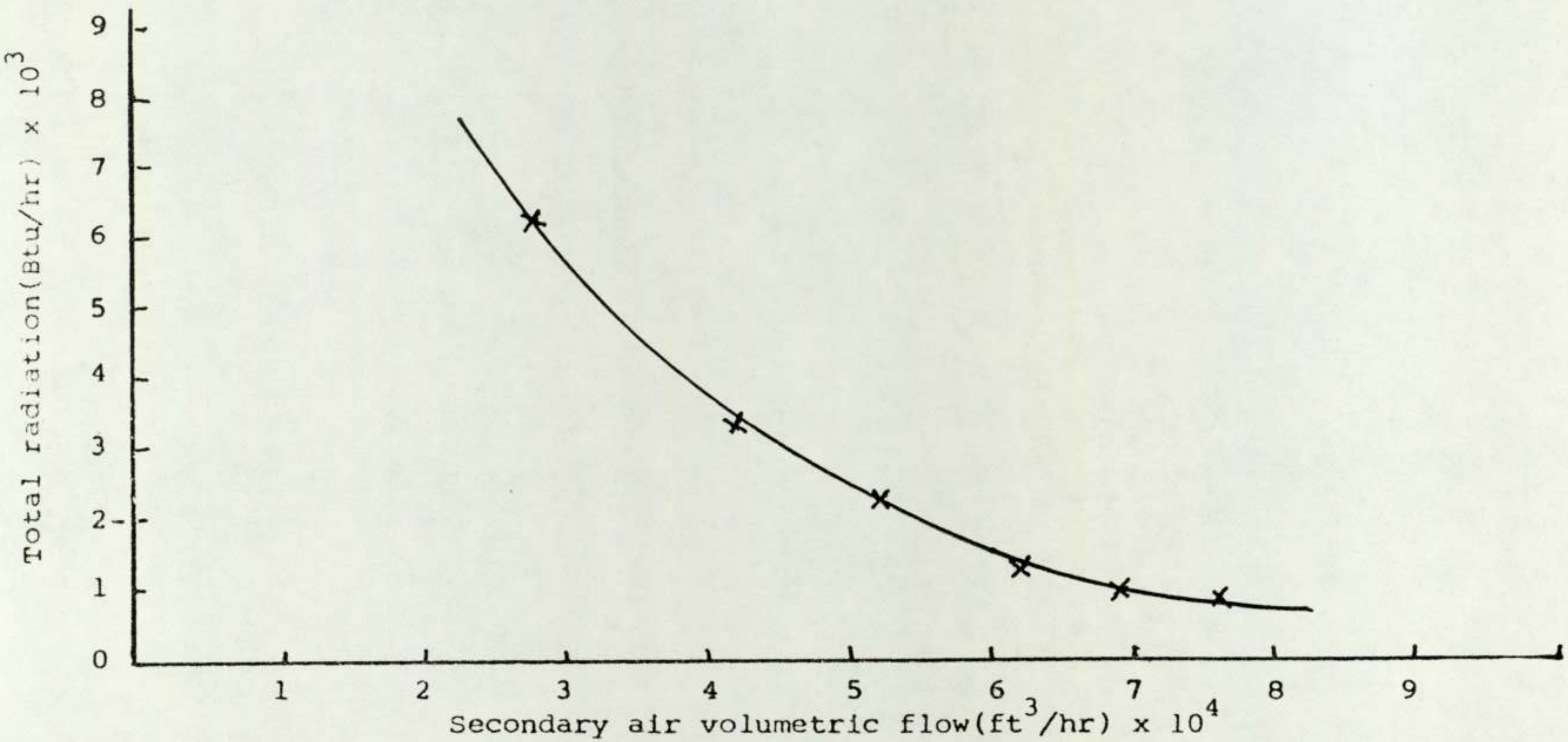

FIG (5.2) variation of total radiation with secondary air flow

5.1.1 Temperature Scanning Through Tubes

As temperature scanning at four radial positions through and along individual tubes was carried out, as shown in figure (5.3), it was observed that temperatures along the tubes in first and second rows were not uniform

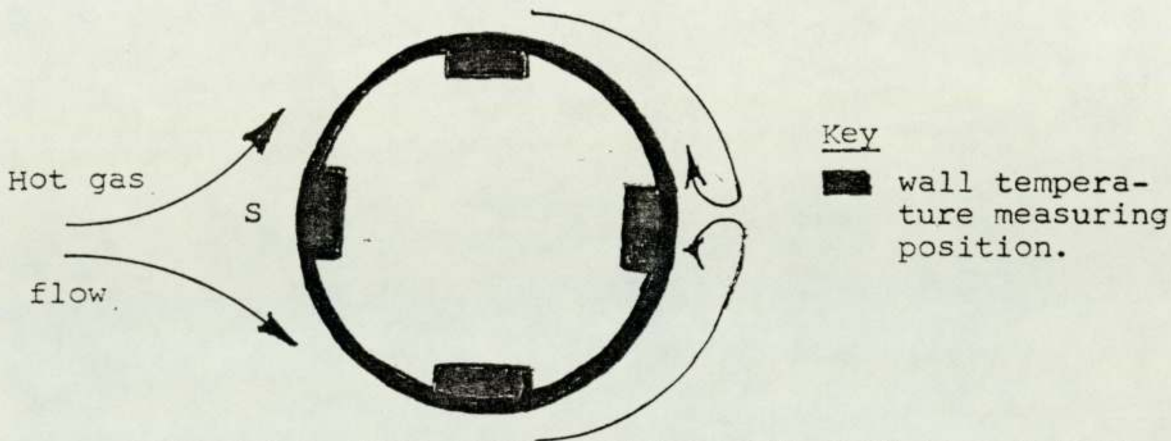

Figure 5.3 Tube cross section with wall temperature measuring positions.

along the tubes. Considering the radial position temperatures, at the stagnation points (S) were showing slightly higher temperatures that the other three positions namely: top, bottom and back of the tube. This slight rise in temperature may be due to the hot gases flowing against the stagnation points where an impact take place, unlike the top and bottom where hot gases sweep passed tube sides, or it may be because of some radiation effect on the front of the bundle.

The other tubes in the bundle, centre and rear, did not show a high degree of temperature profile irregularity. The reason for that was thought to be the hot gas flow in the shell becoming more uniform, as it goes deeper into the bundle.

This kind of scanning was done for the following process conditions:

i) full secondary air flow rate.
ii) low secondary air flow rate
iii) one burner on at a time,
iv) high natural gas flow at constant secondary air flow.
v) low natural gas flow at constant secondary air flow.

Incremental heat transfer coefficients on the tube side were calculated, based on the data obtained from scanning for each tube, at four inch (100mm) intervals along the tubes. It was found that the front tubes, in the first and second rows had very variable heat transfer coefficients along the length, and the central and rear tubes had more constant heat transfer coefficients along the tube length. The calculated errors were higher than the statistical errors so that the assumption of constant heat transfer is valid. As logarithmic mean temperature difference is usually used when the temperature difference varies along the entire tube length as a reasonable average of the mean temperature difference, this seems a suitable method, especially when a correction factor, which is based on the process

Fresh air density	0.049 Lb/ft^3, ($0.882\ Kg/m^3$)
Hot gas density	0.051 Lb/ft^3, ($0.822\ Kg/m^3$)
Reynolds number, tube side	23974
Reynolds number, shell side	17150
Prandtl number, tube side	0.69
Prandtl number, shell side	0.95
Fresh air specific heat capacity	0.219 Btu/Lb $^{\circ}F$ (0.916 KJ/Kg $^{\circ}K$)
Hot gas specific heat capacity	0.23 Btu/Lb $^{\circ}F$ (0.963 KJ/Kg $^{\circ}K$)
Fresh air thermal conductivity	0.012 Btu/hr ft $^{\circ}F$ (0.02 w/m $^{\circ}K$)
Hot gas thermal conductivity	0.019 Btu/hr ft $^{\circ}F$ (0.033 w/m $^{\circ}K$)
Fresh air viscosity	0.046 Lb/ft hr (0.069 Kg/m hr)
Hot gas viscosity	0.05 Lb/ft hr (0.076 Kg/m hr)
Shell equivelant diameter $\left(\frac{4 \text{ x free area}}{\text{wetted perimeter}}\right)$	0.108 ft, (3.3cm)
Outside tube diameter	0.088 ft, (2.7cm)
Inside tube diameter	0.077 ft, (2.35cm)

parameters such as mixing degree in the shell, is used. This method was compared with the linear method, and also with the mean temperature difference based on the practical work as explained in earlier chapter, and it was found that when a correction factor was used for logarithmic mean temperature difference, the mean temperature difference would be almost similar to the practical mean temperature difference. Since the linear method is not corrected by a correction factor and process parameters are not included, it would not be as suitable as the logarithmic mean temperature difference, although it gave a very close mean temperature difference to the logarithmic one. This means that since logarithmic mean temperature difference was used for calculating heat transfer coefficients, and the profile of heat transfer coefficients along the tube was similar at the back and centre of the bundle, logarithmic mean temperature difference, is a suitable method of calculating the mean temperature difference along the tube. Also during the temperature scanning, it was found that there was no irregular temperature profile along the rear and central tubes.

The overall conclusion from temperature scanning, was that the temperature profiles of tubes in the centre and rear regions of the bundle were reasonably uniform and linear and even when a single burner was firing, the profile was only slightly effected.

When operating a single burner at a time the results obtained, when correlated, did not show any significant difference as far as the slope i.e. the power of Reynolds numbers, or the intercept, for a constant secondary air flow rate. In other words it did not matter which burner was in operation. This means that a good degree of mixing was taking place in the shell.

5.1.2 Comparison of the Obtained Correlation to the Published ones.

The heat transfer correlations based on the experimental data obtained from the present work were of the following forms:

Tube side:

$$\frac{h_i D_i}{K} = 0.0028 Re_T^{1.08} Pr^{0.33} \quad \ldots\ldots\ldots\ldots\ldots\ldots (5.5)$$

Shell side:

$$\frac{h_o D_o}{K} = 0.89\ Re_S^{0.42} Pr^{0.33} \quad \ldots\ldots\ldots\ldots\ldots\ldots (5.6)$$

if applied, they would give the correct design values, i.e. no over-design.

A comparison of these practical correlations to the established correlations in the literature, was done, using the following data, which was obtained from the present experimental work:

Applying the practical correlations, which were obtained in the present work:

<u>Tube side correlation</u>

$$\frac{hi \times 0.077}{0.012} = 0.023\ (23974)^{1.08}(0.69)^{0.33}$$

$$hi = 20.7\ \text{Btu/hr ft}^2\ F^{\circ}, (117\ w/m^2\ C^{\circ})$$

<u>Shell side correlation</u>

$$\frac{ho \times 0.088}{0.019} = 0.89(17150)^{0.42} x (0.95)^{0.33}$$

$$ho = 11.34\ \text{Btu/hr ft}^2 F^{\circ}, (644\ w/m^2 K)$$

Now applying, standard and already published heat transfer correlations:

<u>McAdams</u>(16)

$$\left(\frac{hi}{CpG}\right)_i (Pr)^{0.33} = \frac{a/Fs}{(DG/u)_i^{\,1-ni}} \quad \text{..........(5.7)}$$

$$\left(\frac{ho}{CpG}\right)_o (Pr)^{0.33} = \frac{a/Fs}{(DG/u)^{1-no}} \quad \text{..........(5.8)}$$

where

F_s = 1.25

a = 0.023 tube side

n_i = 0.8

n_o = 0.6 for staggered tubes

a = 0.33 for staggered tubes

The above equations (5.7), (5.8) are said to be suitable for both liquid and gaseous heat transfer

taking equation (5.7)

$$\left(\frac{hi}{0.219 \times 14323}\right)_i \times (0.69)^{0.33} = \frac{0.023/1.25}{(23474)^{1-0.8}}$$

$$\therefore \qquad hi = 8.7 \text{ Btu/hr ft}^2 \text{ F}^o$$

$$= (49.2 \text{ w/m}^2 \text{ C}^o)$$

Applying equation (5.8),

$$\left(\frac{ho}{0.23 \times 7372}\right)(0.95)^{0.33} = \frac{0.33/1.25}{(17150)^{1-0.6}}$$

$$\therefore \qquad ho = 12.9 \text{ Btu/hr ft}^2\text{F}^o,$$

$$(73 \text{ w/m}^2\text{C}^o)$$

Nusselt (1)

Applying the following equation presented by Nusselt, where the effect of entrance was introduced

$$\left(\frac{h_i d_o}{K}\right)_b = 0.036\left(\frac{dwG}{u}\right)^{0.8}\left(\frac{cpu}{K}\right)^{0.33}\left(\frac{L}{dw}\right)^{-0.054} \quad \ldots(5.9)$$

$$\frac{hi \times 0.077}{0.012} = 0.036(23974)^{0.8}(0.69)^{0.33}(40)^{-0.054}$$

$\therefore\ h_i \quad = \quad 12.9$ Btu/hr ft^{2}F^o, (73 w/m^2 C^o)

Kern (9)

Tube side

$$\frac{h_i D}{K} = 0.027\ Re^{0.8} Pr^{0.3} \left(\frac{\mu}{\mu w}\right)^{0.14} \qquad \ldots\ldots\ldots\ldots (5.10)$$

Since air was used $\left(\frac{\mu}{\mu w}\right)^{0.14}$ is unity

Applying equation (5.10)

$$\frac{h_i \times 0.077}{0.012} = 0.027(23474)^{0.8}(0.68)^{0.33} \times 1$$

$\therefore\ h_i \quad = \quad 11.8$ Btu/hr ft^{2}F^o, (67 w/m^2 C^o)

Shell side

$$\frac{h_o D_e}{K} = 0.36\left(\frac{D_e G_s}{\mu}\right)^{0.55} (Pr)^{0.33} \left(\frac{\mu}{\mu w}\right)^{0.14} \qquad \ldots . (5.11)$$

Applying equation (5.11)

$$\frac{h_o \times 0.108}{0.0199} = 0.36\left(\frac{7372 \times 0.108}{0.051}\right)^{0.55} \times (0.95)^{0.33} \times 1$$

$\therefore\ h_o \quad = \quad 13.2$ Btu/hr ft^{2}F^o, (74.7 w/m^2 C^o)

Sieder-Tate (4)

The following equation was mainly for turbulent flow up to 100,000.

$$\frac{h_i D}{K} = 0.027\left(\frac{DG}{u}\right)^{0.8}\left(\frac{cpu}{K}\right)^{0.33}\left(\frac{\mu}{\mu w}\right)^{0.14} \quad \ldots\ldots\ldots\ldots(5.12)$$

taking $\left(\frac{\mu}{\mu w}\right)$ equal to 1

Applying equation (5.12).

$$\frac{h_i \times 0.077}{0.012} = 0.027(23474)^{0.8}(0.69)^{0.33} \times 1$$

$$h_i = 11.87 \text{ Btu/hr ft}^2\text{F}^o, (67 \text{ w/m}^2\text{C}^o)$$

Dittus and Boelter (2)

$$\left(\frac{h_i D}{K}\right)_b = 0.023\left(\frac{DG}{u}\right)_b\left(\frac{cpu}{K}\right)_b^{0.33} \quad \ldots\ldots\ldots\ldots(5.13)$$

Applying eqaation (5.13).

$$\frac{h_i \times 0.077}{0.012} = 0.023(23974)^{0.8}(0.69)^{0.33}$$

$$\therefore h_i = 10 \text{ Btu/hr ft}^2\text{F}^o, (56.8 \text{ w/m}^2\text{C}^o)$$

Colburn (3)

$$\left(\frac{h_i}{Gcp}\right)_b \left(\frac{cp\mu}{K}\right)^{2/3}_{T_{0.5}} = 0.023\left(\frac{DG}{u}\right)^{-0.2} \qquad \text{...........(5.14)}$$

Applying equation (5.14)

$$\left(\frac{h_i}{0.219 \times 14323}\right)(0.69)^{2/3} = 0.023(23947)^{-0.2}$$

$$\therefore \qquad h_i = 12.3 \text{ Btu/hr ft}^2 F^{\circ}, (69.9 \text{ w/m}^2 C^{\circ})$$

John L. Boyen

Boyen(63) recommended two correlations in his text book for both tube and shell sides for gaseous heat transfer which are used in industry at the present time. Tube side correlation

$$\frac{h_i D}{K} = 0.0255 \, Re^{0.8} Pr^{0.4} \qquad \text{....................(5.15)}$$

equation (5.15) is only valid when $G > 1650 \, p^{0.645}$ which is no problem in this case, as G = 14323

applying equation (5.15)

$$\frac{h_i \times 0.077}{0.012} = 0.0255(23974)^{0.8}(0.69)^{0.4}$$

$$h_i = 10.9 \text{ Btu/hr ft}^2 F^{\circ}, (61.9 \text{ w/m}^2 C^{\circ})$$

Shell side

$$\frac{h_o D_o}{K} = 0.385\ Re^{0.56} Pr^{0.3} \quad \text{....................(5.16)}$$

applying equation (5.16)

$$\frac{h_o \times 0.088}{0.0199} = 0.385(17150)^{0.56}(0.95)^{0.33}$$

$$h_o = 20\ \text{Btu/hr ft}^2\text{F}^o, (113.6\ \text{w/m}^2\text{C}^o)$$

(unusually high)

L.M.K. Boelter, et al (63) presented the following correlation, which is regarded as a very reliable method for gas heat transfer calculation, with gas flowing across tubes bank.

$$h_o = \frac{0.8(c)(Ta)^{0.33}(G_1)^{(0.6+0.08\ \log d)}}{d^{0.53}} \quad \text{........(5.17)}$$

where

c = constant (usually 1.25) for air

T_a = average gas temperature degree R

G_1 = gas mass flow, $lb/ft^2 sec$.

d = tube o.d

applying euation (5.17)

$$h_o = \frac{0.8(1.25) \times (794)^{0.33} \times (2.04)^{(0.6+0.08\log d)}}{(1.050)^{0.53}}$$

$$= 13.6\ \text{Btu/hr ft}^2\text{F}^o, (77.3\ \text{w/m}^2\text{C}^o)$$

Table (5.1) shows that the practical heat transfer coefficients obtained in this work for tube side were generally higher than those predicted by the standard correlations mentioned earlier. The reasons were discussed earlier. It is important to mention that some factors were ignored, in one correlation or another for example, entrance effect, and in another, the gaseous nature, and so on.

The heat transfer coefficients on the shell side seem to be acceptably near the figures published by other workers, which means that the over design was mainly caused by the inadequate determination of heat transfer coefficients on the tube side.

It has been found in the literature that when hot gases are flowing on the shell side and liquid through tubes, there is no over-design taking place, and since the system gas-liquid is different from the present system gas-gas, most of the change was due to the tube side, concerning the boundary layer differences between gases and liquids.

5.2 General Considerations

The important factors affecting the rate of heat transfer between the walls of a pipe and a fluid flowing through it are usually assumed to be the fluid velocity, the diameter of the pipe, the length of the pipe, the nature of the fluid and the temperature conditions in the fluid from

Table(5.1) Comparison of standard and practical heat transfer coefficients, tube and shell side.

Reference	h_i	h_o
Practical	20.7	11.34
McAdams	8.7	12.9
Nusselt	12.9	-
Kern	11.8	13.2
Sieder-Tate	11.9	-
Dittus-Boelter	10.0	-
Colburn	12.3	-
Boyen	10.9	20.0
L.M.K Boelter	-	13.6

pipe wall to centre line.

Numerous investigators have shown that for fluids in turbulent regimes, the film coefficients of heat transfer between pipe wall and gas vary as the n^{th} power of the mass velocity of the gas, the value of n being about 0.8. The practical data obtained in this particular work, suggested that the n^{th} power mentioned above was higher than 0.8 for the inside tube heat transfer coefficient. This would lead to the conclusion that the mechanism of heat transfer in the present work does not fit the standard and conventional correlations.

In this chapter, general aspects of the present research work, will be discussed in detail.

5.2.1 Instrumentation

All temperatures on the tube walls and in the bulk of fluids were measured using chromel/alumel thermo-couples and an electronic thermocouple meter. Special care was taken, as temperatures were known to be very important design criteria. Wall thermo-couples were attached to the inside surface of the tubes. The reason for choosing this method was mainly because of the thickness of the tube walls, 0.065 inch,(7.65mm) which was regarded as too thin to be grooved so that a thermocouple junction could be embedded in it. Besides, the latter method has been criticised by several research workers, as the thermocouple junction would effect the readings, due to the hot spot established around it. Also the thermal profile would be distorted. For these reasons the method of attaching thermo couples to the walls of the tubes was chosen, as it was the most suitable ona for this specific equipment among other methods.

In measuring the temperature of the fluids flowing through individual tubes, the radiation effect from tube walls to the thermo couple junction was ignored as the temperature difference was found to be small between the wall and the fresh air. Air was considered to be a non-radiative gas.

Considering the temperature measurement of the flue gases in the combustion chamber and the shell, the temperature reading could have been affected by radiation emitted from the refractory walls and radiative gases Co_2 and H_2o, if the thermo couples were not shielded. Therefore, the thermo-couples which were used for measuring the refractory walls were sheath types where the junction was not exposed. Also they were not pushed through the wall fully, they were still covered by a very thin layer of the refractory.

For measuring the temperature of the flue gases, special probes were made, so that the radiation effect would be minimised.

The flow rates in individual tubes measured with a standard pitot tube 3/16 inch diameter would certainly involve some errors because"**Yaw**"might have taken place in some cases where the access to the tubes was not completely free, especially around the edges of the chest in front of the tubes. Therefore three sets of measurments were made to make sure the readings were realistic, and the sum of the flow rates of the individual tubes was checked against the orifice plate measurement of the main fresh air duct and proved to be acceptable.

Errors in air flowrate measurement through tubes could cause considerable inaccuracy when calculating the heat transfer coefficients and Reynolds numbers which would eventually lead to an inaccurate design correlation.

The errors involved in measuring secondary, primary and fresh air flowrates in ducts are of less concern since standard orifice plates were designed and fitted according to B.S 1042. Also the magnitude of the flow was high compared with flowrates in individual tubes, so the pressure differences were much greater and, therefore, easier to measure.

Probe scanning along the inside of the tubes to measure the temperature of the wall and air as explained earlier, would probably involve higher errors than any other experimental work involved, for the following reasons:

i) The probe's presence inside the tube, and against the direction of flow, would create some flow disturbance; a vena contracta may exist between the tube wall and the outside wall of the probe. As in this work the main purpose was to understand the temperature profile along the tube, the error caused by the probe's presence, would be the same at every point along the tube, so this should not effect the pattern of the temperature profile

ii) The other problem was that during measurment of the wall temperatures at several points along the tube maintaining contact between the detecting thermo-couple and the tube wall was not very easy especially at the far end of the tubes. Therefore, the temperature magnitude was used as a guide since with a good contact the highest wall temperature would be obtained. It was ensured that the electronic thermometer, selector, switches and thermo couples, also the flow measuring instrumentation such as orifice plates, manometers and pitot tubes, were all sound and ready before starting any experimental work. In this way the errors were minimised.

5.2.2 Geometrical effects

It was observed during pressure scanning inside the combustion chamber, that in some regions, there were considerable pressure variations, in some areas even suction was noticed. This certainly causes uneven heat distribution within the combustion chamber and leads to an irregular temperature profile at the entrance of the bundle, as the first and second rows of tubes would experience uneven swirling of the gas.

Considering the individual tube air flow rates, there was uneven distribution of flow in the sixty tubes in the bundle, as some tubes show higher air flow than others, as shown in tables(3.1-3.5). This is mainly due to the way in which the main fresh air inlet was connected to the cold end chest, where the flow of air has to turn through a right angle so is likely to hit the wall of the chest producing high turbulence before entering the tubes.

More even flow distribution would result if the main fresh air duct was in line with the tube direction.

The size of the bundle determines the amount of energy required to pump fluids across it since the pressure drop will increase with an increase in the tube size.

The tube arrangement influences the value of friction factor, which directly influences the pressure drop. It has been found that a staggered tube arrangement increased the heat transfer coefficients on the shell side compared with an in-line tube arrangement. This favours high heat transfer coefficients on the shell side in the present work.

5.2.3 Radiation effects on heat transfer coefficient

All the results show that the radiation effect was almost negligible. The following analysis would support this result:

1. The flame in the combustion chamber was a gaseous fuel flame and dark blue in colour which may be regarded as a non-radiative flame.
2. There was always a large amount of secondary air mixed with the combustion gases in the chamber. This causes the partial pressures of Co_2 and H_2o to be very low, and as a result the amount of gas radiation was insignificant.
3. Radiative heat transfer usually starts to be predominent at around $1000^{o}C$, while in the present situation the highest average temperature was around $500^{o}C$.
4. The temperature difference between refractory walls, hot gas and the sink was not great.
5. Inter-tube radiation is almost non existent because the beam length between tubes is very short; more over, the third row and upward to the tenth row do not see any radiation from the refractory walls and flame.
6. The geometry of the tubes and the walls as they are perpendicular to each other, reduces the amount of radiation falling on the bundle by almost 30%.

When hot air was introduced into the combustion chamber, using a steam heat exchanger while the burners were off, it was found that the correlation obtained was very near to the one based on the data with burners running. This means that hot flue gas should show no significant difference from when non-radiative hot air was used.

correlation based on hot air data:

$$NU_{I_{air}} = 0.009 \; Re^{0.98} Pr^{0.33} \quad \ldots\ldots\ldots\ldots\ldots\ldots (5.18)$$

correlation based on burners in operation

$$NU_{I_{Burner}} = 0.01 \; Re^{0.95} Pr^{0.33} \quad \ldots\ldots\ldots\ldots\ldots\ldots (5.19)$$

5.2.4 Insulation inside the chamber

Three layers of insulating material were used to line the combustion chamber and the shell walls, totalling 4 inches of thickness. Since this was fixed on the inner walls, 4 inches of the bundle on each side were masked towards fluids flow, This means that about one fifth of the tube area was masked, which obviously lowers the overall thermal efficiency of the heat exchanger. A thermo-couple shield inside the chamber about 4 inches wide, fixed in front and in the centre of the shell entrance also creates a restriction to the flow of hot gas and forces it to split in the middle. This would increase the irregularity of flow at the entrance of the bundle.

5.2.5 Effect of Physical Properties Changes

Since air was used as the medium for heat transport on both sides, shell and tube, viscosity variations were not very significant as Prandtl number does not exceed unity, therefore, the correction factor $\left(\frac{\mu}{\mu w}\right)^{0.14}$ was not applied in the present calculation as the ratio is always near unity, unlike in oil and some liquids where this ratio becomes crucial.

Taking for example, a typical set of data from the obtained experimental work which is as follows:

	Wall Temperature C°	Air temperature C°
T_o	114.5	78
T_i	61	26.5

using the air viscosity equation for average temperatures.

viscosity of air at the tube wall

$$= 0.044 \quad (393/(87.9 + 273 + 120)) \times \left(\frac{87.9 + 273}{273}\right)^{1.5}$$

$$= 0.055 \text{ lb/ft hr } (0.0013 \text{ Newton/MS})$$

viscosity of air in the bulk

$$= 0.044 \quad (393/(52.25+273+120)) \times \left(\frac{52.25+273}{273}\right)^{1.5}$$

$$= 0.051 \text{ lb/ft hr, } (0.0012 \text{ Newton/MS})$$

$$\left(\frac{\mu}{\mu w}\right)^{0.14} = \left(\frac{0.051}{0.055}\right)^{0.14}$$

$$= 0.99$$

$$\simeq 1.0$$

For the same reason Prandtl number was taken as a weak variable and has very little effect on the Nusselt-Reynolds correlation, so it was used conventionally from the literature as ($Pr^{0.33}$).

Reynolds numbers, based on the inlet temperature for physical properties of air, involve some errors as the density and viscosity change as temperature changes along the tubes. This leads to a change in the air velocity through the tube as the volumetric flowrate changes. To avoid these errors an average Reynolds number based on the inlet and outlet physical properties would be more useful.

Experimental work proved that the averaged Reynolds number was suitable.

5.2.6 Heat Transfer Coefficients

In the present work, the heat transfer coefficients seem to be higher than those calculated by applying turbulent and fully developed boundary layer correlations, such as Seider-Tate, Dittus-Boelter, Kern etc....

Since radiation was proved to have little effect on the heat transfer coefficients for both shell and tube side, it was necessary to justify this rise in the heat transfer coefficients.

Firstly, the standard correlations mentioned above were mainly intended for different conditions of heat transfer, such as liquid-liquid systems, where physical properties respond differently to temperature changes, tubes length to diameter ratio, must be bigger than 60, and the very important condition that a fully developed turbulent boundary, layer exists. In this present work, such conditions cannot be achieved, as the tube length/diameter ratio was 40 and the practical design produces turbulence in the chest before the air enters the tubes which leads to irregularity of air flow through the tubes.

5.2.6.1 Entrance Effect on Heat Transfer Coefficients.

End effects were not allowed for in standard correlations which would tend to create over design.

Using the following end effect correlation reported by Davies (64), for a typical Reynolds number (20000) of this work.

$$\frac{x_{ent}}{d} = C(Re)^{0.25} \qquad (5.20)$$

Where x_{ent} = entrance length using the following equation:
where C was calculated to be 1.41

$$\frac{Yb}{x} = 0.376\ (Re_x)^{-1/5} \quad \ldots\ldots\ldots\ldots\ldots\ldots\ldots (5.21)$$

where Yb = width of boundary layer, perpendicular to wall inch, mm.

x = distance from leading edge inch, mm,

Re_x = Reynolds number based on entrance length.

d = inside tube diameter.

Applying equation (5.21)

$$x_{ent} = 1.41 \times (20000)^{0.25}$$

$$x_{ent} = 15.4 \text{ inch}$$

This shows that for normal situations where tubes are smooth, and there is little preturbulence,the lowest estimate of the length of the entrance effect, before the turbulent boundary layer is fully developed,is over 15 inches. This means that more than a third of the tube length has an undeveloped turbulent boundary layer in which the heat transfer coefficient would be higher than usual, as the resistance (1/h) would be lower.

The front tubes experience high turbulence, on the shell side, as swirling and zoning take place in the combustion chamber. This results in irregularity in the temperature profile and consequently, the differential heat transfer coefficients along the tubes.

Considerable amounts of information are available for the flow of air across banks of tubes. Many are highly theoretical and some_times do not hold in practice when design methods are compared with test results, as the heat transfer coefficient in the shell is influenced by many factors, which may vary from one particular case to another. Some of these factors are the gas temperature, the mass flow, the tube diameter, and clearance, as well as the arrangement of the tubes, in line, or staggered. The relation is shown in the following equation (63).

$$ho = \frac{0.8(c)(Ta)^{1/3}(G)^{(0.6+0.08\log_{10} d)}}{d^{0.53}} \quad \ldots.(5.22)$$

where

ho = outside film coefficient

C = constant usually (1.25) for air

Ta = average gas temperature R^{O}

G = gas mass flow $lb/ft^{2}S$

d = tube outside diameter inch(cm)

Mass flow has an exponential effect on the value of outside heat transfer coefficient, it increases with an increase in the mass flow of gas. This exonential value was given as $(0.6+0.08\log_{10}d)$.

Temperature also has an effect on the heat transfer coefficient, an increase in gas temperature leading to a rise in the outside heat transfer coefficient. This rise is attributed to gas radiation. In the present work, the actual partial pressures of the radiative gases Co_2 and H_2o were very low, therefore, the effect of radiation would almost be negligible, especially when the inter-tube beam length is small. This suggests that correlation (5.17) was not suitable for this kind of condition.

The tube diameter affects both the outside and inside heat transfer coefficients as research shows (63) that heat transfer coefficients vary inversly as D^m, where m ranges from 0.2 to 0.6. The practical value of m was found to be 0.53.

A staggered tube arrangement, which is the arrangement in this work would also contribute to the rise in the outside heat transfer coefficient.

Although Reynolds number calculated for inside tubes or shell side flow of fluids is usually regarded as a measure of the turbulence, it only refers to the magnitude of turbulence. The actual fluctuations of velocity and the violence of eddies are not considered. The heat transfer coefficients on both sides may well be effected by the scale and intensity of this turbulence.
In this particular work the practical pressure drop was found to be higher than the calculated one, also pressure scanning inside the combustion chamber showed large pressure

and suction regions. This indicates the probability of large eddies within the fluids.

5.2.7 Energy Recovered from wastes

All the experimental work completed has been based on natural gas (CH_4) as fuel. Gaseous wastes are in general easier to handle than liquid wastes, provided the gas characteristics are known, so that heat recovery and clean up should be easily achieved.

During inspection of the tubes no sign of corrosion was observed. The operating tube wall temperature was always at a higher temperature than the water dewpoint. Also the flue gases which pass across the bundle, consist predominatly of air; besides, Co formation was minimised by allowing sufficient excess above stochiometric air to the combustion process. No special fouling factor precautions need to be taken; in this present work a fouling factor of 0.001 was used, as a precaution to allow for any coking or dirt that might happen with incorrect air/fuel ratio.

Assuming liquid wastes were used for this particular incinerator, such as heavy oil, paint, paper pulp liquors, or many other organic liquids, then different practical problems may arise, such as viscosity problems when pumping the liquid. Most need some augmenting fuel to start the process of combustion; of concern in this present work was the possibility of a rise in the amount of radiation from firstly the actual partial pressures of Co_2 and H_2o as liquid organic wastes yield higher percentages of Co_2 and H_2o, and secondly, and more important, that the flame from the burners would probably be radiative, and would make a considerable contribution to the amount of radiation in the process. In this case, there might be an appreciable effect on the heat transfer coefficients. Using organic fumes with a high yield of Co_2 and H_2o, such as hydrocarbons, may increase the gaseous radiation as the partial pressure of the radiative gases would be higher. The amount of radiation from sulphur is very small, and would be negligible unless a high sulphur waste were incinerated.

5.2.8 Heat Losses

Proper insulation of heat recovery equipment is important from an economic point of view.

The calculation of heat transfer through insulating walls followed the principles of conduction through a composite wall. Since an average temperature of the inner wall of the combustion chamber, the hot face, was used, some errors were involved in calculating the heat losses, but no error should occur in measuring the cold side, the outside wall in this present work; errors have little effect on the results as this heat represnts only a small proportion of the whole, unlike heat transfer on tubes and shell.

5.2.9 Economics of Gas-Air recovery

As the economical side of this heat recovery process is the main objective, it is important that the design and operation of the process be optimised, to minimise the cost of design and operation.

The over design of the present equipment, means that some construction materials and operating expenses, could be saved.

An increase in the size of the bundle would lead to a higher pumping energy requirement.

Secondly, the tube bundle was found to be masked by about 4 inches each end by the insulating walls, this decreases the contact between the hot gases and the tubes on the shell side and subsequently, lowers themal efficiency.

As it was found that the heat exchanger was over designed, and this was confirmed through this investigation, it would be feasible to think of lowering the pressure drop, caused by the bundle size, which could be achieved by shortening the tubes in the bundle, and if necessary increasing the number of rows. Short tubes lead to the possibility of a less developed turbulent boundary layer giving higher heat transfer coefficients.

Operating at above the H_2o dew point temperature around the tubes avoids corrosion which may be expensive in the case of replacement.

Generally an air-to-air or gas recuperator is economic, provided it is properly designed. Boyen(63) shows inhis text book, for example, that at an air flowrate of 24,000 lb/hr and a temperature change of 900^oF the pay back is £1.7 per operating hour based on fuel cost of $33p/1000ft^3$. This pay back value when compared with the capital investment, fuel gas, maintenace, operation and other costs such as taxes, depreciation which may be £39,820, and even when the facility is shut down 1047h/ year at this rate will pay back in 3 years.

In this work, for example:

$$Q = U_S A_S \Delta T_m \quad \text{.............................(5.23)}$$

also also

$$Q = U_p A_p \Delta T_m \quad \text{..............................(5.24)}$$

where

Q = heat duty Btu/hr,(Kw)

U_S = standard overall heat transfer coefficient

A_S = overall heat exchanger area based on standard correlation

U_p = practical overall heat transfer coefficient

A_p = overall heat exchanger area based on practical correlation from equation (5.23) and (5.24)

$$\frac{A_p}{A_S} = \frac{U_S}{U_p} \quad \ldots\ldots\ldots\ldots\ldots\ldots\ldots\ldots\ldots\ldots\ldots (5.25)$$

Using the following standard correlations (9)

<u>Tube side</u>

$$\frac{h_i D}{K} = 0.023 \ Re^{0.8} Pr^{0.33} \ldots\ldots\ldots\ldots\ldots\ldots (5.26)$$

<u>Shell side</u>

$$\frac{h_o De}{K} = 0.36 \left(\frac{DeG}{\mu}\right)^{0.55} Pr^{0.33} \left(\frac{\mu}{\mu w}\right)^{0.14} \quad \ldots\ldots\ldots (5.27)$$

for standard design fresh air volumetric flowrate of 31,600 ft^3/hr, and shell flow 76,200 ft^3/hr

h_i = 7.6 Btu/hr $ft^{2\,o}F$, (42.6 w/ $m^{2\,o}C$)

h_o = 13 Btu/hr $ft^{2\,o}F$, (73 w/$m^{2\,o}C$)

U = 4.6 Btu/hr $ft^{2\,o}F$, (26 w/$m^{2\,o}C$)

Using the following practical correlation for the same conditions as above

$$\frac{h_i D_i}{K} = 0.0028 \ Re^{1.08} Pr^{0.33} \quad \ldots\ldots\ldots\ldots\ldots (5.28)$$

$$\frac{h_o D_o}{K} = 0.89 \ Re^{0.42} Pr^{0.33} \quad \ldots\ldots\ldots\ldots\ldots (5.29)$$

$h_i = 12$ Btu/ft^{2o}F, (67 w/m^{2o}C)

$h_o = 11.2$ Btu/ft^{2o}F, (62.5 w/m^{2o}C)

$U = 5.75$ Btu/ft^{2o}F, (32 w/m^{2o}C)

Using equation (3)

$$Up = 0.82\ U_S$$

which means that by using the practical correlation, developed in this work the area of the heat exchanger could be made smaller by a fifth for the same heat duty.

Standard correlations from literature for the shell side are suitable for this kind of work, but standard correlation: for tube side are not suitable as using them would cause overdesign.

CHAPTER SIX

Conclusion and Recommendations

6.1 Conclusions

The specific conclusions drawn from this work can be summarised as follows:-

1. The amount of radiation involved in this process was not significant, and had no appreciable effect on the heat transfer coefficients on either shell or tube sides.
2. The following correlations were obtained from the experimental work acheived in this research:-

Tube side

$$Nu_T = 0.0028\, Re_T^{1.08}\, Pr_T^{0.33} \quad \ldots\ldots\ldots\ldots\ldots (6.1)$$

Shell side

$$Nu_S = 0.89\, Re_S^{0.42} Pr_T^{0.33} \quad \ldots\ldots\ldots\ldots\ldots (6.2)$$

3. The practical heat transfer coefficients on the tube side were found to be higher than the calculated ones, using standard published correlations.
4. The heat transfer coefficients on the shell side were found to be around the published values obtained using standard gas correlations such as McAdams, Kern, and others.

5. The secondary air flow rate has a direct effect on the amount of radiation, as the partial pressures of the radiative gases and their temperature drop with the secondary air flow increase. The refractory wall temperature will fall as well.

6. Correlations of heat transfer coefficients can not be based on the frontal tubes in the bundle, namely first and second rows.

7. Keeping either burner in operation, does not effect the form of the correlations.

8. The temperature profile along the central and rear tubes in the bundle, seem to be reasonably linear, unlike the frontal ones.

9. Incremental heat transfer coefficients based on the tube side were found to be reasonably linear, along the length of the tubes, at the centre and rear rows.

10. Increasing the range of Reynolds number on the tube side, by blocking a few tubes in the bundle, did not create any signicant effect on the correlations, and this was verified statistically.

11. Changing fresh air flowrates with secondary air flow rates did not cause any significant incompatibility between sets of data, as this was proved through variance analysis.

6.2 Recommendations

1. In order to show the patterns of heat and flow inside tubes, it would be necessary to visualise the patterns there. Since air is a transparent medium visualisation techniques would have to be adopted such as the following:-

   i) visualisation of the flow direction by means of dye, smoke, or small particles.

   ii) Measurement of spot velocities with the aid of a Lazer Döpler meter

   For the above techniques a transparent tube would be needed.

2. Flow straightners could be connected to the sample tubes, so that entrance effects could be minimised for comparison purposes.

3. A higher and lower Reynolds number range for both shell and tube sides, would be useful to test the heat trans fer correlations, obtained in this work, at higher and lower flowrates.

4. Various organic fume waste should be incinerated especially fumes with high Co_2 and H_2o yield, to test the heat exchnger performance at these conditions.

5. The refractory walls must be rearranged in such a way that they are not covering tube ends on both hot and cold sides as this lowers the hot gas contact with the tubes in the bundle.

6. A liquid medium such as water could be arranged to flow through the tubes so that a system of liquid-gas

could be compared with the present system gas-gas, mainly to compare the heat transfer coefficients obtained from both systems. This would give a clear idea about gaseous and liquid heat transfer nature.

7. The thermo-couple shield in front of the bundle and of 4 inches width restricts the hot gas flow towards the bundle and splits the flow. Since radiation in the chamber was not that great, it could be either removed or thinned down.

8. The bundle size could be optimised, concerning the length of tubes, and depth of rows as this approach will enhance the economical side of the design.

9. Fresh air flow distribution could be improved by either rearranging the inlet duct, or using a flow straightner such as orids placed in the inlet chest.

10. The scale of turbulence in the tubes could be measured by , for example, hot wire anemometer. The intensity of turbulence could be measured in the same way.

REFERENCES

1. Knudson, J.G, Katz, D.L, McGraw-Hill Book Company 1958.
2. Dittus, F.M, and Boelter L.M.K, University of California, published in Eng., 2, 443, (1930).
3. Colburn, A.P, Trans. AIChe., E, 29, 174-210, (1933)
4. Sieder, E.N., and Tate, G.E., ind ENG.Chem., 28 1429-1436 (1936).
5. Drexel R.E., and W.H. McAdams: NACA, W.R, W-108 Feb. 1945.
6. Humble,L.V., W.H. Lowdermilk, and L.G. Demson: NACA Report 1020 (1951).
7. Weiland W.F, Lowdermilk, W.H and J.N.B Livinggood NACA RM E53J07, (1954).
8. Kern, D.Q, Process Heat Transfer (1950).
9. Morris, F.H., and W.G Whitman, ind ENG., Chem., 20, 234 (1928).
10. Short, B.E, Trans, ASME 64 381-392 (1938).
11. Breidenbach, E.P., and O'Connel, H.E., Trans AIChe 42 761-776 (1946).
12. Carpenter, F.G., Colburn, A.P, Schoenborn, E.M, and Wurster, A., Trans AIChe E 42 165-187 (1947).
13. Pierson, O.L, Trans ASME 59, 561 (1937).
14. Grimson E.D, Trans ASME 59 583 (1937).
15. Huge, E.C., Trans ASME 59 573 (1937).
16. McAdams, W.H., 'Heat Transmission', 3rd Ed.,

17. Comings, E.W, Clapp,J.T and Taylor J.F, ind Eng. Chem, 40 1076.

18. Schlichting, H., Boundary Layer Theory, 330, McGraw-Hill.

19. Lin, C.C., Proc. 9th, Inter. Congress Appl. Mech., Brussels 4, 155.

20. Seban, R.A, (1960) Tran ASME, 82 Ser. C, 101.

21. Kestin, J., Macder, P.F and Wang, O.,(1961) Inter. J. Heat and Mass Trasfer 3, 133.

22. Sogin, H.H, Subraminum, V.S, Trans ASME 83 Serc., 483.(1961).

23. Perkins, H.C, and Leppert, G. (1964) Int.J. Heat transfer 7, 143.

24. Hegge Zignen B.G Appl.Sci Res Section A, 7,149.

25. Fallon T.A, Chemical and Process Heat Transfer survey 1957.

26. Thompson, A.S.T, A.W.Scott, A.M.Laird, and H.S. Holden "Procedings of the General Discussion on Heat Transfer, Institution of Mechanical Engineers, New York 177 (1951).

27. Snyder N.W, Chem eng. Progr, Symposium, Ser 5 49:11 (1953).

28. Bergelin, O.P, Brown, G.A, and Doberstein Trans ASME 74 953, 1952.

29. Omhandre G.A, Bergelin O.P, and A.P, Colburn 71 27-34 (1949).

30. Latzko, H.Z, angew, Math. U. Mech., 1 286 (1921).

31. Latzko,H.Z, angew, Math.U.Mech., 1 286(1921).

32. Nusselt, W.Z, ver. deut. Ing., 61 685(1917).

33. Aladyev, I.T, NACA, TM,1356, (1954).

34. Deissler, R.G, NACA, TN, 3016, (1953).

35. Boelter, L.M.K, G. Young, and H.W. Iverson, NACA TN, 1451, (1948).

36. Winding C.C., Ind. Eng. Chem., 30 942 (1938).

37. Gunter and Shaw p.643 (1945) ASME.

38. Patric, E.A.K and Patel, N.G., International Development in Heat Transfer, Part 1.

39. Debaufre, P., ind.Eng.Chem 24 486, (1932).

40. Hottel, H.C, Trans. ASME, 53 256-273, (1931).

41. Mulliken, H.F, Trans. ASME, 57 518, (1935).

42. Orrok, G.A, Trans. ASME, 47 1148, (1925).

43. Wilson R.E, McAdams, W.H, and Seltzer, M, Ind. Eng. Chem., 14, 145, (1922).

44. Wpj;emberg W.J, and Mulliken, H.F, Trans. ASME 57, 531, 1935.

45. Lihou, D.A, Trans IchemE, 55 225-242 (1977).

46. Colburn P.A, ind Eng Chem, 35 873-877 (1933).

47. Bowman R.A, Mueller A.C, and Nagle W.M., Trans ASME, 62, 283-294 (1940).

48. Stevens R.A, Fernandez J, Woolf J.R 79 287

49. Ratzel,W.J, Neuber. Heat Transfer, ASME 101 511, Aug. 1979.

50. Rohesnow W.M, Hunsaker J.P, Applied Mech. ASME, 69, 699 (1947).

51. Co-mark Electronic Ltd.

52. Air Flow Ltd.

53. Coulson, J.M, and J.F. Richardson, Chemical Engineering Volume One (1953).

54. Applied Statistics for Engineers, C.W. Wilson, Applied Science Publishers Ltd. 1972.

55. Statistical Analysis, Allen L. Edwards, Holt, Rinehart and Winston 1958.

56. Statistical theory and methodology in Science and Engineering 2nd ed. Brownlee K.A, 1965, John Wiley and Sons.

57. Weber and mussner, TD for Chemical Engineers 2nd ed. 1957.

58. International Critical tables of Numerical Data, New York, McGraw-Hill Book Company.

59. Obert and Caggloli, TD, McGraw 1963.

60. International Critical Tables of Numerical data, New York, McGraw-Hill B ok Company.

61. J.H. Perry, Chemical Engineers Hand Book, 4th Eddition McGraw-Hill Book Company, New York.

62. Engineering Sciences data "Forced Convection Heat in Circular Tubes", part 111, item no 68007 1968.

63. Boyen, J.L Thermal Energy Recovery

64. J.T. Davies, Turbulence Phenomena, Academic Press, Wiley-Inter Science, 1972.

APPENDIX A.1

EXPERIMENTAL DATA

Fresh air flowrate = 49900 ft^3/hr

Secondary air flowrate = 76200 ft^3/hr

Temperature Measurement C^o

Thermo Couples	Selector A	B	C
1		174.	300.0
2	41.0	109.5	214.0
3	59.5	74.5	68.5
4		71.	102.5
5		119.	72.5
6		72.5	65.5
7		100.5	96.5
8		120.	101.0
9		71.5	110.0
10		67.5	71.0
11	97.0	140.5	42.0
12	95.5		40.0
13	61.0	44.5	63.5
14	104.0		
15	68.5	44.5	74.0
16	96.0	42.0	
17	194.0	53.5	24.5
18	66.5	54.0	
19	67.0	86.0	297.0
20		149.0	184.5

Scanning inside the Chamber C^o

	Temperature (C^o)	Pressure (inch of water)
Left	200	0.053
Centre	206	0.058
Right	202	0.06

Temperature Reading over the Bundle (C^o)

In front of Row	SCAN POSITIONS 3"	6"	9"
1		174	
2	172	170	168
3	167	164.5	163
4	155	160	147
5	159	157	154
6	153	150	142
Behind Bundle		140.5	

EXPERIMENTAL DATA

Fresh air flowrate = 44691 ft^3/hr

Secondary air flowrate = 76200 ft^3/hr

Temperature Measurement C°

Thermo Couples	Selector A	B	C
1		177.5	306.0
2	42.5	118.5	219.0
3	61.5	79.5	69.0
4		79.0	106.0
5		129.0	74.5
6		76.5	67.5
7		108.0	99.5
8		128.0	103.5
9		80.0	115.0
10		69.5	75.0
11	101.5	144.0	44.0
12	99.5		40.5
13	61.0	45.5	71.0
14	111.0		
15	73.0	46.0	75.5
16	101.0	45.5	
17	199.0	56.0	25.0
18	70.0	56.5	
19	72.0	91.0	306.0
20		154.0	188.5

Scanning inside the Chamber C°

	Temperature (C°)	Pressure (inch of water)
Left	200	0.053
Centre	204	0.058
Right	208	0.06

Temperature Reading over the Bundle (C°)

In front of Row	SCAN POSITIONS 3"	6"	9"
1		177.5	
2	182	172.5	160
3	173	165	154
4	169	161	150
5	164	159.5	148
6	160	154	144
Behind Bundle		144	

EXPERIMENTAL DATA

Fresh air flowrate = 38704 ft^3/hr

Secondary air flowrate = 76200 ft^3/hr

Temperature Measurement C°

Thermo Couples	Selector A	B	C
1		178.0	308.0
2	44.5	124.0	222.0
3	65.0	83.5	72.5
4		83.0	111.5
5		133.0	78.5
6		80.0	71.0
7		113.0	105.0
8		133.0	110.0
9		84.5	120.0
10		74.0	77.5
11	107.5	147.0	48.5
12	105.0		41.0
13	65.5	48.0	74.5
14	116.5		
15	76.5	48.5	78.5
16	107.0	48.5	
17	201.0	59.5	25.0
18	73.5	59.5	
19	76.0	93.5	309.0
20		157.0	190.0

Scanning inside the Chamber C°

	Temperature (C°)	Pressure (inch of water)
Left	203	0.053
Centre	208	0.058
Right	206	0.06

Temperature Reading over the Bundle (C°)

In front of Row	SCAN POSITIONS 3"	6"	9"
1		178	
2	180	173	163
3	173	168	160
4	170	163	155
5	166	161	152
6	164	159	149
Behind Bundle		147	

EXPERIMENTAL DATA

Fresh air flowrate = 31602 ft^3/hr

Secondary air flowrate = 76200 ft^3/hr

Temperature Measurement C°

Thermo Couples	Selector A	B	C
1		178.5	307.0
2	47.0	128.0	215.0
3	67.0	86.0	78.5
4		87.0	118.5
5		140.0	83.5
6		87.5	77.0
7		120.5	112.5
8		138.0	117.5
9		87.5	126.5
10		79.0	82.5
11	115.0	150.0	50.5
12	112.0		38.0
13	72.0	51.0	76.0
14	122.0		
15	80.0	51.0	80.0
16	112.0	56.0	
17	202.0	63.0	25.5
18	78.5	62.5	
19	79.5	97.0	311.0
20		157.5	190.0

Scanning inside the Chamber C°

	Temperature (C°)	Pressure (inch of water)
Left	205	0.053
Centre	209	0.058
Right	204	0.06

Temperature Reading over the Bundle (C°)

In front of Row	SCAN POSITIONS 3"	6"	9"
1		178.5	
2	182	173	164
3	180	169	163
4	175	164	159
5	171	163	154
6	169	158.5	152
Behind Bundle		150	

EXPERIMENTAL DATA

Fresh air flowrate = 22346 ft^3/hr

Secondary air flowrate = 76200 ft^3/hr

Temperature Measurement C^{o}

Thermo Couples	Selector A	B	C
1		188.0	308.0
2	53.5	140.0	222.5
3	74.5	95.5	88.0
4		96.5	130.0
5		149.0	93.5
6		95.5	87.5
7		132.5	125.5
8		148.0	128.5
9		97.0	136.5
10		85.0	91.0
11	126.5	155.5	55.5
12	124.5		41.5
13	80.0	55.5	86.0
14	133.5		
15	86.5	56.0	86.0
16	123.0	62.5	
17	202.5	70.5	25.5
18	86.5	68.5	
19	88.5	102.5	310.0
20		158.5	191.0

Scanning inside the Chamber C^{o}

	Temperature (C^{o})	Pressure (inch of water)
Left	206	0.053
Centre	211	0.058
Right	202	0.06

Temperature Reading over the Bundle (C^{o})

In front of Row	SCAN POSITIONS 3"	6"	9"
1		188	
2	181	174	169
3	179	169.5	163
4	175	165	160
5	173	164.5	158
6	172	161	155
Behind Bundle		155.5	

EXPERIMENTAL DATA

Fresh air flowrate = 49900 ft^3/hr

Secondary air flowrate = 69368 ft^3/hr

Temperature Measurement C°

Thermo Couples	Selector A	B	C
1		182.0	324.0
2		114.5	228.0
3	63.0	78.0	76.0
4		74.5	106.5
5		123.0	70.0
6		76.0	65.0
7		104.0	98.0
8		122.5	105.0
9		75.5	113.5
10		71.0	68.0
11	99.0	146.5	41.0
12	99.5		40.5
13	59.5	48.5	74.5
14	109.0		
15	81.5	47.5	78.5
16	103.0	46.0	
17	201.0	57.0	26.5
18	66.5	61.0	
19	70.0		301.0
20		159.5	198.0

Scanning inside the Chamber C°

	Temperature (C°)	Pressure (inch of water)
Left	248	0.04
Centre	250	0.
Right	245	0.

Temperature Reading over the Bundle (C°)

In front of Row	SCAN POSITIONS 3"	6"	9"
1		182.0	
2	180.0	178.0	
3	173.0	168.5	
4	170.0	163.0	
5	163.0	161.0	
6	161.0	183.0	
Behind Bundle		146.5	

EXPERIMENTAL DATA

Fresh air flowrate = 44691 ft^3/hr

Secondary air flowrate = 69368 ft^3/hr

Temperature Measurement C^o

Thermo Couples	Selector A	B	C
1		184.5	325.5
2		123.0	230.0
3	64.5	83.5	78.0
4		83.0	110.0
5		132.5	71.5
6		81.5	67.0
7		113.0	101.0
8		131.5	107.5
9		84.5	118.0
10		74.5	70.5
11	101.5	149.5	43.5
12	102.0		42.5
13	58.5	47.5	76.0
14	113.5		
15	83.5	49.5	79.5
16	107.0	49.5	
17	203.0	60.5	27.5
18	68.0	64.5	
19	76.0		313.5
20	180.5	163.0	200.0

Scanning inside the Chamber C^o

	Temperature (C^o)	Pressure (inch of water)
Left	246	0.04
Centre	251	0.043
Right	247	0.039

Temperature Reading over the Bundle (C^o)

In front of Row	SCAN POSITIONS 3"	6"	9"
1		184.5	
2	186.0	180.0	176.0
3	175.0	170.0	165.0
4	166.0	162.5	160.0
5	168.0	161.5	154.0
6	162.0	158.5	151.0
Behind Bundle		149.5	

EXPERIMENTAL DATA

Fresh air flowrate = 38704 ft^3/hr

Secondary air flowrate = 69368 ft^3/hr

Temperature Measurement C°

Thermo Couples	Selector A	B	C
1		185.0	325.0
2		129.0	230.0
3	68.0	87.0	81.0
4		87.0	114.0
5		138.0	74.0
6		86.0	69.5
7		128.5	105.0
8		136.5	112.5
9		87.5	122.0
10		78.5	69.0
11	107.5	153.0	49.5
12	109.0		49.5
13	64.0	49.5	78.0
14	121.0		
15	88.0	52.0	82.0
16	113.5	53.0	
17	200.5	63.5	27.0
18	72.0	67.0	
19	79.0		317.0
20	164.0	164.0	200.0

Scanning inside the Chamber C°

	Temperature (C°)	Pressure (inch of water)
Left	250	0.04
Centre	252	0.043
Right	249	0.039

Temperature Reading over the Bundle (C°)

In front of Row	SCAN POSITIONS 3"	6"	9"
1		185.0	
2	189.0	180.0	173.0
3	175.0	169.0	161.0
4	174.0	169.0	160.0
5	170.0	165.5	158.0
6	164.0	158.5	153.0
Behind Bundle		153.0	

EXPERIMENTAL DATA

Fresh air flowrate = 31602 ft^3/hr

Secondary air flowrate = 69368 ft^3/hr

Temperature Measurement C^o

Thermo Couples	Selector A	B	C
1		185.5	326.0
2		134.0	229.0
3	70.0	90.5	87.0
4		91.0	121.0
5		144.0	79.5
6		93.5	74.5
7		125.5	113.5
8		141.5	119.5
9		91.5	129.0
10		83.0	73.5
11	113.5	155.5	49.5
12	114.5		49.5
13	68.5	52.0	79.5
14	123.5		
15	90.5	54.0	83.5
16	117.5	57.0	
17	205.0	66.5	27.0
18	77.0	70.0	
19	83.0		315.5
20	163.5	164.0	200.0

Scanning inside the Chamber C^o

	Temperature (C^o)	Pressure (inch of water)
Left		0.04
Centre		0.043
Right		0.039

Temperature Reading over the Bundle (C^o)

In front of Row	SCAN POSITIONS 3"	6"	9"
1		185.5	
2	189.0	181.0	172.0
3	181.0	172.5	167.0
4	178.0	168.5	163.0
5	174.0	166.0	160.0
6	171.0	160.5	155.0
Behind Bundle		155.5	

EXPERIMENTAL DATA

Fresh air flowrate = 22346 ft^3/hr

Secondary air flowrate = 69368 ft^3/hr

Temperature Measurement C°

Thermo Couples	Selector A	B	C
1		186.0	326.0
2		144.5	231.5
3	78.0	99.5	97.5
4		100.0	134.0
5		153.5	90.5
6		101.5	83.0
7		137.5	128.5
8		151.5	132.0
9		101.0	140.0
10		91.0	84.0
11	126.5	161.0	53.0
12	128.5		50.5
13	79.0	55.0	88.5
14	135.5		
15	99.5	60.0	90.0
16	129.5	65.5	
17	200.0	75.0	28.0
18	86.5	78.0	
19	93.5		314.5
20		165.0	200.5

Scanning inside the Chamber C°

	Temperature (C°)	Pressure (inch of water)
Left		0.04
Centre		0.043
Right		0.039

Temperature Reading over the Bundle (C°)

In front of Row	SCAN POSITIONS 3"	6"	9"
1		186.0	
2	191.0	181.0	173.0
3	184.0	174.5	170.0
4	180.0	171.5	167.0
5	173.0	166.0	162.0
6	170.0	162.0	154.0
Behind Bundle		151.5	

EXPERIMENTAL DATA

Fresh air flowrate = 49900 ft^3/hr

Secondary air flowrate = 61720 ft^3/hr

Temperature Measurement C°

Thermo Couples	Selector A	B	C
1		200.5	343.0
2	68.0	125.0	250.0
3	64.0	82.0	78.0
4		78.0	114.0
5		136.0	72.0
6		79.0	65.5
7		113.5	105.0
8		135.0	112.5
9		77.5	124.0
10		73.5	75.5
11	106.5	154.0	43.0
12	107.0		42.0
13	60.5	45.5	73.5
14	120.5		
15	87.5	46.0	79.0
16	111.0	45.5	
17	229.0	56.0	24.5
18	70.0	61.0	
19	74.0	89.0	354.5
20		172.5	209.5

Scanning inside the Chamber C°

	Temperature (C°)	Pressure (inch of water)
Left	290	0.030
Centre	297	0.029
Right	282	0.026

Temperature Reading over the Bundle (C°)

In front of Row	SCAN POSITIONS 3"	6"	9"
1		200.5	
2	199.0	194.0	186.0
3	184.0	178.5	174.0
4	183.0	175.5	171.0
5	180.0	172.5	168.0
6	172.0	164.0	160.0
Behind Bundle		154.0	

EXPERIMENTAL DATA

Fresh air flowrate = 44691 ft^3/hr

Secondary air flowrate = 61720 ft^3/hr

Temperature Measurement C°

Thermo Couples	Selector A	B	C
1		202.0	348.0
2	70.0	133.5	254.0
3	66.0	87.0	79.0
4		86.0	117.5
5		146.0	72.5
6		85.0	67.5
7		123.5	108.0
8		144.5	115.0
9		87.0	129.0
10		77.5	77.5
11	112.0	159.5	41.0
12	112.0		40.0
13	59.5	46.0	75.5
14	126.0		
15	90.0	47.5	80.5
16	116.0	47.5	
17	234.0	59.0	25.0
18	71.0	64.0	
19	78.0	95.0	368.0
20		178.0	214.5

Scanning inside the Chamber C°

	Temperature (C°)	Pressure (inch of water)
Left	291	0.030
Centre	298	0.029
Right	286	0.026

Temperature Reading over the Bundle (C°)

In front of Row	SCAN POSITIONS 3"	6"	9"
1		202.0	
2	200.0	196.0	190.0
3	184.0	178.0	174.0
4	185.0	178.0	176.0
5	182.0	176.0	172.0
6	173.0	164.0	160.0
Behind Bundle		159.5	

EXPERIMENTAL DATA

Fresh air flowrate = 38704 ft^3/hr

Secondary air flowrate = 61720 ft^3/hr

Temperature Measurement C°

Thermo Couples	Selector A	B	C
1		202.5	394.0
2	72.5	137.5	254.5
3	69.5	91.5	184.0
4		90.5	123.5
5		151.0	77.0
6		90.0	70.5
7		129.5	114.0
8		148.5	121.0
9		92.0	133.5
10		82.0	80.5
11	48.5	165.0	43.0
12	118.0		40.5
13	65.0	49.0	77.5
14	134.0		
15	96.0	51.0	83.0
16	123.5	50.5	
17	235.0	63.0	25.0
18	74.5	67.5	
19	83.0	105.0	362.5
20		180.5	215.0

Scanning inside the Chamber C°

	Temperature (C°)	Pressure (inch of water)
Left	289	0.030
Centre	300	0.029
Right	287	0.026

Temperature Reading over the Bundle (C°)

In front of Row	SCAN POSITIONS 3"	6"	9"
1		202.5	
2	200.0	196.5	191.0
3	187.0	181.0	174.0
4	182.0	178.0	172.0
5	181.0	177.0	173.0
6	173.0	169.0	162.0
Behind Bundle		165.0	

EXPERIMENTAL DATA

Fresh air flowrate = 31602 ft^3/hr

Secondary air flowrate = 61720 ft^3/hr

Temperature Measurement C^o

Thermo Couples	Selector A	B	C
1		204.5	350.0
2	45.0	146.0	256.5
3	71.5	96.5	91.5
4		97.5	132.5
5		160.0	84.0
6		100.0	77.0
7		139.0	123.5
8		157.5	130.0
9		98.0	141.5
10		88.0	87.5
11	126.5	169.0	48.0
12	126.0		44.0
13	72.0	53.0	80.5
14	139.5		
15	101.0	54.0	86.0
16	130.0	56.0	
17	235.5	67.5	26.0
18	82.0	72.5	
19	89.0	110.0	364.0
20		182.0	216.0

Scanning inside the Chamber C^o

	Temperature (C^o)	Pressure (inch of water)
Left	300	0.030
Centre	302.5	0.029
Right	289	0.026

Temperature Reading over the Bundle (C^o)

In front of Row	SCAN POSITIONS 3"	6"	9"
1		204.5	
2	200.0	197.0	185.0
3	190.0	183.0	172.0
4	190.0	181.0	173.0
5	192.0	180.0	171.0
6	173.0	169.5	162.0
Behind Bundle		169.0	

EXPERIMENTAL DATA

Fresh air flowrate = 22346 ft^3/hr

Secondary air flowrate = 61720 ft^3/hr

Temperature Measurement C^O

Thermo Couples	Selector A	B	C
1		205.0	352.0
2	78.5	158.5	257.5
3	79.5	107.0	103.5
4		107.5	147.0
5		107.0	95.5
6		110.0	87.0
7		152.5	140.0
8		168.5	143.5
9		109.0	153.5
10		95.0	98.5
11	140.0	176.5	52.5
12	140.0		
13			
14			
15			
16			
17			
18			
19			
20			

Scanning inside the Chamber C^O

	Temperature (C^O)	Pressure (inch of water)
Left	301	0.030
Centre	304	0.029
Right	296	0.026

Temperature Reading over the Bundle (C^O)

In front of Row	SCAN POSITIONS 3"	6"	9"
1		205.0	
2	200.0	197.0	193.0
3	194.0	186.0	184.0
4	192.0	185.5	182.0
5	190.0	183.0	180.0
6	183.0	177.0	173.0
Behind Bundle		176.5	

EXPERIMENTAL DATA

Fresh air flowrate = 49900 ft^3/hr

Secondary air flowrate = 52980 ft^3/hr

Temperature Measurement C°

Thermo Couples	Selector A	Selector B	Selector C
1		235.5	377.0
2		145.5	308.0
3	68.5	93.5	86.5
4		89.0	127.5
5		157.5	78.5
6		90.5	71.5
7		133.5	115.5
8		155.0	127.0
9		88.5	138.5
10		82.5	70.0
11	121.0	175.5	49.0
12	118.5		49.0
13	65.5	49.0	84.0
14	138.5		
15	98.0	48.0	90.0
16	130.5	48.5	
17	270.0	59.5	25.5
18	75.0	67.0	
19	82.5		435.0
20		209.0	236.0

Scanning inside the Chamber C°

	Temperature (C°)	Pressure (inch of water)
Left	362	0.021
Centre	378	0.017
Right	360	0.023

Temperature Reading over the Bundle (C°)

In front of Row	SCAN POSITIONS 3"	6"	9"
1		235.5	
2	230.0	225.0	216.0
3	218.0	208.0	211,0
4	211.0	202.0	200.0
5	210.0	198.0	193.0
6	196.0	185.0	180.0
Behind Bundle		175.5	

EXPERIMENTAL DATA

Fresh air flowrate = 44691 ft^3/hr

Secondary air flowrate = 52980 ft^3/hr

Temperature Measurement C°

Thermo Couples	Selector A	B	C
1		235.5	385.0
2		156.0	313.0
3	71.0	98.5	88.0
4		97.5	131.0
5		167.5	78.5
6		96.0	72.5
7		143.0	118.0
8		165.0	129.0
9		99.5	142.5
10		86.0	71.5
11	126.0	180.5	42.0
12	124.0		40.5
13	65.0	47.5	85.5
14	146.5		
15	102.0	50.0	88.0
16	137.0	52.5	
17	275.0	62.5	25.5
18	77.0	71.0	
19	89.0		437.5
20		216.5	243.0

Scanning inside the Chamber C°

	Temperature (C°)	Pressure (inch of water)
Left	310	0.021
Centre	316	0.017
Right	302	0.023

Temperature Reading over the Bundle (C°)

In front of Row	SCAN POSITIONS 3"	6"	9"
1		235.5	
2	232.0	229.0	219.0
3	220.0	213.0	202.0
4	202.0	198.0	189.0
5	203.0	197.0	186.0
6	194.0	186.5	182.0
Behind Bundle		180.5	

EXPERIMENTAL DATA

Fresh air flowrate = 38704 ft^3/hr

Secondary air flowrate = 52980 ft^3/hr

Temperature Measurement C°

Thermo Couples	Selector A	B	C
1		237.5	384.0
2		162.0	316.0
3	75.0	104.0	94.0
4		102.5	139.0
5		174.5	84.0
6		101.5	77.5
7		149.5	126.5
8		186.0	138.0
9		103.5	150.5
10		90.5	77.0
11	134.0	183.5	44.5
12	132.0		
13	70.0	50.5	90.0
14	153.0		
15	108.0	53.0	92.0
16	144.0	56.5	
17	276.5	67.5	26.0
18	81.5	75.0	
19	94.5		440.0
20		219.0	244.0

Scanning inside the Chamber C°

	Temperature (C°)	Pressure (inch of water)
Left	320	0.021
Centre	331	0.017
Right	311	0.023

Temperature Reading over the Bundle (C°)

In front of Row	SCAN POSITIONS 3"	6"	9"
1		237.5	
2	235.0	229.0	219.0
3	222.0	216.0	200.0
4	212.0	201.0	189.0
5	209.0	200.0	186.0
6	197.0	190.0	182.0
Behind Bundle		183.5	

EXPERIMENTAL DATA

Fresh air flowrate = 31602 ft^3/hr

Secondary air flowrate = 52980 ft^3/hr

Temperature Measurement C^o

Thermo Couples	Selector A	B	C
1		238.0	387.0
2		170.0	317.0
3	79.0	110.0	103.0
4		111.0	150.0
5		184.0	92.0
6		113.0	85.0
7		160.5	138.0
8		180.0	148.0
9		110.5	160.0
10		98.5	83.5
11	146.0	190.0	48.0
12	143.0		45.0
13	80.0	54.5	92.0
14	162.0		
15	112.0	57.0	94.5
16	153.0	63.0	
17	279.0	72.5	26.5
18	90.0	81.0	
19	100.0		441.0
20		222.0	245.5

Scanning inside the Chamber C^o

	Temperature (C^o)	Pressure (inch of water)
Left	350	0.021
Centre	360	0.017
Right	341	0.023

Temperature Reading over the Bundle (C^o)

In front of Row	SCAN POSITIONS 3"	6"	9"
1		238.0	
2	237.0	228.0	219.0
3	228.0	217.0	210.0
4	218.0	207.0	200.0
5	217.0	204.0	194.0
6	208.0	195.0	187.0
Behind Bundle		190.0	

EXPERIMENTAL DATA

Fresh air flowrate = 22346 ft^3/hr

Secondary air flowrate = 52980 ft^3/hr

Temperature Measurement C^o

Thermo Couples	Selector A	Selector B	Selector C
1		239.5	389.0
2		184.5	318.0
3	88.0	123.5	118.0
4		123.5	166.0
5		195.0	107.5
6		126.5	96.5
7		177.0	158.0
8		197.0	163.0
9		125.0	175.0
10		108.0	96.5
11	161.5	198.5	54.0
12	160.0		50.5
13	91.5	58.0	105.0
14	177.0		
15	124.0	63.5	103.0
16	166.5	72.0	
17	280.0	82.0	26.5
18	101.5	90.0	
19	114.0		442.0
20		223.0	247.0

Scanning inside the Chamber C^o

	Temperature (C^o)	Pressure (inch of water)
Left	410	0.021
Centre	415	0.017
Right	402	0.023

Temperature Reading over the Bundle (C^o)

In front of Row	SCAN POSITIONS 3"	6"	9"
1		239.5	
2	235.0	230.0	219.0
3	217.0	215.0	210.0
4	210.0	208.0	201.0
5	213.0	207.0	198.0
6	206.0	199.5	196.0
Behind Bundle		198.5	

EXPERIMENTAL DATA

Fresh air flowrate = 49900 ft^3/hr

Secondary air flowrate = 42479 ft^3/hr

Temperature Measurement C^O

Thermo Couples	Selector A	B	C
1		277.5	427.0
2	95.0	161.5	371.5
3	73.0	103.0	91.0
4		94.0	134.0
5		165.5	79.0
6		100.0	75.0
7		145.0	119.0
8		150.0	134.0
9		98.0	146.0
10		87.0	71.5
11	126.5	192.0	40.5
12	125.0		43.0
13	67.0	51.0	93.0
14	152.0		
15	106.0	49.0	95.0
16	144.0	50.0	
17	302.5	61.0	24.5
18	78.5	74.0	
19	89.0	61.0	483.0
20		257.5	278.0

Scanning inside the Chamber C^O

	Temperature (C^O)	Pressure (inch of water)
Left	401	0.019
Centre	413	0.02
Right	405	0.021

Temperature Reading over the Bundle (C^O)

In front of Row	SCAN POSITIONS 3"	6"	9"
1		277.5	
2	272.0	261.5	251.0
3	240.0	234.0	223.0
4	231.0	220.0	212.0
5	220.0	217.5	211.0
6	210.0	204.5	197.0
Behind Bundle		192.0	

EXPERIMENTAL DATA

Fresh air flowrate = 44691 ft^3/hr

Secondary air flowrate = 42479 ft^3/hr

Temperature Measurement C°

Thermo Couples	Selector A	B	C
1		290.0	444.0
2	97.0	180.5	391.0
3	77.5	114.0	95.0
4	136.5	110.5	141.0
5		190.0	81.5
6		110.0	77.5
7		160.0	126.0
8		162.0	140.5
9		114.0	153.0
10		94.0	75.5
11	136.5	200.0	42.0
12	134.0		45.0
13	68.5	50.0	96.0
14	166.0		
15	115.0	51.5	98.0
16	157.5	52.5	
17	318.0	66.0	24.5
18	84.5	79.5	
19	101.0	70.5	501.0
20		272.0	294.0

Scanning inside the Chamber C°

	Temperature (C°)	Pressure (inch of water)
Left	522	0.019
Centre	534	0.02
Right	511	0.021

Temperature Reading over the Bundle (C°)

In front of Row	SCAN POSITIONS 3"	6"	9"
1		290.0	
2	280.0	272.5	251.0
3	249.0	239.0	222.0
4	246.0	230.0	215.0
5	231.0	222.5	210.0
6	225.0	218.0	209.0
Behind Bundle		200.0	

EXPERIMENTAL DATA

Fresh air flowrate = 38704 ft^3/hr

Secondary air flowrate = 42479 ft^3/hr

Temperature Measurement C°

Thermo Couples	Selector A	B	C
1		292.5	447.0
2	101.0	188.0	396.5
3	81.5	122.0	103.0
4		118.0	151.5
5		194.0	88.5
6		116.5	83.0
7		168.5	135.5
8		170.0	149.5
9		122.0	163.5
10		102.0	82.0
11	146.0	208.0	45.0
12	143.0		47.0
13	74.0	53.5	101.0
14	171.5		
15	121.0	56.5	103.5
16	163.5	57.0	
17	318.0	71.5	25.5
18	90.0	86.0	
19	105.0	77.0	506.0
20		275.0	295.0

Scanning inside the Chamber C°

	Temperature (C°)	Pressure (inch of water)
Left	463	0.019
Centre	469	0.02
Right	452	0.021

Temperature Reading over the Bundle (C°)

In front of Row	SCAN POSITIONS 3"	6"	9"
1		292.5	
2	282.0	274.5	270.0
3	261.0	254.0	248.0
4	241.0	235.0	230.0
5	236.0	228.0	220.0
6	232.0	221.5	211.0
Behind Bundle		208.0	

EXPERIMENTAL DATA

Fresh air flowrate = 31602 ft^3/hr

Secondary air flowrate = 42479 ft^3/hr

Temperature Measurement C^o

Thermo Couples	Selector A	B	C
1		294.5	449.0
2	106.0	195.0	400.0
3	88.5	126.0	112.0
4	161.0	126.0	162.5
5	157.0	202.0	97.0
6	86.5	127.0	92.0
7	186.5	178.5	148.5
8	13.0	176.0	162.0
9		127.0	175.5
10		111.0	90.0
11	161.0	216.0	49.0
12	157.0		52.0
13	86.5	57.0	106.5
14	186.5		
15	132.5	60.0	108.0
16	175.5	64.5	
17	322.5	78.0	26.0
18	98.5	93.0	
19	114.0	80.5	508.0
20	277.0	277.0	297.0

Scanning inside the Chamber C^o

	Temperature (C^o)	Pressure (inch of water)
Left	567	0.019
Centre	561	0.02
Right	552	0.021

Temperature Reading over the Bundle (C^o)

In front of Row	SCAN POSITIONS 3"	6"	9"
1		294.5	
2	281.0	270.0	260.0
3	262.0	256.5	245.0
4	245.0	237.5	228.0
5	242.0	232.0	221.0
6	234.0	225.0	215.0
Behind Bundle		216.0	

EXPERIMENTAL DATA

Fresh air flowrate = 22346 ft^3/hr

Secondary air flowrate = 42479 ft^3/hr

Temperature Measurement C°

Thermo Couples	Selector A	B	C
1		294.5	453.0
2	99.0	220.5	396.0
3	98.5	142.5	132.5
4		143.0	184.5
5		221.5	118.5
6		142.5	108.0
7		197.0	175.5
8		143.0	182.0
9		143.0	196.5
10		122.0	108.5
11	180.5	225.5	57.0
12	176.5		58.5
13	102.0	61.5	119.5
14	203.0		
15	144.0	67.5	117.5
16	190.5	75.0	
17	324.0	89.0	26.5
18	114.0	102.0	
19	131.0	89.0	507.0
20		278.0	298.0

Scanning inside the Chamber C°

	Temperature (C°)	Pressure (inch of water)
Left	568	0.019
Centre	574	0.02
Right	552	0.021

Temperature Reading over the Bundle (C°)

In front of Row	SCAN POSITIONS 3"	6"	9"
1		294.5	
2	290.0	276.0	262.0
3	262.0	251.0	242.0
4	254.0	247.0	236.0
5	241.0	235.0	221.0
6	239.0	231.0	225.0
Behind Bundle		225.5	

EXPERIMENTAL DATA

Fresh air flowrate = 49900 ft^3/hr

Secondary air flowrate = 28319 ft^3/hr

Temperature Measurement C°

Thermo Couples	Selector A	B	C
1		373.0	551.5
2	96.0	201.0	496.0
3	94.5	150.0	107.0
4		122.5	155.0
5		205.5	91.5
6		131.0	89.0
7		175.0	138.0
8		182.5	156.0
9		148.5	173.0
10		104.5	87.0
11	150.5	227.5	43.5
12	146.0		48.0
13	77.0	58.0	122.5
14	188.5		
15	133.0	56.5	131.0
16	175.0	55.5	
17	408.0	71.5	25.5
18	92.0	100.0	
19	111.0	74.0	600.0
20		369.5	391.0

Scanning inside the Chamber C°

	Temperature (C^o)	Pressure (inch of water)
Left	600	0.01
Centre	630	0.012
Right	602	0.013

Temperature Reading over the Bundle (C^o)

In front of Row	SCAN POSITIONS 3"	6"	9"
1		373.0	
2	352.0	341.5	325.0
3	309.0	299.0	282.0
4	284.0	277.0	270.0
5	271.0	260.0	251.0
6	330.0	316.0	305.0
Behind Bundle		227.5	

EXPERIMENTAL DATA

Fresh air flowrate = 44691 ft^3/hr

Secondary air flowrate = 28319 ft^3/hr

Temperature Measurement C^o

Thermo Couples	Selector A	B	C
1		380.5	565.0
2	99.0	219.0	512.0
3	97.0	161.0	111.0
4		140.0	162.0
5		226.5	95.0
6		139.5	92.0
7		190.0	144.0
8		201.5	161.5
9		165.5	181.0
10		108.5	90.5
11	158.0	235.5	45.0
12	151.0		49.0
13	77.0	57.5	123.0
14	201.0		
15	141.5	58.0	132.0
16	186.5	58.5	
17	420.0	76.0	26.25
18	98.0	104.5	
19	123.0	86.5	609.0
20		376.5	404.5

Scanning inside the Chamber C^o

	Temperature (C^o)	Pressure (inch of water)
Left	615	0.01
Centre	623	0.012
Right	608	0.013

Temperature Reading over the Bundle (C^o)

In front of Row	SCAN POSITIONS 3"	6"	9"
1		380.5	
2	356.0	348.0	331.0
3	311.0	303.0	294.0
4	295.0	283.0	264.0
5	289.0	270.0	255.0
6	280.0	263.0	252.0
Behind Bundle		235.5	

EXPERIMENTAL DATA

Fresh air flowrate = 38704 ft^3/hr

Secondary air flowrate = 28319 ft^3/hr

Temperature Measurement C°

Thermo Couples	Selector A	B	C
1		387.0	564.5
2	108.0	233.5	570.0
3	106.0	171.5	120.0
4		147.0	174.0
5		240.0	102.0
6		148.0	99.0
7		198.0	150.0
8		213.5	172.0
9		174.0	191.5
10		120.5	98.0
11	170.5	242.5	50.0
12	163.0		88.0
13	84.0	60.0	131.0
14	214.5		
15	150.0	62.0	135.5
16	198.0	63.5	
17	425.5	81.5	26.75
18	105.0	111.5	
19	133.0	93.5	613.5
20		400.0	408.0

Scanning inside the Chamber C°

	Temperature (C°)	Pressure (inch of water)
Left	618	0.01
Centre	629	0.012
Right	609	0.013

Temperature Reading over the Bundle (C°)

In front of Row	SCAN POSITIONS 3"	6"	9"
1		387.0	
2	366.0	351.5	340.0
3	315.0	321.5	311.0
4	294.0	287.5	279.0
5	286.0	279.0	265.0
6	280.0	269.0	260.0
Behind Bundle		242.5	

EXPERIMENTAL DATA

Fresh air flowrate = 31602 ft^3/hr

Secondary air flowrate = 28319 ft^3/hr

Temperature Measurement C^o

Thermo Couples	Selector A	B	C
1		388.0	571.0
2	115.0	243.0	509.0
3	114.0	179.0	133.0
4		156.0	191.5
5		253.0	148.0
6		162.5	110.5
7		214.0	183.0
8		225.0	188.0
9		183.0	207.0
10		127.5	109.0
11	190.0	253.0	58.5
12	180.0		56.5
13	98.0	65.0	137.5
14	231.0		
15	161.0	68.5	
16	211.0	75.0	
17	430.5	90.5	27.5
18	118.0	122.5	
19	143.0	99.0	613.0
20		390.0	411.0

Scanning inside the Chamber C^o

	Temperature (C^o)	Pressure (inch of water)
Left	619	0.01
Centre	630	0.012
Right	612	0.013

Temperature Reading over the Bundle (C^o)

In front of Row	SCAN POSITIONS 3"	6"	9"
1		388.0	
2	364.0	352.5	341.0
3	330.0	318.0	310.0
4	305.0	293.0	281.0
5	395.0	286.5	277.0
6	292.0	275.0	262.0
Behind Bundle		255.0	

EXPERIMENTAL DATA

Fresh air flowrate = 22346 ft^3/hr

Secondary air flowrate = 28319 ft^3/hr

Temperature Measurement C^{o}

Thermo Couples	Selector A	B	C
1		390.0	576.0
2	133.0	268.0	518.0
3	130.0	197.0	157.0
4		180.0	220.0
5		280.5	173.0
6		182.0	134.0
7		241.0	214.5
8		254.0	214.0
9		207.5	235.5
10		145.0	131.5
11	213.0	275.5	65.0
12	209.0	67.0	67.0
13	121.0	72.0	155.5
14	255.0		
15	177.0	78.5	154.5
16	234.5	92.5	
17	434.0	106.5	28.25
18	139.0	137.5	
19	163.5	111.5	618.0
20		393.0	415.0

Scanning inside the Chamber C^{o}

	Temperature (C^{o})	Pressure (inch of water)
Left	633	0.01
Centre	650	0.012
Right	614	0.013

Temperature Reading over the Bundle (C^{o})

In front of Row	SCAN POSITIONS 3"	6"	9"
1		390.0	
2	370.0	356.0	340.0
3	352.0	337.0	322.0
4	325.0	314.0	302.0
5	323.0	311.0	300.0
6	399.0	290.0	281.0
Behind Bundle		275.5	

A.1.2

Blocked Tube Experiments

EXPERIMENTAL DATA

Fresh air flowrate = 40594 ft^3/hr

Secondary air flowrate = 76200 ft^3/hr

Temperature Measurement C^o

Thermo Couples	Selector A	Selector B	Selector C
1		195.0	
2	51.5	173.5	
3	63.5	70.5	62.0
4		71.5	87.0
5		102.5	58.5
6		87.5	62.0
7		88.5	94.5
8		107.5	109.0
9		74.5	106.0
10		71.5	56.5
11		159.0	39.5
12	98.0		37.0
13	55.0	45.5	129.5
14	109.0		
15	75.0	48.0	86.0
16	143.0	48.5	
17	222.0	61.0	25.5
18	61.0	115.0	
19	64.5	55.0	
20		168.5	

Scanning inside the Chamber C^o

	Temperature (C^o)	Pressure (inch of water)
Left	225	0.05
Centre	246	0.057
Right	249	0.061

Temperature Reading over the Bundle (C^o)

In front of Row	SCAN POSITIONS 3"	6"	9"
1		195.0	
2	194.0	189.0	183.0
3	191.0	185.5	182.0
4	190.0	182.0	180.0
5	186.0	180.0	175.0
6	180.0	174.5	169.5
Behind Bundle		159.0	

EXPERIMENTAL DATA

Fresh air flowrate = 36308 ft^3/hr

Secondary air flowrate = 76200 ft^3/hr

Temperature Measurement C°

Thermo Couples	Selector A	B	C
1		196.0	
2	52.5	176.0	
3	65.5	73.5	95.5
4		78.0	65.5
5		125.0	61.5
6		87.0	63.5
7		105.0	99.5
8		113.0	113.0
9		80.0	110.0
10		74.0	60.0
11		161.0	42.0
12	102.5		39.0
13	56.0	46.5	129.0
14	115.5		
15	77.5	49.5	85.0
16	147.0	50.5	
17	225.5	62.5	26.0
18	65.0	120.5	
19	68.5	54.5	
20		172.5	

Scanning inside the Chamber C°

	Temperature (C°)	Pressure (inch of water)
Left	250	0.05
Centre	249	0.057
Right	251	0.061

Temperature Reading over the Bundle (C°)

In front of Row	SCAN POSITIONS 3"	6"	9"
1		196.0	
2	192.5	187.5	180.0
3	188.5	185.5	178.0
4	188.0	184.0	176.0
5	184.0	182.0	173.0
6	180.0	175.5	171.0
Behind Bundle		161.0	

EXPERIMENTAL DATA

Fresh air flowrate = 31444 ft^3/hr

Secondary air flowrate = 76200 ft^3/hr

Temperature Measurement C^o

Thermo Couples	Selector A	B	C
1		196.5	
2	57.0	179.5	
3	69.5	79.5	100.0
4		82.5	69.5
5		126.0	67.0
6		95.5	69.5
7		103.0	108.0
8		120.0	123.0
9		79.5	116.0
10		81.0	65.5
11		165.0	45.0
12	112.5		42.0
13	62.5	50.5	134.0
14	124.0		
15	84.5	53.5	92.0
16	152.5	54.0	
17	230.0	68.0	27.0
18	69.5	127.5	
19		60.0	
20		174.5	

Scanning inside the Chamber C^o

	Temperature (C^o)	Pressure (inch of water)
Left	255	0.05
Centre	254	0.057
Right	256	0.061

Temperature Reading over the Bundle (C^o)

In front of Row	SCAN POSITIONS 3"	6"	9"
1		196.5	
2	198.0	190.5	184.5
3	194.0	188.5	182.0
4	195.0	184.5	180.0
5	190.0	184.0	177.0
6	183.0	177.5	172.0
Behind Bundle		165.0	

EXPERIMENTAL DATA

Fresh air flowrate = 25674 ft^3/hr

Secondary air flowrate = 76200 ft^3/hr

Temperature Measurement C°

Thermo Couples	Selector A	B	C
1		197.5	
2	61.5	184.0	
3	76.5	87.0	110.5
4		92.5	71.0
5		141.5	77.5
6		105.0	78.5
7		113.0	123.5
8		134.0	135.0
9		91.5	130.5
10		89.0	76.0
11		170.0	50.5
12	126.5		46.5
13	72.0	53.5	145.5
14	135.0		
15	90.0	58.0	96.0
16	158.5	60.0	
17	229.0	75.5	27.0
18	79.5	133.0	
19	83.0	65.5	
20		175.5	

Scanning inside the Chamber C°

	Temperature (C°)	Pressure (inch of water)
Left	256	0.05
Centre	260	0.057
Right	262	0.061

Temperature Reading over the Bundle (C°)

In front of Row	SCAN POSITIONS 3"	6"	9"
1		197.5	
2	200.0	191.0	185.0
3	194.0	188.0	181.0
4	191.0	185.5	179.0
5	189.0	184.0	178.0
6	184.0	181.0	173.0
Behind Bundle		170.0	

EXPERIMENTAL DATA

Fresh air flowrate = 18534 ft^3/hr

Secondary air flowrate = 76200 ft^3/hr

Temperature Measurement C°

Thermo Couples	Selector A	B	C
1		196.5	
2	78.0	190.0	
3	95.0	101.0	130.0
4		110.0	73.0
5		165.0	94.5
6		129.0	99.0
7		138.0	150.0
8		156.5	154.5
9		108.0	151.0
10		104.0	92.5
11		178.5	65.0
12	150.0		59.5
13	90.5	70.0	159.5
14	156.0		
15	103.5	75.5	112.5
16	169.0	81.5	
17	229.0	95.0	28.0
18	100.0	148.5	
19	102.0	84.5	
20		175.5	

Scanning inside the Chamber C°

	Temperature (C°)	Pressure (inch of water)
Left	260	0.05
Centre	262	0.057
Right	253	0.061

Temperature Reading over the Bundle (C°)

In front of Row	SCAN POSITIONS 3"	6"	9"
1		196.5	
2	200.0	190.5	182.0
3	195.0	188.0	180.0
4	193.0	187.0	178.0
5	192.0	185.0	174.0
6	190.0	182.0	173.0
Behind Bundle		178.5	

EXPERIMENTAL DATA

Fresh air flowrate = 40594 ft^3/hr

Secondary air flowrate = 69368 ft^3/hr

Temperature Measurement C°

Thermo Couples	Selector A	B	C
1		204.0	
2	52.5	179.0	
3	66.0	115.0	68.5
4		74.5	115.5
5			59.5
6		86.5	61.5
7			103.0
8		111.0	113.5
9		75.5	110.5
10		73.5	57.0
11	107.5	165.5	40.0
12	108.5		39.5
13	57.5	44.5	138.5
14	113.5		
15	77.5	49.0	90.0
16	148.5	49.5	
17		63.5	25.5
18	69.5	122.0	
19	67.0	57.5	
20	193.5	176.0	

Scanning inside the Chamber C°

	Temperature (C°)	Pressure (inch of water)
Left	223	0.04
Centre	241	0.041
Right	231	0.033

Temperature Reading over the Bundle (C°)

In front of Row	SCAN POSITIONS 3"	6"	9"
1		204.0	
2	201.0	197.5	181.0
3	199.0	195.0	183.0
4	195.0	194.0	186.0
5	194.0	191.5	184.0
6	187.0	183.0	176.0
Behind Bundle		165.5	

EXPERIMENTAL DATA

Fresh air flowrate = 36308 ft^3/hr

Secondary air flowrate = 69368 ft^3/hr

Temperature Measurement C^{o}

Thermo Couples	Selector A	B	C
1		205.5	
2	53.5	183.0	
3	67.5	122.0	71.5
4		81.0	121.0
5		119.0	63.0
6		90.0	63.5
7		120.0	109.0
8		118.0	118.0
9		81.5	115.5
10		77.5	61.5
11	113.5	168.0	42.5
12	112.5		42.0
13	59.5	46.0	137.5
14	120.0		
15	82.0	50.5	89.5
16	153.0	51.5	
17		65.5	26.5
18	72.5	127.5	
19	71.5	56.5	
20		182.0	

Scanning inside the Chamber C^{o}

	Temperature (C^{o})	Pressure (inch of water)
Left	229	0.04
Centre	240	0.041
Right	233	0.033

Temperature Reading over the Bundle (C^{o})

In front of Row	SCAN POSITIONS 3"	6"	9"
1		205.5	
2	202.0	199.5	195.0
3	200.0	196.5	192.0
4	199.5	195.0	189.0
5	194.0	191.5	186.0
6	191.0	185.0	181.0
Behind Bundle		168.0	

EXPERIMENTAL DATA

Fresh air flowrate = 31444 ft^3/hr

Secondary air flowrate = 69368 ft^3/hr

Temperature Measurement C^o

Thermo Couples	Selector A	B	C
1		205.0	
2	58.0	186.0	
3	71.5	127.0	77.0
4		86.0	129.5
5			67.5
6		98.5	69.0
7		120.0	110.5
8		124.0	127.5
9		82.5	123.5
10		83.0	67.0
11	121.5	172.0	45.0
12	125.5		44.5
13	65.0	50.5	142.5
14	129.0		
15	86.5	54.5	96.0
16	158.5	51.5	
17		70.5	26.5
18	78.5	134.5	
19	81.0	61.5	
20		185.0	

Scanning inside the Chamber C^o

	Temperature (C^o)	Pressure (inch of water)
Left	226	0.04
Centre	242	0.041
Right	236	0.033

Temperature Reading over the Bundle (C^o)

In front of Row	SCAN POSITIONS 3"	6"	9"
1		205.0	
2	205.0	200.0	194.0
3	201.0	197.0	192.0
4	200.0	194.0	186.0
5	198.0	192.5	183.0
6	192.0	186.5	180.0
Behind Bundle		172.0	

EXPERIMENTAL DATA

Fresh air flowrate = 25674 ft^3/hr

Secondary air flowrate = 69368 ft^3/hr

Temperature Measurement C°

Thermo Couples	Selector A	B	C
1		207.0	
2	63.5	190.5	
3	79.5	125.0	88.5
4		96.0	143.0
5			79.5
6		110.0	79.0
7		124.0	127.5
8		140.0	141.0
9		95.0	137.0
10		94.0	78.0
11	135.0	178.0	51.5
12	130.5		50.0
13	76.0	53.5	148.0
14	140.5		
15	93.5	60.0	101.0
16	165.5	60.5	
17		79.5	27.0
18	90.5	141.5	
19	87.0	68.5	
20		186.0	

Scanning inside the Chamber C°

	Temperature (C°)	Pressure (inch of water)
Left	224	0.04
Centre	243	0.041
Right	236	0.033

Temperature Reading over the Bundle (C°)

In front of Row	SCAN POSITIONS 3"	6"	9"
1		207.0	
2	209.0	202.5	197.0
3	201.0	198.0	192.0
4	199.0	195.5	190.0
5	196.0	193.5	186.0
6	193.0	190.0	185.0
Behind Bundle		178.0	

EXPERIMENTAL DATA

Fresh air flowrate = 18534 ft^3/hr

Secondary air flowrate = 69368 ft^3/hr

Temperature Measurement C°

Thermo Couples	Selector A	Selector B	Selector C
1		208.0	
2	81.5	199.0	
3	99.0	136.0	109.5
4		115.5	167.5
5			97.0
6		135.0	100.5
7		160.0	156.0
8		164.0	162.0
9		114.0	156.5
10		114.5	96.0
11	160.5	188.5	67.0
12	56.0		63.5
13	95.0	72.0	164.0
14	163.5		
15	108.0	78.0	119.0
16	177.5	84.0	
17		84.5	28.5
18	111.5	157.5	
19	107.0	88.0	
20		187.0	

Scanning inside the Chamber C°

	Temperature (C^O)	Pressure (inch of water)
Left	225	0.04
Centre	244	0.041
Right	236	0.033

Temperature Reading over the Bundle (C^O)

In front of Row	SCAN POSITIONS 3"	6"	9"
1		208.0	
2	208.0	202.5	197.0
3	206.0	200.0	194.0
4	203.0	197.0	193.0
5	201.0	196.0	194.0
6	196.0	193.5	187.0
Behind Bundle		188.5	

EXPERIMENTAL DATA

Fresh air flowrate = 40594 ft^3/hr

Secondary air flowrate = 52980 ft^3/hr

Temperature Measurement C^o

Thermo Couples	Selector A	B	C
1		219.5	
2	54.0	195.5	
3	68.5	125.0	71.5
4		79.5	124.5
5			62.5
6		92.5	64.5
7			123.5
8		122.0	122.5
9		80.5	120.5
10		78.0	59.5
11	117.5	176.5	40.0
12	128.5		40.0
13	60.5	46.5	146.0
14	124.5		
15	82.5	50.5	94.0
16	162.0	51.0	
17		64.0	25.5
18	74.0	130.5	
19	71.0	60.0	
20		192.5	

Scanning inside the Chamber C^o

	Temperature (C^o)	Pressure (inch of water)
Left	242	0.034
Centre	236	0.039
Right	251	0.036

Temperature Reading over the Bundle (C^o)

In front of Row	SCAN POSITIONS 3"	6"	9"
1		219.0	
2	220.0	213.5	209.0
3	215.0	210.0	205.0
4	210.0	205.0	199.0
5	208.0	202.5	197.0
6	200.0	194.5	192.0
Behind Bundle		176.5	

EXPERIMENTAL DATA

Fresh air flowrate = 36308 ft^3/hr

Secondary air flowrate = 52980 ft^3/hr

Temperature Measurement C^o

Thermo Couples	Selector A	B	C
1		222.5	
2	56.5	199.5	
3	90.5	134.0	75.5
4		86.5	131.0
5			65.5
6		98.5	67.0
7		125.0	70.0
8		130.5	128.0
9		88.5	125.5
10		82.0	64.5
11	124.5	180.0	43.5
12	124.5		43.0
13	62.5	48.0	144.5
14	131.5		
15	85.0	53.0	94.0
16	68.0	54.0	
17		67.5	26.5
18	78.5	135.5	
19	76.5	59.5	
20		199.5	

Scanning inside the Chamber C^o

	Temperature (C^o)	Pressure (inch of water)
Left	250	0.034
Centre	260	0.039
Right	253	0.036

Temperature Reading over the Bundle (C^o)

In front of Row	SCAN POSITIONS 3"	6"	9"
1		222.5	
2	221.0	214.5	210.0
3	218.0	211.0	208.0
4	213.0	207.5	204.0
5	210.0	205.0	201.0
6	202.0	196.5	192.0
Behind Bundle		180.0	

EXPERIMENTAL DATA

Fresh air flowrate = 31444 ft^3/hr

Secondary air flowrate = 52980 ft^3/hr

Temperature Measurement C°

Thermo Couples	Selector A	B	C
1		223.0	
2	61.0	204.5	
3	76.0	128.0	82.0
4		93.5	141.0
5			72.0
6		108.0	73.5
7		140.0	131.0
8		137.0	139.5
9		90.5	137.0
10		89.0	71.5
11	133.0	184.5	47.0
12	135.5		45.5
13	70.0	53.0	152.0
14	142.0		
15	93.0	57.5	102.0
16	174.0	58.0	
17		74.0	27.5
18	84.0	145.5	
19	88.0	65.0	
20		202.5	

Scanning inside the Chamber C°

	Temperature (C°)	Pressure (inch of water)
Left	251	0.034
Centre	257	0.039
Right	256	0.036

Temperature Reading over the Bundle (C°)

In front of Row	SCAN POSITIONS 3"	6"	9"
1		223.0	
2	224.0	216.5	209.0
3	218.0	212.5	205.0
4	214.0	209.0	202.0
5	212.0	207.0	200.0
6	210.0	200.0	193.0
Behind Bundle		184.5	

EXPERIMENTAL DATA

Fresh air flowrate = 25674 ft^3/hr

Secondary air flowrate = 52980 ft^3/hr

Temperature Measurement C°

Thermo Couples	Selector A	Selector B	Selector C
1		226.0	
2	67.0	210.0	
3	84.5	141.0	95.0
4		109.0	156.0
5			84.5
6		122.0	84.5
7		150.0	149.5
8		154.5	153.5
9		103.5	150.5
10		101.0	83.5
11	149.5	192.5	53.0
12	150.0		51.5
13	82.5	56.0	158.5
14	155.5		
15	101.0	62.5	108.0
16	182.0	63.0	
17		80.5	28.0
18	98.0	151.5	
19	95.0	72.5	
20		205.0	

Scanning inside the Chamber C°

	Temperature (C°)	Pressure (inch of water)
Left	252	0.034
Centre	261	0.039
Right	259	0.036

Temperature Reading over the Bundle (C°)

In front of Row	SCAN POSITIONS 3"	6"	9"
1		226.0	
2	230.0	217.0	212.0
3	226.0	214.5	206.0
4	221.0	211.0	201.0
5	217.0	209.5	193.0
6	211.0	203.0	190.0
Behind Bundle		192.5	

EXPERIMENTAL DATA

Fresh air flowrate = 18534 ft^3/hr

Secondary air flowrate = 52980 ft^3/hr

Temperature Measurement C^o

Thermo Couples	Selector A	B	C
1		227.0	
2	86.5	219.0	
3	106.5	155.0	121.5
4		175.0	184.5
5		188.5	106.0
6		150.0	110.0
7			177.5
8		181.0	176.5
9		125.0	179.5
10		127.0	105.5
11	177.5	204.0	71.0
12	175.5		67.0
13	105.0	76.5	176.0
14	181.0		
15	117.5	83.0	127.5
16	195.0	89.0	
17	268.0	106.0	29.5
18	125.0	168.0	
19	118.0	94.0	
20		205.0	

Scanning inside the Chamber C^o

	Temperature (C^o)	Pressure (inch of water)
Left	252	0.034
Centre	253	0.039
Right	259	0.036

Temperature Reading over the Bundle (C^o)

In front of Row	SCAN POSITIONS 3"	6"	9"
1		227.0	
2	239.0	216.0	210.0
3	231.0	215.0	209.0
4	225.5	213.5	206.0
5	219.0	212.0	201.0
6	215.0	207.5	198.0
Behind Bundle		204.0	

EXPERIMENTAL DATA

Fresh air flowrate = 40594 ft^3/hr

Secondary air flowrate = 42479 ft^3/hr

Temperature Measurement C°

Thermo Couples	Selector A	B	C
1		256.5	
2	59.0	225.5	
3	75.0	140.0	78.0
4		90.0	137.5
5			68.0
6		105.0	71.0
7			125.0
8		141.0	137.0
9		95.5	135.0
10		87.0	66.0
11	132.5	200.0	43.0
12	122.5		42.0
13	67.0	48.5	167.5
14	142.5		
15	94.0	54.0	105.0
16	186.0	55.0	
17		71.0	27.0
18	80.0	150.0	
19	79.0	66.0	
20		234.0	

Scanning inside the Chamber C°

	Temperature (C°)	Pressure (inch of water)
Left	290	0.019
Centre	294	0.022
Right	299	0.017

Temperature Reading over the Bundle (C°)

In front of Row	SCAN POSITIONS 3"	6"	9"
1		256.5	
2	257.0	249.0	240.0
3	252.0	246.5	236.0
4	250.0	241.5	231.0
5	247.0	234.0	228.0
6	232.0	221.0	217.0
Behind Bundle		200.0	

EXPERIMENTAL DATA

Fresh air flowrate = 36308 ft^3/hr

Secondary air flowrate = 42479 ft^3/hr

Temperature Measurement C°

Thermo Couples	Selector A	Selector B	Selector C
1		266.0	
2	60.5	231.5	
3	77.0	147.0	82.5
4		98.0	145.5
5		100.5	73.0
6		113.0	74.5
7		96.0	133.5
8		151.0	143.5
9		103.0	142.0
10		93.0	70.5
11	138.5	205.0	45.5
12	139.0		44.5
13	68.5	51.5	167.0
14	149.5		
15	96.0	56.5	105.0
16	191.5	57.0	
17		74.0	27.5
18	86.0	156.0	
19	85.0	65.0	
20		245.0	

Scanning inside the Chamber C°

	Temperature (C°)	Pressure (inch of water)
Left	298	0.019
Centre	300	0.022
Right	301	0.017

Temperature Reading over the Bundle (C°)

In front of Row	SCAN POSITIONS 3"	6"	9"
1		266.0	
2	260.0	250.5	241.0
3	257.0	249.0	240.0
4	252.0	242.5	236.0
5	248.0	237.5	232.0
6	240.0	226.0	229.0
Behind Bundle		205.0	

EXPERIMENTAL DATA

Fresh air flowrate = 31444 ft^3/hr

Secondary air flowrate = 42479 ft^3/hr

Temperature Measurement C^o

Thermo Couples	Selector A	B	C
1		268.0	
2	67.0	238.0	
3	84.0	154.0	92.5
4		106.5	160.0
5		107.5	82.0
6		120.0	84.0
7		104.5	148.0
8		159.5	158.0
9		110.0	152.0
10		101.0	79.5
11	151.0	211.5	51.0
12	143.0		49.0
13	79.0	56.5	163.0
14	164.0		
15	107.0	62.0	115.5
16	200.5	63.0	
17		82.0	30.0
18	96.0	167.0	
19	101.0	72.0	
20		250.5	

Scanning inside the Chamber C^o

	Temperature (C^o)	Pressure (inch of water)
Left	299	0.019
Centre	305	0.022
Right	301	0.017

Temperature Reading over the Bundle (C^o)

In front of Row	SCAN POSITIONS 3"	6"	9"
1		268.0	
2	257.0	250.5	241.0
3	252.0	248.0	234.0
4	250.0	244.5	228.0
5	247.0	243.0	219.0
6	239.0	232.0	214.0
Behind Bundle		211.5	

EXPERIMENTAL DATA

Fresh air flowrate = 25674 ft^3/hr

Secondary air flowrate = 42479 ft^3/hr

Temperature Measurement C^o

Thermo Couples	Selector A	B	C
1		265.0	
2	73.5	243.0	
3	94.0	160.0	108.5
4		112.5	177.0
5		111.0	95.0
6		126.5	95.0
7		109.0	158.0
8		168.5	174.5
9		116.5	174.0
10		115.0	94.0
11	168.0	217.0	57.5
12	161.0		55.0
13	93.0	62.0	181.0
14	179.0		
15	118.0	68.0	123.0
16	209.0	68.0	
17	314.0	92.0	30.0
18	111.0	173.0	
19	109.5	80.0	
20		253.0	

Scanning inside the Chamber C^o

	Temperature (C^o)	Pressure (inch of water)
Left	299	0.019
Centre	293	0.022
Right	298	0.017

Temperature Reading over the Bundle (C^o)

In front of Row	SCAN POSITIONS 3"	6"	9"
1		265.0	
2	262.0	256.0	248.0
3	260.0	253.0	243.0
4	254.0	243.5	240.0
5	250.0	242.0	237.0
6	245.0	232.0	227.0
Behind Bundle		217.0	

EXPERIMENTAL DATA

Fresh air flowrate = 18534 ft^3/hr

Secondary air flowrate = 42479 ft^3/hr

Temperature Measurement C^o

Thermo Couples	Selector A	B	C
1		264.0	
2	97.5	257.5	
3	121.0	166.0	141.5
4		118.0	214.0
5		117.0	123.5
6		133.0	126.0
7		126.0	200.0
8		173	204.0
9		124.5	200.0
10		149.0	121.0
11	205.5	235.5	79.0
12	198.0		75.0
13	120.0	85.5	217.0
14	213.5		
15	136.0	93.0	146.0
16	227.5	98.5	
17		121.0	32.5
18	140.5	195.0	
19	139.0	106.5	
20		255.0	

Scanning inside the Chamber C^o

	Temperature (C^o)	Pressure (inch of water)
Left	300	0.019
Centre	302	0.022
Right	306	0.017

Temperature Reading over the Bundle (C^o)

In front of Row	SCAN POSITIONS 3"	6"	9"
1		264.0	
2	269.0	257.0	248.0
3	266.0	255.0	242.0
4	261.0	252.0	240.0
5	257.0	250.0	239.0
6	253.0	247.0	236.0
Behind Bundle		235.5	

APPENDIX A.1.3

One Burner in Operation

A.1.3.1	Burner "1" on
A.1.3.2	Burner "1" on
A.1.3.3	Burner "2" on
A.1.3.4	Burner "2" on

(A.1.3.1)

EXPERIMENTAL DATA

Fresh air flowrate = 49900 ft^3/hr

Secondary air flowrate = 76200 ft^3/hr

Temperature Measurement C^o

Thermo Couples	Selector A	B	C
1		115.5	126.5
2	40.0	82.5	142.0
3	39.0	59.5	54.5
4		51.0	86.0
5		91.0	60.5
6		54.0	45.5
7		70.0	80.5
8		78.0	81.0
9		62.0	88.0
10		51.5	45.5
11	78.0	100.0	30.5
12	74.5		30.0
13	41.5	34.0	43.0
14	81.5		
15	56.0	32.0	44.0
16	76.5	33.5	
17	167.0	35.0	23.5
18	56.0	40.0	
19	48.5	33.0	270.0
20		109.5	95.0

Scanning inside the Chamber C^o

	Temperature (C^o)	Pressure (inch of water)
Left	126	0.051
Centre	130	0.056
Right	133	0.059

Temperature Reading over the Bundle (C^o)

In front of Row	SCAN POSITIONS 3"	6"	9"
1		115.5	
2	108.0	98.0	94.0
3	102.0	93.0	89.0
4	100.0	92.0	86.0
5	94.0	89.0	85.0
6	92.0	86.5	82.0
Behind Bundle		100.0	

EXPERIMENTAL DATA

Fresh air flowrate = 44691 ft^3/hr

Secondary air flowrate = 76200 ft^3/hr

Temperature Measurement C°

Thermo Couples	Selector A	B	C
1		116.5	129.0
2	41.0	87.5	144.0
3	39.5	63.0	56.5
4		55.5	88.0
5		97.0	62.0
6		56.0	46.5
7		74.5	83.5
8		82.5	83.5
9		66.5	92.0
10		52.5	47.0
11	81.0	98.5	32.0
12	77.5		31.0
13	41.5	33.5	44.0
14	86.0		
15	59.0	32.5	44.5
16	81.0	35.5	
17	168.0	36.5	24.5
18	57.5	41.5	
19	52.0	36.0	273.5
20		112.0	96.5

Scanning inside the Chamber C°

	Temperature (C°)	Pressure (inch of water)
Left	126	0.051
Centre	131	0.056
Right	132	0.059

Temperature Reading over the Bundle (C°)

In front of Row	SCAN POSITIONS 3"	6"	9"
1		116.6	
2	100.0	96.0	90.0
3	98.0	93.5	89.0
4	96.0	92.0	83.0
5	94.0	91.0	86.0
6	94.0	90.0	84.0
Behind Bundle		98.5	

EXPERIMENTAL DATA

Fresh air flowrate = 38704 ft^3/hr

Secondary air flowrate = 76200 ft^3/hr

Temperature Measurement C°

Thermo Couples	Selector A	B	C
1		117.5	130.0
2	42.0	92.0	145.5
3	40.5	65.5	68.5
4		58.5	91.0
5		102.0	64.5
6		58.0	48.0
7		78.0	86.5
8		86.5	86.5
9		69.0	94.5
10		54.5	49.0
11	84.0	101.5	32.5
12	81.0		31.5
13	43.5	35.0	45.0
14	89.0		
15	60.0	34.0	45.5
16	84.5	37.0	
17	169.0	37.5	24.5
18	60.0	43.0	
19	53.5	37.5	272.5
20		113.0	97.0

Scanning inside the Chamber C°

	Temperature (C°)	Pressure (inch of water)
Left	127	0.051
Centre	139	0.056
Right	136	0.059

Temperature Reading over the Bundle (C°)

In front of Row	SCAN POSITIONS 3"	6"	9"
1		117.5	
2	110.0	99.5	93.0
3	108.0	96.0	91.0
4	105.0	95.0	89.0
5	99.0	91.0	86.0
6	98.0	91.0	84.0
Behind Bundle		101.5	

EXPERIMENTAL DATA

Fresh air flowrate = 31602 ft^3/hr

Secondary air flowrate = 76200 ft^3/hr

Temperature Measurement C°

Thermo Couples	Selector A	B	C
1		119.0	130.0
2	43.0	95.0	145.5
3	42.0	67.5	62.5
4		61.0	93.0
5		107.0	69.0
6		61.5	51.5
7		82.5	92.5
8		89.5	92.5
9		71.0	100.0
10		58.5	52.0
11	89.0	103.5	34.0
12	87.0		33.0
13	47.5	35.5	46.0
14	94.0		
15	64.5	35.0	46.5
16	89.0	39.5	
17	169.0	39.5	24.5
18	63.5	44.5	
19	57.0	38.5	274.0
20		113.5	97.0

Scanning inside the Chamber C°

	Temperature (C°)	Pressure (inch of water)
Left	129	0.051
Centre	121	0.056
Right	122	0.059

Temperature Reading over the Bundle (C°)

In front of Row	SCAN POSITIONS 3"	6"	9"
1		119.0	
2	111.0	105.0	100.0
3	105.0	96.5	90.0
4	102.0	95.0	89.0
5	100.0	92.0	87.0
6	99.0	92.0	85.0
Behind Bundle		103.5	

EXPERIMENTAL DATA

Fresh air flowrate = 22346 ft^3/hr

Secondary air flowrate = 76200 ft^3/hr

Temperature Measurement C^o

Thermo Couples	Selector A	B	C
1		119.0	128.5
2	44.0	103.5	145.0
3	43.0	72.5	69.0
4		68.0	102.0
5		117.0	75.5
6		66.5	57.0
7		92.5	102.0
8		99.0	101.5
9		97.5	109.0
10		63.0	58.0
11	93.0	107.5	35.5
12	93.0		35.0
13	51.5	37.5	49.0
14	99.0		
15	69.0	37.5	49.0
16	93.5	42.0	
17	171.0	42.5	25.5
18	68.0	46.5	
19	60.0	41.0	274.5
20		113.5	96.5

Scanning inside the Chamber C^o

	Temperature (C^o)	Pressure (inch of water)
Left	137	0.051
Centre	139	0.056
Right	132	0.059

Temperature Reading over the Bundle (C^o)

In front of Row	SCAN POSITIONS 3"	6"	9"
1		119.0	
2	109.0	103.0	100.0
3	100.0	96.5	92.0
4	101.0	96.5	91.0
5	102.0	96.0	91.0
6	100.0	95.0	90.0
Behind Bundle		107.5	

(A.1.3.2)

EXPERIMENTAL DATA

Fresh air flowrate = 49900 ft^3/hr

Secondary air flowrate = 28319 ft^3/hr

Temperature Measurement C^o

Thermo Couples	Selector A	B	C
1		228.0	278.0
2	40.5	150.0	311.0
3	47.5	70.0	62.0
4		79.0	63.0
5		163.0	57.0
6		98.0	57.5
7		107.0	106.5
8		146.0	124.0
9		77.0	134.5
10		73.0	58.5
11	115.0	165.0	31.0
12	107.0		31.0
13	60.0	40.0	58.0
14	143.5		
15	74.0	36.0	58.0
16	133.0	36.0	
17	327.0	42.5	25.0
18	64.0	52.5	
19	68.0	43.5	505.0
20		207.5	208.0

Scanning inside the Chamber C^o

	Temperature (C^o)	Pressure (inch of water)
Left	170	0.018
Centre	177	0.019
Right	173	0.021

Temperature Reading over the Bundle (C^o)

In front of Row	SCAN POSITIONS 3"	6"	9"
1		228.0	
2	181.0	173.0	167.0
3	180.0	172.5	165.0
4	179.0	172.0	166.0
5	165.0	158.0	150.0
6	153.0	147.5	140.0
Behind Bundle		165.0	

EXPERIMENTAL DATA

Fresh air flowrate = 44691 ft^3/hr

Secondary air flowrate = 28319 ft^3/hr

Temperature Measurement C^o

Thermo Couples	Selector A	B	C
1		231.0	289.0
2	42.5	166.0	320.0
3	49.0	73.0	63.0
4		90.0	67.5
5		188.5	58.5
6		106.5	59.0
7		123.5	112.0
8		163.0	127.5
9		91.0	141.0
10		77.0	61.0
11	122.0	170.5	33.0
12	135.0		33.0
13	61.5	40.5	59.5
14	155.0		
15	79.0	37.5	59.5
16	142.5	38.0	
17	36.0	45.0	25.0
18	66.5	56.5	
19	75.0	46.0	510.0
20		217.5	221.0

Scanning inside the Chamber C^o

	Temperature (C^o)	Pressure (inch of water)
Left	185	0.018
Centre	190	0.019
Right	188	0.021

Temperature Reading over the Bundle (C^o)

In front of Row	SCAN POSITIONS 3"	6"	9"
1		231.0	
2	190.0	181.0	173.0
3	188.0	180.0	171.0
4	185.0	178.5	172.0
5	182.0	163.0	152.0
6	164.0	151.5	141.0
Behind Bundle		170.5	

EXPERIMENTAL DATA

Fresh air flowrate = 38704 ft^3/hr

Secondary air flowrate = 28319 ft^3/hr

Temperature Measurement C^o

Thermo Couples	Selector A	B	C
1		232.0	291.0
2	45.0	175.0	322.0
3	51.5	79.0	67.5
4		96.0	70.5
5		198.0	62.5
6		113.0	63.0
7		132.0	122.0
8		171.0	137.0
9		94.0	150.5
10		82.0	66.0
11	131.0	171.0	34.0
12	122.5		33.5
13	66.5	41.0	62.0
14	162.5		
15	84.0	40.0	62.0
16	151.0	41.0	
17	332.0	47.0	25.5
18	70.0	59.0	
19	80.5	48.5	510.0
20		219.5	224.0

Scanning inside the Chamber C^o

	Temperature (C^o)	Pressure (inch of water)
Left	182	0.018
Centre	187	0.019
Right	186	0.021

Temperature Reading over the Bundle (C^o)

In front of Row	SCAN POSITIONS 3"	6"	9"
1		232.0	
2	195.0	188.0	181.0
3	190.0	185.0	175.0
4	188.0	182.0	175.0
5	183.0	177.0	170.0
6	159.0	155.0	150.0
Behind Bundle		177.0	

EXPERIMENTAL DATA

Fresh air flowrate = 31602 ft^3/hr

Secondary air flowrate = 28319 ft^3/hr

Temperature Measurement C°

Thermo Couples	Selector A	B	C
1		234.0	294.0
2	47.0	187.0	324.0
3	54.0	86.0	75.0
4		104.0	74.0
5		211.5	70.0
6		125.0	70.0
7		145.5	136.5
8		184.5	149.5
9		103.5	163.0
10		90.0	73.0
11	145.0	186.0	36.0
12	136.0		35.0
13	75.0	43.0	64.0
14	174.0		
15	91.0	41.5	64.0
16	161.5	45.0	
17	319.0	50.5	25.5
18	78.0	62.5	
19	87.0	51.0	512.0
20		221.0	225.0

Scanning inside the Chamber C°

	Temperature (C°)	Pressure (inch of water)
Left	184	0.018
Centre	188	0.019
Right	189	0.021

Temperature Reading over the Bundle (C°)

In front of Row	SCAN POSITIONS 3"	6"	9"
1		234.0	
2	195.0	187.0	180.0
3	190.0	180.5	171.0
4	173.0	161.0	156.0
5	165.0	154.0	149.0
6	162.0	153.5	147.0
Behind Bundle		186.0	

EXPERIMENTAL DATA

Fresh air flowrate = 22346 ft^3/hr

Secondary air flowrate = 28319 ft^3/hr

Temperature Measurement C°

Thermo Couples	Selector A	B	C
1		235.0	292.0
2	52.0	214.5	323.0
3	60.0	95.0	89.0
4		123.0	78.0
5		229.0	81.5
6		141.5	81.5
7		169.0	162.0
8		209.0	168.5
9		118.0	183.5
10		102.0	85.0
11	165.0	196.5	40.0
12	58.5		39.0
13	88.0	45.5	71.5
14	194.0		
15	101.0	45.5	69.5
16	179.0	51.0	26.5
17	340.0	56.0	
18	90.0	68.0	
19	100.0	56.0	514.0
20		221.0	225.0

Scanning inside the Chamber C°

	Temperature (C°)	Pressure (inch of water)
Left		0.018
Centre		0.019
Right		0.021

Temperature Reading over the Bundle (C°)

In front of Row	SCAN POSITIONS 3"	6"	9"
1		235.0	
2	192.0	184.0	180.0
3	191.0	183.0	176.0
4	190.0	183.0	174.0
5	188.0	181.0	173.0
6	179.0	170.5	164.0
Behind Bundle		196.5	

(A.1.3.3)

EXPERIMENTAL DATA

Fresh air flowrate = 49900 ft^3/hr

Secondary air flowrate = 76200 ft^3/hr

Temperature Measurement C°

Thermo Couples	Selector A	B	C
1		129.0	324.0
2		73.0	171.5
3	62.0	65.5	59.5
4		62.5	68.0
5		73.0	63.5
6		64.0	66.5
7		68.5	70.0
8		70.0	67.0
9		66.0	70.0
10		56.0	54.5
11	71.5	117.5	43.0
12	64.5		41.5
13	52.5	49.0	72.0
14	69.0		
15	62.5	47.5	
16	68.5	50.5	
17	103.0	54.5	27.5
18	68.5	67.0	
19	59.0	50.5	144.0
20		100.5	189.0

Scanning inside the Chamber C°

	Temperature (C°)	Pressure (inch of water)
Left	260	0.057
Centre	270	0.052
Right	271	0.053

Temperature Reading over the Bundle (C°)

In front of Row	SCAN POSITIONS 3"	6"	9"
1		129.0	
2	149.0	140.0	130.0
3	139.0	131.0	129.0
4	137.0	130.0	128.0
5	135.0	127.0	120.0
6	130.0	119.0	113.0
Behind Bundle		117.5	

EXPERIMENTAL DATA

Fresh air flowrate = 44691 ft^3/hr

Secondary air flowrate = 76200 ft^3/hr

Temperature Measurement C^o

Thermo Couples	Selector A	Selector B	Selector C
1		125.5	324.0
2		76.5	171.0
3	62.5	68.5	60.0
4		66.0	68.0
5		76.0	63.0
6		65.0	56.0
7		70.0	69.5
8		73.0	67.0
9		70.0	70.0
10		56.5	55.0
11	73.0	113.5	44.0
12	65.5		42.0
13	51.5	44.0	72.5
14	71.0		
15	65.5	47.0	
16	70.5	55.5	
17	103.0	56.0	27.5
18	70.0	68.0	
19	62.0	56.5	143.0
20		100.0	188.0

Scanning inside the Chamber C^o

	Temperature (C^o)	Pressure (inch of water)
Left	255	0.057
Centre	272	0.052
Right	260	0.053

Temperature Reading over the Bundle (C^o)

In front of Row	SCAN POSITIONS 3"	6"	9"
1		125.5	
2	146.0	137.0	130.0
3	149.0	140.5	132.0
4	142.0	134.0	128.0
5	140.0	130.0	121.0
6	130.0	121.0	111.0
Behind Bundle		113.5	

EXPERIMENTAL DATA

Fresh air flowrate = 38704 ft^3/hr

Secondary air flowrate = 76200 ft^3/hr

Temperature Measurement C°

Thermo Couples	Selector A	B	C
1		127.0	321.0
2		78.0	170.0
3	64.5	70.0	61.0
4		68.5	69.0
5		78.0	64.5
6		67.0	57.5
7		72.0	71.5
8		75.0	69.0
9		72.0	71.5
10		58.5	57.0
11	74.0	128.0	46.0
12	67.0		43.0
13	53.5	46.0	74.5
14	72.0		
15	66.0	49.5	86.0
16	71.5	57.5	
17	102.0	59.0	27.5
18	70.0	71.0	
19	62.5	58.5	143.0
20		99.5	187.0

Scanning inside the Chamber C°

	Temperature (C°)	Pressure (inch of water)
Left	280	0.057
Centre	272	0.052
Right	270	0.053

Temperature Reading over the Bundle (C°)

In front of Row	SCAN POSITIONS 3"	6"	9"
1		127.0	
2	145.0	137.0	130.0
3	143.0	136.0	128.0
4	141.0	134.0	126.0
5	140.0	131.5	127.0
6	132.0	121.0	115.0
Behind Bundle		128.0	

EXPERIMENTAL DATA

Fresh air flowrate = 31602 ft^3/hr

Secondary air flowrate = 76200 ft^3/hr

Temperature Measurement C°

Thermo Couples	Selector A	B	C
1		125.0	321.0
2		77.5	169.0
3	67.0	70.5	64.0
4		70.0	72.5
5		78.5	68.0
6		70.0	61.0
7		74.0	74.5
8		75.0	72.0
9		72.0	74.0
10		60.0	59.5
11	76.5	122.5	48.5
12	70.0		44.0
13	58.0	47.0	75.5
14	74.5		
15	69.0	51.5	77.0
16	74.0	61.0	
17	101.5	61.5	27.5
18	73.5	72.5	
19	65.6	60.0	140.5
20		97.0	186.0

Scanning inside the Chamber C°

	Temperature (C°)	Pressure (inch of water)
Left	270	0.057
Centre	281	0.052
Right	290	0.053

Temperature Reading over the Bundle (C°)

In front of Row	SCAN POSITIONS 3"	6"	9"
1		125.0	
2	145.0	138.0	131.0
3	140.0	134.0	329.0
4	133.0	127.0	120.0
5	131.0	125.0	119.0
6	128.0	120.0	114.0
Behind Bundle		122.5	

EXPERIMENTAL DATA

Fresh air flowrate = 22346 ft^3/hr

Secondary air flowrate = 76200 ft^3/hr

Temperature Measurement C°

Thermo Couples	Selector A	B	C
1		121.5	312.0
2		80.0	162.0
3	71.0	73.0	67.5
4		75.0	74.5
5		81.0	72.5
6		74.0	65.5
7		77.5	78.0
8		79.0	75.0
9		77.0	77.0
10		63.0	64.5
11	78.0	122.0	50.5
12	73.0		47.5
13	63.5	48.0	81.5
14	77.0		
15	72.5	54.0	
16	76.5	66.0	
17	97.0	66.0	26.0
18	75.0	75.0	
19	70.0	63.0	136.0
20		91.5	180.0

Scanning inside the Chamber C°

	Temperature (C°)	Pressure (inch of water)
Left	116	0.057
Centre	120	0.052
Right	121	0.053

Temperature Reading over the Bundle (C°)

In front of Row	SCAN POSITIONS 3"	6"	9"
1		121.0	
2	145.0	138.0	136.0
3	136.0	131.0	125.0
4	139.0	130.5	123.0
5	130.0	124.0	120.0
6	132.0	124.0	120.5
Behind Bundle		122.0	

(A.1.3.4)

EXPERIMENTAL DATA

Fresh air flowrate = 44900 ft^3/hr

Secondary air flowrate = 28319 ft^3/hr

Temperature Measurement C^o

Thermo Couples	Selector A	B	C
1		258.0	514.0
2	61.5	119.0	337.0
3	83.5	98.5	71.5
4		91.5	101.0
5		116.5	68.0
6		92.0	71.0
7		86.0	90.0
8		114.0	98.0
9		92.0	103.0
10		75.5	66.0
11	101.0	185.0	52.0
12	91.0		51.0
13	67.5	52.0	97.0
14	112.5		
15	83.0	52.0	108.0
16	120.0	52.0	
17	111.0	68.0	26.0
18	230.0	101.5	
19	73.0	75.5	270.5
20	85.0	203.0	326.0

Scanning inside the Chamber C^o

	Temperature (C^o)	Pressure (inch of water)
Left	303	0.012
Centre	312	0.014
Right	310	0.019

Temperature Reading over the Bundle (C^o)

In front of Row	SCAN POSITIONS 3"	6"	9"
1		258.0	
2	253.0	247.0	240.0
3	227.0	217.5	212.0
4	210.0	200.0	194.0
5	211.0	192.0	186.0
6	200.0	187.0	180.0
Behind Bundle		185.0	

EXPERIMENTAL DATA

Fresh air flowrate = 44691 ft^3/hr

Secondary air flowrate = 28319 ft^3/hr

Temperature Measurement C°

Thermo Couples	Selector A	B	C
1		271.0	527.0
2	66.0	132.5	353.0
3	87.5	110.0	73.0
4		104.0	106.0
5		129.5	72.0
6		100.5	74.0
7		90.0	95.0
8		127.5	103.5
9		107.0	109.5
10		80.0	69.0
11	107.0	192.0	53.5
12	96.0		52.5
13	68.0	52.5	115.0
14	122.0		
15	87.5	54.5	110.0
16	118.0	54.5	~~26.0~~
17	242.5	74.0	26.0
18	76.0	109.0	
19	93.0	78.5	284.0
20	218.0	218.5	345.0

Scanning inside the Chamber C°

	Temperature (C°)	Pressure (inch of water)
Left	305	0.012
Centre	317	0.014
Right	315	0.019

Temperature Reading over the Bundle (C°)

In front of Row	SCAN POSITIONS 3"	6"	9"
1		271.0	
2	260.0	254.0	250.0
3	236.0	225.0	220.0
4	215.0	207.0	201.0
5	207.0	199.0	192.0
6	201.0	191.0	183.0
Behind Bundle		192.0	

EXPERIMENTAL DATA

Fresh air flowrate = 38704 ft^3/hr

Secondary air flowrate = 28319 ft^3/hr

Temperature Measurement C°

Thermo Couples	Selector A	B	C
1		271.0	530.0
2	70.5	138.0	356.0
3	92.5	115.5	77.5
4		111.0	112.0
5		136.0	76.0
6		109.0	79.0
7		96.0	101.0
8		134.0	109.0
9		113.5	115.0
10		85.5	73.5
11	113.0	200.0	56.0
12	102.0		57.0
13	75.0	57.5	116.0
14	128.5		
15	93.5	59.5	116.5
16	125.0	59.0	
17	246.5	79.5	26.5
18	81.5	117.5	
19	98.0	84.0	289.0
20		224.5	351.0

Scanning inside the Chamber C°

	Temperature (C°)	Pressure (inch of water)
Left	306	0.012
Centre	322	0.014
Right	319	0.019

Temperature Reading over the Bundle (C°)

In front of Row	SCAN POSITIONS 3"	6"	9"
1		271.0	
2	260.0	252.0	246.0
3	241.0	233.0	227.0
4	219.0	208.5	298.0
5	209.0	203.0	294.0
6	210.0	196.0	190.0
Behind Bundle		200.0	

EXPERIMENTAL DATA

Fresh air flowrate = 31602 ft^3/hr

Secondary air flowrate = 28319 ft^3/hr

Temperature Measurement C^o

Thermo Couples	Selector A	B	C
1		271.0	534.0
2	77.0	144.0	360.0
3	98.0	121.0	87.5
4		119.0	123.5
5		143.5	84.5
6		118.5	87.0
7		103.0	112.0
8		131.0	118.0
9		122.0	125.0
10		93.0	81.0
11	124.0	206.0	60.0
12	112.0		59.0
13	84.5	60.5	117.0
14	136.5		
15	101.0	63.0	120.0
16	134.0	66.5	
17	250.0	85.5	27.5
18	91.5	123.5	
19	100.0	90.0	291.0
20		227.0	354.0

Scanning inside the Chamber C^o

	Temperature (C^o)	Pressure (inch of water)
Left	306	0.012
Centre	323	0.014
Right	319	0.019

Temperature Reading over the Bundle (C^o)

In front of Row	SCAN POSITIONS 3"	6"	9"
1		271.0	
2	261.0	252.0	241.0
3	252.0	233.0	220.0
4	231.0	212.0	199.0
5	217.0	206.0	293.0
6	219.0	204.0	194.0
Behind Bundle		206.0	

EXPERIMENTAL DATA

Fresh air flowrate = 22346 ft^3/hr

Secondary air flowrate = 28319 ft^3/hr

Temperature Measurement C°

Thermo Couples	Selector A	B	C
1		274.0	531.0
2	91.0	137.0	362.0
3	114.0	135.0	101.5
4		157.0	140.0
5		133.5	100.0
6		111.0	102.0
7		155.5	130.5
8		140.0	133.5
9		125.0	140.0
10		107.0	96.0
11	140.0	222.5	70.0
12	129.0		68.0
13	98.5	67.0	119.0
14	151.0		
15	117.0	73.0	135.0
16	145.5	81.0	
17	252.0	99.0	29.0
18	105.5	139.0	
19	121.0	100.5	292.0
20		229.0	358.0

Scanning inside the Chamber C°

	Temperature (C°)	Pressure (inch of water)
Left	307.	0.012
Centre	327	0.014
Right	322	0.019

Temperature Reading over the Bundle (C°)

In front of Row	SCAN POSITIONS 3"	6"	9"
1		274.0	
2	257.0	250.0	241.0
3	248.0	240.5	231.0
4	236.0	224.0	218.0
5	234.0	222.0	209.0
6	225.0	215.0	201.0
Behind Bundle		222.5	

<u>A.1.4</u>

Hot air across the bundle

EXPERIMENTAL DATA

Fresh air flowrate = 49900 ft^3/hr

Secondary air flowrate = 69368 ft^3/hr

Temperature Measurement C^o

Thermo Couples	Selector A	B	C
1		110.0	86.0
2	37.0		90.0
3	43.0	56.0	46.5
4		48.0	68.0
5			46.0
6		56.5	45.0
7		49.5	60.0
8		66.0	66.0
9		57.0	68.0
10	27.0	50.0	46.0
11	65.5	88.0	
12	61.5		40.0
13	44.0		47.5
14	67.0	27.0	
15	49.0	36.5	49.0
16	67.5	34.0	
17	104.0	41.0	27.0
18	48.0		
19	49.0	40.5	93.5
20	90.0	90.0	96.5

Scanning inside the Chamber C^o

	Temperature (C^o)	Pressure (inch of water)
Left	100	0.04
Centre	95	0.042
Right	98	0.031

Temperature Reading over the Bundle (C^o)

In front of Row	SCAN POSITIONS 3"	6"	9"
1		110.0	
2	119.0	109.0	101.0
3	110.0	102.0	98.0
4	0.6.0	100.0	96.0
5	101.0	94.5	95.0
6	97.0	92.0	93.0
Behind Bundle		88.0	

EXPERIMENTAL DATA

Fresh air flowrate = 44691 ft^3/hr

Secondary air flowrate = 69368 ft^3/hr

Temperature Measurement C^o

Thermo Couples	Selector A	Selector B	Selector C
1		110.0	87.5
2	38.0		91.0
3	43.5	58.0	46.5
4		51.5	69.0
5			47.0
6		57.0	46.0
7		50.0	61.0
8		69.0	66.0
9		55.5	69.0
10	97.5	51.0	47.0
11	66.5	88.0	
12	62.5		34.0
13	43.5		48.5
14	70.0	25.5	
15	50.0	37.0	49.0
16	69.0	35.5	
17	105.0	42.0	27.0
18	48.5		
19	52.0	40.5	95.0
20		91.5	98.0

Scanning inside the Chamber C^o

	Temperature (C^o)	Pressure (inch of water)
Left	101	0.04
Centre	98	0.042
Right	99	0.031

Temperature Reading over the Bundle (C^o)

In front of Row	SCAN POSITIONS 3"	6"	9"
1		110.0	
2	116.0	108.0	101.0
3	109.0	103.0	98.0
4	104.0	99.5	94.0
5	100.0	95.5	93.0
6	97.0	92.0	90.0
Behind Bundle		88.0	

EXPERIMENTAL DATA

Fresh air flowrate = 38704 ft^3/hr

Secondary air flowrate = 69368 ft^3/hr

Temperature Measurement C^o

Thermo Couples	Selector A	B	C
1		111.5	88.0
2	42.0		93.5
3	47.5	61.0	51.0
4		56.0	74.0
5			51.0
6		61.0	50.0
7		54.0	66.5
8		74.0	71.0
9		59.0	74.5
10		55.5	51.5
11	71.5	92.5	
12	68.0		37.5
13	48.0		52.5
14	75.0	29.0	
15	54.0	41.0	53.0
16	73.5	37.5	
17	107.0	45.5	30.0
18	52.0		
19	65.5	44.0	96.5
20		93.5	99.0

Scanning inside the Chamber C^o

	Temperature (C^o)	Pressure (inch of water)
Left	102	0.04
Centre	105	0.042
Right	96	0.031

Temperature Reading over the Bundle (C^o)

In front of Row	SCAN POSITIONS 3"	6"	9"
1		111.5	
2	121.0	111.0	103.0
3	115.0	104.0	99.0
4	111.0	102.5	95.0
5	103.0	98.0	92.0
6	100.0	96.0	91.0
Behind Bundle		92.5	

EXPERIMENTAL DATA

Fresh air flowrate =31602 ft^3/hr

Secondary air flowrate = 69368 ft^3/hr

Temperature Measurement C^o

Thermo Couples	Selector A	B	C
1		112.0	90.0
2	44.0		94.0
3		63.5	54.0
4		58.0	78.0
5			54.0
6		63.5	53.0
7		57.0	70.5
8		77.5	75.0
9		62.0	78.0
10		58.0	54.0
11	75.0	94.0	
12	71.5		39.0
13	51.5		53.0
14	77.0	30.0	
15	56.5	42.5	54.0
16	76.0	40.5	
17	107.0	47.5	31.0
18	54.0		
19		46.0	97.0
20	95.0	95.0	100.0

Scanning inside the Chamber C^o

	Temperature (C^o)	Pressure (inch of water)
Left	104	0.04
Centre	97	0.042
Right	99	0.031

Temperature Reading over the Bundle (C^o)

In front of Row	SCAN POSITIONS 3"	6"	9"
1		112.0	
2	120.0	111.5	105.0
3	115.0	108.0	103.0
4	109.0	106.0	99.0
5	106.0	101.5	95.0
6	103.0	99.0	94.0
Behind Bundle		94.0	

EXPERIMENTAL DATA

Fresh air flowrate = 22346 ft^3/hr

Secondary air flowrate = 69368 ft^3/hr

Temperature Measurement C^o

Thermo Couples	Selector A	B	C
1		111.5	89.5
2	47.0		94.0
3	52.0	67.0	58.5
4		63.0	83.0
5			58.5
6		69.0	57.5
7		60.0	76.5
8		83.0	79.5
9		68.0	83.0
10		61.5	58.5
11	80.0	96.0	
12	77.0		41.0
13	56.0		57.0
14	82.0	30.0	
15	59.0	45.0	57.0
16	81.0	43.5	
17	107.0	51.0	31.0
18	56.5		
19	62.0	50.0	96.5
20	95.0	95.0	100.0

Scanning inside the Chamber C^o

	Temperature (C^o)	Pressure (inch of water)
Left	99	0.04
Centre	103	0.042
Right	101	0.031

Temperature Reading over the Bundle (C^o)

In front of Row	SCAN POSITIONS 3"	6"	9"
1		111.5	
2	120.0	111.5	108.0
3	113.0	108.5	103.0
4	110.0	106.5	99.0
5	108.0	101.0	93.0
6	103.0	100.0	92.0
Behind Bundle		96.0	

APPENDIX A.2

(A.2.1)

COMPUTER NOMENCLATURE

ACS	total furnace wall area
AKON1	fresh air thermal conductivity at tube inlet temperature
AKON2	fresh air thermal conductivity at tube exit temperature
AKON3	hot gas thermal conductivity on shell side
AKONV	overall fresh air thermal conductivity
AL	longitudinal inner tube area
ALO	longitudinal outer tube area
AM	linear mean temperature difference
AT	tube cross sectional area
AS	shell flow area
ASR	radiative sink area
C1,C2,C3,C4	constants for parameters
CFL	total fresh air flowrate
cp1	fresh air specific heat capacity at tube inlet temperature
cp2	fresh air specific heat capacity at tube exit temperature
cpB	hot gas specific heat capacity at shell temperature
cpp	total fresh air specific heat capacity
cpv	overall fresh air specific heat capacity
D	tube internal diameter
De	shell equivalent diameter
DEN	density at fresh air at inlet temperature
Dens1	fresh air density at tube inlet temperature
Dens2	fresh air density at tube outlet temperature
DensB	density of hot gas at the bundle
Denss	hot gas density at shell temperature
DensV	overall fresh air density
ECo2	radiative heat transfer
EHo	error involved in calculating heat transfer coefficient on shell side

ERC	error involved in calculating heat transfer coefficient on tube side
EReS	errors involved in calculating Reynolds number on shell side
EW	emissivity of water vapour
F	degree of variance
FK	thermal conductivity of insulation wall
FTS	Practical correction factor
FTW	calculated correction factor
GN	natural gas flowrate
HEEFE	heat exchanger efficiency
HFL	hot gas flow rate
HI	heat transfer coefficient on tube side
HO	heat transfer coefficient on shell side
OD	outer tube diameter
Pair	primary air flow rate
Prs	Prandtl number on shell side
Prt	Prandtl number on tube side
QCo2	radiative heat transfer rate from Co2
QCON	heat transfer rate to fresh air
QF	heat taken out by flue gases
QL	heat losses rate
QP	heat recovered by fresh air
QRT	total radiative heat transfer rate
QRW	radiative heat transfer rate
QRWT	radiative heat transfer rate from furnace walls
QW	radiative heat transfer rate from water vapour
RCoF	true counter current
RCRF	r(cross flow), temperature group
REH1	ratio of error to the actual heat transfer coefficient on tube side
REHO	ratio of error to the actual heat transfer coefficient on shell side
RERE	ratio of error to the actual Reynolds number on tube side
Res	Reynold number on shell side

SAir	secondary air flow rate
SDA2	standard deviation in group A
SDB2	standard deviation in group B
TA	fresh air temperature
TB	temperature of gas surrounding a sample tube
TF	furnace wall temperature
TL	practical mean temperature difference
TLC	logarithmic mean temperature difference shell side
TM	logarithmic mean temperature difference tube side
TW	tube wall temperature
WK	tube wall thermal conductivity
XF	furnace wall thickness
XT	tube wall thickness
V	fresh air velocity through a sample tube
VS	hot gas velocity through shell

Subscripts

(i)	tube entrance
(i + i)	tube exit

(A.2.2)

```
      LEAST SQUARE FIT PROGRAMME WITH STATISTICAL ANALYSIS
      ----------------------------------------------------
      USED FOR OVER-ALL CORRELATION ON THE SHELL SIDE
      ------------------------------------------------
      TRACE2
      MASTER ADIL
      DIMENSION X(200),Y(200),XE(200),YE(200),RR(20)
      DO 999 I=1,50
C     X=REYNOLDS NUMBER
      ----------------
C     Y=NUSSELT NUMBER
      ------------------
      READ(1,7)X(I),Y(I)
    7 FORMAT(2F0.0)
      XE(I)=ALOG10(X(I))
      YE(I)=ALOG10(Y(I))
  999 CONTINUE
C     STATISTICAL COMPUTER PACKAGE
       ----------------------------
      IFAIL=0
      CALL G02CAF(50,XE,YE,RR,IFAIL)
      WRITE(2,23) RR(5), RR(6),RR(7),RR(8),RR(9)
   23 FORMAT(1H0,'CORR COEFF=',F12.4,'SLOPE=',F12.4,'INTERCEPT=',
     1F12.4,'STANDARD ERROROF SLOPE=',F12.4,'STEROFINT=',F12.4)
      STOP
      END
      FINISH
```

(A.2.3)

```
C     PROGRAMME FOR STATISTICAL ANALYSIS OF''HI'' VARIATION ALONG TUBES
      ------------------------------------------------------------------
      TRACE2
      MASTER ADIL
      DIMENSION TW(200),HI(200),TA(200),V(200)
      READ (1,17) (V(I),I=1,4)
   17 FORMAT(4F0.0)
      READ(1,6) (TW(I), I = 1, 48)
    6 FORMAT(12F0.0)
      READ(1,3)(TA(I),I=1,48)
    3 FORMAT(12F0.0)
      DO 99 K=1,4
      AL=0.046
      D=0.0792
      AT=0.00492
      DO 19 J=1,11
      I=(K-1)*(12)+J
      IF(J.GT.1)AL=0.092
      DENS1=(14.7*144.0)/(53.36*1.8*(TA(1)+273.0))
      CP1=(6.713+(0.4967*(TA(I)+273.0)/1000.0))*1.0/29.0
      CP2=(6.713+(0.4967*(TA(I+1)+273.0)/1000.0))*1.0/29.0
      VISC1=0.044*(393.0/(TA(I)+273.0+120.0))*
     1((TA(I)+273.0)/273.0)**1.5
      VISC2=0.044*(393.0/(TA(I+1)+273.0+120.0))*
     1((TA(I+1)+273.0)/273.0)**1.5
      QCON=(DENS1)*V(K)*0.8*AT*((CP1+CP2)/2.)*((TA(I+1)*(9./
     15.)+32.)-(TA(I)*(9./5.)+32.))
      RET=DENS1*V(K)*D/((VISC1+VISC2)/2.)
      HI(J)=QCON/(AL*((((TW(I)*9./5.+32.)+(TW(I+1)*9./5.+32.))/
```

```
 12.)-(((TA(I)*9./5.+32.)+(TA(I+1)*9./5.+32.))/2.)))
  A=2*((TA(I+1)-TA(I))**2)+((TW(I)+TW(I+1)-2.*TA(I+1)-2.*TA(I))**
 12)+((TW(I)+TW(I+1))**2)
  B=(TW(I)+TW(I+1)-TA(I)-TA(I+1))**4
  C=DENS1*V(K)*0.8*AT*(CP1+CP2)/AL
  ERC=(0.25*C/HI(J))*((A/B)**0.5)
  WRITE(2,29)HI(J),QCON,RET,ERC
29 FORMAT(10X,'HI=',F10.2,5X,'QCON=',F10.2,'RET=',F10.2,5X,'ERC=',
 1F10.3)
19 CONTINUE
  S=0.
  STD=0.
  DO 120 J=1,11
  S=S+HI(J)
120 CONTINUE
  XMEAN=S/11.
  DO 130 J=1,11
  STD=STD+(HI(J)-XMEAN)**2
130 CONTINUE
  STD=(STD/11.)**0.5
  RATIO=STD/XMEAN
  WRITE(2,98)XMEAN,STD,RATIO
98 FORMAT(10X,'XMEAN=',F10.2,'STD=',F10.2,'RATIO=',F10.2)
99 CONTINUE
  STOP
  END
  FINISH
```

(A.2.4)

```
C       PROGRAMME OF COMPARING DIFFERENT TYPES OF MEAN TEMPERATURE
        ----------------------------------------------------------
      TRACE2
      MASTER ADIL
      DIMENSION TW(25),TA(25),TF(4),V(24),T(9),DP(25),TB(24),
     1XE(300),YE(300),RR(30)
      READ(1,6) (DP(I), I = 1, 5)
    6 FORMAT(5F0.0)
      DO 999 K=1,5
      READ(1,3)(TW(I),I=1,24)
    3 FORMAT(8F0.0)
      READ(1,3)(TA(I),I=1,24)
      READ(1,7)(V(I),I=1,24,2)
    7 FORMAT(6F0.0)
      READ(1,9)(TF(I),I=1,4)
    9 FORMAT(4F0.0)
      READ(1,10)(T(J),J=1,8)
   10 FORMAT(8F0.0)
      READ (1,77)(TB(I),I=1,24,2)
   77 FORMAT(6F0.0)
      GN=450.
      DP12=0.8
      PAIR=9600.
      CFL=(526.7*(DP(K)*0.785)**0.5)*60.0
      QC=GN*895.
      SAIR=527.73*((DP12*0.785)**0.5)*60.0
      ASR=1.94
      DEV=0.108
      LT=3.5
```

```
FK=2.2
D=0.077
AS=0.85
OD=0.0875
AT=0.00492
AL=0.9962
AC=42.47
XT=0.0054
XF=0.3745
WK=26.0
HFL=SAIR+GN+PAIR
DENSS=(14.7*144.0)/(53.36*1.8*(T(2)+273.0))
AKONS=0.01391*(398.0/((T(2)+273.0)+125.0))*
1((T(2)+273.0)/273.0)**1.5
CPS=(6.713+0.4697*((T(2)+273.0)/1000.0))*1.0/29.0
VISCS=0.044*(393.0/(T(2)+273.0+120.0))*((T(2)+273.0)/273.0)**1.5
VS=HFL*((T(2)+273.)/(T(7)+273.))/AS
RES=(DENSS*VS*DEV)/VISCS
PRS=VISCS*CPS/AKONS
DEN=(14.7*144.)/(53.36*1.8*(T(4)+273.))
QS=(SAIR+GN+PAIR)*DEN*CPS*((T(8)*(9./5.)+
132.)-(T(5)*(9./5.)+32.))
TV=((T(3)+T(7))/2.)+273.
DENSV=(14.7*144.)/(53.36*1.8*TV)
VISCV=0.044*(393./(TV+120.))*(TV/273.)**1.5
AKONV=0.0139*(398./(TV+125.))*((TV)/273.)**1.5
CPV=(6.713+(0.4967*TV/1000.))*1./29.
REO=DENSV*D*(CFL/(60.*0.00492))/VISCV
PRO=CPV*VISCV/AKONV
```

```
      US=1./(1./((1.7/OD)*AKONS*RES**0.35*PRS**0.33)+1./((0.0023/D)*
     1AKONV*REO**1.12*PRO**0.33)+(XT/WK))
C     PRACTICAL MEAN TEMPERATURE DIFFERENCE
      -------------------------------------
      TL=QS/(US*AL*60.)
      A=T(8)*(9./5.)+32.
      B=T(5)*(9./5.)+32.
      C=T(7)*(9./5.)+32.
      D=T(3)*(9./5.)+32.
C     LOGARITHMIC MEAN TEMPERATURE DIFFERENCE
      ----------------------------------------
      TLC=((A-D)-(B-C))/ALOG((A-D)/(B-C))
C     LINEAR MEAN TEMPERATURE DIFFERENCE
      -----------------------------------
      AM=(A+B)/2.-(C+D)/2.
C     PRACTICAL CORRECTION FACTOR
      ---------------------------
      FTS=TL/TLC
      XK=(A-B)/(A-C)
      S=(D-C)/(A-C)
      RCOF=(XK-S)/ALOG((1.-S)/(1.-XK))
      RCRF=S/(ALOG(1./(1.-S/XK*ALOG(1./(1.-XK)))))
C     CROSS FLOW MEAN TEMPERATURE DIFFERENCE,(LITERATURE)
       ----------------------------------------------------
      FTW=RCRF/RCOF
      WRITE(2,100)QS,TL,TLC,AM,FTS,FTW,US
  100 FORMAT(10X,'QS=',F10.2,'TL=',F10.3,'TLC=',F10.3,'AM=',F10.3,
     1'FTS=',F10.3,'FTW=',F10.3,'US=',F10.3)
  999 CONTINUE
```

```
STOP
END
FINISH
```

(A.2.5)

PROGRAMME FOR VARIANCE CALCULATIONS ''F TEST''

```
      TRACE2
      MASTER ADIL
      DIMENSION A(180),B(180)
      READ(1,9) (A(I), I=1,30)
      READ(1,10) (B(I), I=1,30)
    9 FORMAT(10F0.0)
   10 FORMAT(10F0.0)
      S1=0.0
      S2=0.0
      DO  11  M=1,30
      S1=S1+A(M)
   11 CONTINUE
      DO 55 K=1,30
      S2=S2+B(K)
   55 CONTINUE
      SDA2=0.0
      SDB2=0.0
      DO 13  J=1,30
      SDA2=SDA2+((A(J)-S1/30.)**2/(30.-1))
   13 CONTINUE
      DO 19 LL=1,30
      SDB2=SDB2+((B(J)-S2/30.)**2/(30.-1))
   19 CONTINUE
      F=SDA2/SDB2
      WRITE(2,15)F
   15 FORMAT(5X,'F=',F10.3)
      STOP
```

```
END
FINISH
```

(A.2.6)

```
C       ''PROGRAMME TO CALCULATE RADIATION AND CONVECTION
          ---------------------------------------------
C         HEAT TRANSFER''
          --------------
        TRACE2
        MASTER ADIL
        DIMENSION TW(25),TA(25),TF(4),V(24),T(9),DP(25),TB(24),
       1XE(300),YE(300),RR(30)
        READ(1,6) (DP(I), I = 1, 5)
      6 FORMAT(5F0.0)
        DO 999 K=1,5
        READ(1,3)(TW(I),I=1,24)
      3 FORMAT(8F0.0)
        READ(1,3)(TA(I),I=1,24)
        READ(1,7)(V(I),I=1,24,2)
      7 FORMAT(6F0.0)
        READ(1,9)(TF(I),I=1,4)
      9 FORMAT(4F0.0)
        READ(1,10)(T(J),J=1,7)
     10 FORMAT(7F0.0)
        READ (1,77)(TB(I),I=1,24,2)
     77 FORMAT(6F0.0)
        S=0.0
        DO 19 I=1,12
        S=S+TW(I)
     19 CONTINUE
        GN=450.
        DP12=5.8
        CFL=(526.7*(DP(K)*0.785)**0.5)*60.0
```

```
      QC=GN*895.
      SAIR=527.73*((DP12*0.785)**0.5)*60.0
      EW=0.006
      EC=0.015
      ASR=1.94
      DEV=0.108
      LT=3.5
      FK=2.2
      D=0.077
      AS=0.85
      OD=0.0875
      AT=0.00492
      ALO=0.9962
      AL=0.71
      AC=42.47
      XT=0.0042
      XF=0.3745
      WK=26.0
      PAIR=6900.
C     RADIATIVE HEAT TRANSFER CALCULATIONS
      -------------------------------------
      TF1=TF(1)*(9./5.)+492.
      TF2=TF(2)*(9.0/5.0)+492.0
      TF3=TF(3)*(9.0/5.0)+492.0
      TF4=TF(4)*(9.0/5.0)+492.0
      TAV=(S*9.0/(12.0*5.0))+492.0
      QRW1=(0.15*0.0864*0.173*12.900*1.0/(10.0**8))*(TF1**4-TAV**4)
      QRW2=(0.15*0.0864*0.173*12.900*1.0/(10.0**8))*(TF2**4-TAV**4)
      QRW3=(0.36*0.0864*0.173*14.160*1.0/(10.0**8))*(TF3**4-TAV**4)
```

```
      QRW4=(0.36*0.0864*0.173*14.160*1.0/(10.0**8))*(TF4**4-TAV**4)
      QRWT=QRW1+QRW2+QRW3+QRW4
      QW=0.173*EW*((T(1)*(9.0/5.0)+492.0)/100.0)**4
      QCO2=0.173*EC*((T(1)*(9.0/5.0)+492.0)/100.0)**4
      QRT=QRWT+'QW+QCO2)*ASR
      WRITE(2,11)QRT
   11 FORMAT(50X,'QRT=',F10.2)
      HFL=SAIR+GN+PAIR
      VS=HFL*((T(2)+273.0)/(T(7)+273.0))/AS
      QL=AC*FK*((T(6)*(9.0/5.0)+?2.0)-(T(7)*(9.0/5.0)+32.0))/XF
C     HEAT TAKEN OUT BY FLUE GASES
      ----------------------------
      CPB=(6.713+0.4697*(T(5)+273.0)/1000.0)*1.0/29.0
      DENSB=(14.7*144.0)/(53.36*1.8*(T(7)+273.0))
      QF=HFL*DENSB*CPB*((T(5)*(9.0/5.0)+32.0)-(T(7)*(9.0/5.0)+32.0))
C     HEAT RECOVERED BY FRESH AIR
      ---------------------------
      DENSP=(14.7*144.0)/(53.36*1.8*(T(4)+273.0))
      CPP=(6.713+(0.4697*(((T(3)+T(4))/2.0)+273.0)/1000.0))*1.0/29.0
      QP=CFL*DENSP*CPP*((T(3)*(9.0/5.0)+32.0)-(T(4)*(9.0/5.0)+32.0))
C     HEAT AND RIG EXCHANGER EFFICIENCIES
     ------------------------------------
      HEEFF=QP/(QC-QL)
      ER=QP/QC
C     RE AND PR (ON SHELL SIDE ) CALCULATIONS
      ---------------------------------------
      DENSS=(14.7*144.0)/(53.36*1.8*(T(2)+273.0))
      AKONS=0.01391*(398.0/((T(2)+273.0)+125.0))*((T(2)+
     1273.0)/273.0)**1.5
```

```
      CPS=(6.713+0.4697*((T(2)+273.0)/1000.0))*1.0/29.0
      VISCS=0.044*(393.0/(T(2)+273.0+120.0))*((T(2)+273.0)/273.0)**1.5
      RES=(DENSS*VS*DEV)/VISCS
      PRS=VISCS*CPS/AKONS
      WRITE(2,17)QL,QF,QP,QC,HEEFF,PRS,RES,ER
   17 FORMAT(2X,'QL=',F10.3,5X,'QF=',F10.3,5X,'QP=',
     2F10.3,5X,'QC=',F10.3,5X,'HEEFF=',F5.2,5X,'PRS=',
     3F5.2,5X,'RES=',F8.2,5X,'ER=',F3.2)
C     TUBE (INSIDE AND OUT SIDE WALL)CALCULATIONS
      -----------------------------------------
      DO 34 I=1,24,2
      DENS1=(14.7*144.0)/(53.36*1.8*(TA(I)+273.0))
      DENS2=(14.7*144.0)/(53.36*1.8*(TA(I+1)+273.0))
      CP1=(6.713+(0.4967*(TA(I)+273.0)/1000.0))*1.0/29.0
      CP2=(6.713+(0.4967*(TA(I+1)+273.0)/1000.0))*1.0/29.0
      AKON1=0.01391*(398.0/(TA(I)+273.0+125.0))*((TA(I)+
     1273.0)/273.0)**1.5
      AKON2=0.0139*(398.0/(TA(I+1)+273.0+125.0))*((TA(I+1)+
     1273.0)/273.0)**1.5
      VISC1=0.044*(393.0/(TA(I)+273.0+120.0))*((TA(I)+
     1273.0)/273.0)**1.5
      VISC2=0.044*(393.0/(TA(I+1)+273.0+120.0))*((TA(I+1)+
     1273.0)/273.0)*1.5
C     LOGARITHMIC MEAN TEMPERATURE DIFFERENCE CALCULATIONS
       ----------------------------------------------------
      A=TW(I+1)*(9.0/5.0)+32.0
      B=TW(I)*(9.0/5.0)+32.0
      C=TA(I+1)*(9.0/5.0)+32.0
      R=TA(I)*(9.0/5.0)+32.0
```

```
      TM=((A-C)-(B-R))/ALOG((A-C)/(B-R))
      RET=((DENS1+DENS2)/2.)*D*V(I)/((VISC1+VISC2)/2.)
      PRT=((VISC1*CP1/AKON1)+(VISC2*CP2/AKON2))/2.0
      QCON=((DENS1+DENS2)/2.0)*V(I)*AT*((CP1+CP2)/2.0)*
     1((TA(I+1)*(9.0/5.0)+32.0)-(TA(I)*(9.0/5.0)+32.0))
      HI=QCON/(AL*TM)
      HO=QCON/(AL*((TB(I)*)+32.0)-((TW(I)+TW(I+1)/2.0)*
     1(9.0/5.0)+32.0)))
      XNUO=HO*OD/AKONS
      XNUM=HI*D/((AKON1+AKON2)/2.0)
      XNUI=XNUM*(T(3)/TA(I+1))**4
      WRITE(2,100)QCON,HI,HO,U,XNUI,XNUO,RET,PRT
  100 FORMAT(4X,'QCON=',F6.1,'HI=',F5.1,'HO=',F5.1,'U=',F5.1,'XNUI=',
     1F7.2,'XNUO=',F7.2,'RET=',F9.1,'PRT=',F5.3)
      U=1./((1./HO)+(1./HI)+(XT/WK)+0.001)
      INT=6*(K-1)+((I-13)/2)+1
      IF(I.LT.13) GO TO 34
      IF(I.GT.23) GO TO 34
      XE(INT)=ALOG10(RET)
      YE(INT)=ALOG10(XNUI)
   34 CONTINUE
  999 CONTINUE
C     STATISTICAL ANALYSIS COMPUTER PACKAGE
      ------------------------------------
      IFAIL=0
      CALL G02CAF(30,XE,YE,RR,IFAIL)
      WRITE(2,23) RR(5), RR(6),RR(7),RR(8),RR(9)
   23 FORMAT(1H0,'CORR COEFF=',F12.4,'SLOPE=',F12.4,'INTERCEPT=',
     1F12.4,'STANDARD ERROROF SLOPE=',F12.4,'STEROFINT=',F12.4)
```

```
STOP
END
FINISH
```

(A.2.7)

```
C       PROGRAMME FOR CALCULATING ERRORS IN ''RE,H''TUBE AND SHELL SIDES
        ----------------------------------------------------------------
      TRACE1
      TRACE2
      MASTER ADIL
      DIMENSION TW(25),TA(25),TF(4),V(24),T(9),DP(25),TB(24)
      READ(1,6) (DP(I), I = 1, 5)
    6 FORMAT(5F0.0)
      DO 999 K=1,5
      READ(1,3)(TW(I),I=1,24)
    3 FORMAT(8F0.0)
      READ(1,3)(TA(I),I=1,24)
      READ(1,7)(V(I),I=1,24,2)
    7 FORMAT(6F0.0)
      READ(1,9)(TF(I),I=1,4)
    9 FORMAT(4F0.0)
      READ(1,10)(T(J),J=1,7)
   10 FORMAT(7F0.0)
      READ (1,77)(TB(I),I=1,24,2)
   77 FORMAT(6F0.0)
      GN=450.
      DP12=5.8
      CFL=(526.7*(DP(K)*0.785)**0.5)*60.0
      SAIR=527.73*((DP12*0.785)**0.5)*60.0
      ASR=1.94
      DEV=0.108
      LT=3.5
      D=0.077
      AS=0.85
```

```
      OD=0.0875
      AT=0.00492
      ALO=0.9962
      AL=0.71
      AC=42.47
      XT=0.0042
      XF=0.3745
      WK=26.0
      PAIR=6900.
      HFL=SAIR+GN+PAIR
      VS=HFL*((T(2)+273.0)/(T(7)+273.0))/AS
      DENSS=(14.7*144.0)/(53.36*1.8*(T(2)+273.0))
      AKONS=0.01391*(398.0/((T(2)+273.0)+125.0))*((T(2)+
     1273.0)/273.0)**1.5
      CPS=(6.713+0.4697*((T(2)+273.0)/1000.0))*1.0/29.0
      VISCS=0.044*(393.0/(T(2)+273.0+120.0))*((T(2)+
     1273.0)/273.0)**1.5
      RES=(DENSS*VS*DEV)/VISCS
      ERS=(DENSS*DEV/VISCS)**2*(0.065*VS)**2
      RERS=ERS**0.5/RES
      WRITE(2,17)RERS
   17 FORMAT(50X,'RERS=',F10.5)
      DO 34 I=1,24,2
      DENS1=(14.7*144.0)/(53.36*1.8*(TA(I)+273.0))
      DENS2=(14.7*144.0)/(53.36*1.8*(TA(I+1)+273.0))
      CP1=(6.713+(0.4967*(TA(I)+273.0)/1000.0))*1.0/29.0
      CP2=(6.713+(0.4967*(TA(I+1)+273.0)/1000.0))*1.0/29.0
      AKON1=0.01391*(398.0/(TA(I)+273.0+125.0))*((TA(I)+
     1273.0)/273.0)**1.5
```

```
AKON2=0.0139*(398.0/(TA(I+1)+273.0+125.0))*((TA(I+1)+
1273.0)/273.0)**1.5
VISC1=0.044*(393.0/(TA(I)+273.0+120.0))*((TA(I)+
1273.0)/273.0)**1.5
VISC2=0.044*(393.0/(TA(I+1)+273.0+120.0))*((TA(I)+
1273.0)/273.0)**1.5
A=TW(I+1)*(9.0/5.0)+32.0
B=TW(I)*(9.0/5.0)+32.0
C=TA(I+1)*(9.0/5.0)+32.0
R=TA(I)*(9.0/5.0)+32.0
TM=((A-C)-(B-R))/ALOG((A-C)/(B-R))
RET=((DENS1+DENS2)/2.)*D*V(I)/((VISC1+VISC2)/2.)
QCON=((DENS1+DENS2)/2.0)*V(I)*AT*((CP1+CP2)/2.0)*((TA(I+1)*
1(9.0/5.0)+32.0)-(TA(I)*(9.0/5.0)+32.0))
HI=QCON/(AL*TM)
HO=QCON/(AL*((TB(I)*)*(9.0/5.0)+32.0)-((TW(I)+TW(I+1)/2.0)*
1(9.0/5.0)+32.0)))
C1=DENS1*AT*(CP1+CP2)*0.5/AL
DENOM=(B+A-R-C)**2
X=(C1*V(I)*(C-R)/DENOM)**2*(0.5)**2
Y=(C1*V(I)*(2*C-B-A)/DENOM)**2*(0.5)**2
Z=(C1*V(I)*(B+A-2*R)/DENOM)**2*(0.5)**2
W=(C1*(C-R)/(DENOM**0.5))**2*(0.13*V(I))**2
EHI=2*X+Y+Z+W
REHI=EHI**0.5/HI
C2=DENS1*AT*(CP1+CP2)*0.5/ALO
DEN= (TB(I)*(9./5.+32.)-(A+B)*0.5)**2
S1=(C2*V(I)/(DEN**0.5))**2*(0.5)**2
S2=(C2*V(I)*(C-R)/DEN)**2*(0.5)**2
```

```
      S3=(0.5*C2*V(I)*(C-R)/DEN)**2*(0.5)**2
      S4=(0.5*C2*V(I)*(C-R)/DEN)**2*(0.5)**2
      S5=(C2*(C-R)/(DEN)**0.5)**2*(0.13*V(I))**2
      EHO=2*S1+S2+S3+S4+S5
      REHO=EHO**0.5/HO
      ERE=((DENS1+DENS2)*D/(VISC1+VISC2))**2*(0.13*V(I))**2
      RERE=ERE**0.5/RET
      WRITE(2,100)QCON,HI,HO,REHI,REHO,RERE,RET
  100 FORMAT(4X,'QCON=',F6.1,'HI=',F5.1,'HO=',F5.1,'REHI=',F5.2,
     1'REHO=',F7.4,'RERE=',F7.2,'RET=',F9.1)
   34 CONTINUE
  999 CONTINUE
      STOP
      END
      FINISH
```